NASA Contractor Report 3957

A Review of Fracture Mechanics Life Technology

Philip M. Besuner, David O. Harris,
and Jerrell M. Thomas

CONTRACT NAS8-34746
FEBRUARY 1986

NASA

NASA Contractor Report 3957

A Review of Fracture Mechanics Life Technology

Philip M. Besuner, David O. Harris,
and Jerrell M. Thomas
Failure Analysis Associates
Palo Alto, California

Prepared for
George C. Marshall Space Flight Center
under Contract NAS8-34746

NASA
National Aeronautics
and Space Administration

**Scientific and Technical
Information Branch**

1986

Table of Contents

Table of Contents
(continued)

Table of Contents
(continued)

Section 1

INTRODUCTION

The purpose of this report is to provide a review of current fracture mechanics technology for the prediction of the lifetime of structural components subjected to cyclic loads. The central objectives of the review are to report the current state and recommend future development of fracture mechanics-based analytical tools applicable to modeling and forecasting the subcritical fatigue crack growth in structures. A wide variety of information and opinion sources were used in performing the review; ranging from the published literature through interviews and including the authors' experiences and opinions. The application of these tools to day-to-day problems for practical engineering design, development and decision is emphasized. At the request of the National Aeronautics and Space Administration (NASA), special emphasis was given to the following areas:

- Retardation
- Plasticity
- Thermal stress fields
- Plane stress and strain
- Surface effects on stress intensity
- High compressive load effects on crack growth
- Effects of pressure in cracks on stress intensity
- Threshold effect for high cycle low positive stress ratios
- Mixed low and high cycle environments
- Frequency effects
- Uniaxial and multiaxial stress fields
- Breakthrough criteria
- Residual stress effects
- Stress ratio effects
- Automated stress intensity computer programs
- Proof test criteria for tough ductile materials exhibiting stable flaw growth
- Weld cracks
- Probabilistic fracture mechanics

This limited scope, combined with the seemingly unlimited volume of available, related information and opinions, has led to a deemphasis of the following related subjects:

- non-metallic materials
- metallurgical and material aspects and techniques
- micromechanics
- experimental aspects and techniques
- creep crack growth
- creep-fatigue interactions
- analytical tools with severely limited potential for timely, cost-effective applications
- analysis tools not based on the principles of continuum mechanics

To a lesser extent, there is also a deemphasis of brittle fracture and other cracking and failure modes not directly involving subcritical fatigue crack growth.

Before proceeding with the survey, the remaining portions of Section 1 will provide some background material.

1.1 FRACTURE MECHANICS BACKGROUND

The traditional approach to structural fatigue life prediction has been the alternating stress-versus-cycles (S-N) technique. Initially smooth or notched test specimens are polished so that all surface defects are removed. These specimens are tested to failure (which can be defined as crack initiation or fracture of the specimen) and the resulting cyclic lives for various alternating stresses serve as a basis for the design of a component against fatigue failure. For example, in the ASME Pressure Vessel Code design procedure [1-1] the S-N approach is used to establish usage factors for the component. However, the principles of the more recent linear elastic fracture

mechanics (LEFM) approach have been adopted recently by the Code to (1) assure adequate material toughness at the start of life, and (2) provide flaw evaluation procedures for defects found during service so that rules for flaw acceptability and component operation without repair could be established. Linear elastic fracture mechanics approaches cannot always replace S-N techniques, because LEFM is based on a crack being initially present. Unfortunately, this is all too often the case. However, the S-N approach is still applicable in situations where the initiation of cracks occupies a significant portion of the component lifetime; especially when the cycles to initiation (rather than failure) is considered.

The application of linear elastic fracture mechanics has three major advantages over the S-N technique of life prediction. Specifically and ideally, when valid laboratory data, stress analysis, and stress intensity factor solutions are available, LEFM:

(1) Accounts for initial crack-like defects and growing cracks,

(2) Allows generation of a family of S-N curves from one specimen (exclusive of natural fatigue life "scatter"); that is, nominal load or stress distribution is essentially eliminated as a test variable at considerable savings in replicate specimen and test time costs, and

(3) Allows the lives of other component or crack geometries to be predicted from the results of the one test; thus, eliminating geometry as a test variable, again at considerable savings.

In order to obtain these valuable advantages, more intensive experimental and analytical efforts must be performed for these fewer specimens that are employed as part of a LEFM analysis. For example:

(1) Fatigue crack growth rate laboratory data are still required for actual operating conditions since present theory does not account for the effects of many variables. These include temperature, time at load, environment (e.g., corrosion), material composition and microstructure, and complicated load interaction effects (e.g., overload) and significant plastic activity. These items must therefore be considered test variables just as for the S-N approach.

(2) Surface or maximum stress estimates may not be sufficient. An estimate of internal stress must often be made, at least along the crack locus, to enable a sufficiently accurate calculation of K.

(3) An "initial" or reference crack configuration must be specified.

There are other less obvious advantages of LEFM that become apparent after a few typical structural applications. Examples are:

- Often, a structural detail like a weld bead or rim slot has an extremely high or unestimable stress concentration factor (say, $K_t > 4$). The detail can often be modeled as a crack to obtain useful lower bounds on fatigue life and other performance parameters. This is especially true if the highest stresses are extremely local or if crack-like defects are numerous, as in welds.

- Probabilistic systems can be created which account for stochastic variations in key input parameters and for the occasional presence of a true fatigue crack or crack-like defect. The engineer is no longer restricted to representing occasionally-flawed structures to structures with "worst-case" cracks.

- LEFM accounts for the important physical size effect of the structural detail or notch. Crack propagation data shows that for a given initial crack size, concentrated stress and nominal stress, the larger the notch the lower the fatigue crack growth life to failure. Since LEFM accounts for the notch's stress field, which decays (with distance from the notch surface) more slowly for larger notches, it often can predict this life decrease.

- LEFM data interpretation allows a formulation of a simple cumulative damage hypothesis in which the crack growth rate for each cycle in a loading block are summed

to calculate the growth rate per block. The hypothesis can account for the experimentally observed contribution to crack growth of the smaller stress cycles in a transient which increases in relative importance as crack size increases. This damage hypothesis is both a restatement and an extension of Miner's rule [1-2] in that it accounts for the effect of a "change of state" (i.e., crack growth) upon the relative contributions of high- and low-stress cycles. As detailed in Section 3.4.3, the hypothesis appears to adequately model certain failure modes involving both low cycle (LCF) and high cycle fatigue (HCF) in the absence of significant overloads.

1.2 KEY DEFINITIONS IN LEFM

The fracture mechanics equations effectively link three parameters -- the defect size, the material/environment's intrinsic fracture toughness or subcritical crack growth rate, and the applied stress, so that if any two of these are known, the third can be quantified. The complete stress distribution for any arbitrary mode of loading and shape of body and crack can be quite difficult to determine; however, near the tip of the crack, essentially only three things can occur; the faces can be pulled apart (Mode I) or sheared perpendicular or parallel to the leading edge of the crack (Modes II or III). These three load modes are shown schematically in Figure 1-1a. The crack opening mode or Mode I is generally regarded as by far the most common of the three modes. Thus, unless otherwise indicated by context of discussion or by subscripts, Mode I cracking will always be assumed in this report. The character of the near-crack-tip stress distribution is illustrated in Figure 1-1b. The stress intensity factor, K, for each mode defines the magnitude of stress distribution and is calculated from the relation

$$K = \sigma F\sqrt{\pi a}, \quad \sigma < \sigma_y \tag{1-1}$$

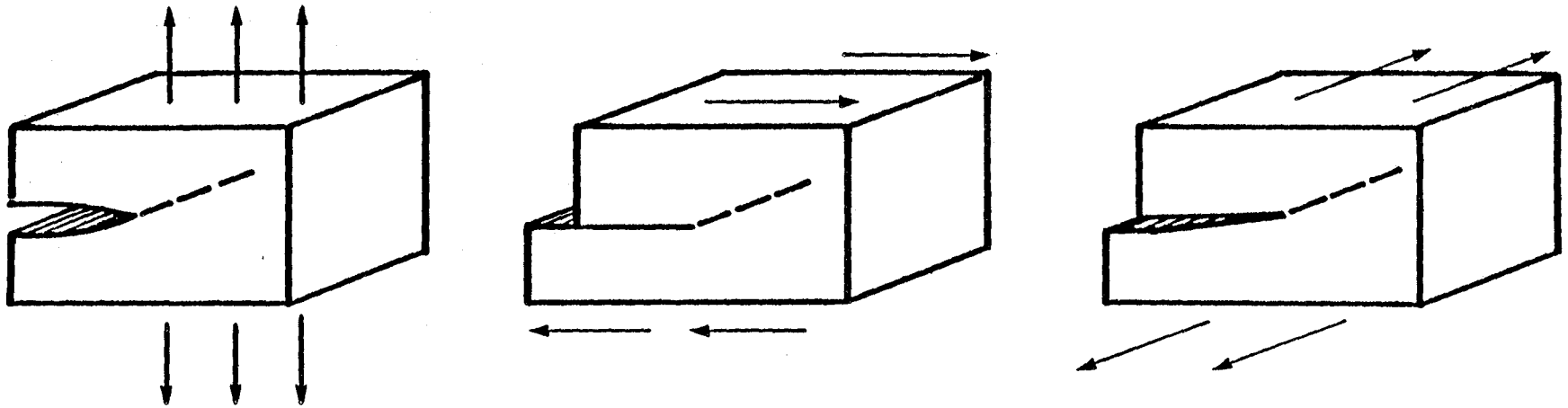

a) Crack Tip Loading Modes

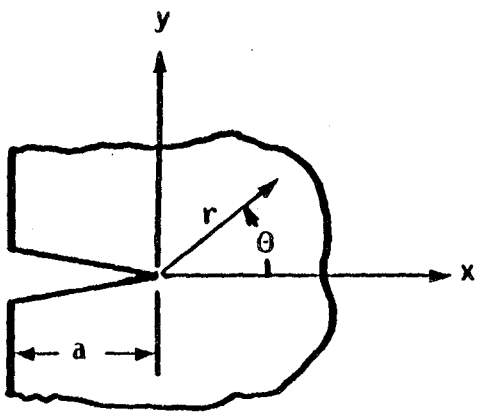

All Stress Components Have the Form:

$$\sigma_{ij} = \frac{K_k}{\sqrt{2\pi r}} f_{ij}^{(k)}(\theta)$$

Where i = x, y, z; j = x, y, z, and k=I,II,III.

No Summation is Implied and Stress Intensity Factor, K, is Roughly Proportional to

(Nominal Stress) $\sqrt{(\text{Crack Length})}$.

b) Near-Crack Tip Stress Components

Figure 1-1. Review of Linear Elastic Fracture Mechanics.

where σ is the applied stress, σ_y is the yield strength, "a" is the crack length, and F is a correction factor that depends on the flaw size, "a", and the geometry of the structure and flaw, the mode of loading, stress gradients, and the structural displacement constraints or other boundary conditions. For the case of a center-cracked infinitely wide plate under uniform tensile stress, F is unity (note that in this case "a" is the half length from the crack center line to each crack tip).

When the value of K reaches a critical value, K_c, fracture will occur in an unstable manner. Thus, if K_c were a fixed material property and F nearly constant with respect to crack size, then the critical flaw size, a_c, can be determined by rearranging Equation 1-1 to yield

$$a_c = \frac{1}{\pi}\left(\frac{K_c}{F\sigma}\right)^2 \qquad (1\text{-}2)$$

For many LEFM-based fatigue applications, Equation 1-2 should provide a sufficiently accurate estimate of critical crack size, particularly when it is noted that a final flaw size usually has very little effect on crack growth life compared to the influence of an initial flaw size.

1.3 FATIGUE CRACK GROWTH RATE REPRESENTATION

For the assessment of a fatigue failure mode, the fracture mechanics analyst assumes that the flaw of initial size, a_i, can grow to some final size, a_f or a_c, under the action of cyclic loading during the lifetime of the structure. Crack growth rate-per-load cycle (da/dn) is dependent on the stress intensity factor

$$da/dn = f(K) \tag{1-3}$$

For problems containing elements of stress corrosion or creep propagation, crack growth rate-per-time, "t", can be similarly correlated,

$$da/dt = g(K) \tag{1-4}$$

The subcritical crack growth life (n or t) can be determined by rearranging and integrating Equation 1-3 or Equation 1-4 over the appropriate range of crack size so that

$$N = \int_{a_i}^{a_c} \frac{da}{f(K)} \tag{1-5}$$

One standard way to characterize the crack growth behavior of a material is to test a center-flawed specimen with a saw-cut slot in the center to act as a crack starter. The specimen is cyclically loaded at a low stress level until a fatigue crack grows far enough out of the slot to eliminate the effect of the slot-tip dimensions and residual stresses on crack growth. Crack length is periodically measured and recorded along with the number of load cycles. From this information, a curve for crack length versus cycles is determined as shown in Figure 1-2a. The slope of this curve, da/dn, can then be computed at any crack length, "a". The stress intensity factor, K, can be calculated from the same "a" and a plot made of da/dn versus K, as shown in Figure 1-2b. In most cases ΔK (which equals $K_{max} - K_{min}$ or equivalently $(1-R)\ K_{max}$ where $R = K_{min}/K_{max}$) is used (see Figure 1-3) because it has been

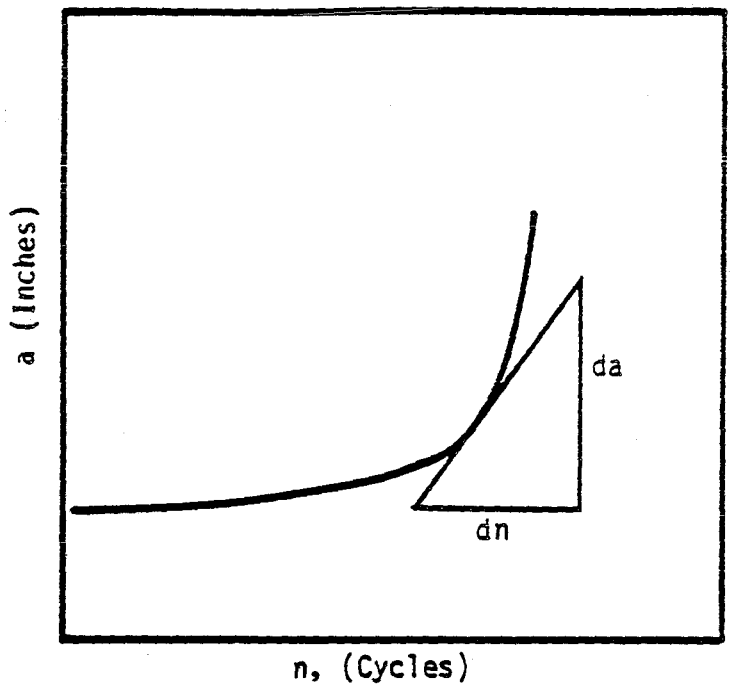

a) Crack Length versus Applied Cycles. (Should be Smoothed to Avoid False Representation of da/dn Scatter.)

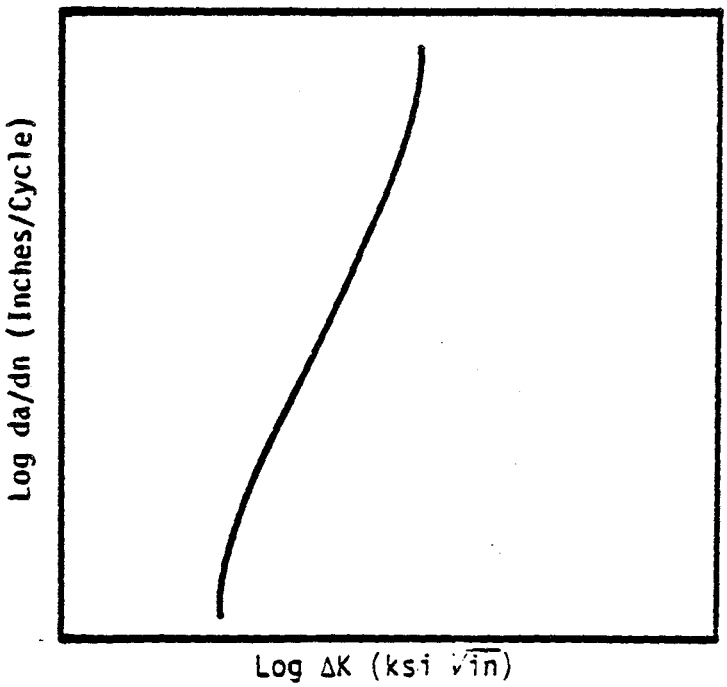

b) Crack Growth Rate Representation.

Figure 1-2. Schematic of Fatigue Crack Growth Data Representation.

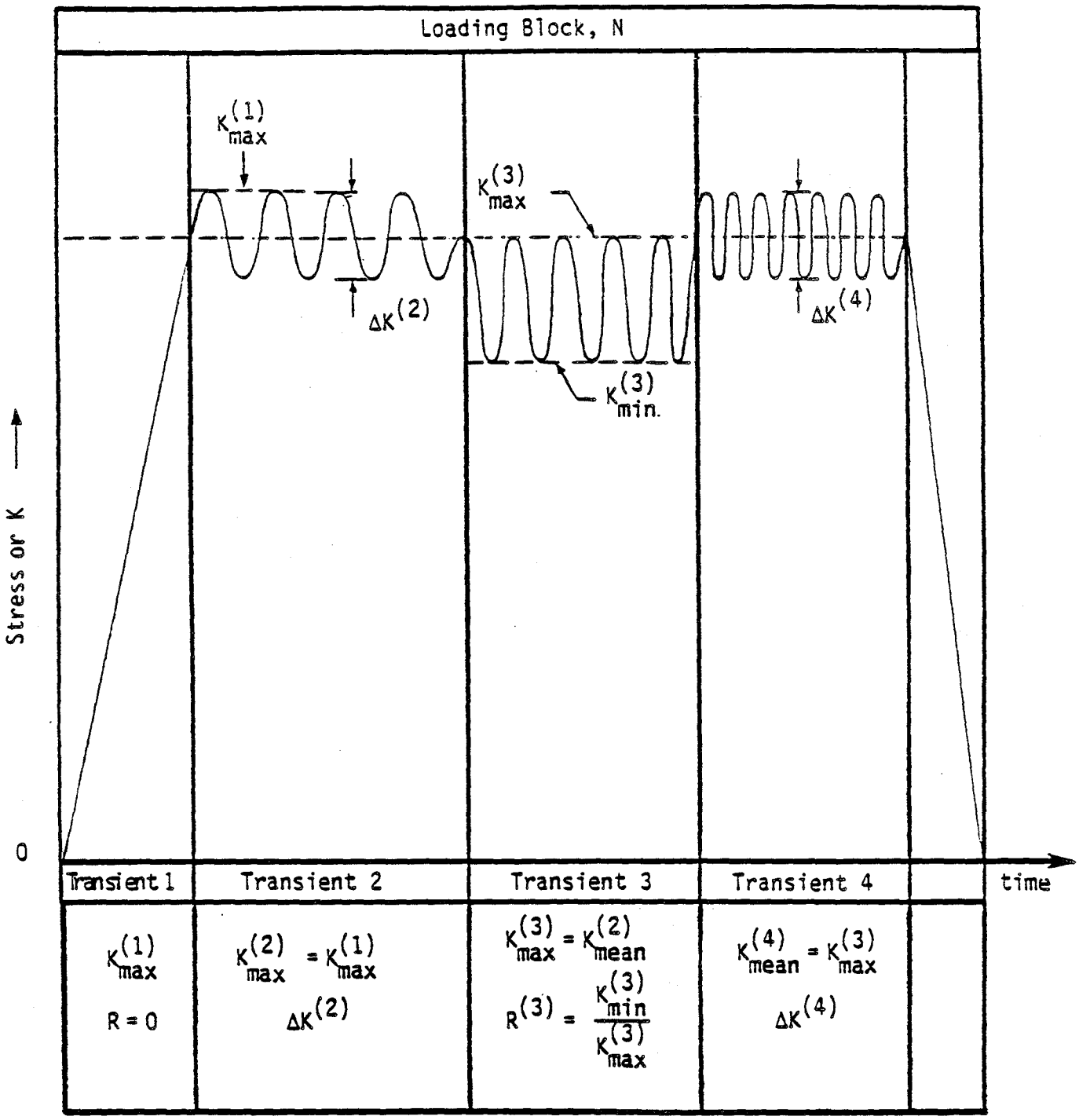

Figure 1-3. Schematic Showing Five Cyclic Stress Intensity Factor Parameters.

shown to correlate da/dn data for a wide variety of geometries. An "R-ratio" value of approximately 0.1 is commonly specified for the experiment (because testing with $K_{min} = 0$ is often difficult) although higher values such as R = 0.5, 0.9 are used for appropriate applications involving high steady stresses. A similar technique for determining crack growth under steady stress (da/dt versus K_{max}) can also be applied to correlate stress corrosion or creep cracking for specimen or structural loads.

The da/dn versus ΔK curve thus produced is independent of load magnitude and geometry and can be used for general life prediction. Empirical relations, often incorrectly called "laws", to express da/dn behavior have been proposed to fit the data represented by Figure 1-2b. The earliest and most well known relation is from Paris [1-3], and takes the form

$$da/dn = C\,\Delta K^{m} \qquad \Delta K > \Delta K_{th} \qquad *(1\text{-}6)$$

where C and m are constants determined from the relevant data. The advantages of the Paris rule is that it is simple in form (straight line on a log-log plot) and fits experimental data well in the middle range of ΔK away from threshold* effects (low ΔK region) and K_{max} effects (high ΔK region). One major disadvantage of the Paris rule is that it does not account for mean stress effects (R-variation) on fatigue crack propagation.

*The material/environment parameter ΔK_{th} is used herein to denote the fatigue threshold stress intensity factor which defines a limit on ΔK below which no fatigue crack growth is observed.

A popular expression which accounts for mean stress was developed by Forman, et al., [1-4]:

$$da/dn = \frac{C\ \Delta K^m}{K_c\ (1-R) - \Delta K} \qquad \Delta K > \Delta K_{th}(R) \qquad R \geq 0 \qquad *(1\text{-}7)$$

where C and m are material constants (not the same as those in Equation 1-6), and K_c is the fracture toughness as originally proposed by Forman or can serve as an additional parameter for data fit. The added feature of Forman's relation is to correct for positive* minimum stress and to increase the calculated fatigue crack growth rate at the onset of failure.

The equational forms described above and many others are available, along with additional options which allow the analyst to consider any da/dn (ΔK, R) relationship by, for example, expressing it as a piecewise, tabulated, univariable or multivariable function. It is important to note that since expression of a valid da/dn (ΔK, R) data is no more than a numerical curve-fitting exercise, and has little to do with physics or engineering, choice of the equational or piecewise tabular form and calculation of the constants need not follow a prescribed format as long as two conditions are met:

(1) For any given value of da/dn, the equation should agree with plotted median ΔK values to within say $\pm$ 5%. (This will contribute integrated life errors of (usually much) less than $\pm$ 20% if the second condition is also met. Greater errors may have to be tolerated in high-slope regions such as near the threshold but goodness-of-fit is the analyst's only goal). The use of a two- or three-parameter equational representation of da/dn (ΔK,

*Forman's relation severely overpredicts the crack growth rate when R is decreased below zero.

R) often leads to errors greatly in excess of ± 20% of life (e.g., Reference 1-5).

(2) The equation must not be extrapolated outside the data range without extreme caution. Experience indicates that it is surprisingly easy to inadvertantly violate this condition.

In general, the practice should be to "let the data draw the curve". When actual material data is not available, the analyst will have to rely on comparable literature data. In the absense of strong environmental effects, such reliance rarely introduces large errors since material subcritical crack growth properties are very consistant and predictable compared to material crack initiation and toughness properties. For example, compilation of crack growth rate and toughness data for high strength alloys is provided in Reference 1-6. Section 3.5 details the effect of environment upon crack growth rates.

1.4 FATIGUE CYCLE DESCRIPTION AND PARAMETRIC DEFINITION

A schematic showing the most often used fatigue cycle definitions is shown in Figure 1-3. A group of constant amplitude cycles could be defined as a transient or as a block.

For a given stress intensity factor fatigue cycle, there exist at least five, conventionally-defined, useful parameters as shown in Figure 1-3. Once any two parameters are known, the remaining three are easily determined. For purpose of discussions through the report five parameters are defined as:

- K_{max}
- K_{min}
- $\Delta K = K_{max} - K_{min}$

- $K_{mean} = (K_{max} + K_{min})/2$
- $R = K_{min}/K_{max}$

These five parameters are used frequently in conjunction with the other definitions introduced in Section 1. Where more complex fatigue cycles and concepts than introduced so far are treated, additional definitions are given.

1.5 REFERENCES

1-1. ASME Boiler and Pressure Vessel Code, Section III, 1977 Edition, Summer Addenda.

1-2. Miner, M.A., "Cumulative Damage in Fatigue," Transactions of the ASME, Vol. 67, pages A159-A164, September 1945.

1-3. Paris, P.C., Gomez, M.P., and Anderson, W.E., "A Rational Analytic Theory of Fatigue," The Trend in Engineering, Vol. 13, No. 1, January 1961.

1-4. Forman, R.G., Kearney, V.E., and Engle, R.M., "Numerical Analysis of Crack Propagation in A Cyclic Loaded Structure," Journal of Basic Engineering, pages 459-464, September 1967.

1-5. Vroman, G., Personal Communication with Besuner, P.M., December 1982. According to Mr. Vroman, significant errors are present in an important material data library of the NASA contractor-employed computer program FLAGRO. This library contains da/dn (ΔK, R) data for more than 80 material-environment combinations. The errors arise from the poor data fit acheived by the employed "Collipriest da/dn Law", a three-parameter function that is a sigmoid on log-log plots like Figure 1-2b, in the near-threshold domain of ΔK, say, for $\Delta K_{th} < \Delta K \leq 2\Delta K_{th}$.

1-6. Damage Tolerant Design Handbook, "A Compliation of Fracture and Crack Growth Data for High Strength Alloys," Metals and Ceramics Information Center, Battelle Columbus NTIS HB-01, September 1973.

Section 2

ELASTIC STRESS ANALYSIS OF CRACKS

Linear elastic fracture mechanics (LEFM) and its applications to fatigue life prediction are the major subjects of this review. LEFM is based on the application of classical linear elasticity to bodies that contain cracks. Therefore, the assumptions made in the development of linear elasticity are inherent in linear elastic fracture mechanics. These assumptions include small displacement and linearity between stresses and strains. Generally, the assumptions of homogeneity and isotropy are also made. With respect to the geometry and mechanics of mathematical models, a crack is a slit or planar surface in a body that does not transmit loads, and has a zero radius at it's tip.

This section will review the stress analysis of linear elastic bodies with cracks by use of the classical theory. Two-dimensional bodies will be discussed first, because the basic important analytical techniques and results are most easily illustrated by use of this less complex case. Three-dimensional considerations will be covered in Section 2.2.

2.1 CRACKS IN TWO-DIMENSIONAL BODIES

As introduced in Section 1, and described in detail now, three different modes of deformation are possible for material relative to a crack front. These modes are based on kinematic considerations and are independent of elasticity theory or the dimensionality of the body. Figure 2-1 shows these three modes of deformation [2-1 through 2-3] which are referred to as follows:

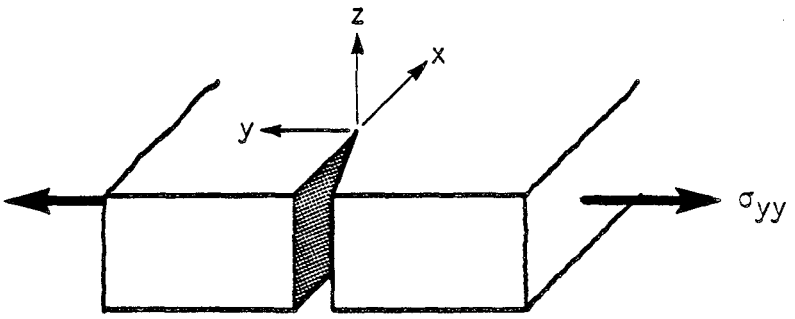

Mode I

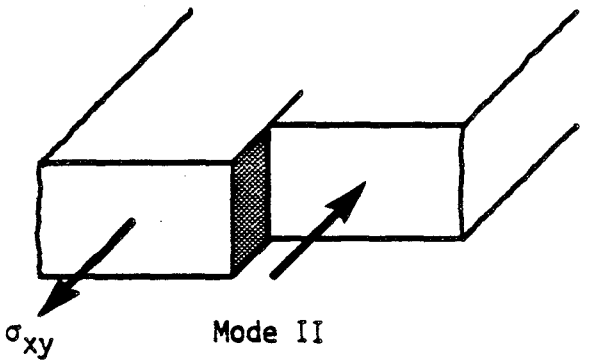

Mode II

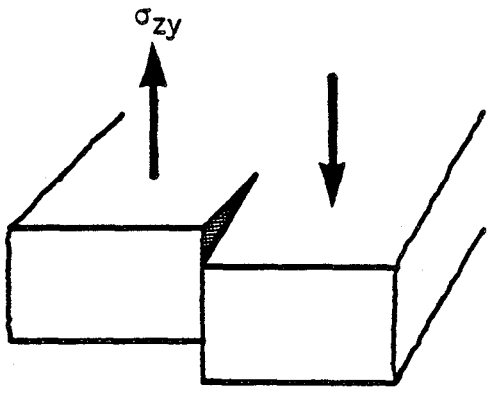

Mode III

Figure 2-1. Characteristic Crack Modes.

I	opening
II	sliding
III	tearing

A stress analysis of a cracked body subjected to loads that impose each of these modes of deformation can be performed. Under the assumption of classical elasticity (including isotropy and homogeneity) a general stress analysis can be performed that concentrates on the region near the crack tip. Using a coordinate system centered on the crack tip (as shown in Figure 2-2) and retaining the dominant terms for small "r" provides the following results:

For Mode I cracking

$$\sigma_{xx} = \frac{K_I}{\sqrt{2\pi r}} \cos\frac{\theta}{2}\left(1 - \sin\frac{\theta}{2}\sin\frac{3\theta}{2}\right)$$

(2-1)

$$\sigma_{yy} = \frac{K_I}{\sqrt{2\pi r}} \cos\frac{\theta}{2}\left(1 + \sin\frac{\theta}{2}\sin\frac{3\theta}{2}\right)$$

$$\sigma_{zz} = \begin{cases} 2\dfrac{\nu K_I}{\sqrt{2\pi r}}\cos\dfrac{\theta}{2} & \text{if crack front under plane strain} \\ 0 & \text{if crack front under plane stress} \end{cases}$$

$$\sigma_{xy} = \frac{K_I}{\sqrt{2\pi r}} \sin\frac{\theta}{2}\cos\frac{\theta}{2}\cos\frac{3\theta}{2}$$

$$\sigma_{yz} = \sigma_{xy} = 0$$

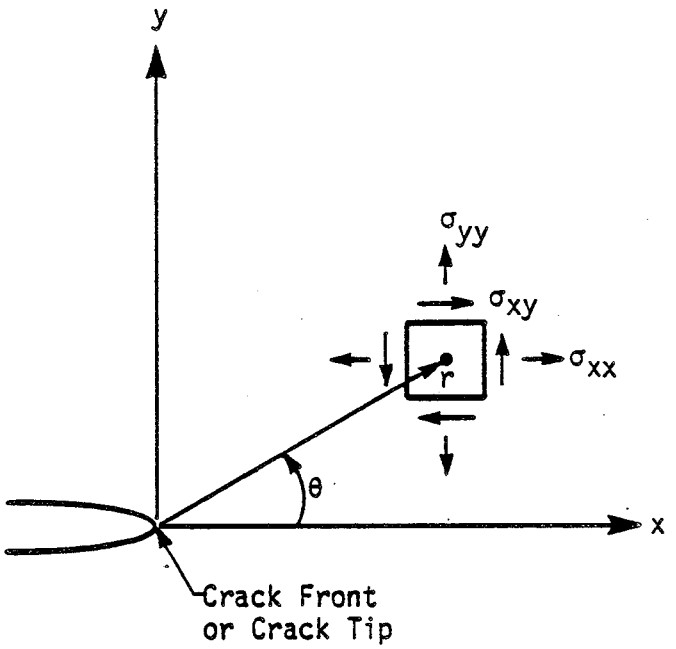

Figure 2-2. Planar Crack and Dimensions to a Point for Definition of Local Stress.

For Mode II cracking,

$$\sigma_{xx} = -\frac{K_{II}}{\sqrt{2\pi r}} \sin\frac{\theta}{2}\left(2 + \cos\frac{\theta}{2}\cos\frac{3\theta}{2}\right)$$

(2-2)

$$\sigma_{yy} = \frac{K_{II}}{\sqrt{2\pi r}} \sin\frac{\theta}{2}\cos\frac{\theta}{2}\cos\frac{3\theta}{2}$$

$$\sigma_{zz} = \begin{cases} -2\dfrac{\nu K_{II}}{\sqrt{2\pi r}}\sin\dfrac{\theta}{2} & \text{if crack front under plane strain} \\ 0 & \text{if crack front under plane stress} \end{cases}$$

$$\sigma_{xy} = \frac{K_{II}}{\sqrt{2\pi r}} \cos\frac{\theta}{2}\left(1 - \sin\frac{\theta}{2}\sin\frac{3\theta}{2}\right)$$

$$\sigma_{yz} = \sigma_{xz} = 0$$

For Mode III cracking, the stresses are

$$\sigma_{xx} = \sigma_{yy} = \sigma_{zz} = \sigma_{xy} = 0$$

$$\sigma_{yz} = \frac{K_{III}}{\sqrt{2\pi r}} \cos\frac{\theta}{2}$$

(2-3)

$$\sigma_{xz} = -\frac{K_{III}}{\sqrt{2\pi r}} \sin\frac{\theta}{2}$$

where ν is the Poisson's ratio and r and θ are defined on Figure 2-2. These equations are applicable for small "r" relative to other in-plane dimensions of the body. The above results reveal that, for a given mode of loading, the spatial distribution of the stress is always the same, and that the stresses are predicted to be very large in the vicinity of the crack tip ($r \to 0$) and infinite (singular) at the tip ($r = 0$). Real materials undergo finite, non-linear plastic, strains at the crack tip which eliminate this LEFM-predicted singularity. Nevertheless, as long as this region of plasticity is small and well contained, experiments have shown repeatedly that, for a given mode of loading, the stresses near the crack tip are controlled by a single parameter, K, which is known as the stress intensity factor. All of the geometrical parameters in the crack problem such as plate width, crack length, etc., are present in the stress intensity factor. As shown in the above equations, there is a stress intensity factor associated with each mode of crack deformation.

The realization that the spatial distribution of the stresses near the crack tip are always the same, and that they are controlled by a single parameter (for each mode) formed the basis of linear elastic fracture mechanics. The stress intensity factors can be related to strain energy release rates, so that the theory based on stress intensity factors can be tied to the earlier energy approaches to fracture such as devised by Griffith [2-4].

Since a linear theory was employed in the development of the crack tip stress fields, these stresses must be linearly related to applied loads. This, in conjunction with dimensional considerations, requires that stress

intensity factors have units of $F\text{-}L^{-3/2}$ or $(F/L^2)\text{-}L^{1/2}$. In common engineering usage, stress intensity factors are expressed in units like $ksi\text{-}in^{1/2}$ or $MPa\text{-}m^{1/2}$, etc.

Mode I (opening) stress intensity factors (K_I) are by far the most commonly encountered in engineering practice, and this particular mode will be concentrated upon in the remainder of this report. For the sake of convenience, K will be used to represent K_I unless otherwise specified.

Obviously, an important aspect of applying fracture mechanics to engineering problems is the determination of the stress intensity factors for the loading and body geometry being analyzed.

2.1.1 Two-Dimensional Crack Analyses and Models

As detailed immediately above, the stresses in the vicinity of a crack tip in a body subjected to opening mode loading (i.e., everything symmetric with respect to the crack plane) are completely characterized by the stress intensity factor K (or K_I). Additionally, as introduced in Section 1 and as will be detailed in Section 3, the behavior of an elastic body that contains a crack is also dependent on K. The stress intensity factor in turn depends upon loading, crack size and shape, and geometric boundaries. K serves as a measure of the magnitude of stress occurring in the material near the crack tip. As such, the principal uses of K are to relate stress analysis to material properties and to provide a common parameter to characterize the stress field near crack tips. One simple example of the power of such a common parameter may be derived from the wide class of problems in which, given geometrical similarity and proportioned loads, K is proportional to the

product of the applied stress, σ, and the square root of the crack's characteristic size dimension, $\sqrt{a}$. For these problems, useful rules of thumb* may be stated such as "for a single load cycle, doubling the stress is comparable to quadrupling the crack size". The problem of elastic stress analysis of cracks reduces essentially to a problem of determining the stress intensity factor.

The following discussion presents various methods of stress intensity factor determination for two-dimensional elasticity models including the use of handbooks and other literature, conventional finite element methods, finite element methods with special elements, other numerical methods, and elastic superposition methods. By the term "two-dimensional," we refer to the level of elasticity theory (i.e., plane stress, plane strain, generalized plane strain, or axisymmetric states of stress) required to determine K which, by this definition, is constant along the crack front. We do not refer to the number of dimensions or "degrees-of-freedom" (DOF) needed to specify the crack geometry. While most crack problems possess some three-dimensional and inelastic aspects, two-dimensional elastic models often provide adequate solutions or bounds, especially if one tempers accuracy requirements for K computations by considering the variability and errors of such input as loads and material properties.

---

*Several investigators have extrapolated these rules incorrectly for fatigue, or other subcritical crack growth calculations, by expressing fatigue life as a function of only the initial (K_i) and final (K_f) values of K (or of ΔK, the alternating stress intensity factor). This expression fails to account for the rate at which K changes as the crack grows (dK/da). This rate is much faster for a high-stress, small-crack problem than for a low-stress, large-crack problem. The proper procedure for life computation is always to integrate the differential equation involving da/dn (K), as discussed in Section 1.

In addition, the effect of crack face pressure and surface effects on stress intensity factors will be discussed. While these topics are not limited strictly to two-dimensional problems, they are elementary compared to topics explored in following sections and they lend themselves to explanation in the context of two-dimensional models.

The choice of method for the determination of the stress intensity factor is an engineering decision that depends on several criteria. Familiarity, cost, time available, required accuracy and the type of application are a few of the important aspects involved in the decision. For example, in looking at the required accuracy criteria, it may be determined that readily available solutions (i.e., handbook solutions) may provide adequate bounds on the stress intensity factor such that the actual values may never need to be solved for accurately. Finally, it may be that several methods of computing a stress intensity factor will need to be performed and cross-checked to ensure accuracy of the final model and solution.

Comprehensive reviews of the different methods of stress intensity factor determination are found in References 2-1 thru 2-8.

2.1.2 Handbooks

Stress intensity factor solutions for a wide variety of two-dimensional configurations have been compiled, tabulated and graphed in several reference books or handbooks [2-1, 2-3, 2-5 through 2-8]. For simple geometries or complex problems that may be approximated or bounded by simple models, readily available solutions may be obtained from these references. These solutions have been determined by various analytical mathematical or semi-numerical

theory-of-elasticity techniques including boundary collocation, Westergaard's solutions, conformal mapping, Mushkelishvili's method, asymptotic approximation, and others. While it cannot be claimed that all useful solutions from the mathematical theory-of-elasticity have already been derived, it is probable that most have been and that the development of useful mathematical solutions has necessarily slowed. The difficulty in applying the mathematical elasticity techniques to complex geometries and loading states, and the existence of many competing numerical tools, further reduces the current value of the mathematical techniques for day-to-day engineering applications to new problems.

Reference 2-5 lists various determined solutions for each problem with reference lists for details on the analyses. Reference 2-3 also lists various solutions and in addition states which (few) solutions are exact and, for the others, provides the solution authors' estimation of accuracy.

Handbooks can often be used to obtain bounds on complicated problems, thereby eliminating the need for more costly and difficult solution methods. Also, various handbook solutions to the same problem can be checked against each other for consistency. Similar answers obtained from various approximate solutions may often eliminate the need for more advanced solution methods.

While clever use of handbook solutions and bounds can be used to model the geometrical aspects of most two-dimensional problems, handling high stress gradients is usually more difficult. This is because the great majority of handbook and published solutions are for loads which produce uniform or bending (linear spatial gradient) stress fields remote from the crack. The methods discussed in the following paragraphs are used to account for stress

gradients and other complications outside the scope of most literature solutions.

2.1.3 Conventional Finite Element Methods

Although handbooks provide the most direct approach to solving two-dimensional fracture mechanics problems, situations arise in which the problem is too complicated to be modeled such that the stress intensity factor can be determined from a known solution. In addition, in many cases exact solutions to the actual problem are too costly, time consuming and difficult, if not impossible, to obtain. Conventional finite element methods provide a numerical method of stress intensity factor determination which allows complex structures with general shape, boundary and loading conditions to be readily handled. By "conventional" we refer to models which use the same element types throughout and have no means of handling high crack tip stress/strain gradients beyond mesh refinement. The use of special elements is discussed later.

Using conventional finite element computer programs, there are three major methods of determining the crack tip stress intensity. These include, in the order of increasing accuracy, the stress method, the displacement method, and the strain energy release rate method. These three methods are discussed and compared in References 2-9 through 2-12.

The stress method of determining stress intensity factors correlates nodal stresses determined from the finite element analysis with the well-known crack tip stress equations (i.e., Equation 2-1). Due to the inability of the conventional finite elements to represent the crack tip singularity (i.e., the

$r^{-1/2}$ term in Equation 2-1), poor estimates result in the area very near the crack tip. In addition, stress results relatively far away from the crack tip are of little use in estimating K as the stress equations are only accurate in the limit of $r \to 0$ (typically, for $r < a/10$). The singularity problem is lessened by the use of a very fine finite element mesh around the crack tip. In addition, Chan, et al. [2-13] suggest a method in which an estimate of K, $\hat{K}(r) \propto \sigma(r)\, r^{1/2}$, is plotted as a function of the distance, r. As r increases, the $\hat{K}(r)$ versus r curve rapidly approaches a constant, shallow slope. By extrapolation back to the vertical, $\hat{K}(r)$ axis where $r = 0$, a good estimate of the crack tip stress intensity factor often may be obtained. For very fine meshes, Chan reports an accuracy within 5%* using the extrapolation process.

The displacement method is very similar to the stress method. In this method, nodal point displacements are correlated with the well-known displacement equations [of a form $u(r,\theta) \propto \hat{K}\sqrt{r}\, f(\theta)$]. The inability of the conventional finite element to represent the (stress) singularity at $r = 0$ is again present in this method. Thus, as presented in the stress method, extrapolation of the stress intensity estimation $\hat{K}(r)$ versus r curve is suggested. Again, the accuracy of the results depend on the size of the finite element mesh. Oglesby and Lomacky [2-14] report a K-computation accuracy of 5% for fine meshes (element size of $A/a^2 = 1.2 \times 10^{-6}$ where A = element area and a = crack length) compared to an accuracy of within 9% for relatively coarser meshes ($A/a^2 = 312 \times 10^{-6}$).

*Most accuracy values reported herein are for uniform tension or bending problems with no extraordinary aspects like ultra high thermal stress gradients. Errors can increase significantly as a result of such aspects.

Both the stress and displacement methods suffer some significant weaknesses. Although the displacement method generally produces better results than the stress method, the accuracies of both depend heavily upon finite element mesh refinement. In both methods, an excessively large number of degrees-of-freedom is often required in determining the stress intensity factor. This is directly related, of course, to time and money involved preparing and executing these solution methods. Another major disadvantage, reported in References 2-15 and 2-16, is that the determination of stress intensity from these methods often lacks consistency among investigators using the same finite element procedures and even the same finite element runs.

The strain energy release rate method is based upon the relationship between the strain energy release rate $G = dU/da$ and stress intensity factor, of the form $K^2 = HG$ ($H = E$ for plane stress and $H = E/(1-\nu^2)$ for plane strain, where E is the modulus of elasticity and ν is Poisson's ratio) for plane strain.

G can be determined numerically in at least three ways [2-17]. In one way, the strain energy U(a) is computed for several finite element runs, each with a different value of a. Using any regression method, such as least-square error minimization, U(a) can be expressed in equational form and fit to the numerical data as a smooth function. The G(a) is computed by evaluating, analytically or numerically, the derivative of the U(a) regression equation.

The second method consists of computing the change in strain energy U for two computer models with slightly different crack lengths ($\Delta U/\Delta a$). This "perturbation" method is described in greater detail in References 2-15 and 2-16. This method has several advantages over the stress and displacement

methods. First, because the strain energy release rate, which is directly related to the stress intensity factor, is determined solely from the difference of two finite element runs which differ only by a slight, say 0.1%, increase in crack depth, the results are not as dependent on localized finite element results of crack tip stress/strain or displacements. Specifically, if strain energy errors are the same for each run, ΔU may be relatively error free. (Care must be taken, though, that the basic element mesh and nodal point coordinates remain the same from one run to the next. The stress intensity factor result depends on the difference of the two similar finite element runs in which only the crack depth changes. A change in mesh refinement could produce a change in stress and strain numerical results that are not due to change in crack depth. Reference 2-18 provides guidelines for perturbing the crack.) Another advantage of this method is that accurate results may be obtained for relatively coarse meshes, this being directly linked to time and cost of the stress intensity factor analysis. The third may to compute G is to calculate the J-integral parameter [2-19], normally used for elastic-plastic analysis of cracks and to take advantage of the fact that J and G are identical for the linear elastic case. As detailed in discussions of elastic plastic-fracture mechanics (Section 4), J can be calculated for numerical results some distance from the crack tip. This tends to reduce error.

The accuracy of these three G-based methods has been reported, typically, to be better than 2% (e.g., Reference 2-15). Often the error associated with using the displacement method is halved by using G. It has been speculated that using G tends to cancel numerical errors, since G involves the product of stress and strain and the numerical estimates of stress are often too low

while corresponding strain estimates are too high. Another feature is that the need to plot the $\hat{K}$ versus r curves is eliminated as K is calculated directly from energy values obtained from the finite element results. Finally, Watwood [2-15] suggests that the strain energy release rate produces bounds on the actual stress intensity factor. He suggests that if K is increasing with crack depth, the method leads to a lower bound while if K is decreasing with crack depth, an upper bound is determined.

The major disadvantage in this method is the inability to separate the stress intensity factors for Modes I and II (K_I and K_{II}) from the calculated results. Watwood suggests this problem may be alleviated by constraining the appropriate nodes to obtain the stress intensity factors for the separate modes. Another disadvantage which has been pointed out in Reference 2-11 is that uncertainty regarding the accuracy of the solution results when arbitrary crack surface tractions applied close to the crack tip must be considered.

In general, though, the advantage in accuracy and reduced mesh refinement requirements makes the strain energy release rate method the preferable alternative in the conventional finite element stress intensity determination methods.

2.1.4 Finite Elements with Special Crack Tip Elements

To alleviate the singularity problem with conventional finite element methods, several special crack tip finite elements have been developed which directly model the singularity at the crack tip. These include those elements developed by Byskov [2-20], Tracey [2-21], Wilson [2-22], and Hilton and Hutchinson [2-23]. Atluri [2-24] provides a recent review of this field.

Methods and examples for use of these elements are discussed and compared in References 2-9, 2-11 and 2-16. Use of these special elements generally requires modification of finite element routines, but excellent accuracy is obtained using fewer elements than stress intensity factor evaluations made with conventional finite elements.

The special element developed by Tracey is an isoceles trapezoidal-shaped isoparametric element focused into the crack tip. It was shown to yield very accurate values of the stress intensity factor from relatively coarse meshes. The edge cracked rectangle was modeled and compared to the problem solved by Chan, et al. [2-13] with 2000 degrees-of-freedom and yielded results within 5% accuracy of a known solution.

Wilson developed a circular-shaped element with the crack tip located at the center of the element with the crack extending radially away from the center to the outer edge. This element embeds the asymptotic expansion into the finite element mesh at the crack tip. Byskov developed a similar element except that it was triangular in shape. The crack tip was again located in the center of the element with the crack extending to a corner. Westmann [2-25] has developed a library of "singularity elements", including a crack tip element, that can be embedded in a mesh of ordinary elements using what he terms a "global-local" formulation.

These special elements, used in conjunction with standard finite element routines, provide stress intensity factors with excellent accuracy and good convergence with relatively coarse meshes. Depending on the problem configuration, loading, degrees-of-freedom and type of special element adjoining the

general elements that model the continuum away from the crack tip, accuracy often is proven to be within 5% of known solutions.

Additional discussions on particular computer codes that are available for evaluating stress intensity factors by finite element techniques are provided in Section 2.3. The three K-computation procedures described above, stress, displacement, and strain energy release rate, can be used with the special elements or with any numerical and many experimental methods, including those described below.

2.1.5 Other Numerical Methods

Many other numerical methods exist for determining the stress intensity factor. Three of the most widely applied methods are the boundary integral equation method, boundary collocation, and the finite difference method.

In the boundary integral equation (BIE) method, the governing partial differential equations are replaced with integral identities. Use of the integral identities reduces the dimensionality of the problem by one. In other words, to solve problems in plane or axisymmetric elasticity theory, only the boundary need be discretized, modeled, and expressed in terms of line (i.e., one-dimensional) integrals. Similarly, the three-dimensional continuum need be modeled numerically only on its surface (for multiply-connected continua, the inner surface of, for example, holes must also be discretized), thus reducing the number of dimensions to two. Also, the equations of the BIE methods are precise representations of the continuum mechanics theory being modeled. The typical finite element errors associated with matching some of the field equations but not the others at internal points in the numerical

mesh model are not suffered in the BIE method. For ideal circumstances, such as those reported in References 2-26 and 2-27 tremendous savings are available in both central processing unit time on the computer and, thanks to the fact that the user need model only the boundary, the engineering time to prepare the idealization. Typically, where the BIE method is well developed, as in the two-dimensional and three-dimensional elasticity problems of References 2-26 and 2-27 and the more general continuum mechanics theories described in References 2-28 and 2-29, some significant accuracy improvement is noted versus standard finite element programs.

Simultaneous integral constraint equations are obtained which relate displacements to boundary conditions and are then solved numerically. Review of both the BIE method and its applications are given in References 2-26 through 2-29, and, of special note for its depth and scope, in Reference 2-29 by Bannerjee and Shaw. Although advanced mathematical and numerical analyses are involved for formulating and solving singular integral equations, and the scope of this method is somewhat limited by its complexity and its relatively recent introduction, the BIE method usually results in reduced problem size with increased accuracy compared to the finite element method.

Boundary collocation of stress functions provides another numerical means of evaluating stress intensity factors for planar bodies. This technique makes use of a stress function that automatically satisfies the stress-free boundary conditions on the crack surfaces and includes the stress singularity at the crack tip. The stress function includes unknown functions that can be adjusted to satisfy boundary conditions away from the crack such as loaded and free surfaces. These adjustable functions are expanded in an infinite series

with unknown coefficients, and then truncated. The now finite number of unknown coefficients are evaluated by solving the set of simultaneous linear algebraic equations that result from satisfying the boundary conditions at a finite number of points. The coefficients are usually evaluated so as to minimize the least squares error in satisfaction of the boundary conditions at a number of boundary points that is larger than the number of unknown coefficients. Conformal mapping may also be applied to advantage in treatment of complex geometries. The value of the stress intensity factor follows directly from values of the coefficients of the series representation of the stress function. This technique was one of the earliest schemes used for evaluation of stress intensity factors for planar elastic bodies of finite in-plane dimensions [2-30, 2-31]. The need for solution of a large number of simultaneous equations precluded the use of this approach prior to the availability of electronic computers. Most of the standard stress intensity factor and crack surface displacement equations used in current testing were obtained by boundary collocation. For two-dimensional problems, no other method has matched the accuracy that is obtained by this method, which has been subject to improvement [2-32] and is in current use. However, the increased availability, familiarity and generality of alternative approaches, such as finite elements, has led to a relative decrease of the use of boundary collocation approaches.

In the finite difference method, the governing partial differential equations (for any theoretical level of boundary value problems ranging from two-dimensional elasticity through three-dimensional viscoplasticity) are solved by approximating the equations with ordinary differential equations and algebraic expressions. The approximations are then solved by discretizing the

continuum with a finite number of mesh points, nodes, or grid points [2-33]. As with the finite element method, a large number of simultaneous equations again results and these are solved numerically.

Of particular interest to this area and to the entire survey of methods and analytical fracture mechanics, is the development of a series of computer codes which use the explicit (time-dependent) finite difference method to solve general problems in continuum mechanics. The two families of computer codes, STEALTH and HEMP were both developed and based entirely on the published technology of the Lawrence Livermore National Laboratory (LLNL), Livermore, California, and Sandia Laboratory, Albuquerque, New Mexico. It is our understanding that the person most responsible for the developments is Dr. Mark Wilkins of LLNL with a considerable amount of work also done by Walt Herrmann of Sandia and Ronald Hofmann of Science Applications, Inc. While a thorough survey of these particular codes has not been made, the most useful references noted to date are those of Hofmann [2-33] and Wilkins [2-34]. We recommend that these powerful (partially) publically available codes be considered for those analytical models of a complexity beyond the capabilities of other analytical computer programs and methods. The codes, while relatively expensive to run, may be the "ultimate" in analysis scope and depth for most categories of continuum mechanics problems.

2.1.6 Elastic Superposition Methods

Linear elastic fracture mechanics is based on the linear theory of elasticity -- as the name implies. Therefore, linear-superposition is applicable to LEFM crack problems. This often allows stress intensity factors for

some complex loading conditions to be devised from the superposition of simpler results, such as may be obtainable from handbooks. Additionally, there are two techniques for evaluation of stress intensity factors that make explicit use of linear superposition. These are the alternating method and the weight function method (also known as the influence function or Green's function method).

A weight function is merely the stress intensity factor due to equal and opposite unit concentrated loads at a given position on the two crack surfaces. The weight function method makes use of the simple elastic superposition illustrated in Figure 2-3. The original problem is broken down into two simpler portions. First, the complete boundary value problem without the crack is analyzed, and stresses, $\sigma(x)$, are determined at the future crack site (or locus). In the second portion of the problem the crack is "created" by removing all loads by means of the introduction of equal and opposite crack-face stresses or pressures ($-\sigma(x)$) of those determined for the uncracked state, so as to create a traction-free crack face. Since the uncracked body has no stress intensity factor, the original problem thus reduces to determining the stress intensity factor for the "pressurized crack"; that is, for the cracked surface with the stresses or pressures determined from the uncracked body applied to the crack face. Figure 2-3b shows how these pressures are discretized along the crack face, multiplied by weight functions. References 2-1, 2-6 and 2-7 contain good descriptions of this procedure with solved problems using these methods referenced. In addition, the BIGIF computer code [2-17] is based on these methods. As discussed by various authors [2-35 through 2-38], the weight function for a cracked configuration can be obtained from information on the stress intensity factor and corresponding crack

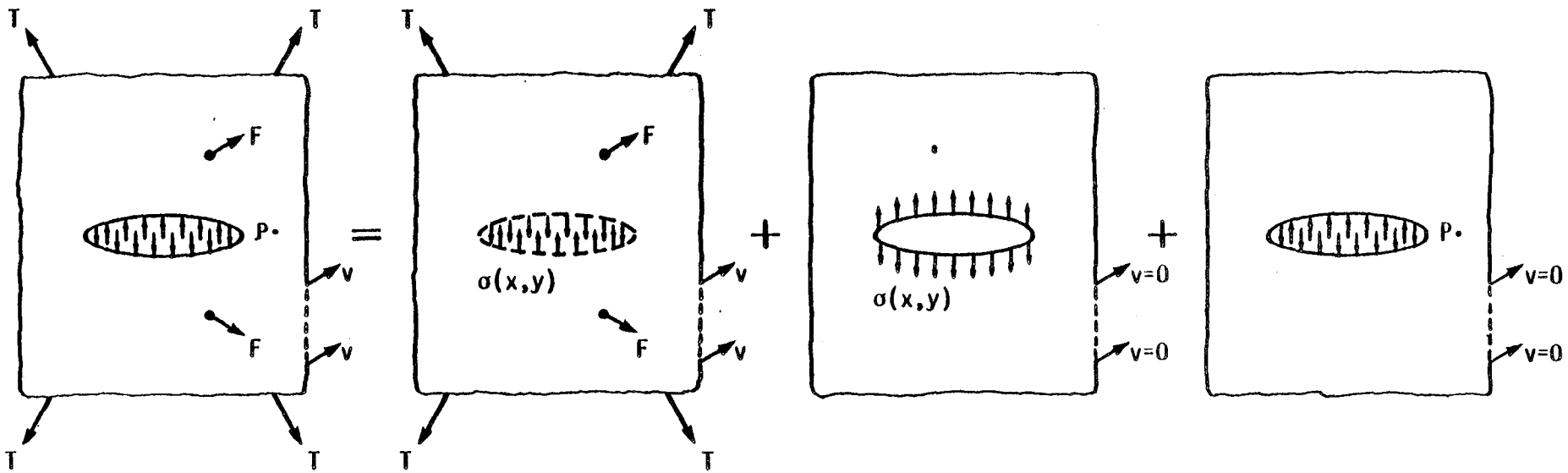

a. Body with Applied Tractions (T), Body Force (F) Displacements (v), and Internal Pressure Applied to Crack Face.

b. Uncracked Body with Applied Tractions and Displacements. Determined Stress $\sigma(x,y)$ at Location of Future Crack.

c. No Tractions or Body Forces; Zero-Prescribed Displacements. Equal and Opposite Stress $\sigma(x,y)$ Shown at Crack Location.

d. Internal Pressure (P•) Applied to Crack Face.

Figure 2-3. Representation of the Use of Superposition to Generate Stress Intensity Factors for Complex Loading From Combinations of Simpler Loadings.

surface opening displacements for an arbitrary (non-zero) loading. Hence, as mentioned by Rice [2-35], inclusion of crack surface displacements in conjunction with stress intensity factors for a particular loading, allows the results to be greatly generalized to include arbitrary loads on the crack surfaces. Such an approach can be extended to general three-dimensional problems [2-35, 2-38], but only RMS-weighted averages of the stress intensity factor are obtained, rather than details of the variation of K along the crack front. This approach is used in BIGIF for its treatment of elliptical cracks [2-17].

The weight function method handles general stress gradients and, properly applied, suffers minimal increase in error with increasing complexity of the problem. Typically it is the least expensive technique available for handling complex fracture mechanics problems and is enthusiastically recommended for day-to-day engineering fracture mechanics applications. The authors know of several cases in which more than $100,000 savings has been credited directly to the substitution of the weight function method for the finite element method and a recent application has been documented* in which nearly a million dollars were saved.

The alternating method, sometimes known as the Schwarz alternating technique, also uses the principle of superposition. The method involves using several component solutions, each of which satisfies a portion of the total boundary conditions. Through a successive iterative procedure a solution is obtained such that the boundary conditions are satisfied everywhere. A

*"The BIGIF Computer Program," EPRI Technology Application Brochure No. 3106B (RP700-5), Electric Power Research Institute and Pennsylvania Electric Company, March 1983.

thorough review of this method is presented by Hartranft and Sih [2-39]. This method has also been used by Smith [2-40 through 2-42] and, especially, by Shah and Kobayashi [2-43, 2-44] as will be discussed in the three-dimensional crack analyses discussion (Section 2.2). The alternating method has some of the same features of the weight function method. At their current stages of development, the alternating method provides a more complete solution to some three-dimensional problems than the weight function method, but does not handle as wide a class of loadings and does not have nearly as much publically available, user-oriented software as does the weight function method.

2.1.7 Experimental Techniques

The analytical techniques discussed above have generally been much more widely used than experimentally based procedures. However, for cracks in complicated structures or simple geometries in which it would be difficult to analytically model the boundary conditions, experimental techniques may be used to advantage. These may involve direct measurement on a model, such as by the use of photoelasticity or strain gages, or observations of crack surface opening displacements near the crack tip. Additionally, the stress intensity factor may be determined by experimental load-deflection measurements using the relationship between compliance, strain energy release rates and stress intensity factors [2-1, 2-3, 2-7].

2.1.8 Surface Effects

The stress intensity factor can be greatly affected by the proximity and shape of connected or nearby surfaces which modify the boundary conditions. Because most potentially troublesome design details where cracks start involve

surface-connected geometric stress raisers, the understanding and ability to quantify these effects are extremely important.

A simple example of the stress intensity factor dependency on surface conditions is shown in the cases of an edge crack and a center crack in finite width plates subjected to a uniaxial tensile stress, σ. (This case is of practical significance as it is often found in structural members.)

Two curves are plotted in Figure 2-4. The curve shown is a graph of the ratio of stress intensity to a normalization parameter (K_I/K_0) versus a ratio of crack length to sheet width (a/W) for a center crack of length 2a. (The normalizing parameter $K_0 = \sigma\sqrt{\pi a}$, is the stress intensity factor in the infinite media, and would be equal to K_I in the absence of any surface or boundary effect.) By symmetry, the center crack problem may be modeled by cutting the sheet in half and replacing the removed half sheet with "rollers" which eliminate normal displacement and shear traction.

An edge crack is modeled in the same manner except the rollers are removed which allows bending to take place. If the plate is wide the bending is localized near the cracked surface but if the plate is narrow, bending is largely global. The top curve in Figure 2-4 is a plot of K_I/K_0 versus (a/W) for the edge crack.

For a semi-infinite sheet, where the ratio of $a/W \to 0$, the stress intensity factor is increased by only 12% (i.e., $K = 1.12\ \sigma\sqrt{\pi a}$) which may be thought of as the effect of local surface "bending" due to "roller removal". As the ratio a/W is increased, though, a very large increase in the edge crack stress intensity factor results. This large increase is due to the more

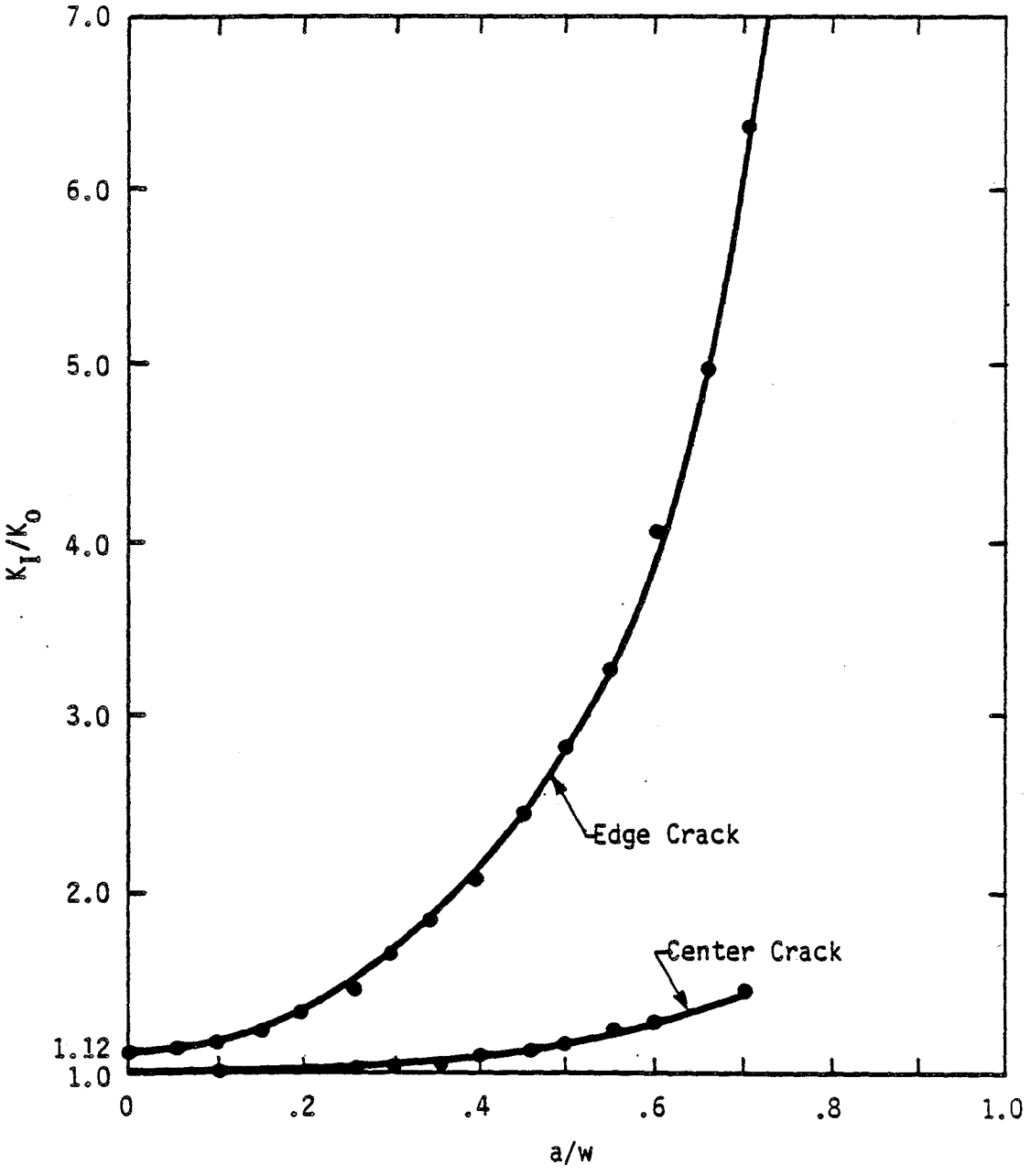

Figure 2-4. Comparison of Two Stress Intensity Factor Solutions which Illustrate the Rapidly Increasing Effect of a Free Surface as Crack Size is Increased.

global bending caused by the eccentric load path of the remote tensile stress. Thus, the stress intensity factor is shown to be only mildly dependent on connected surfaces for small cracks ($a/W \to 0$) but is very dependent on the presence of connected boundaries or surfaces for larger cracks ($a/W \to 1$).

Stress intensity factors which have been modified due to surface effects are most commonly determined by the finite element method and elastic superposition method (i.e., weight function and alternating method). Several simple and useful appropriate methods, though, which often may be used for obtaining a first estimate for the effect of stress concentrations on the crack are given in Reference 2-6. Experimental methods may also be used when surface effects complicate the determination of the stress intensity factor to such a degree that numerical determination is questionable or impossible.

As dicussed in Section 2.3, surface effects in three-dimensional problems are often both more complicated and (fortunately) smaller than surface effects in two-dimensional problems (which may therefore serve as bounds).

Another class of problems, not considered in detail herein, are near-surface cracks which have the additional complication of a sequential failure mode consisting of brittle or ductile failure of the surface-connected ligament followed by brittle fracture of the dynamically formed edge crack. Because this ligament tearing may not be quasi-static a bounding model which accounts for maximum dynamic effects, as shown schematically in Figure 2-5, may have to be employed to envelop the deterious effects of these insidious, difficult to inspect cracks.

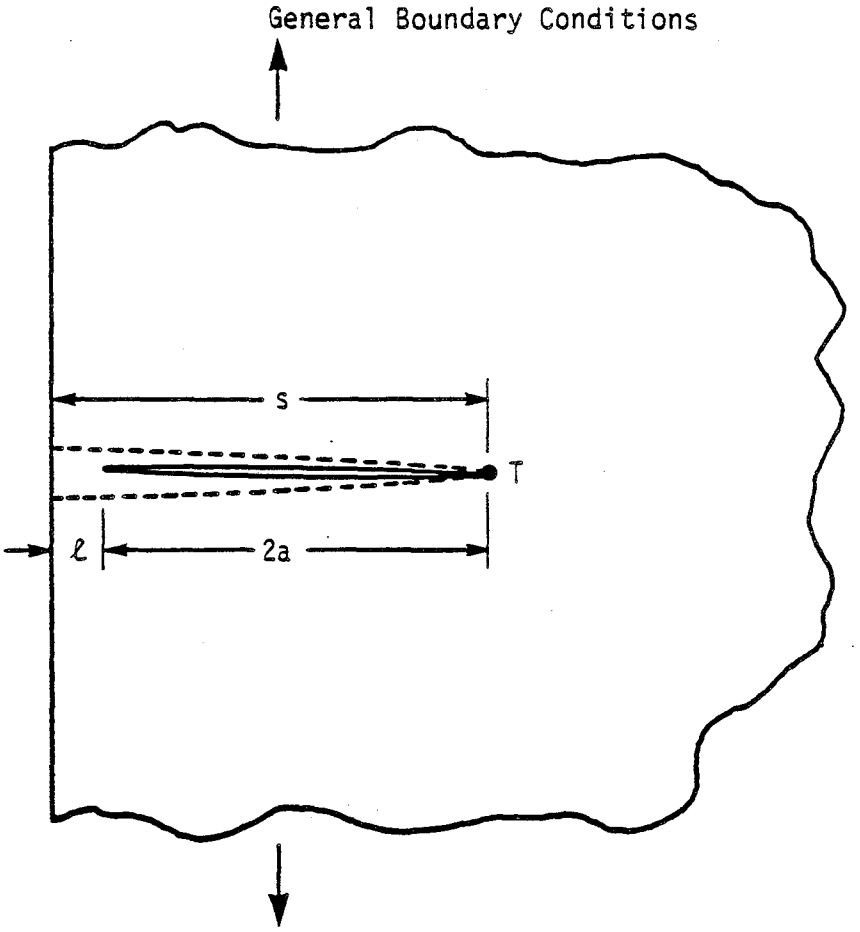

PROCEDURE	RESULT FOR UNIFORM REMOTE STRESS σ_o
Compute quasi-static K_T for near-surface Crack, 2a.	$K_{T2a} \simeq \sigma_o\sqrt{\pi a}$
Compute quasi-static K_T for hypothetical surface crack, $s = 2a+\ell$.	$K_{Ts} = 1.12\sigma_o\sqrt{\pi s}$
Superimpose K_{T2a} and K_{Ts} to account for dynamic factor ≤ 2.	$K_T = K_{T2a} + 2\left[K_{Ts} - K_{T2a}\right]$
Compare K_T with dynamic, rather than static, fracture toughness K_{Id}	$K_T = 2.24\sigma_o\sqrt{\pi s} - \sigma_o\sqrt{\pi a}$

Figure 2-5. Procedure to Account for the Effect of Dynamic Failure of Ligament ℓ on the Upper Bound of the Stress Intensity Factor K_T at Crack Tip, T. Similar Procedures are Available for Bounding Other Elastic Parameters near T.

2.1.9 Effects of Pressure in Cracks

In pressure vessels and piping, the crack tip stress intensity factor may be increased due to pressure on the crack face surface. It is a commonly known fact that pressure on a crack surface develops the same K as if it were a tensile stress applied to the gross section. At NASA's request, some amplification of this fact is provided and the need to include the pressure term in the stress intensity factor determination is shown in the "proof" below.

An interesting case history, with proprietary details, which emphasizes the importance of the effects of pressure on the stress intensity, and consequently, on fatigue crack growth rates occurred in the testing of gun barrels. Because a very high ratio of internal pressure to hoop stress is present in these thick-walled pressure vessels, it is important that crack face pressure is accounted for in the fracture mechanics calculation or testing. In the case of the gun barrels, several field failures occurred after fracture mechanics-based testing determined the fatigue crack growth life to be much greater than that eventually experienced in the field. The overestimation was traced back to the fluid used in the fatigue life testing. The high frequency pressure cycling in the testing had been performed using a hydraulic fluid. Apparently, due to the oil's viscosity, the full effect of the in-service gas pressure could not be reproduced on the crack face during testing. Consequently, the test lives were much longer than those later experienced in catastrophic failures during actual field firings. Analytical studies of this pressure effect predicted differences sufficient to explain the significant reduction in life of test gun barrels between the hydraulic testing and the field firing.

The effective crack face stresses due to both a crack face pressure, p_o, and a crack-locus stress, is $\sigma(x,y) + p_o$. This is generally known and easily proven. However, for some unknown reason, some investigators still dispute the approach. Due to this controversy, we offer the development below.

Figure 2-3a shows a cracked body with applied displacements and tractions acting on the body and pressure, p_o, acting on the crack face. Using the superposition principle discussed previously, the problem can first be analyzed by looking at the body without the crack but with all applied tractions and displacements still acting on the body. The stress in the uncracked body at the future location of the crack is determined using standard analytical, numerical or experimental means. This stress, $\sigma(x,y)$ is represented in Figure 2-3b. Next, as shown in Figure 2-3c, a crack is introduced to the same body with all applied tractions and displacements acting on the body reduced to zero. To obtain a stress-free surface normal to the crack face, a stress or pressure equal and opposite to the normal stress in the uncracked body $\sigma(x,y)$ must act on the crack.

Using the weight function method, the stress intensity factor due to the precracked stress distribution, $\sigma(x)$ can be represented as

$$K = \int_0^a \sigma(x)\, h(a,x)\, dx \qquad (2\text{-}4)$$

where the function, $h(a,x)$, is dependent on the geometry and the integral is summed over the length of the crack, "a".

As shown in Figure 2-1d, the crack face is also subjected to the pressure, p_o. (This pressure, although considered in this example as a constant,

may actually vary over the crack face.) The stress intensity factor due to this pressure is treated in the same manner as above for the precracked stress distribution.

$$K = \int_0^a p_0 \, h(a,x) \, dx \qquad (2\text{-}5)$$

where the function, $h(a,x)$, is the identical function used in Equation 2-4.

By superposition, the combined effect due to the applied traction and displacements and crack face pressure is simply the sum of the two individual stress intensity factors

$$K = \int_0^a \sigma(x) \, h(a,x) \, dx + \int_0^a p_0 \, h(a,x) \, dx$$

or

$$K = \int_0^a [\sigma(x) + p_0] \, h(a,x) \, dx$$

Thus the effective crack face stress can be modeled directly as $\sigma(x) + p_0$.

2.2 CRACKS IN THREE-DIMENSIONAL BODIES

The two-dimensional idealizations of cracked bodies discussed in Section 2.1 are widely applicable and can be used in a wide variety of engineering problems. However, there are situations in which the three-dimensional nature of a problem can not be "idealized or bounded away". A simple example of this is the planar crack of elliptical shape embedded in a body for which an accurate solution is required. This particular problem was solved by analytical means for uniform pressure on the crack face [2-45] and still constitutes one

of the basic crack stress intensity factor solutions for three-dimensional bodies.

Three-dimensional elasticity theory applied to crack problems reveals that the local stresses near the crack tip have the same angular variation and inverse square root singularity as those in a two-dimensional body [2-46]. Thus, the crack tip stress fields given in Equations 2-1 through 2-3 are also applicable to cracks in three dimensional bodies and the stress field near such cracks is still characterized in terms of K_I, K_{II} and K_{III}. In principle, the extension of linear elastic fracture mechanics from two- to three-dimensions is therefore quite straightforward. However, for three-dimensional problems, the stress intensity factor(s) will vary along the crack front and the evaluation of stress intensity factors is more difficult by either analytical or numerical means.

Three-dimensional elastic crack problems may be defined as a configuration of loading, solid body, and crack geometry for which a subdivision of loadings or symmetry cannot be made to reduce the problem to one of lesser dimensions. The problem of cracks in curved shells, which is clearly not a two-dimensional or lesser problem, does offer simplifications not available to the general three-dimensional solid body problem. For this reason, cracks in shells are discussed separately in Section 2.2.3. Three-dimensional crack problems represent an inherently greater variety of configurations that could be modeled than is possible for two-dimensional problems. On the other hand, three-dimensional elastic analysis for stresses around cracks represents a considerably more difficult problem than is the case for two-dimensional and axial symmetric problems. First, the apparatus of complex variable theory with conformal mapping and expansions of analytic functions has no analogue in

three-dimensional elasticity. Second, either the stress function is often not harmonic (e.g., if the Galerkin [2-47] vector is used), or a harmonic construction requires as many as four independent harmonic functions for solution (i.e., the Papkovich-Neuber [2-48] potentials $\Phi = \phi_o + x_j \phi_j$, $j = 1, 2, 3$). As a consequence, only the simplest configurations have received in-depth analytical attention. At the same time for many engineering applications, results have depended on the execution of special experimental and numerical analysis efforts. Of necessity, the published results of such efforts are sparse and often of uncertain accuracy and limited to the particular engineering cases studies.

Essentially four approaches have been used for three-dimensional crack problems. These are:

1. solid mechanics procedures in which exact or approximate results are derived as a formula,
2. solid mechanics procedures in which approximate results are obtained by numerical methods,
3. finite element and related methods, or
4. experimental methods.

Finite element and related methods and experimental methods have been discussed in Section 2.1. For three-dimensional crack problems, solid mechanics procedures which produce results in a parametric form include:

(1) Potential function methods including the Papkovich-Neuber potentials and derivative solutions obtained as extensions of previously developed results through superposition and integration.

(2) Asymptotic limits of stress concentration solutions given in the form of Papkovich-Neuber potential functions. As indicated in Tada's handbook [2-3], stress function solutions for stresses around various three-dimensional voids such as hyperboloids and ellipsoids [Neuber, 2-48] have been

degenerated into solutions for stresses around the correspondingly shaped cracks.

The usefulness of these methods is largely limited to such problems as infinite bodies with embedded penny, elliptic, parabolic, or hyperbolic flaws, or penny or elliptic stamps between semi-infinite bodies under various point and distributed loads. While of limited direct utility, may of these solutions are in closed form and can be used as building blocks with approximate methods, such as the alternating methods, fór obtaining solutions to cracked body configuratins of engineering interest.

Approximate solid mechanics procedures with more flexible application to simple cracked bodies of engineering interest include:

(3) Eigenfunction expansions which were used with some success by Hartranft and Sih [2-49] in obtaining results for cracks in finite thickness bodies.

(4) The line method in which Gyekenesi [2-50, 2-51], using ideas of Fadeeva [2-52], converts the system of coupled partial differential equations of elasticity into a system of ordinary differential equations for numerical solution. While possibly promising, this methods has not been observed in extensive use outside NASA Lewis.

(5) Integral transform methods which include a variety of numerical techniques associated with integral transforms, weight functions, and solution of singular integral equations. These methods have seen wide use by a number of investigators in numerous applications for cracked structures of simple configuration.

(6) The alternating method which iteratively combines simple body solutions (e.g., semi-infinite and cracked infinite bodies) into cracked body solutions of engineering interest.

For general applicability to comprehensive analysis to cracked structures of arbitrary and complex configurations, the method of choice is most often that of finite element and related methods supported by experiment. However,

for day-to-day engineering modeling of three-dimensional problems, the handbook, weight function, and alternating methods are most often applied.

2.2.1 Status of Available K Solutions

Several three-dimensional crack problems have been solved analytically. Such results are summarized in Sih's handbook [2-5]. In view of the use of asymptotic limits of stress concentration solutions for crack problems in the form of the Papkovich-Neuber potentials, the book on the subject by Neuber [2-48] should be most useful. The configurations covered by solutions given in the form of parametric stress functions include embedded penny and elliptic, external penny and elliptic, parabolic, hyperbolic, and semi-infinite cracks in an infinite body under a variety of point and distributed loading on or away from the crack face. A number of these solutions are available, some in closed form as exact results. Clearly, the range of configurations in this class of solutions is severely limited. However, embedded small flaws remote from free boundaries under arbitrary distributions of applied and residual stress are a frequent concern so that the solutions available provide directly applicable stress intensity factors. In addition, stress function solutions give complete stress-strain fields throughout the modeled simple geometries so that they provide excellent building blocks for solution of more complex configurations using such methods as the alternating method. Finally, exact solutions where available provide the best possible standard against which a new or proposed method of solution can be tested for baseline accuracy.

Complete three-dimensional results for cracks in simple bodies have been used as building blocks to provide approximate results for more complex geometries. These include the following configurations:

- embedded penny and elliptical cracks near the free boundary of a semi-infinite body,
- embedded elliptical cracks in a plate of finite thickness,
- semi-elliptical surface flaw in a semi-infinite body,
- corner flaw in a quarter infinite body,
- corner flaw emanating from a hole in a plate, and
- cracks in cylindrical bars and discs.

The generation of K solutions for less idealized geometries, such as for a semi-elliptical surface crack in a plate of finite thickness, requires more advanced techniques, such as finite elements, boundary integral equations, or alternating techniques. These were discussed in Section 2.1 within the context of two-dimensional problems, but the discussion there is generally also applicable to three-dimensions. However, application of numerical techniques to three-dimensional problems can frequently produce erroneous results. Investigators have tended to gradually discover and correct the causes of such errors with subsequently published work. As traced by Newman [2-53], the development of a solution for the surface flaw in a finite thickness plate under uniaxial tension is a case in point (Figure 2-6). That is, as indicated by Newman in the figure, the value of stress intensity factor has differed significantly from one investigator to another and from one time to another by the same investigator (see also Table 2-1). However, the most recent solutions are in reasonable agreement which evidence, at least circumstancially, a gradual improvement in the state-of-the-art and the convergence to the "right answer". Consequently, it is clear that extensive and informed checking and corroboration of results and sources are essential before solution of a given cracked structure problem can be considered to be established.

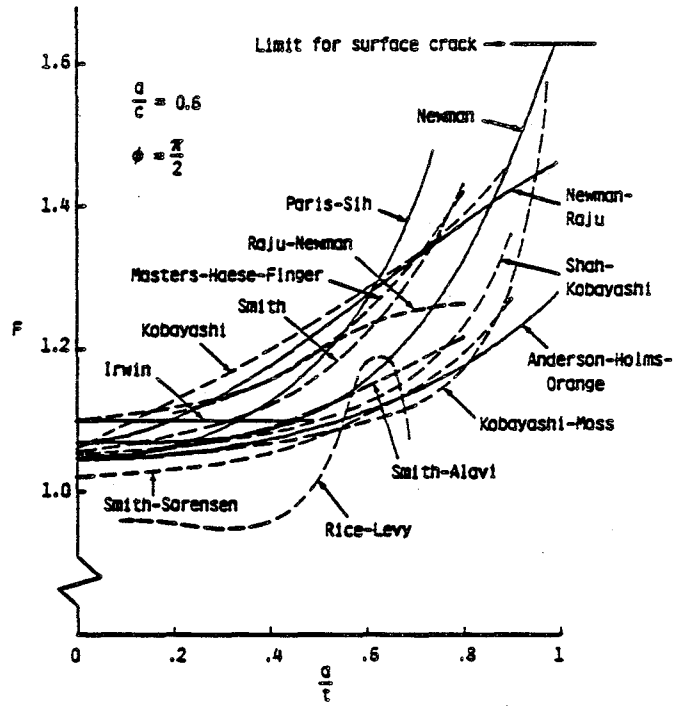

Figure 2-6. Stress Intensity Correction Factor at Maximum Depth Point for Semi-Elliptical Surface Crack (a/c = 0.6).

Table 2-1
Stress Intensity Factor Soultions For Surface Crack
In Chronological Order [2-53]

Investigator(s)	Date	Method[a]	Limitations			Form of Results
			a/t	a/c	2c/W	
Irwin	1962	EE	<0.5	0 to 1	b	equation
Paris-Sih	1965	EE	<0.75	0 to 1	b	equation
Smith	1966	AM and EE	f(a/c)	0.2 to 1	b	graph
Kobayashi-Moss	1969	AM and EE	<0.98	0 to 1	b	graph
Masters-Haese-Finger	1969	EM	<0.85	0.1 to 0.8	b	graph
Smith-Alavi	1969	AM and EE	<0.8	0.4 to 1	b	graph
Rice-Levy	1970	LSM	<0.7	0 to 1	b	graph
Anderson-Holms-Orange	1970	EE	<1.0	0 to 1	b	equation
Newman	1972	EE	<1.0	0.02 to ∞	< 1	equation
Shah-Kobayashi	1972	AM	<0.9	0.1 to 1	b	graph
Smith-Sorensen	1974	AM	<0.9	0.1 to 1	b	graph
Kobayashi	1976	AM and EE	<0.9	0.2 to 1	b	graph
Raju-Newman	1977	FEM	<0.8	0.2 to 2	b	graph
Newman-Raju	1978	FEM and EE	<1.0	0.03 to ∞	< .5	equation

a Engineering estimate (EE), alternating method (AM), line spring model (LSM), finite element method (FEM).
b Effects of finite width were not considered.

Examples of numerical results for stress intensity factors for cracks in three-dimensional bodies are becoming more numerous. They consist primarily of semi-elliptical surface cracks in plates and cylindrical bodies, such as pipes and pressure vessels. This includes early estimates for fairly simple stress systems [2-54] to more recent results that provide the variation of K along the crack front for stresses that vary as a polynomial of distance into the cracked body and for general elastic stress fields [2-17, 2-18]. References 2-55 through 2-57 provide examples of such results, which are available for only certain crack sizes. Additional results are available in the form of influence functions for semi-elliptical cracks in pipes. Such results are applicable to arbitrary stresses and to a much wider variety of crack sizes than have been analyzed by finite element techniques. Examples of work in this area are included in References 2-17 and 2-58.

Several other finite element analysis efforts related to nozzle cracks in pressure vessels have been executed and published including Smith [2-59], Atluri & Kathiresan [2-60], and Schmitt, et al. [2-61, 2-62]. In some cases, the analysis methods applied to the nozzle cracks were first applied to more classic crack problems (e.g., surface flaw in a plate) with varying results. In one case [Smith, 2-59], the surface flaw solution for the semi-elliptic case was compared with experimentally derived stress intensity factors for a naturally shaped surface flaw. However, in addition to flaw shape, valid comparison is confounded by unwanted out of plane bending in the experiment and by the criterion used to choose the ellipse to represent the natural flaw in question.

As mentioned earlier, another class of three-dimensional crack problems for which considerable information is available is corner cracks emanating

from holes or corners of quarter spaces. Such results are of interest in the aerospace industry because they can be used to model cracks that initiate at bolt or rivet holes in plates. References 2-63 through 2-65 provide representative results for these configurations. Such results are generally produced by finite element or boundary integral equation techniques.

Other procedures for evaluating stress intensity factors for cracked three-dimensional bodies include line spring models and the alternating techniques. Both of these are reported to provide considerable savings in computer expense as compared to finite elements. The line spring model was originally devised for elastic bodies [2-66], but has been extended to elastic-plastic problems [2-67, 2-68] which is an area in which its use is probably most advantageous because of the savings in computer costs.

The alternating and weight function methods, which were discussed in Section 2.1.6, provide a powerful means of analyzing three-dimensional crack problems. The application of weight function methods to three-dimensional problems is similar to that described in Section 2.1.6 for two-dimensional problems, and will not be repeated here. The weight function method now enjoys widespread successful application [2-17] to three-dimensional problems and handles stress gradients of high severity and complexity with reasonable accuracy. Its drawbacks are its restriction to LEFM and certain contained plasticity problems and its current use of weighted averages of K around the crack front rather than complete description of the K variation.

Additional discussion will be included here for the alternating method because of its special applicability to such complex problems. A drawback of this technique is its limitation to linear elastic problems. Essentially, the method consists of iteratively superposing the solutions of two or more simple

elastic problems until the results converge on a solution for some given composite of the simple problems. In general, each simple problem will contribute the solution for one set of boundary conditions, for example tractions on a semi-infinite body or tractions on the surface of an elliptic crack in an infinite body. The composite would then have the combination of boundaries in common with the contributing simple problems.

As an example, consider a surface flaw in an finite thickness plate of infinite in-plane extent loaded on its surface (Figure 2-7). The simple elastic problems, from which this example elastic problem can be constructed consist of:

(1) a surface-loaded elliptic crack embedded in an infinite body,

(2) a semi-infinite body arbitrarily loaded on its surface for the front surface of the plate, and

(3) a second arbitrarily loaded semi-infinite body for the back surface of the plate.

The procedure begins by application of the surface flaw applied loads on the surface of the infinite body elliptic crack. A solution for stress intensity factors (singular stresses) along the crack front are then obtained together with stresses over the planar regions corresponding to the front and back surfaces of the original cracked plate. Second, the semi-infinite body representing the front surface of the plate is loaded to estimate the stresses obtained on the corresponding planar region in the infinite body solution. The results will produce additional stresses on the regions corresponding to both the crack surface and the back surface of the original plate. Moreover, stresses applied to correct singular boundary stresses imposed by the infinite body solution at the intersection of the crack front with the front surface will produce secondary singular stresses (by Poisson's ratio) in the semi-

Original finite thickness plate with loaded semi-elliptic surface flaw and stress-free boundaries

Simple problem 1:

Elliptic crack embedded in an infinite body

Simple problem 2:

Surface loads on a semi-infinite body (front surface)

Simple problem 3:

Surface loads on a semi-infinite body (back surface)

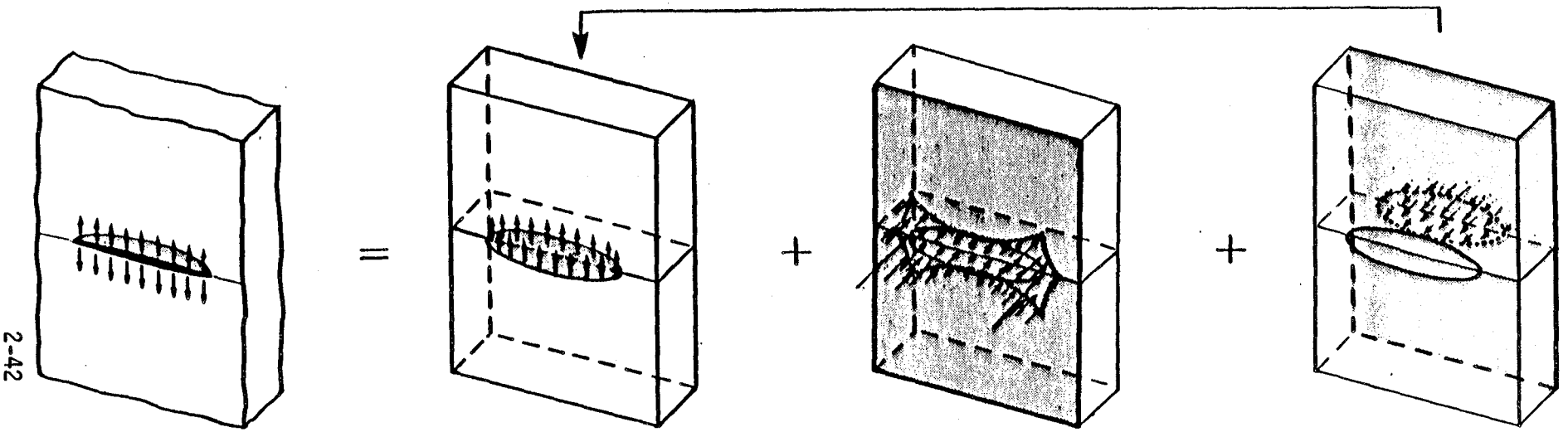

First trial: Apply original loads for original stress intensity factors.

Subsequent trials: Apply loads to eliminate stresses from problems 2 and 3 on crack surface for correction to stress intensity factors.

First and subsequent trials: Apply loads to eliminate stresses from problems 1 and 3 on front surface boundary and for secondary correction to stress intensity factors from singular loads.

First and subsequent trials: Apply loads to eliminate stresses from problems 1 and 2 on back surface boundary.

[Stop when stresses from 2 and 3 are negligible.]

Figure 2-7. Alternating Method Applied to the Surface Flaw in a Finite Thickness Plate Problem.

infinite body in the region around the crack front as well as on the crack surface. Consequently, these secondary singular stresses must be added directly as a correction to the stress intensity factor solution. Third, the semi-infinite body for the back surface of the plate is loaded to eliminate stresses from the infinite body analysis and the front surface semi-infinite body calculations. The trial sequence is completed with the first simple problem as the start of the next sequence. That is, the impact of the two semi-infinite body boundary stress corrections on the crack surface region is imposed on the surface of the elliptic crack in the infinite body to correct the stress intensity factor along the crack front. The entire sequence of alternating corrections is repeated until it is seen that further repetition will not improve the results. Convergence is assured since it is known that with each subsequent sequence of corrections, the stresses produced diminish asymptotically to zero.

Application of the alternating method for non-singular elastic stresses can proceed essentially by the usual brute-force numerical techniques. However, the singular stresses produced on the region corresponding to the front surface and their singular stress impact on the crack surface will require special, perhaps analytic, treatment to avoid errors in the results. Moreover, as the crack approaches the back surface, near singular stresses will appear on the free boundary represented by the semi-infinite body for the back surface and these can affect validity of results if not properly treated. Another source of error occurs when insufficient areas on the semi-infinite bodies are used to represent the stress-free boundaries so that the unrepresented areas are left analytically with unknown levels of stress applied to the cracked plate. In addition, overly gross representations of loads to correct for stresses at the free boundaries can also add to errors in the

results [2-39, 2-53, 2-69]. Finally, it must be noted that the solution to a composite of simple elastic problems cannot be more accurate than the solutions used to represent each of the simple elastic problems comprising the composite.

Recent advances in the solution for an embedded elliptical crack [2-70] in conjunction with finite element calculations have led to a more economical means of generating stress intensity factors for semi-elliptical surface cracks [2-71]. Such advances may lead to more widespread use of alternating techniques in the future.

2.2.2 Estimates By Re-Idealization

In some cracked structure situations, a solution may not be available for the actual configuration but may be composed as the solution to a nearly equivalent idealization that is available. As an illustration, an idealization is depicted in Figure 2-8 of a crack in an integrally stiffened sheet growing through the sheet into a stiffener. Comparative rates of crack growth through stiffener and skin have been measured and reported by Poe for a few selected cases [2-72]. From his results, Poe conservatively suggested that a crack may be assumed to grow at the same rate through a stiffener as along the skin. Poe further recommends that the stress intensity factor correction for the partially broken stiffener be linearly interpolated from the crack size upon entering the still unbroken stiffener to the crack size at which the stiffener is broken through (Figure 2-8). Other examples of re-idealization may be found in an irregular shaped flat embedded crack by Paris & Sih [2-1] and Westmann [2-73].

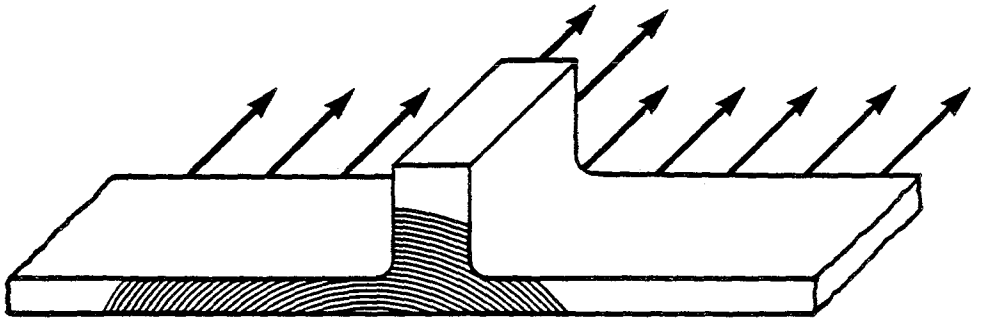

Crack Growth Through Skin and Stiffener Until Stiffener Breaks

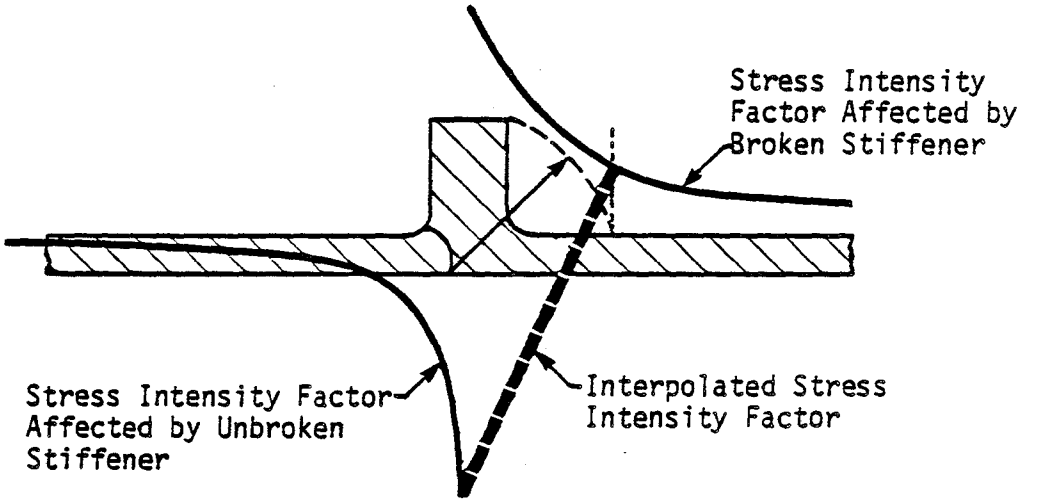

Linear Interpolation of Idealized Crack

Figure 2-8. An Example of Idealizations to Make Estimation of Stress Intensity Factors Tractable.

In the case of larger cracks, subject to the influence of nearby free boundaries and stiffeners, etc., rough estimates of stress intensity factors can be obtained by compounding of magnification factors. That is, a complete stress intensity factor estimate may be expressed in a manner following Paris & Sih [2-1] and Kobayashi [2-74, 2-75] as

$$K = \sigma\sqrt{\pi a}\, \gamma_1 \cdot \gamma_2 \cdot \ldots \cdot \gamma_N$$

where σ is applied stress, a is crack size, and $\gamma_1, \gamma_2, \ldots, \gamma_N$ are correction (magnification) factors representing each component influence. For example, consider a through crack as depicted in the axially loaded finite width stiffened plate on Figure 2-9. Here the estimated stress intensity factor may be expressed by

$$K = \sigma\sqrt{\pi a}\gamma_1\gamma_2\gamma_3\gamma_4$$

where we can use

- γ_1 the Sanders [2-76] tabulated correction for effect of a stiffener broken through by through crack in a stiffened sheet (see [Davis, 2-77] for curve fit equation).
- γ_2 the Greif and Sanders [2-78] correction for effect of the near stiffener on the right (see [Davis, 2-77] for curve fit equation).
- γ_3 the Greif and Sander [2-78] correction for effect of the far stiffener on the left.
- γ_4 Isida's [2-79] correction for a center crack in a sheet with two stiffened edges (see [Davis, 2-77] for curve fit equation). Note that Isida's correction includes the effect of finite width.

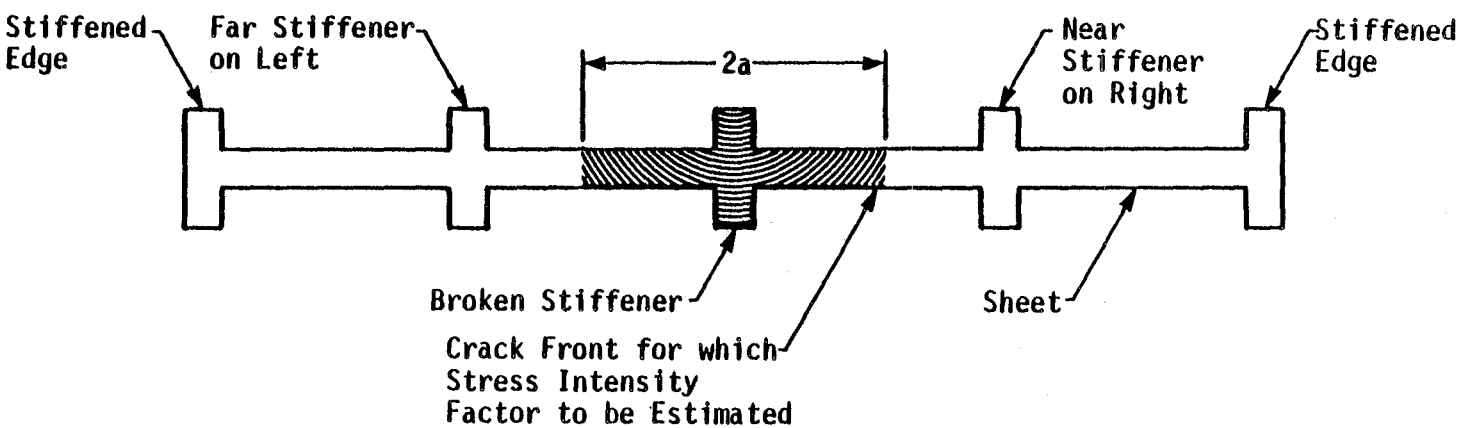

Figure 2-9. Integrally Stiffened Sheet with Center Through Crack.

A somewhat different approach to compounding the influence of boundaries and other elements of a structure may be obtained from Cartwright and Rooke [2-7].

Procedures such as this provide a powerful means of estimating stress intensity factors for complex finite bodies. The relatively simple results summarized in handbooks are obviously very useful in such exercises.

2.2.3 Cracks in Plates and Shells

Plates and shells are structural elements that are of particular interest in aerospace applications because of their inherent light weight. The stress analysis of cracks in such elements will therefore be given special attention.

The stress analysis of bodies which are thin relative to their in-plane dimensions can be considerably simplified over that for fully three-dimensional bodies. Plates subjected to bending loads can often be analyzed by classical plate theory, such as presented in Reference 2-80. The major assumptions of plate theory that are of relevance to this discussion are:

- small displacements,
- straight lines initially normal to the middle surface remain straight and normal to that surface. (Vertical shear strains are therefore neglected), and
- stress resultants rather than detailed stress patterns are considered.

Application of the classical (fourth order) plate theory to cracked plates [2-81] revealed that the angular variation of the singular stresses at the crack tip was different than that predicted from elasticity theory. In other words, the θ-variation in plates in bending was not the same as in Equations 2-1 through 2-3. Equations 2-1 through 2-3 are supposedly appli-

cable to any elastic body, and a discrepancy is apparent. This discrepancy is due to the omission of vertical shear strains, which assumes a certain type of rigidity not consistent with the isotropy assumed in the derivation of Equations 2-1 through 2-3. Additionally, stating the boundary conditions in terms of stress resultants is an approximation to the true case that causes errors in localized regions of high stress gradients (such as in the vicinity of crack tips).

More advanced analyses of cracked plates in bending have been performed that employ the higher order theory of Reissner [2-82]. Such results, as reported by Hartranft and Sih [2-83], provide an agreement between the angular variation of crack tip stresses for bending and extension. Figure 2-10 summarizes these results for the stress intensity factor at the tension surface of a plate of thickness "h" subjected to all-around bending at infinity. This figure shows that the stress intensity factors approaches that for corresponding tension problems as "h" gets very large and that the behavior is strongly dependent on h/a for small values of this ratio.

Turning to cracks in shells, these solutions are an outgrowth of analysis methods for the more general problem of stresses in uncracked elastic shells. In the case of very heavy section shells where the thickness dimension is large compared to the radius so that stress analysis is treated as a three-dimensional elasticity problem, then the crack problem is also three-dimensional. However, for a broad class of shells, the wall thickness dimension is small compared to other dimensions. Such a shell may be thought of as a membrane except for possession of thickness to resist bending. The thinness of a shell means that the two free surfaces are too close to perceptibly deflect relative to one another, to develop significant cross thickness

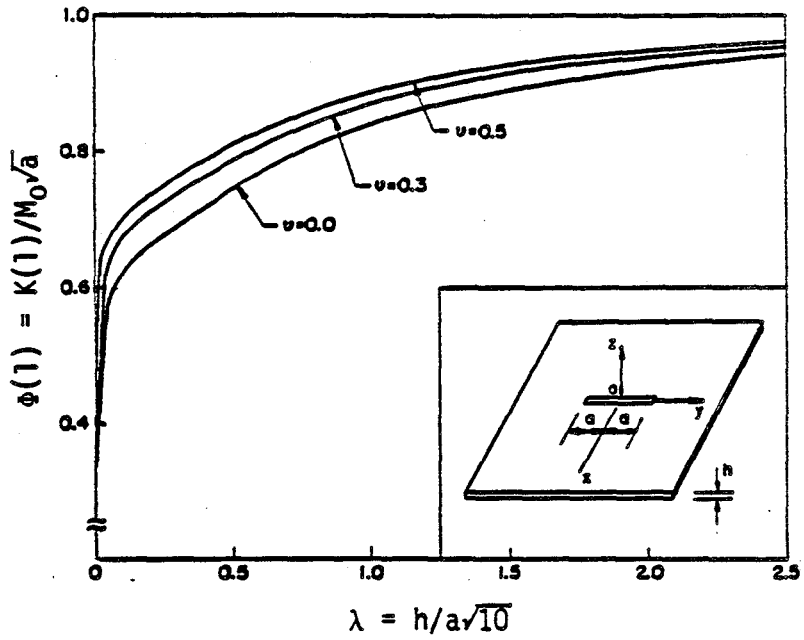

Figure 2-10. Moment Intensity versus Ratio of Plate Thickness to Half Crack Length.

stresses, or to act other than as a unit for in or out of plane deflection. In view of these observations, simplifying assumptions have been developed to reduce and simplify the equations of three-dimensional elasticity so as to create a theory of thin shells whose equations can be more easily solved for the significant stresses to be found in an elastic shell. This is analogous to the case of elastic plates discussed above.

With the advent of fracture mechanics in the 50's and 60's, the problem of stresses around cracks was viewed as a simple adaptation of the existing elasticity theory to the new problems thus generated. Consequently, the existing classical theory of thin shells, which had been quite successful for analysis of stresses in shells, was simply adopted without modification for the solutions of cracks in shell problems. As a result, a considerable body of literature containing classical shell theory solutions for stresses around cracks in shells was created by the early 1970's. However, disturbing signs as to the validity of such results began to appear as early as 1960. The differences in the angular variation in the crack tip stress fields for differing plate theories discussed above is a primary example.

By the early 1970's, it became clear that since the classical theory of thin shells is limited to smooth transitions of the shell surface, the classical theory cannot be depended upon for computing stresses near abrupt discontinuities of the shell surface, including cracks. The primary cause of the discrepancies in the theory was identified by Reissner [2-82], Sih and Haggendorf [2-84] and others to be the neglect of transverse shear deformation in the classical theory. Accordingly, a shear deformation theory of shells was developed to correct the problem [2-84]. Subsequent publications [2-85, 2-86] have indicated another new but simpler shear deformation theory of

shells to have also entirely eliminated the anomalous differences so that shell results will agree with the results from three-dimensional and two-dimensional elasticity for the angular distribution of singular stresses around cracks. Because of these findings and the importance of shells in aerospace structures, a comparison of the classical and the two shear deformation shell theories is presented next. With the comparison as a basis, the methods and sources applicable to solution of cracked shell problems is then mentioned, followed by a review on the current status of available solutions.

The primary assumptions that have been developed for stresses in shells are as follows [2-86]:

1. Planes normal to the middle surface remain plane during bending.
2. Lines normal to the middle surface neither contract nor expand during deformation.
3. Stresses are represented by their resultants or couples across the shell thickness.

The further simplifying assumptions after Kirchhoff to complete the classical theory of thin shells are the following:

4. The squares of the derivatives $\frac{\partial w\ (x,y)}{\partial x}$ and $\frac{\partial w\ (x,y)}{\partial y}$, where w is the middle surface displacement, can be neglected.
5. The transverse shear resultants in the equations of equilibrium can be neglected.
6. The tangential displacements in the expressions for transverse shear stress can be neglected.

The first assumption would obviously be unappropriate for a part-through crack in a shell, because it would not be possible to reproduce the crack surface displacements and stress singularity present for a part-through crack.

Hence, shell theories are limited to through-wall cracks, and fully three-dimensional elasticity theory, such as summarized in Section 2.2.1, must be utilized for part-through cracks.

The membrane resultants of stress across the thickness combined with two-dimensional stress compatibility leads to an Airy stress function for the membrane stresses. The strain-displacement relations and constitutive relations combined with equilibrium and compatibility, in line with the symmetries from the assumptions lead to the use of the displacement function $w(x,y) = u_3$ for bending, (note that u_3 is the out of plane deflection of the shell).

In contrast to the classical shell theory, Sih and Haggendorf [2-84] used only the first four of the six assumptions of shell theory. That is, Sih and Haggendorf, by not neglecting transverse shear, developed a 10^{th} order system of shallow shell equations with all 5 boundary conditions on the free edge of the shell (Figure 2-11).

For Sih and Haggendorf's shear theory of shells, the equations of equilibrium and other equations of elasticity as constrained by the first four simplifying assumptions for shells are used to construct a set of shell equations in terms of five measures of displacement. For this shear theory, the five measures replace the stress function and single measure of displacement of the classical theory. These five measures are as follows:

$u_1(x,y)$	is the in-plane displacement of the shell along the x-coordinate
$u_2(x,y)$	is the in-plane displacement of the shell along the y-coordinate
$w(x,y) = u_3$	is the out of plane displacement of the shell

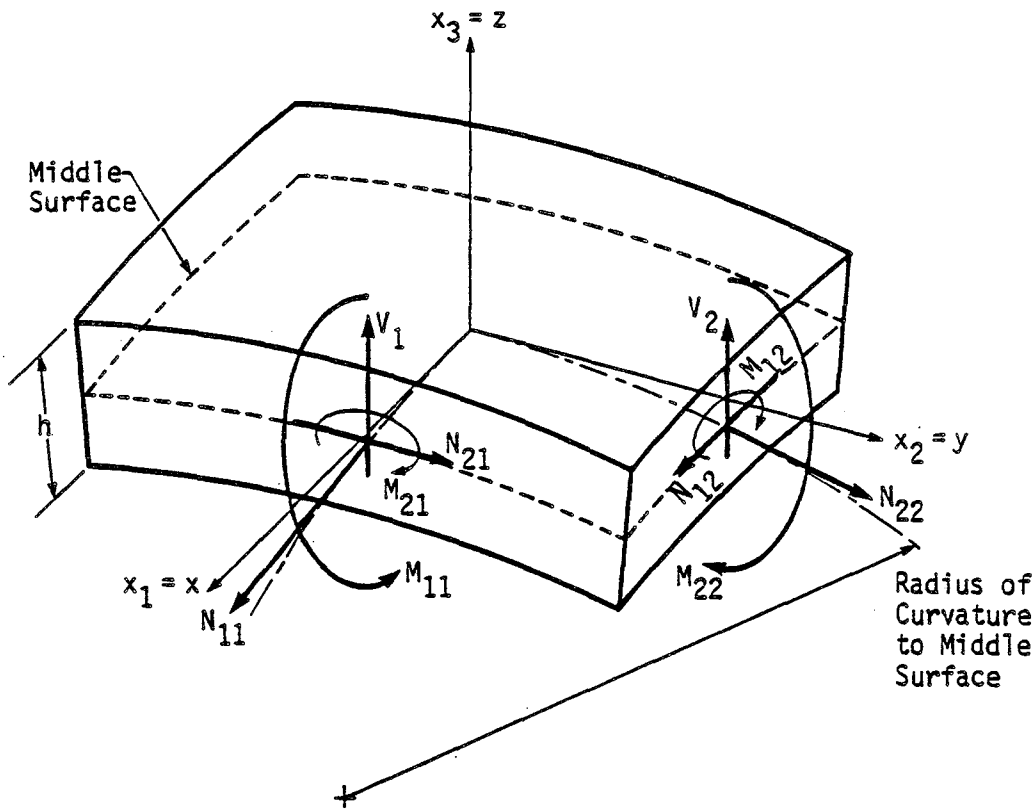

Perspective View of Shell Element

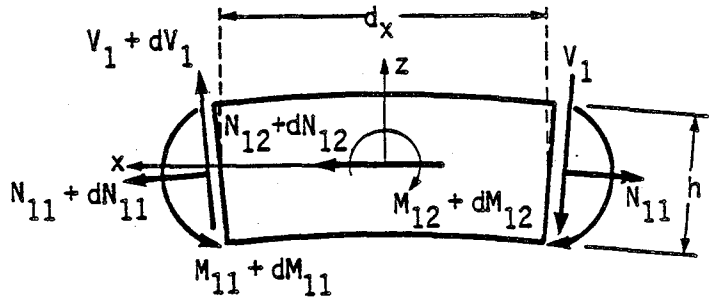

Shell Element as Viewed Along y Axis to Show Differentials for Equilibrium

Figure 2-11. Illustrations of a Shell Element to Show Resultant Forces and Moment Couples Acting on Faces of Element Which Would be the Free Edges of the Shell.

$\beta_1(x,y)$ is the angle through which the normal to the middle surface upon displacement rotates in the direction of the x-coordinate

$\beta_2(x,y)$ is the angle through which the normal to the middles surface upon displacement rotates in the direction of the y-coordinate

The governing equations have been applied to the problem of through cracks in spherical shells with the crack faces loaded in stretching and bending [2-84]. As shown on Figures 2-12 and 2-13, a comparison of the resulting stress intensity factor solutions with the classical shell theory solutions indicates significant and sometimes dramatic differences in the stress intensity factors for both stretching (membrane) and bending loads on a crack. In particular, the Sih and Haggendorf shear theory of shells have produced the following three results:

1. The angular distribution of singular stresses around a crack in a shell are the same for all loading components in that they all agree with the classic Mode I, Mode II, and Mode III stress fields derived for two- and three-dimensional bodies. This is in contrast to the classical theory which predicted different angular distributions of singular stresses for bending as compared to membrane loads.

2. The stress intensity factor under crack face stretch loads for shear theory in shells with R/h = 10 and ν = 1/3 rises from 2% higher than classical prediction at crack size 2a = h to 50% higher at 2a = 5h to beyond 100% higher when 2a exceeds 10h. (See Figure 2-12.)

3. In the case of a crack face under bending loads, the trend in stress intensity factor for shear theory is opposite to that expected from the classical theory. That is, as the crack gets longer the effect of bending reduces instead of increasing as we were led to believe by the classical theory. (See Figure 2-13.)

Krenk [2-85] and Delale and Erdogan [2-86] have developed a simplified form for a transverse shear theory of stresses in shallow thin shells. In their development, which loosely follows the Sih and Haggendorf derivation,

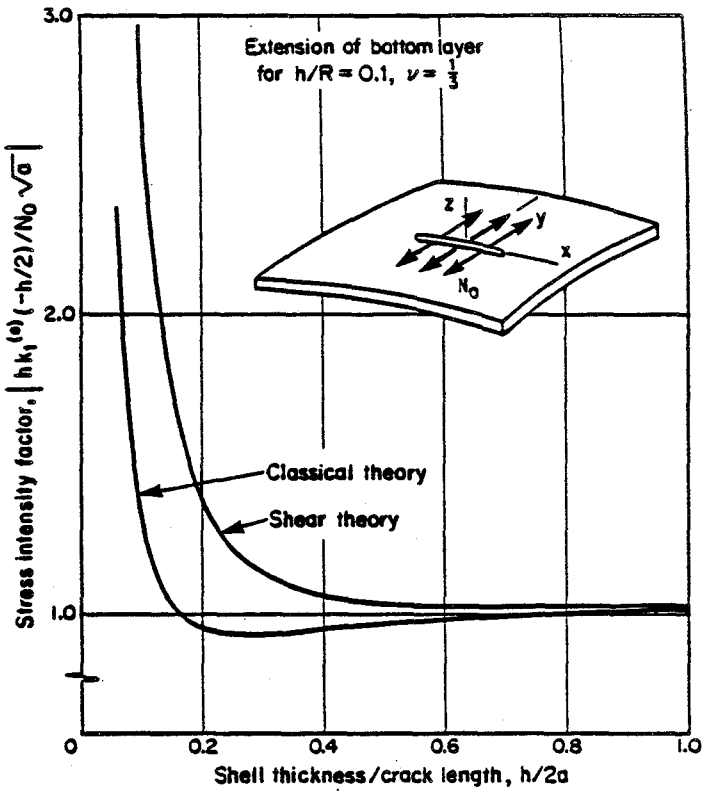

Figure 2-12. Classical Theory versus Shear Theory for Stretching Load in Spherical Shells [2-84].

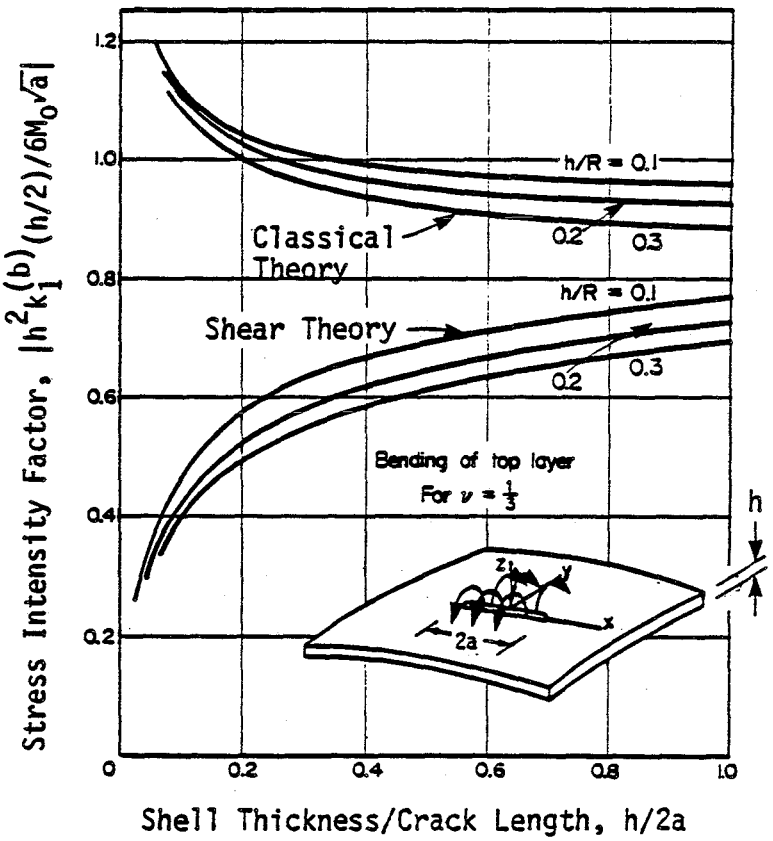

Figure 2-13. Comparison of Classical and Shear Deformation Theory for Bending Load in Spherical Shells [2-84].

Krenk and coworkers have selectively neglected u_i/R displacements and V_i/R transverse shear ratios to arrive at a reduced number of governing shell equations. In particular, the stress function is reintroduced from the classical shell theory so that the new shear membrane equilibrium equation is the same as it was in the classical theory. The displacement function from the equilibrium of bending resultants [2-84] is introduced into the equilibrium of transverse resultants so that the transverse equilibrium equations of Sih and Haggendorf in their new form are reduced to nearly the classical form for bending equilibrium.

Krenk [2-85] and Delale and Erdogan [2-86] have also developed and applied their shear theory of thin shells to axial and circumferential cracks in cylindrical shells. In both cases, comparisons were made with the classical theory. Representative results for an axial crack in a cylindrical shell are shown in Figures 2-14 and 2-15.

Figure 2-14 shows the dimensionless membrane and bending stress intensity for the cylindrical shell subjected only to hoop membrane stress σ_m far from the crack. K_m is the value of K at the mid-surface of the shell, which must be equal to a flat plate in tension when $R \to \infty$. Thus $K_m = \sigma_m (\pi a)^{1/2}$ as λ approaches zero, as shown in the upper portion of Figure 2-14. K_b is related to bending in the shell and is proportional to the difference between K at the shell tension surface and K at the mid-surface. [K_b = K (outer surface) - K (mid-surface)]. Note that for $R \to \infty$ ($\lambda = 0$), the bending contribution to K due to a membrane stress is zero. Also, the classical results are seen to be quite close to the more precise theory.

Figure 2-15 shows similar results for a shell subjected to a through-thickness bending moment on the faces of the crack; σ_b is the maximum stress

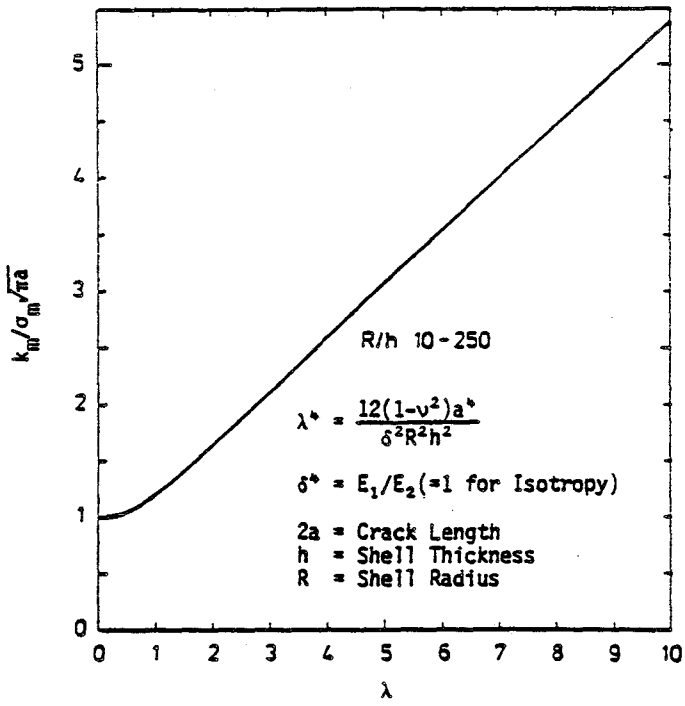

Stress Intensity Factor K_{mm}

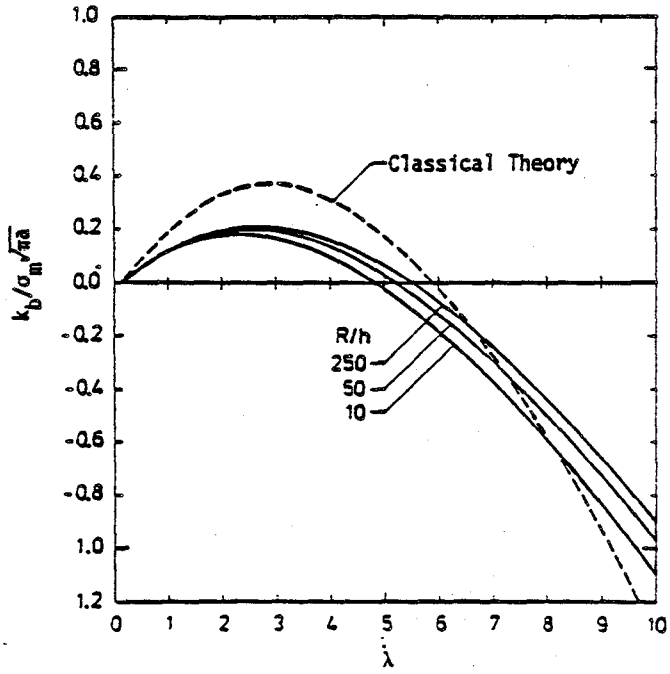

Stress Intensity Factor K_{bm}

Figure 2-14. Bending and Tension Stress Intensity Factors Due to Membrane Stresses in a Cylindrical Shell with a Through-Wall Axial Crack.

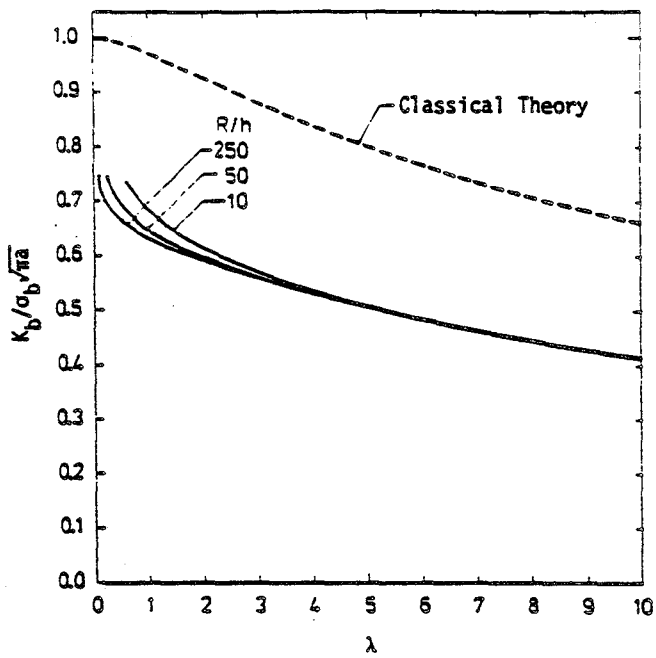

Stress Intensity Factor K_{bb}

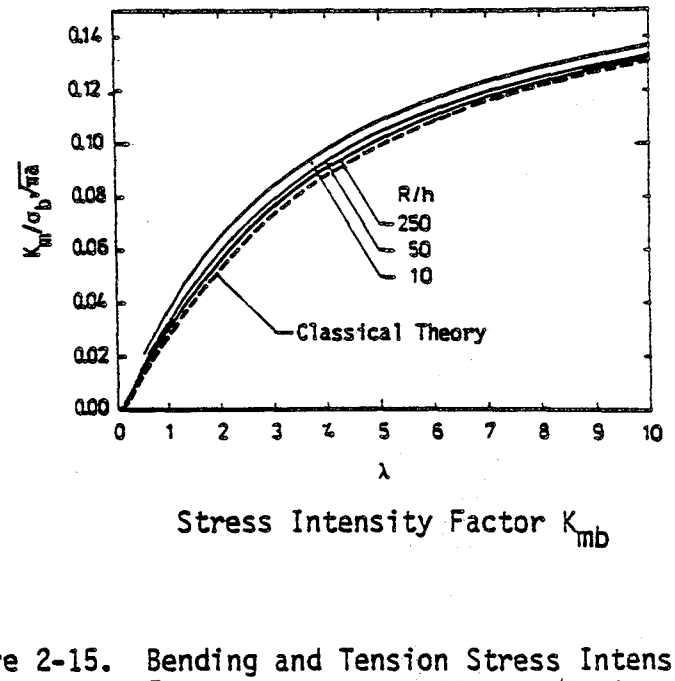

Stress Intensity Factor K_{mb}

Figure 2-15. Bending and Tension Stress Intensity Factors Due to Bending Loads in a Cylindrical Shell with a Through-Wall Axial Crack.

that would be produced by the bending moment in the absence of the crack. In this case, the classical theory is seen to provide consistently large results for the bending component of K, which again demonstrates the inadequacy of the classical theory for the determination of stresses near crack tips.

From the figures, and statements by Delale and Erdogan [2-86] the following results were obtained:

1. As in the Sih and Haggendorf theory, the Krenk shear theory predicts the angular distribution of singular stresses around a crack in a shell to be the same for all loading components in that they all agree with the classic Mode I and Mode II stress fields.

2. The stress intensity factors for membrane loads are not much different than those predicted by the classical shell theory. Indeed, membrane stress intensity factors due to membrane loads are identical between the Krenk shear theory and the classical theory for thin shell stresses.

3. For a crack face under bending loads, the classical shell theory produced bending stress intensity factors 50% higher than those based on the Krenk shear theory for longitudinal cracks in cylindrical shells (Figure 2-15). For circumferential cracks under crack face bending major differences between the Krenk shear and classical theories were also reported.

To complete the comparison, these results should be compared with those of Sih and Haggendorf who found more significant differences between shear and classical theory predictions of stress intensity factor due to membrane loadings than did Krenk or Delale and Erdogan. It is true that the Sih and Haggendorf comparisons were for a cracked spherical shell while the Krenk and Delale and Erdogan comparisons were for cracked cylindrical shells. However, comparison of the resultants expressions and the governing equations for the three shell theories applied to crack problems does show disturbing similarities between the Krenk shear and classical theories that are not shared by the Sih and Haggendorf theory -- especially for the membrane equilibrium

governing equations. Therefore, the competing shear theories for stresses in thin shells should be carefully studied to decide whether or within what limitations the Krenk shear theory can safely be used.

2.3 AUTOMATED COMPUTER PROGRAMS FOR COMPUTATION OF IMPORTANT CRACK TIP STRESS PARAMETERS

General procedures for numerical evaluation of crack surface displacement and stress intensity factors, such as the finite element method, were reviewed in Section 2.1. Such procedures are of general applicability but are quite expensive, both in labor and computer costs. Several automated computer programs for evaluation of stress intensity factors by use of previously calculated and stored results are available and will be reviewed in this section. Some of these computer programs can very ecomonically provide suitable results, even for some fairly complex geometries and especially for complex stress fields.

Automated stress intensity factor programs are defined for the current review as computer codes which compute stress intensity factors "automatically", i.e., without recourse to explicit crack modeling (or meshing) and detailed stress analysis. Because of the desireability to obtain quick stress intensity factor solutions for specific flaw geometries, rather than performing detailed modeling of the cracked geometry or component, only "non-stress analysis" programs which store previously generated stress intensity solutions have been reviewed. Consequently, the following areas have been excluded from the current survey: 1) stress analysis programs such as NASTRAN, ANSYS, and MARC (available through commercial computer centers) which model the crack and compute stress intensities directly from mesh refinement or indirectly using such methods as nodal point displacements, strain energy

release rates, J-integrals, etc., 2) special crack tip finite elements which incorporate the crack tip singularity into the displacement formulation and are embedded into general purpose finite element codes, and 3) other stress analysis techniques such as boundary integral equations which model the cracked geometry and provide stresses and displacements for automatically calculating stress intensities by such methods as strain energy release rate. (PESTIE, developed at and proprietary to Pratt and Whitney Aircraft, as an example). A general review of such codes is provided in Section 2.1.

No detailed discussion is provided in this section on the methods used to obtain the stress intensity solutions found in the reviewed computer codes. However, for the reader's interest, an excellent, concise review of available methods -- both theoretical and experimental -- is found in an article by Cartwright and Rooke [2-7]. Their paper discusses many of the popular approaches, such as discussed in earlier portions of Section 2.

In practice, automated stress intensity programs are generally combined with computer flaw growth programs to provide a single package convenient for analysis of subcritical crack growth. This section will concentrate on the automated evaluation of stress intensity factors, and the discussion on subcritical crack growth programs will be deferred to Section 3.6 -- which follows a detailed discussion of the fracture mechanics bases of such calculations. Table 2-2 lists automated stress intensity evaluation programs, each of which also contains capabilities for crack growth analysis. This list is by no means complete, since 1) many private companies and university researchers involved in such work have developed their own programs to suit their particular applications, and 2) our review has been restricted to codes which are available to the public. Table 2-3 provides a list of several

Table 2-2
Automated Stress Intensity and Flaw Growth
Computer Programs Included in Review

Code Name	Sponsor	Principal Developer [Reference]
BEWICH*	Beech Aircraft	S. Imtiaz [2-87]
BIGIF	Failure Analysis Assoc.	P. Besuner [2-17]
CGR-LaRC	NASA Langley	S. Johnson [2-88]
CRACKS 4**	Wright Patterson	R. Engle [2-89]
CRACKGRO**	Wright Patterson	R. Engle (J. Chang) [2-90]
EFFGRO	Rockwell North American	J. Vroman, J. Chang [2-91]
FAST-2	NASA Langley	J. Newman [2-92]
FATPAC	Central Electricity Research Labs	G. Chell [2-93]
FLAGRO 4	NASA: JSC	A. Liu [2-94]
MSFC-2*	NASA: MSFC	M. Creager [2-95]

* Acronym assigned code for current review. No acronym issued with publication.
** Documentation ordered but not received at time of current review.

Table 2-3
Special Application Computer Programs. No Detailed Review Of These Codes Was Conducted In Current Program.

CODE NAME	SPONSOR (developer) [Reference]	APPLICATION	FEATURES
FACET	EPRI (R. Cipolla) [2-96]	Flaw evaluation specified in Appendix A, Section XI of ASME Boiler and Pressure Vessel Code, Surface Flaws & Embedded Ellipses only.	Determines crack-tip stress intensity factor range, the corresponding crack growth, and whether maximum crack size which could develop in remaining life will approach minimum crack size allowable, General Stress Gradients (Weight Function).
OCA1	Oak Ridge National Lab (S. Iskander) [2-97]	Part-Through Infinitely Long Cracks in Cylindrical Geometries. Thermal and Pressure Loading on Cylinders. Nuclear Power Plants.	Thermal stress & pressure stress analyses combined with CUFIGHT Function Stress Intensity Program. $K > K_{Ic}$ produces crack growth until $K < K_{Ia}$ (arrest stress intensity) and crack stops. Cycle repeats, $K > K_{Ic}$, $K < K_{Ia}$. K_{Ic}, $K_{Ia} = f(T,\text{radiation})$.
PERFCT	Failure Analysis Assoc. (P. Besuner) [2-98]	Probabilistic fracture mechanics crack growth code used to make run/repair/retire decisions of structural components in service, especially gas turbine disks.	Monte Carlo simulation to determine the in-service impact of almost any systematic and random error that can be expressed with numbers and equations. Distributions on inspection, stress, flaw size (growth), usage, and constraints of safety, logistics, economy.
STRAP	EPRI (C.H. Wells) [2-99]	Stress and crack propagation analyses for General Electric or Westinghouse steam turbine rotors from Cr-Mo-V material.	Combines preprocessor mesh generator (PP MESH) with general finite element stress analysis program (ANSYS) and uses stress output for flaw growth program, FRAC. Four flaw geometries available.
TIFFANY	Lawrence Livermore National Laboratory (D.O. Harris) [2-100]	Evaluation of stress intensity factors for semi-elliptical cracks in pipes subject to radial gradient thermal stresses. Cladded Pipe Applications.	Solves heat conduction equations to obtain temperature distributions and subsequently calculates stresses. Stress intensity values are then evaluated using weight functions. Evaluates K versus "a" only. No fatigue calculations.
*EPRI NP-2425	EPRI (D.O. Harris) [2-101]	Calculated stress intensity factors for interior surface cracks in cylinders using weight function approach.	Models complete circumferential, long longitudinal, and semi-elliptical cracks. Accepts arbitrary stresses on plane of crack. Radial stress variation only for circumferential and longitudinal crack geometries.

*No acronym assigned but the developers sometime call it "Little IF".

additional computer codes for evaluation of stress intensity factors. Brief descriptions of the codes are provided in the table, but detailed review of them were not performed for the current project.

The programs listed in Table 2-2 all contain multiple crack geometries, ranging in number from 8 to 47, and use one or several of the following three techniques for automatically generating stress intensity values: 1) programming closed-form "handbook" stress intensity solutions which generally restrict loading to uniform tension, and possibly, bending, 2) allowing input of stress intensity as a function of crack length by the user if the K solution is known, or 3) using weight functions (discussed in detail in Section 2.1) which allow computation of stress intensity factors for general stress gradients.

Figures 2-16 through 2-23 illustrate the various crack geometries and load conditions for the programs listed in Table 2-2. The libraries and loadings shown in Figures 2-16 and 2-18 through 2-23 are from programs which utilize the "handbook" stress intensity solution technique. In addition, the programs represented by these figures have primarily been developed for aircraft/spacecraft applications. Considering the common approach and application, it is not surprizing that many of the crack geometries and loading conditions are similar in these programs. As illustrated, all of the handbook-based stress intensity algorithms address the two-dimensional geometries of edge and center through-thickness cracks and the three-dimensional geometries of surface, and corner cracks. Particular emphasis is also placed on cracks emanating from holes, which is most likely due to the abundance of bolt and fastener holes and other notches in aircraft structures. Surface flaw stress intensities are typically calculated for two positions along the

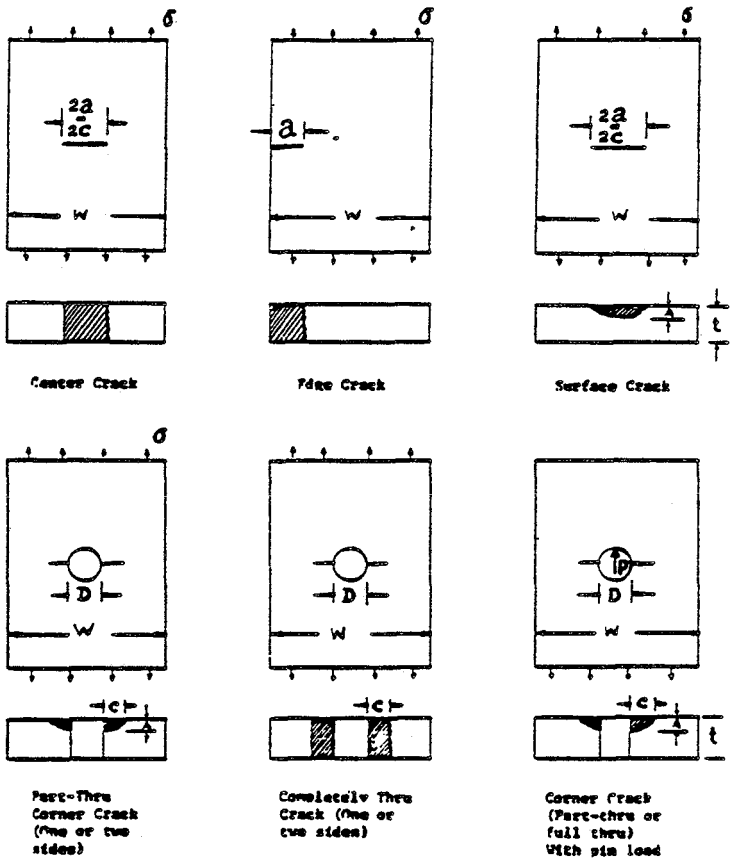

Types of crack specimens

Figure 2-16. Crack Geometry Library and Loading Conditions Available in Flaw Growth Program BEWICH [2-87].

Library Class	Subroutine	Class Index (IFI)	Crack Geometry Description	Degrees-of-Freedom (IDOF)	Crack Shape	Crack Mode	Finite Width Effects	Variable Thickness (NTH)	Curvature	Stress(1) Input
Special Cases	SIMPLK	101	Center Cracked Infinite Plate in Tension	1	Straight	I	No	No	No	Uniform
	SIMPLK	102	Edge Cracked Semi-Infinite Plate in Tension	1	Straight	I	No	No	No	Uniform
Two-Dimensional	CENTER	201	Center Cracked Plate, Mode I	1	Straight	I	Yes	Yes	No	General(2)
	CENTER	202	Center Cracked Plate, Mode II	1	Straight	II	Yes	Yes	No	General(2)
	CENTER	203	Center Cracked Plate, Mode III	1	Straight	III	Yes	Yes	No	General(2)
	EDGE	204	Edge Cracked Plate, Mode I	1	Straight	I	Yes(3)	Yes	No	General
	EDGE	205	Edge Cracked Plate, Mode II (Inactive)	1	Straight	II	Yes	Yes	No	General
	EDGE	206	Edge Cracked Plate, Mode III (Inactive)	1	Straight	III	Yes	Yes	No	General
	TELEFI	207	Edge Notched Plate, Mode I	1	Straight	I	Yes	Yes	Yes	General
	PIPE	208	Longitudinal Pipe Crack	1	Straight	I	Yes	Yes	Yes	General(2)
	PIPE	209	Circumferential Pipe Crack	1	Straight	I	Yes	No	Yes	General(2)
Three-Dimensional	TELEFI	300	Nozzle Blend Radius Circular Corner Crack	1 or 3	1/2 Circular	I	No	No	No	General
	ØNEDØF	301	Buried Circular Crack	1	Circular	I	No	No	No	General
	ØNEDØF	302	Circular Surface Crack	1	1/2 Circular	I	No	No	No	General
	ØNEDØF	303	Circular Corner Crack	1	1/4 Circular	I	No	No	No	General
	BUR4	304	Buried Elliptical Crack	4	Elliptical	I	No	No	No	General
	SUR3	305	Elliptical Surface Crack	3	1/2 Elliptical	I	No	No	No	General
	CØR2	306	Elliptical Corner Crack	2	1/4 Elliptical	I	No	No	No	General
	ELNØZ	307	Elliptical Nozzle Crack	3	Near Elliptical	I	No	No	No	General

NOTES: (1) General stress input for two-dimensional crack models implies any $\sigma(x)$ variation; for three-dimensional models, the general stress variation is $\sigma(x,y)$.
(2) $\sigma(x)$ must be symmetric about the z axis (axisymmetric for IFI = 209).
(3) The influence function is accurate for $0 < a/W < 0.6$. Beyond this, the model is converted to IFI = 207, which is accurate for $a/W > 0.6$.

Figure 2-17. Crack Geometry Library and Loading Conditions Available in Flaw Growth Program, BIGIF [2-17].

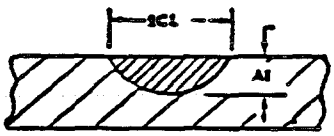

Surface Crack

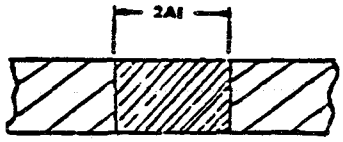

Through Crack

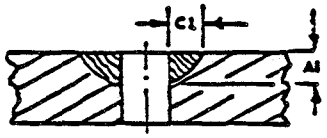

Part-Through Crack at a Hole

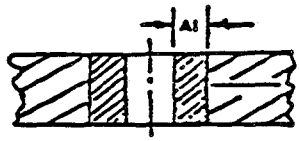

Through Crack at a Hole

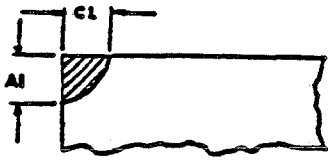

Corner Crack Where AI = CL

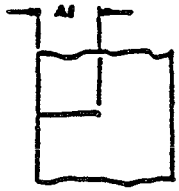

Edge Crack

VARIABLE INPUT	FLAW
1	Part-through surface crack
2	Through-the-thickness crack
3	Corner crack originating at a hole under tensile loading
4	Corner crack originating at a hole under bearing loads
5	Corner crack originating at a hole under both tensile and bearing loads
6	Through-the-thickness crack originating at a hole under tensile loading
7	Through-the-thickness crack originating at a hole under bearing loads
8	Through-the-thickness crack originating at a hole under both tensile and bearing loads
9	Corner crack emanating from an edge
10	Single edge crack

Figure 2-18. Crack Geometry Library and Loading Conditions Available in Flaw Growth Program CGR-LaRC [2-88].

PART THROUGH CRACKS (PTC)

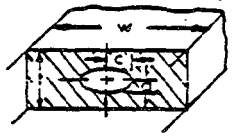

$K=1.0\,\sigma\sqrt{\pi a/Q}$

Embedded Crack:
a/2c ≤ 1/2
t_{equiv} = 1/2 t
half w = 1/2 w
const = .91
HOLE = blank

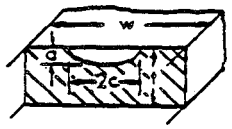

$K=1.1\,\sigma\sqrt{\pi a/Q}$

Shallow or Semi-Circular Surface Flaw:
a/2c ≤ 1/2
t_{equiv} = t
half w = 1/2 w
const = blank or 1.0
HOLE = blank

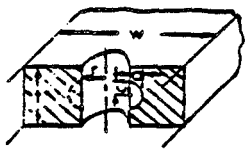

$K=1.0\,\sigma\sqrt{\pi a/Q}\ f(a/r)$

Shallow or Semi-Circ. Surf. Flaw from Hole:
a/2c ≤ 1/2
t_{equiv} = (c/a)(t/2)
half w = 1/2 w
const. = .91
HOLE = punched "hole"
Use BOWIE series for one or two cracks on CARDS 5 & 6 (series).

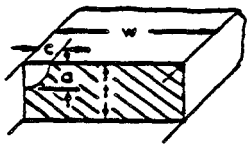

$K = 1.2\,\sigma\sqrt{\pi a/Q}$

Corner Crack in Uniform Stress Field
a/2c = 1/2
t_{equiv} = t
half w = w
const = 1.1
HOLE = blank

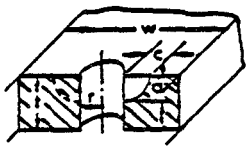

$K=1.1\,\sigma\sqrt{\pi a/Q}\ f(a/r)$

Corner Crack from Hole:
a/2c = 1/2
t_{equiv} = t
half w = 1/2 w
const = blank or 1.0
HOLE = punched "hole"
Use BOWIE series for one or two cracks on CARDS 5 & 6 (series).

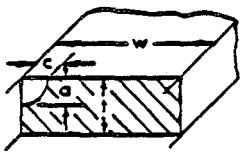

$K = 1.2\,\sigma\sqrt{\pi a/Q}\ f(x)$

Corner Crack in Stress Gradient:
a/2c = 1/2
t_{equiv} = t
half w = w
const = 1.1
HOLE = punched "hole"
use f(x) series on CARDS 5 & 6 (series) where f(x) is the normalized stress distribution (normalized to the peak stress, and r = 1.0

Figure 2-19. Crack Geometry Library and Loading Conditions Available in Flaw Growth Program EFFGRO [2-91].

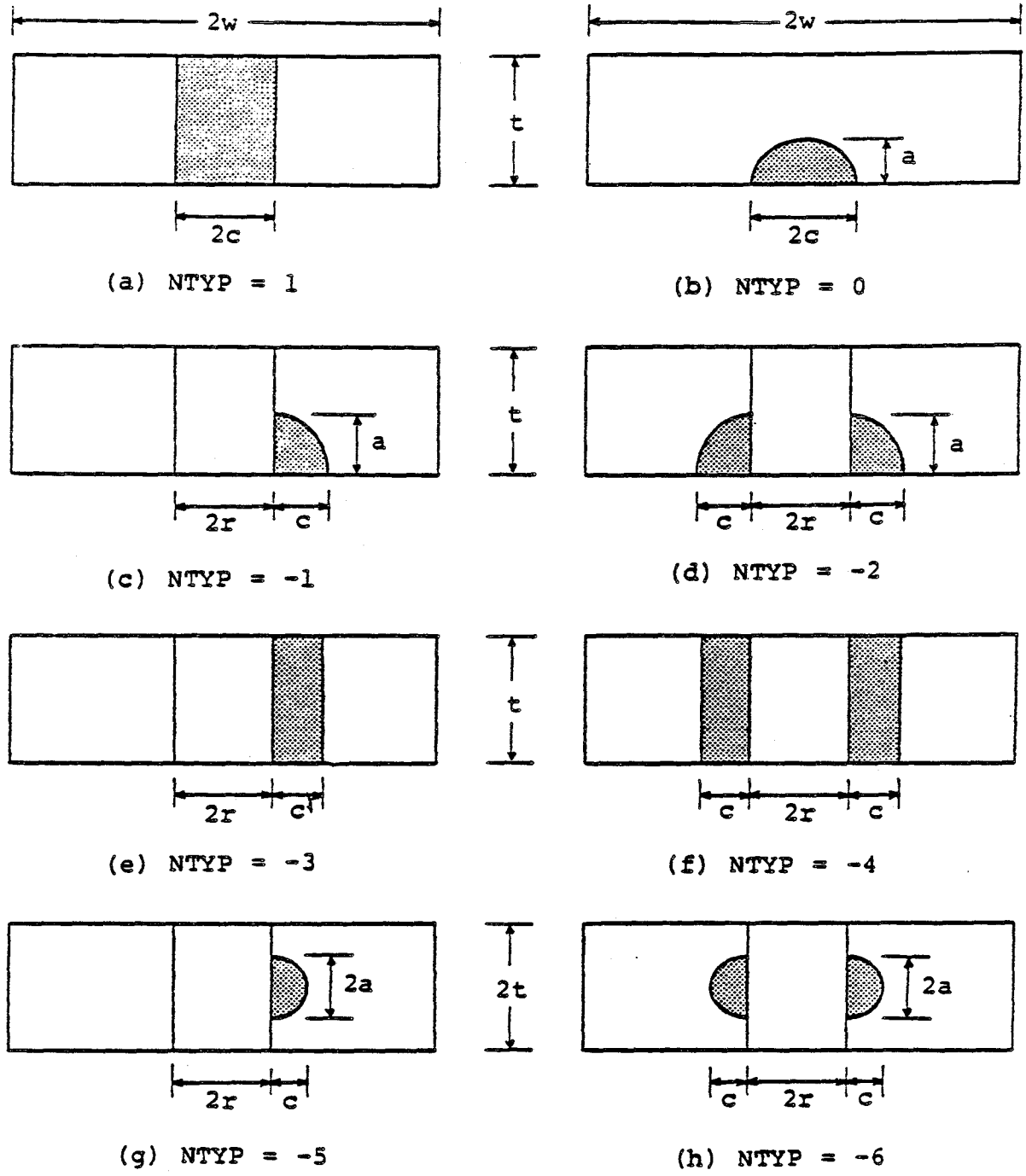

Crack configurations analyzed.

Figure 2-20. Crack Geometry Library and Loading Conditions (Uniform Load Only) Available in Flaw Growth Program FAST-2 [2-92].

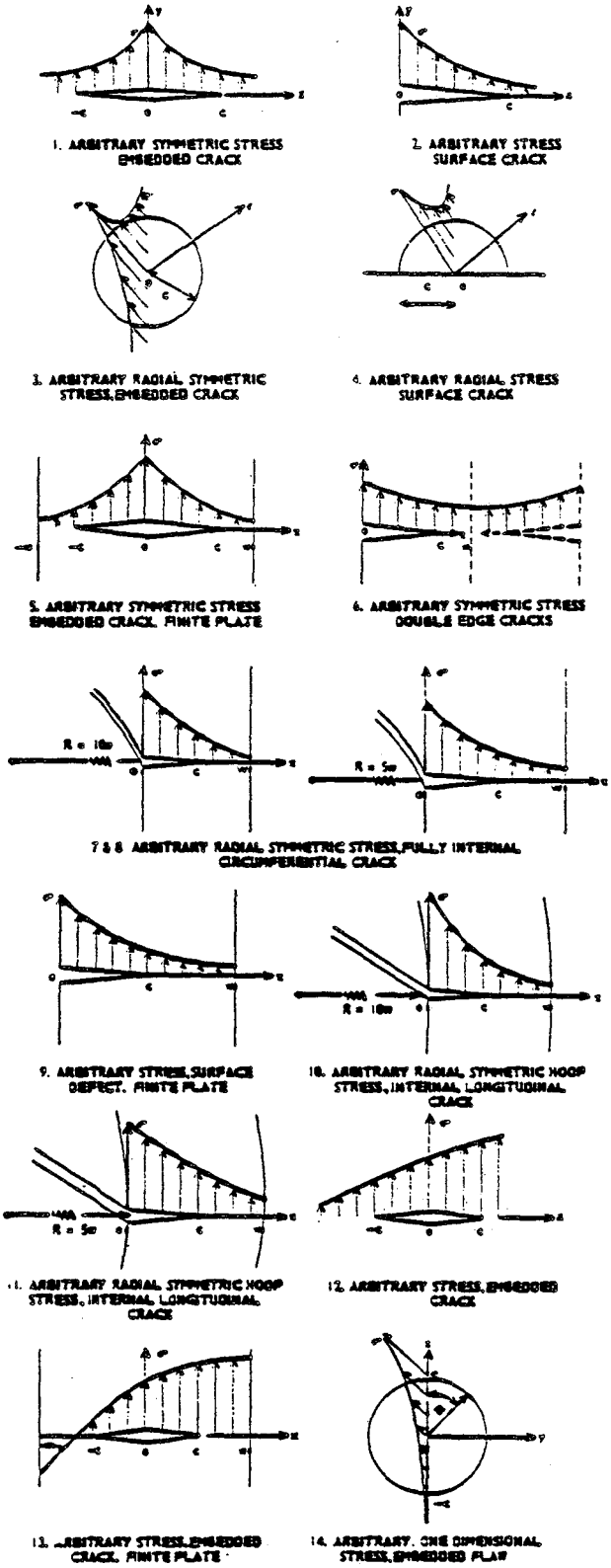

Figure 2-21.- Crack Geometry Library and Loading Conditions Available in Flaw Growth Program FATPAC [2-93].

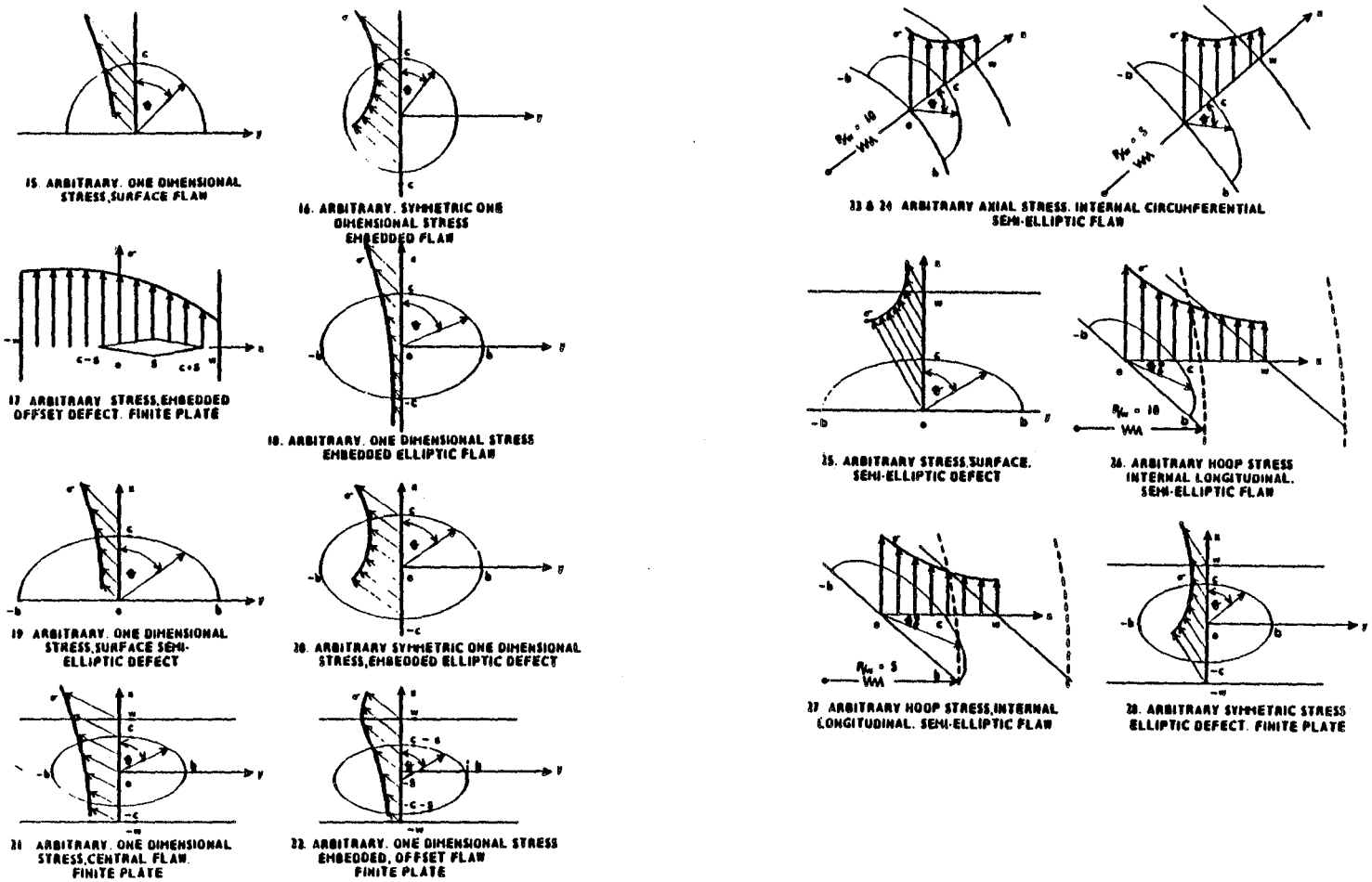

Figure 2-21 (Continued).

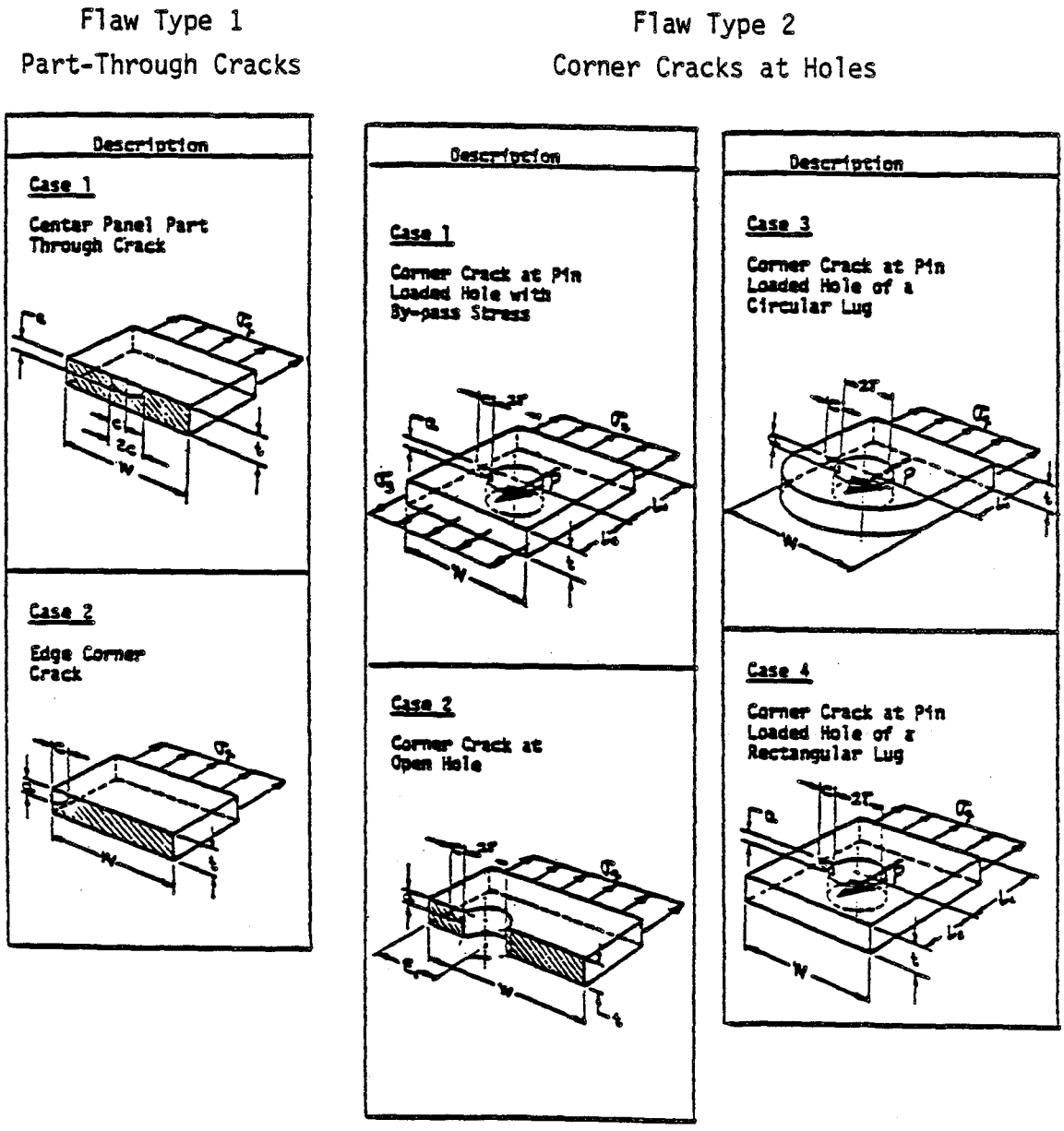

Figure 2-22. Crack Geometry Library and Loading Conditions Available in Flaw Growth Program FLAGRO-4 [2-94].

Flaw Type 3
Through Cracks

Flaw Type 4
Through Cracks at Holes

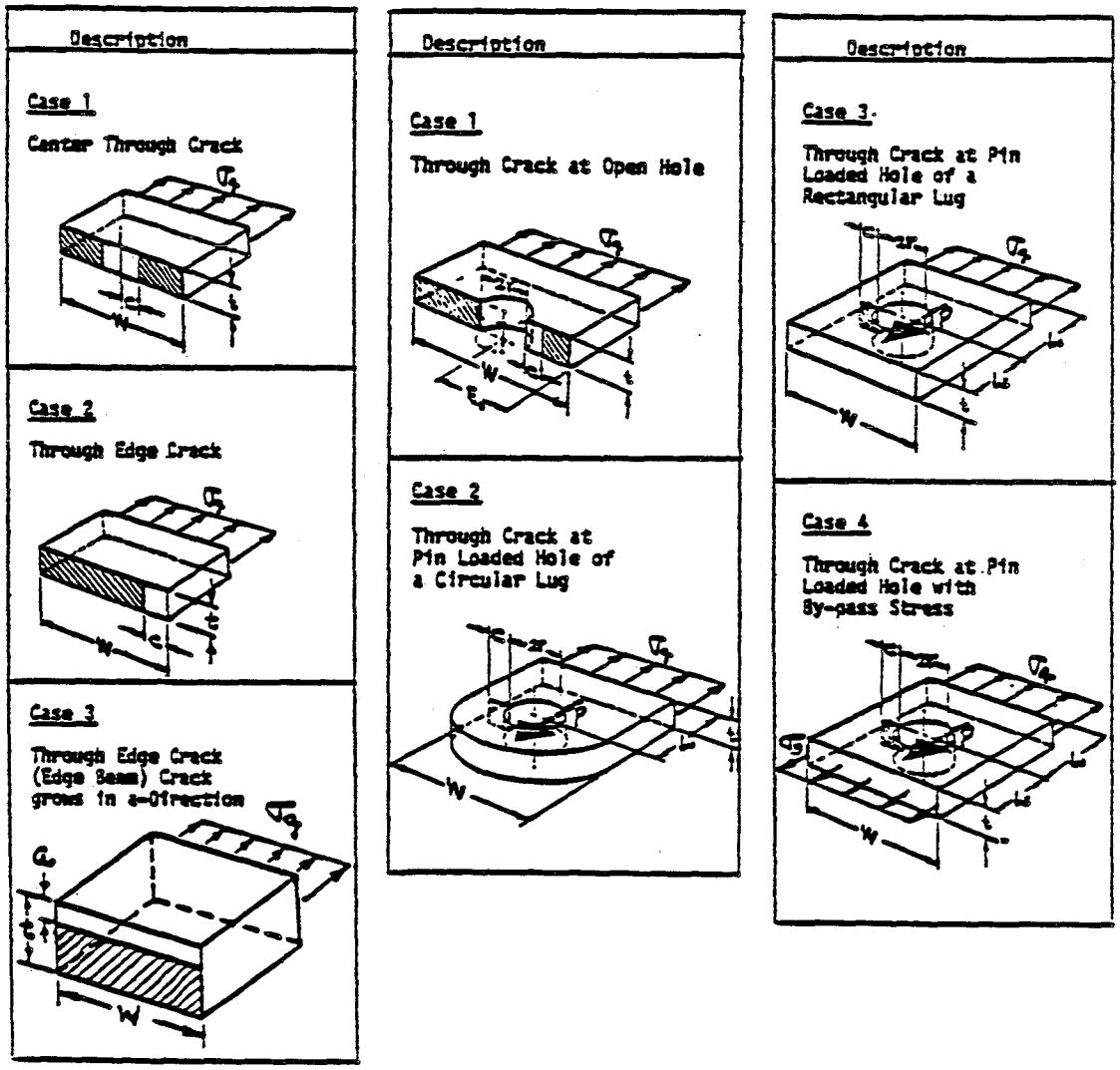

Figure 2-22 (Continued).

The module which performs stress intensity calculations currently includes stress intensity equations for the following geometries:

1) Crack in a finite width finite thickness plate - part-through crack, transition crack, through crack.

2) ASTM E399 compact specimen - through crack.

3) Single crack emanating from a hole - corner crack, internal crack, transition crack, through crack.

4) Two cracks emanating from a hole - corner crack, internal crack, transition crack, through crack.

5) Single crack emanating from a pin loaded lug - corner crack, internal crack, transition, crack, through crack.

6) Two cracks emanating from a pin loaded lug - corner crack, internal crack, transition crack, through crack.

7) Crack emanating from a notch - corner crack, internal crack, transition crack, through crack.

8) Cracks emanating from double notches - corner crack, internal crack, transition crack, trough crack.

Figure 2-23. Excerpt from flaw growth program, MSFC-2 [2-95], illustrating crack geometry library and load conditions (under tension unless otherwise noted).

crack front -- the point of maximum crack depth, a, and the intersection of the crack at the free surface -- which allows simultaneous surface flaw growth in two directions. However, a less sophisticated technique is sometimes employed as in BEWICH [2-87] which calculates stress intensities at only one location on the surface flaw and uses the assumption that the aspect ratio, 2c/a, remains constant to calculate crack growth in the second direction.

Applied loading is essentially restricted to uniform tension and pin loading in the "handbook" flaw geometries computer programs with the occasional exception of applied bending stress distribution for a surface flaw as found in FAST-2. Another option in several of these programs -- most notably MSFC-2 [2-95] -- provide a tabular input of stress intensity versus crack length, which may give the impression of complete generality of the stress distribution. However, the K-solution and distribution must be known a priori for it must be input by the user.

In contrast to the handbook-based stress intensity programs, BIGIF [2-17] and FATPAC [2-93] employ the "weight function" stress intensity calculation approach for similar flaw geometries and are capable of great generality in load or stress distribution input. For these programs, the user selects the appropriate flaw geometry and subsequently inputs a general stress field for the uncracked geometry. Figures 2-17 and 2-21 indicate the extensive libraries which have evolved for these two programs using the weight function approach. It is interesting to note in these two figures that no stress intensity solutions are specified for a specific component geometry such as a crack emanating from a hole, but rather concentrate on the flaw shape and cracking mode (I, II, or III). This is a direct consequence of the capability of inputting general stress distributions which can be determined analytically

or numerically for any desired component geometry and the relatively weak dependence of weight functions upon low-curvature surfaces and their geometrical features remote from the crack tip.

A major advantage of the BIGIF influence function (weight function) approach involves three-dimension, multidegree-of-freedom crack geometries such as surface flaws, corner cracks, and buried ellipses. In their most general form, weight functions are capable of calculating or estimating a) stress intensity factors at every point along the curved crack front, K(s), b) root-mean-square (RMS) values of stress intensities, $\bar{K}$, defined over a local area, and c) point estimates of stress intensities of the major and minor axes of the curved crack geometry. However, the weight functions for three-dimensional problems in BIGIF provide only the local RMS-averaged* values of stress intensity factor ($\bar{K}$); one value for each "degree-of-freedom (growing crack dimension)" built into the given crack model. The options presented by the weight function approach allow flexibility in allowing continuous crack geometry changes as propagation occurs. For example, a four degree-of-freedom buried elliptical crack uses four $\bar{K}$ values which allow independent growth of the major and minor axes and also two planar translations of the crack centroid. In other words, opposite ends of both the major and minor axes can grow at different rates. Four degrees-of-freedom may be necessary to analyze growth of embedded elliptical cracks under stress fields that are not symmetric with respect to the elliptical axes.

* The RMS-average corresponds to the strain energy release rate caused by perturbing a single crack degree-of-freedom, while holding all other degrees-of-freedom constant [2-17].

Stress gradients due to temperature gradients and residual stress fields in the vicinity of a crack are extremely important in subsequent crack propagation. Of the programs surveyed in Table 2-2, except for the influence function-based BIGIF and FATPAC Programs, none could model thermal or residual stress gradients, except for the very simple, but rarely occurring, cases of uniform distributions or, for some programs, linear spatial gradients (as arise from beam bending). Because of the general stress gradient input capabilities, BIGIF and FATPAC can accurately model many thermal and residual stress effects.

Plasticity effects on subsequent crack growth are divided into two categories in the programs reviewed. The first category is Irwin's [2-102] first order plasticity correction for crack tip yielding and involves modifying the actual crack length by adding on to it half the plastic zone size. The modified defect is then treated linear elastically. The plastic zone size is proportional to the square of the stress intensity divided by the material yield strength and depends upon the condition of plane stress or plane strain of the crack tip. Several of the computer programs, including BEWICH and FATPAC, have incorporated Irwin's plasticity correction. Application of the crack tip plasticity correction is straightforward for two-dimensional, one degree-of-freedom crack geometries, but various assumptions are usually made when applying it to the dimensional multi degree-of-freedom geometries. For example, FATPAC determines the plastic zone size for an embedded crack by using the value of K which is the greater of the two values corresponding to the two crack tips. Each half of the defect is then increased by half of this amount. Two errors often made by analysts seeking to employ these first order "corrections" are:

1. Use of monotonic yield stress failures to model cyclic plastic zones,

2. Use of da/dn (ΔK,R) data obtained from experiments in which the data reduction included no first order plasticity corrections.

The second category of plasticity effects, which have been included in the weight function programs BIGIF and FATPAC, is "constrained or contained plasticity" in which the plastic stress redistribution resulting from some significant load component is constrained by the primary elastic structure but still has non-negligible effects on the rate of subcritical crack growth [2-103]. The most common example of a contained plasticity problem is a stress concentration, such as a hole, causes local plastic response which is well constrained by the primary elastic structure surrounding it. FATPAC models the contained plasticity effect by calculating a plastic stress intensity factor, K_p, based on crack tip opening displacement which is calculated from weight functions defined within a Bilby, Coltrell and Dugdale yield model. BIGIF, does not use crack opening displacement, but calculates the yielded off stresses by employing a) Neuber's elastic plastic notch solution, b) the Ramberg-Osgood material stress-strain relation, and c) stress equilibrium perpendicular to the crack plane. The yielded-off stresses are subsequently used to propagate the flaw. FATPAC has been successfully benchmarked against solutions based upon dislocation models of extended symmetric cracks emanating from elliptic holes. BIGIF has been benchmarked by comparing its calculated elastic-plastic stress distribution to stress distributions obtained by elastic-plastic finite element analyses [2-103]. Section 4.2 discusses the procedures in BIGIF for contained plasticity in more detail.

As mentioned earlier, many of the codes listed in Table 2-2 also have capabilities of analyzing subcritical crack growth. Such capabilities are

discussed in Section 3.7, which also provides additional details on some aspects of their stress intensity factor evaluation capabilities.

2.4 REFERENCES

2-1. Paris, P.C., and Sih, G.C., "Stress Analysis of Cracks," Fracture Toughness Testing and Its Applications, ASTM Special Technical Publication 381, pages 30-81, 1965.

2-2. Broek, D., Elementary Engineering Factors Mechanics, Sijthoff and Noordhoff, Alphen aan den Rijn, Netherlands, 1978.

2-3. Tada, H., Paris, P.C., and Irwin, G.R., "The Stress Analysis of Cracks Handbook," Del Research Corporation, Hellertown, Pennyslvania, 1973.

2-4. Griffith, A.A., "The Phenomena of Rupture and Flow in Solids," Philosophical Transactions of the Royal Society of London, Series A, Vol. 221, pages 163-198, 1920.

2-5. Sih, G.C.M., "Handbook of Stress Intensity Factors," Lehigh University, Bethlehemn, Pennyslvania, 1973.

2-6. Cartwright, D.J., "Stress Intensity Factor Determination," Developments in Fracture Mechanics, Vol. 1, edited by G.G. Chell, Applied Science Publishers, London, pages 26-66, 1979.

2-7. Cartwright, D.J., and Rooke, D.P., "Evaluation of Stress Intensity Factors," Journal of Strain Analysis monograph, Vol. 10, No. 4, pages 260-263, Mechanical Engineering Publications, Ltd., London, October 1975.

2-8. Rooke, D.P., and Cartwright, D.J., Compendium of Stress Intensity Factors, Her Majesty's Stationery Office, London, 1975.

2-9. Rice, R.J., and Tracey, D.M., "Computational Fracture Mechanics," presented at Symposium on Numerical and Computer Methods in Structural Mechanics, University of Illinois, Urbana, September 8-10, 1971.

2-10. Hellen, T.K., "Numerical Methods in Fracture Mechanics," Developments in Fracture Mechanics, Vol. 1, edited by G.G. Chell, pages 145-181, Applied Science Publishers, London, 1979.

2-11. Wilson, W.K., "Finite Element Methods for Elastic Bodies Containing Cracks," Mechanics of Fracture I, edted by G.C. Sih, Chapter 9, pages 484-515, Noordhoff, 1973.

2-12. Kobayashi, A.S., editor, Experimental Techniques in Fracture Mechanics, Society for Experimental Stress Analysis Monograph No. 1, 1973.

2-13. Chan, S.K., Tuba, I.S., and Wilson, W.K., "On the Finite Element Method in Linear Fracture Mechanics," Engineering Fracture Mechanics, Vol. 2, pages 1-17, 1970.

2-14. Oglesby, J.J., and Lomacky, O., "An Evaluation of Finite Element Methods for the Computation of Elastic Stress Intensity Factors," Journal of Engineering for Industry, pages 177-184, February 1973.

2-15. Watwood, V.B., "The Finite Element Method for Prediction of Crack Behavior," Nuclear Engineering and Design, Vol. 11, No. 2, pages 323-332, November 1969.

2-16. Hilton, P.D., and Sih, G.C., "Applications of the Finite Element Method to the Calculations of Stress Intensity Factors," Mechanics of Fracture I, edited by G.C. Sih, Chapter 8, pages 426-483, Noordhoff, 1973.

2-17. Besuner, P.M., et al., BIGIF - Fracture Mechanics Code for Structures, Electric Power Research Institute RP700-5, EPRI Report NP-1830-CCM, 1981.

2-18. Besuner, P.M., "The Influence Function Method for Fracture Mechanics and Residual Life Analysis of Cracked Components Under Complex Stress Fields," Nuclear Engineering and Design, Vol. 43, No. 1, pages 115-154, August 1977.

2-19. Rice, J.R., "A Path Independent Integral and the Approximate Analysis of Strain Concentration by Notches and Cracks," Journal of Applied Mechanics, Vol. 35, pages 370-386, 1968.

2-20. Byskov, E., "The Calculation of Stress Intensity Factors Using the Finite Element Method with Cracked Elements," International Journal of Fracture Mechanics, Vol. 6, No. 2, pages 159-167, June 1970.

2-21. Tracey, D.M., "Finite Elements for Determination Crack Tip Elastic Stress Intensity Factors," Engineering Fracture Mechanics, Vol. 3, pages 255-265, 1971.

2-22. Wilson, W.K., "On Combined Mode Fracture Mechanics," University of Pittsburgh, Ph.D. Dissertation, 1969.

2-23. Hilton, P.D., and Hutchinson, J.W., "Plastic Intensity Factors for Cracked Plates," Journal of Engineering Fracture Mechanics, Vol. 3, pages 435-451, 1971.

2-24. Atluri, S., "Higher Order, Special and Singular Elements," Finite Element Methods, edited by A.K. Noor and W. Pilken, ASME New York, 1983.

2-25. Westmann, R., "GLASS II -- Global-Local Finite Element Analysis of Structural Systems," Electric Power Research Institute Report EPRI NP-1089, Palo Alto, California, 1979.

2-26. Besuner, P.M., and Snow, D.W., "Applications of the Two-Dimensional Integral Equation Method to Engineering Problems," Boundary Integral Equation Method: Computational Applications in Applied Mechanics, American Society of Mechanical Engineers AMD-Vol. 11, pages 101-117, New York, 1975.

2-27. Lachat, J.C., and Watson, J.O., "A Second Generation Boundary Integral Equation Program for Three-Dimensional Elastic Analysis," Boundary Integral Equation Method: Computational Applications in Applied Mechanics, American Society of Mechanical Engineers AMD Vol. 11, pages 85-100, New York, 1975.

2-28. Developments in Boundary Element Methods - 1, edited by P.K. Bannerjee and R. Butterfield, Applied Science Publishers, Ltd., London, 1979.

2-29. Developments in Boundary Element Methods - 2, edited by P.K. Bannerjee and R.P. Shaw, Applied Science Publishers, Ltd., London, 1982.

2-30. Gross, B., Srawley, J.E., and Brown, W.R,. Jr., "Stress Intensity Factors for a Single-Edge-Notch Tension Specimen by Boundary Collocation of a Stress Function," NASA Technical Note NASA-TN-D-2395, Lewis Research Center, Ohio, August 1964.

2-31. Kobayashi, A.S., Cherepy, R.B., and Kensil, W.C., "A Numerical Procedure for Estimating Stress Intensity Factor of a Crack in a Finite Plate," ASME Paper 63-WA-24, New York, 1963.

2-32. Newman, J.C., Jr., "An Improved Method of Collocation for the Stress Analysis of Cracked Plates with Various Shaped Boundaries," NASA Technical Note D-6376, 1971.

2-33. Hofmann, R., "Stealth: A Lagrange Explicit Finite-Difference Code for Solids, Structural and Thermohydraulic Analysis," Electric Power Research Institute Report NP-176, Palo Alto, California, 1976.

2-34. Wilkins, M.L., "Calculation of Elastic-Plastic Flow," Methods in Computational Physics, Vol. 3, Fundamental Methods in Hydrodynamics, edited by B. Alder, S. Feinbach and M. Rotenberg, pages 211-263, Academic Press, New York, 1964.

2-35. Rice, J.R., "Some Remarks on Elastic Crack-Tip Stress Fields," International Journal of Solids and Structures, Vol. 8, pages 751-758, 1972.

2-36. Bueckner, H.F., "A Novel Principle for the Computation of Stress Intensity Factors," Zeifschrift fur Angewandte Mathematik und Mechanik, Vol. 50, page 529, 1970.

2-37. Paris, P.C., McMeeking, R.M., and Tada, H., "The Weight Function Method for Determining Stress Intensity Factors," Cracks and

Fracture, ASTM Special Technical Publication 601, pages 471-489, 1976.

2-38. Cruse, T.A., and Besuner, P.M., "Residual Life Prediction for Surface Cracks in Complex Structural Details," Journal of Aircraft, Vol. 12, No. 4, pages 369-375, April 1975.

2-39. Hartranft, R.J., and Sih, G.C., "Alternating Method Applied to Edge and Surface Crack Problems," Mechanics of Fracture I, edited by G.C. Sih, Chapter 4, pages 179-238, Noordhoff, 1973.

2-40. Smith, F.W., Emery, A.F., and Kobayashi, A.S., "Stress Intensity Factors for Semicircular Cracks," Journal of Applied Mechanics, Vol. 34, pages 953-959, 1967.

2-41. Smith, F.W., and Alavi, M.J., "Stress Intensity Factors for a Penny Shaped Crack in a Half Space," Engineering Fracture Mechanics, Vol. 3, pages 241-254, 1971.

2-42. Smith, F.W., and Alavi, M.J., "Stress Intensity Factors for a Part Circular Surface Flaw," Department of Mechanical Engineering, Colorado State University, 1969.

2-43. Shah, R.C., and Kobayashi, A.S., On the Surface Flaw Problem, The Surface Crack: Physical Problems and Computational Methods, American Society of Mechanics Engineers, New York, 1972.

2-44. Shah, R.C., and Kobayashi, A.S., "Stress Intensity Factor for an Elliptical Crack Approaching the Surface of a Plate in Bending," Stress Analysis and Growth of Cracks, ASTM Special Technical Publication 513, pages 3-21, 1972.

2-45. Green, A.E., and Sneddon, I.N., "The Distribution of Stress in the Neighborhood of a Flat Elliptical Crack in an Elastic Solid," Proceedings of the Cambridge Philosophical Society, Vol. 46, pages 159-164, 1950.

2-46. Kassir, M.K., and Sih, G.C., "Three-Dimensional Stress Distribution Around an Elliptical Crack Under Arbitrary Loadings," Journal of Applied Mechanics, Vol. 33, pages 601-611, 1966.

2-47. Fung, Y.C., Foundations of Solid Mechanics, Prentice-Hall, Inc., Englewood Cliffs, New Jersey, 1965.

2-48. Neuber, H., Kerbspannungslehre, Springer, Berlin, 1937 and 1958.

2-49. Hartranft, R.J., and Sih, G.C., "The Use of Eigenfunction Expansions in The General Solution of Three-Dimensional Crack Problems," Journal of Mathematical Mechanics, Vol. 19, No. 2, pages 123-138, August 1969.

2-50. Gyekenyesi, J.P., Mendelson, A., and Kring, J., "Three-Dimensional Elastic Stress and Displacement Analysis of Finite Circular Geometry Solids Containing Cracks," NASA TN-D-7266, International Journal of Fracture, Vol. 11, No. 3, pages 409-429, June 1975.

2-51. Gyekenyesi, J.P., "Solution of Some Mixed Boundary Value Problems of Three-Dimensional Elasticity by the Method of Lines," Ph.D. Thesis, Michigan State University, 1972.

2-52. Faddeeva, V.N., "The Method of Lines Applicable to Some Boundary Problems," Trudy Mat. Institute, Steklov, Vol. 28, pages 73-103, 1949.

2-53. Newman, J.C., Jr., "A Review and Assessment of the Stress Intensity Factors for Surface Cracks," Part-Through Crack Fatigue Life Predictions, ASTM Special Technical Publication 687, pages 16-42, 1979.

2-54. Kobayashi, A.S., Polvnichi, N., Emery, A.F., and Love, W.J., "Inner and Outer Cracks in Internally Pressurized Cylinders," Journal of Pressure Vessel Technology, Vol. 99, Series J, No. 1, pages 83-89, February 1977.

2-55. Heliot, J., Labbens, R.C., and Pellisier-Tanon, A., "Semi-Elliptical Cracks in a Cylinder Subjected to Stress Gradients," Fracture Mechanics, ASTM Special Technical Publication 677, pages 341-364, 1979.

2-56. McGowan, J.J., and Raymund, M., "Stress Intensity Factor Solutions for Internal Longitudinal Semi-Elliptical Surface Flaws in a Cylinder Under Arbitrary Loading," Fracture Mechanics, ASTM Special Technical Publication 677, pages 365-380, 1979.

2-57. Raju, I.S., and Newman, J.C., Jr., "Stress Intensity Factor Influence Coefficients for Internal and External Surface Cracks in Cylindrical Vessels," Aspects of Fracture Mechanics in Pressure Vessels and Piping, ASME-PVP-Vol. 58, pages 37-48, New York, 1982.

2-58. Dedhia, D.D., and Harris, D.O., "Improved Influence Functions for Part-Circumferential Cracks in Pipes," to be presented at ASME Pressure Vessel and Piping Conference, Portland, Oregon, June 1983.

2-59. Smith, C.W., "Observations on Prediction on Non-Self-Similar Sub-critical Crack Growth and Stress Intensity Factor Distributions," Advances in Fracture Research, Vol. 1, pages 3-10, Pergamon Press, Oxford, England, 1982.

2-60. Atluri, S.N., and Kathiresan, K., "Stress Intensity Factor Solutions for Arbitrarily Shaped Surface Flaws in Reactor Pressure Vessel Nozzle Corners," International Journal of Pressure Vessels and Piping, Vol. 8, pages 313-322, 1980.

2-61. Schmitt, W., Keim, E., Wellein, R., and Bartholome, G., "Linear Elastic Stress Intensity Factors for Cracks in Nuclear Pressure Vessel Nozzles Under Pressure and Temperature Loadings," International Journal of Pressure Vessels and Piping, Vol. 8, pages 41-68, 1980.

2-62. Schmitt, W., Bartholome, G., Grostad, A., and Miksch, M., "Calculation of Stress Intensity Factors of Cracks in Nozzles," International Journal of Fracture, Vol. 12, No. 3, pages 381-390, June 1976.

2-63. Kobayashi, A.S., and Enetanya, A.N., "Stress Intensity Factor for a Corner Crack," Mechanics of Crack Growth, ASTM Special Technical Publication 590, pages 477-495, Pennsylvania, 1976.

2-64. Palisamy, S.S., and Raymond, M., "Stress Intensity Factor for a Corner Crack at the Edge of a Hole in a Plate," Fracture Mechanics: Thirteenth Conference, ASTM Special Technical Publication 743, pages 438-455, 1981.

2-65. Raju, I.S., and Newman, J.C., Jr., "Stress Intensity Factors for Two Symmetric Corner Cracks," Fracture Mechanics, ASTM Special Technical Publication 677, pages 411-430, 1979.

2-66. Rice, J.R., and Levy, N., "The Part-Through Surface Crack in an Elastic Plate," Journal of Applied Mechanics, Vol. 39, pages 185-194, 1972.

2-67. Rice, J.R., "The Line Spring Model for Surface Flaws," The Surface Crack: Physical Problems and Computational Solutions, pages 171-185, American Society of Mechanical Engineers, New York, 1972.

2-68. Parks, D.M. and White,C.S., "Elastic-Plastic Line Spring Finite Elements for Surface-Cracked Plates and Shells," Aspects of Fracture Mechanics in Pressure Vessels and Piping, ASME-PVP-Vol. 58, pages 159-174, New York, 1982.

2-69. Smith, F.W., and Sorensen, D.R., "The Semi-Elliptical Surface Crack -- A Solution by the Alternating Method," International Journal of Fracture, Vol. 12, No. 1, pages 47-57, February 1976.

2-70. Vijayakumar, K., and Atluri, S.N., "An Embedded Elliptical Flaw in an Infinite Solid Subjected to Arbitrary Crack-Free Tractions," Journal of Applied Mechanics, Vol. 48, pages 88-96, 1981.

2-71. Nishioka, T., and Atluri, S.N., "Analysis of Surface Flaw in Pressure Vessels by a New Three-Dimensional Alternating Method," Aspects of Fracture Mechanics in Pressure Vessel and Piping, ASME-PVP-Vol. 58, pages 17-35, 1982.

2-72. Poe, C.C., Jr., "Fatigue Crack Propagation in Stiffened Panels," Damage Tolerance in Aircraft Structures, ASTM Special Technical Publication 486, pages 79-97, 1971.

2-73. Westmann, R.A., "Notes on Estimating Critical Stress for Irregularly Shaped Planar Cracks," International Journal of Fracture Mechanics, Vol. 2, page 561, 1960.

2-74. Kobayashi, A.S., Ziv, M., and Hall, L.R., "Approximate Stress Intensity Factors for an Embedded Elliptical Crack Near Two Parallel Free Surfaces," International Journal of Fracture, Vol. 1, No. 2, pages 81-95, 1965.

2-75. Kobayashi, A.S., Emery, A.F., Love, W.J., and Antipas, A., "Embedded Elliptical Crack at a Corner," ASME Paper 78-PVP-5, Journal of Pressure Vessel Technology, Vol. 100, pages 28-33, February 1978.

2-76. Sanders, J.L., Jr., "Effect of a Stringer on the Stress Concentration Due to a Crack in a Thin Sheet," Langley Research Center, Virginia, NASA TR-R-13, Washington, D.C., 1959.

2-77. Davis, C.S., "Inclusion of Crack Growth and Fracture Constraints in Automated Design," Ph.D. Dissertation, University of California, Los Angeles, March 1976.

2-78. Greif, R. and Sanders, J.L., "The Effect of a Stringer on the Stress in a Cracked Sheet," Journal of Applied Mechanics, Vol. 32, No. 1, pages 59-66, March 1965.

2-79. Isida, M., "Analysis of Stress Intensity Factors for the Tension of a Centrally Cracked Strip with Stiffened Edges," Engineering Fracture Mechanics, Vol. 5, No. 3, pages 647-665, September 1973.

2-80. Timoshenko, S.P., and Woinowsky-Krieger, S., Theory of Plates and Shells, McGraw-Hill, New York, 1959.

2-81. Williams, M.L., "The Bending Stress Distribution at the Base of the Stationary Crack," Journal of Applied Mechanics, Vol. 28, pages 78-82, March 1961.

2-82. Reissner, E., "The Effect of Transverse Stress Deformation on the Bending of Elastic Plates," Journal of Applied Mechanics, Vol. 12, pages A-69 - A-77, 1945.

2-83. Hartranft, R.J., and Sih, G.C., "Effect of Plate Thickness on the Bending Stress Distribution Around Through Cracks," Journal of Mathematics and Physics, Vol. 47, No. 3, pages 276-291, September 1968.

2-84. Sih, G.C., and Haggendorf, H.C., "A New Theory of Spherical Shells with Cracks," Thin Shell Structures: Theory, Experiment and Design,

edited by Y.C. Fung and E.E. Sechler, Prentice-Hall, New Jersey, pages 519-545, 1974.

2-85. Krenk, S., "Influence of Transverse Shear on an Axial Crack in a Cylindrical Shell," International Journal of Fracture, Vol. 14, No. 2, pages 123-143, April 1978.

2-86. Delale, F., and Erdogen, F., "Transverse Shear Effect in a Circumferentially Cracked Cylindrical Shell," Quarterly of Applied Mathematics, pages 239-257, October 1979.

2-87. Imtiaz, S. K. and Smith, B. L., "A Computer Program for Predicting Fatigue Crack Propagation," SAE Technical Paper N-810594, Beech Aircraft Corporation, Wichita, Kansas, 1981.

2-88. Johnson, W.S., "Input/Output Guide, CGR-LaRC, Crack Growth Prediction Program," NASA-LRC Documentation.

2-89. Engle, R.M., "Cracks, A Fortran IV Digital Computer Program for Crack Propagation Analysis," AFFDL-TR-70-107, Air Force Flight Dynamics Laboratory, Wright Patterson Air Force Base, 1970.

2-90. Engle, R.M., "CRACKGRO, Theoretical Background and Input Manual," Wright Patterson Air Force Base.

2-91. Szamossi, M., "Crack Propagation Analysis by G. Vroman's Model, Computer Analysis Summary, Program EFFGRO," Rockwell International, North American Aircraft Division, NA-72-94, 1972.

2-92. Newman, J.C., "Instructions for Use of FAST-2, A Program for the Fatigue-Crack Growth Analysis of Various Crack Configurations," NASA Langley Research Center, 1982.

2-93. Chell, G.G., "FATPAC: A Computer Program for Calculating Fatigue Crack Growth," Central Electricity Research Laboratories, England, RD/L/N205/78, 1979.

2-94. Hu, T., "Advanced Crack Propagation Predictive Analysis Computer Program FLAGRO 4, Software Documentation," (COSMIC), MSC-18718, 1979.

2-95. Creager, M., "MSFC Crack Growth Analysis Computer Program, Version II (User's Manual)," NASA:MSFC, NASA CR-150153, 1976.

2-96. Cipolla, R., "Computational Method to Perform the Flaw Evaluation Procedure as Specified in the ASME Code, Section XI, Appendix A," Failure Analysis Associates Report to EPRI, FAA-76-2-1 (I), 1976.

2-97. Iskander, R.D., Cheverton, R.D., and Ball, D.G., "OCA-1, A Code for Calculating the Behavior of Flaws on the Inner Surface of a Pressure

Vessel Subject to Pressure and Temperature Transients," U.S. Nuclear Regulatory Commission Report NUREG/CR-2113, August 1981.

2-98. Besuner, P., "Preliminary Analysis of Weld Cracks in A Petroleum Refinery Pressure Vessels," Failure Analysis Associates Report FAA-82-1-2 to Engineering Advancement Association of Japan and Chiyoda Chemical Engineering and Construction Co., Ltd., January 1982.

2-99. Pennick, H.G., Cook, T.S., and Wells, C.H., "General Description Manual for Turbine Rotor Lifetime Prediction Analysis Systems, EPRI Task RP502, 1977-1978.

2-100. Dedhia, D.D., Harris, D.O., and Denny, V.E., "TIFFANY -- A Computer Code for Thermal Stress Intensity Factors for Surface Cracks in Clad Piping," Lawrence Livermore National Laboratory Final Report, Contract 8679501, 1982.

2-101. Dedhia, D.D., and Harris, D.O., "Stress Intensity Factors for Surface Cracks in Pipes: A Computer Code for Evaluation by Use of Influence Functions," EPRI Final Report NP-2425, 1982.

2-102. Irwin, G., "Plastic Zone Near a Crack and Fracture Toughness," Proceedings of the Seventh Sagamore Conference, pages IV-63, 1960.

2-103. Besuner, P., and Rau, S., "Stress and Subcritical Crack Growth Analysis Under Contained Plastic Conditions," EPRI Key Phase Report NP-81-8-LD, April 1981.

Section 3

SUBCRITICAL GROWTH OF CRACKS

Cyclic loading is one of the most common causes of failure of structural and machine components. This is especially true in the aerospace field. Such failures can occur in an initially "flaw-free" material, and the familiar "S-N" curve approach is used for design purposes. In such an approach, the combined effects of both crack initiation and propagation are included in the cycles to failure. Many structural components contain crack-like defects that were introduced during fabrication. Such cracks can grow in a subcritical manner leading to a failure when they reach a critical size. One of the major uses and powers of fracture mechanics is its application for analyzing such subcritical crack growth.

3.1 BASIC REVIEW OF FATIGUE CRACK GROWTH

Cracks can grow in a subcritical manner due to a number of factors, including cyclic loading (or fatigue), stress corrosion cracking or hydrogen induced crack growth [3-1]. Various combinations of these growth mechanisms can occur, with environmentally accelerated fatigue crack growth (often known as corrosion fatigue) being a common example.

Fatigue crack growth will be concentrated upon in this report because of its importance in aerospace applications. Environmental influences on fatigue crack growth will be considered. A simple discussion of fatigue crack growth, and an example of its use will be presented before proceeding to a review of

the current state-of-the-art of this aspect of linear elastic fracture mechanics.

The hypothesis that the rate of fatigue crack growth per cycle of loading (da/dn) is dependent on the magnitude of the cyclic stresses in the vicinity of the crack-tip, in conjunction with the observation that the magnitude of these cyclic stresses in a nominally elastic body is controlled by the value of the cyclic stress intensity factor (ΔK), leads to the realization that [3-2]*

$$\frac{da}{dn} = F\ (\Delta K) \qquad (3\text{-}1)$$

The function $F(\Delta K)$ depends on the material, of course, as well as other parameters, such as the mean value of K and the environment (air, vacuum, salt water, etc.). The function $F(\Delta K)$ can be determined experimentally under laboratory conditions and the information then used to calculate the growth behavior of cracks under service conditions. This ability to predict service performance for a wide range of cyclic stresses and crack and structural geometries is one of the major uses of fracture mechanics.

The following is a commonly observed form of Equation 3-1

$$\frac{da}{dn} = C\ (\Delta K)^m \qquad (3\text{-}2)$$

*Crack growth under cyclic loading conditions that involves extensive plastic deformation may require the use of concepts beyond linear elastic fracture mechanics. Section 4.2 includes a discussion of such considerations.

This form is applicable to an amazingly wide range of materials and ΔK levels and is commonly referred to as the Paris "law". As will be discussed in detail in later portions of Section 3, this relationship is subject to numerous modifications to account for the influence of thresholds, mean value of K, non-uniform value of ΔK, environment, imminence of catastrophic failure, etc.

As an example of the use of fracture mechanics in analysis of fatigue crack growth, consider a panel of width, W, with a central crack of length $2a_0$, subjected to a cyclic stress $\Delta\sigma = \sigma_{max} - \sigma_{min}$. This panel is composed of a material whose crack growth relation is

$$\frac{da}{dn} = C\,\Delta K^4 \tag{3-3}$$

This material has a fracture toughness value K_{Ic}.

One form of the K-relation for this geometry is given by the following expression [3-3]

$$K = \sigma\,(\pi a)^{1/2}\,\frac{1 - 0.5\,(2a/W) + 0.326\,(2a/W)^2}{(1 - 2a/W)^{1/2}} \tag{3-4}$$

The number of cycles of loading of $\Delta\sigma$ that the panel can sustain without failure is of interest. Obviously, this is the number of cycles (n_f) required to grow the crack from the initial size, a_0, to the critical size, a_c. The first step is to determine the critical crack size. This is accomplished by solving the following equation, which is usually done by trial and error

$$K_{Ic} = \sigma_{max} (\pi a_c)^{1/2} \frac{1 - 0.5 (2a_c/W) + 0.326 (2a_c/W)^2}{(1 - 2a_c/W)^{1/2}} \qquad (3\text{-}5)$$

If the number of cycles to failure is large, the crack size as a function of the number of fatigue cycles can be determined by considering the crack growth "law" as a differential equation which is solved by separation of variables and integrating. The following parameters are defined for convenience:

$$\alpha = a/W$$

$$Y(\alpha) = \frac{1 - 0.5 (2\alpha) + 0.326 (2\alpha)^2}{(1 - 2\alpha)^{1/2}} \qquad (3\text{-}6)$$

The following first order ordinary differential equation is obtained by combining Equations 3-3, 3-4 and 3-6 and using the definition of α

$$\frac{da}{dn} = C (\Delta K)^4 = C(\Delta\sigma)^4 \pi^2 a^2 [Y(\alpha)]^4$$

$$W \frac{d\alpha}{dn} = C(\Delta\sigma)^4 \pi^2 W^2 \alpha^2 [Y(\alpha)]^4$$

Separating variables, integrating, and using the initial and final conditions provide the following result

$$n_f = \frac{1}{C (\Delta\sigma)^4 \pi^2 W} \int_{\alpha_0}^{\alpha_c} \frac{dx}{x^2 [Y(x)]^4} \qquad (3\text{-}7)$$

The integral in this expression cannot be evaluated in closed form because of the complexity of the form of $Y(\alpha)$. The integral can be easily evaluted by numerical techniques. In the literature, $Y(\alpha)$ is often taken to be a constant equal to its initial value. This allows the integral in Equation 3-7 to be easily evaluated in closed form. However, the approximate nature of this procedure should be borne in mind. In the case where the number of cycles to failure is not large, the integration procedures in Equation 3-7 can be replaced by cycle-by-cycle calculations.

The above procedure for evaluating remaining lifetime is intended to provide a simple example of the use of fatigue crack growth analysis in the evaluation of remaining lifetime. Many complicating factors occur in most actual situations, such as the influence of cyclic stress levels that vary from cycle-to-cycle. Detailed review of the various factors involved in more detailed and complex analyses will be provided in the remaining portion of Section 3.

3.2 STRESS RATIO EFFECTS

Stress ratio effects refer to variations in fatigue crack growth rate (da/dn) for a given ΔK that result from differences in the mean value of K. The load ratio

$$R = \frac{K_{min}}{K_{max}}$$

is used as a measure that is related to the mean value of K. The stress ratio has been shown to have a significant influence [3-4] as shown in Figure 3-1.

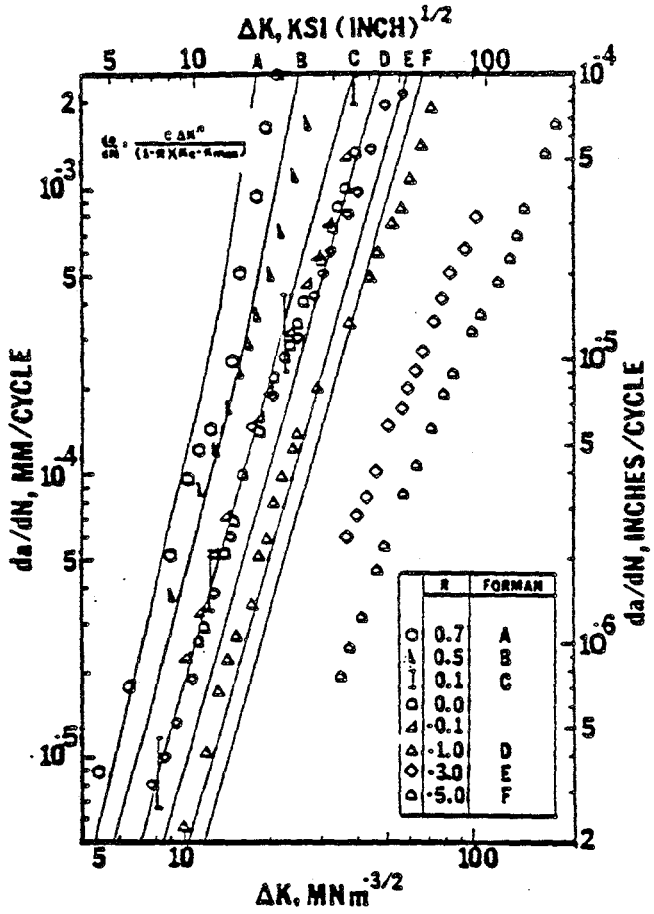

Figure 3-1. Crack Growth Rate in Ti-6Aℓ-4V as a Function of Stress Intensity Range for the Various R Ratios Using Forman's Equation [3-4].

Several relationships between da/dn and ΔK that include R have been suggested, with Forman's relation [3-5] being one of the most widely used. This relation is as follows:

$$\frac{da}{dn} = \frac{C(\Delta K)^m}{(1 - R) K_c - K_{max}} \tag{3-8}$$

Figure 3-1 shows a comparison of experimental data with predictions based on this relationship. Good agreement for positive R is observed, but the agreement for negative R is poor.

The dominant mechanism behind the stress ratio effect on fatigue crack growth rate remains unclear. Crack closure arguments have been used by some researchers to explain the stress ratio effect. Elber's empirical relation [3-6]

$$U = \frac{(S_{max} - S_{op})}{(S_{max} - S_{min})} = 0.5 + 0.4\ R \quad (-0.1 < R < 0.7) \tag{3-9}$$

implies that the minimum stress, S_{min}, never exceeds the crack opening stress, S_{op}, for 2024-T3 aluminum in the range of R between -0.1 and 0.7; therefore, the crack growth rate for this range of R is dominated by closure and dependent on R through U in the relation

$$\frac{da}{dn} = C(U\Delta K)^m \tag{3-10}$$

The aluminum sheet specimens tested by Elber were 5 mm thick. Although it is not known for certain, large amounts of residual plasticity associated with these thin specimens may have resulted in a high crack opening stress. Radon

[3-7], in his research on thresholds in steel, showed a marked influence of specimen thickness on the crack opening stress. Thicker specimens were found to have a much lower crack opening stress than thin specimens in a range of thicknesses from 12 - 50 mm. Radon does point out, however, that data exists showing the opposite trend for aluminum. Yuen, et al. [3-4], in experiments of Ti-6Aℓ-4V, have shown a linear dependence of ΔK_{eff} on R-ratio for values of R above which the crack is fully open. The value of R above which the crack always remains open was determined by Shih and Wei [3-8] to be 0.1 in this material.

Further studies by Yuen, et al., revealed that the following relationship provided close correlation for R in the range from -5 to 0.7.

$$\frac{da}{dn} = C(\Delta K_{eff})^m \qquad (3\text{-}11)$$

$$\Delta K_{eff} = \frac{1.63}{1.73 - R} \Delta K$$

Figure 3-2 shows the good correlation obtained by use of this relationship. Equation 3-11 is closely related to correlations observed by numerous other investigators as exemplified by James [3-9].

Crack closure is not the only phenomenon influencing the stress ratio effect. Musuva and Radon [3-10] have presented arguments indicating environmental effects may be significant in the observed variation in growth rate with stress ratio, making reference to data for steels in vacuum which show no stress ratio effect. The higher value of K_{max} associated with high stress ratios creates a large stress gradient to promote hydrogen diffusion and thus

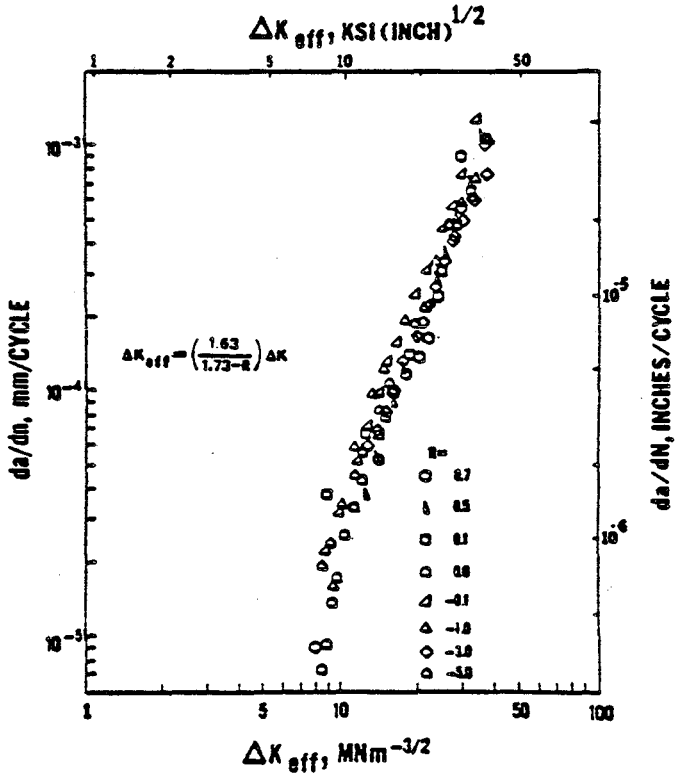

Figure 3-2. Crack Growth Rate as a Function of the Effective Stress Intensity Range for the Various R-Ratios [3-4].

increase crack growth rate. Higher test frequencies would not provide favorable conditions for hydrogen diffusion to the crack-tip because of the higher velocity of the advancing crack at faster growth rates. At low growth rates and low frequencies, however, environmental effects may have much more influence on the R-ratio effect. Although adequate empirical relations exist to quantify the effect of stress ratio on fatigue crack growth rate, more research is necessary to identify the dominant mechanisms. Additional discussions on the influence of environment on fatigue crack growth rates is included in Section 3.5.

3.3 THRESHOLD EFFECTS

Threshold stress intensity factors, ΔK_{th}, exist, below which opening mode fatigue crack growth does not occur or occurs at a rate too slow to measure. Although a general concensus has not been reached, crack growth rates below 10^{-8}in/cycle are seldom reported in the literature. Large amounts of data have been generated which support the existence of a fatigue crack propagation threshold. Throughout the 1960's and early 1970's, it was generally assumed that fatigue threshold for a material was dependent on the stress ratio, R, essentially independent of mechanical properties and only slightly affected by frequency of loading and environment. Since the early 1970's, however, extensive research conducted in the area of loading frequency and environmental effects has shown a significant influence of these variables on fatigue threshold. The frequency and environmental effects on threshold will not be covered here as they are addressed under the general heading of frequency and environmental effects on fatigue.

The increased research on fatigue threshold has produced a great deal of enlightening data, but has spawned numerous controversies over the mechanisms used to explain observations and the experimental methods for obtaining useful values of fatigue threshold. Following Elber's development of fatigue crack closure arguments in the early 1970's, researchers began to explain many threshold effects using crack closure theories. Many of these theories and approaches were presented at an international conference [3-11] on Fatigue Thresholds, Fundamentals and Engineering Applications. At this conference, Paris noted that despite the vast amount of existing data on thresholds, unified theories do not yet exist and need to be developed. Paris also commented that the key questions to be resolved are those on crack closure relative to fatigue thresholds and growth. Noted researchers such as Smith [3-12], Cadman [3-13], agree that due to the sensitivity of threshold values to load history and environment, the best method for determining ΔK_{th} is through experimental testing under conditions which best simulate service and that published data is often relevant only for the specific conditions used during the tests.

It is generally accepted that fatigue threshold decreases with increasing stress ratio. Empirical relations have been developed to model this variation with R, yet controversy still exists over the range of applicability for these relations. The commonly used empirical relations for the variation of ΔK_{th} with R are of the general form

$$\Delta K_{th} = [1 - C\ R]\ \Delta K_{th_o} \qquad (3\text{-}12)$$

where ΔK_{th_o} is the threshold at R = 0, and C is a constant. Rolfe and Barsom [3-14], using data published by various researchers for a wide variety of steels (Figure 3-3), state that for R > 0.1, conservative predictions of ΔK_{th} can be obtained using

$$\Delta K_{th} = [1 - 0.85\ R]\ 6.4\ \text{ksi}\sqrt{\text{in}} \qquad (3\text{-}13)$$

and for R < 0.1, ΔK_{th} is independent of R and has a value of 5.5 $\text{ksi}\sqrt{\text{in}}$. It is believed that the constant value of ΔK_{th} for negative values of R results from considering only the portion of the loading cycle in which K_{min} is positive (i.e., K_{min} is taken as zero if the actual calculated value is negative). Chalant and Rémy [3-15] argue that an equation of the form of Equation 3-13, with C = 1, is applicable for any load ratio R, where -1.0 < R < 1.0. Radon [3-7], however, conducted tests in low alloy steel BS4360-50D and obtained, using crack closure arguments, the expression

$$\Delta K_{th} = (1 - R)\ (K_{CL} + \Delta K_{C,th}) \qquad (3\text{-}14)$$

where K_{CL} is the crack closure stress intensity factor and $\Delta K_{C,th}$ is the threshold ΔK at the specific R-ratio, R_C, for which the applied K_{min} is equal to K_{CL}. Radon also states that there is no variation in ΔK_{th} for increases in R above the R_C level. Radon attributes the knee in the high-R end of Figure 3-4 to this R_C level. Tests conducted by Chalant and Rémy [3-15] on a Co33Ni alloy at various crack growth rates (Figure 3-5) have shown that as the growth rate at which the threshold is measured decreases, the knee at high R values disappears, indicating closure may not be the controlling mechanism. Data for

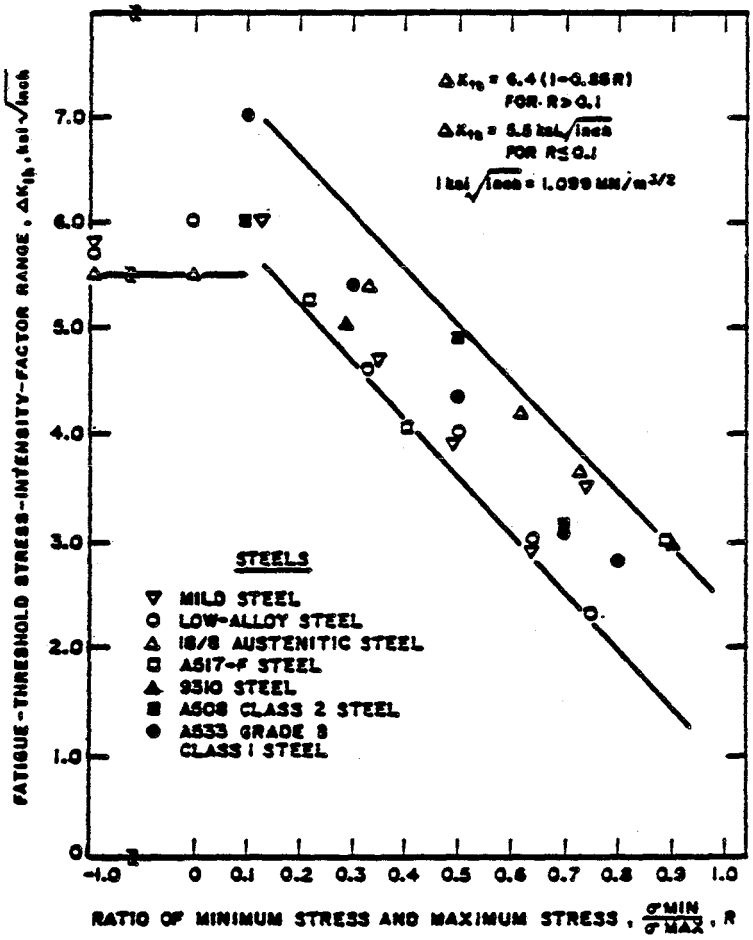

Figure 3-3. Variation of Threshold Stress Intensity Factor with R-Ratio for a Wide Variety of Steels Showing Linear Decrease with Increasing R [3-14].

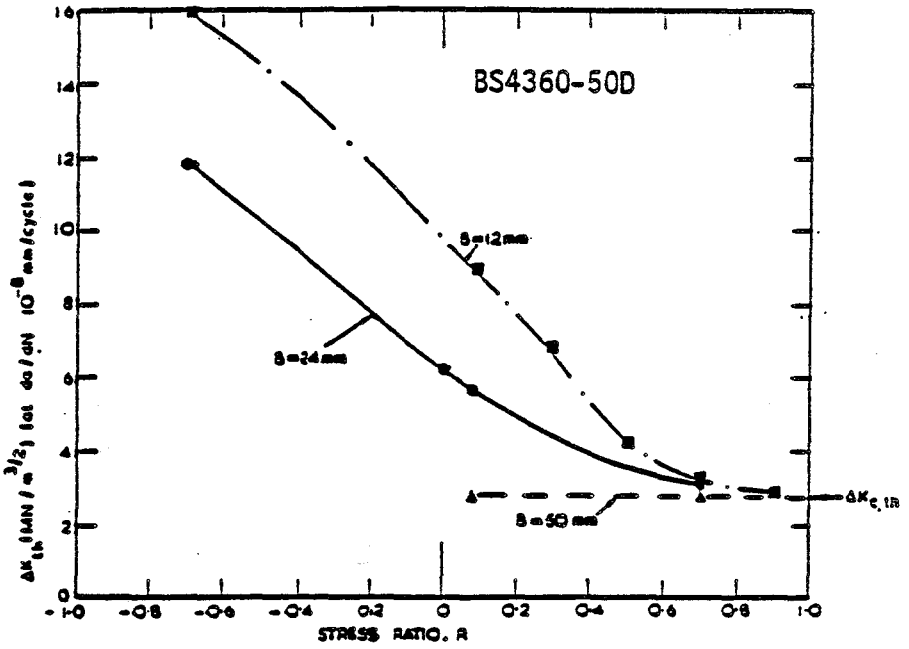

Figure 3-4. Influence of R-Ratio on Threshold ΔK for BS4360-50D Steel (Data of Radon [3-7]).

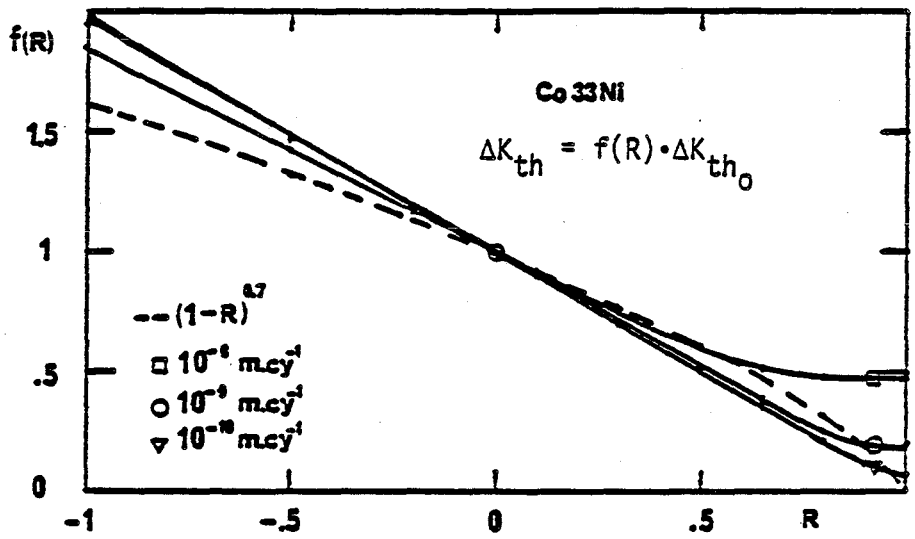

Figure 3-5. Influence of R-Ratio on Threshold ΔK for Co33Ni Alloy (Data of Chalant and Rémy [3-15]).

a titanium alloy (Figure 3-6), Ti-6Al-4V, presented by Hopkins, et al. [3-16] shows the linear decrease in threshold with increasing R continues for R-ratios above 0.3, the observed closure value for the material. In the absence of a clear understanding of the mechanisms which cause the variations in fatigue threshold values with increases in load ratio, R, at values of R above the closure level, it is important that thresholds be experimentally determined for high R-ratio applications such as fatigue life predictions involving mixed low and high cycle fatigue.

In recent years, there has been a growing concern over the application of continuum mechanics principles and test data for long cracks to the analysis of short cracks. Such concerns have led to specially developed techniques applicable to short cracks, with Reference 3-17 providing an example of efforts in this area. The purpose of the current discussion is not to review this area in general, but to discuss the special aspects of relevance to thresholds for fatigue crack growth.

A short crack can be defined as a crack that propagates at a different rate than a long crack in the same material and subject to the same "equivalent" driving force [3-18]. Problems can arise when cracks are (i) of a size comparable to the scale of plasticity, (ii) of a size comparable to the scale of the microstructure, or (iii) physically small such that closure, geometry, or environment can significantly affect behavior relative to that of long cracks. In fact, many of the differences in behavior between long and short cracks can be attributed to their different crack closure behavior [3-19]. The primary differences between the growth of short cracks and long cracks have been summarized by Schijve [3-20] and are presented in Table 3-1.

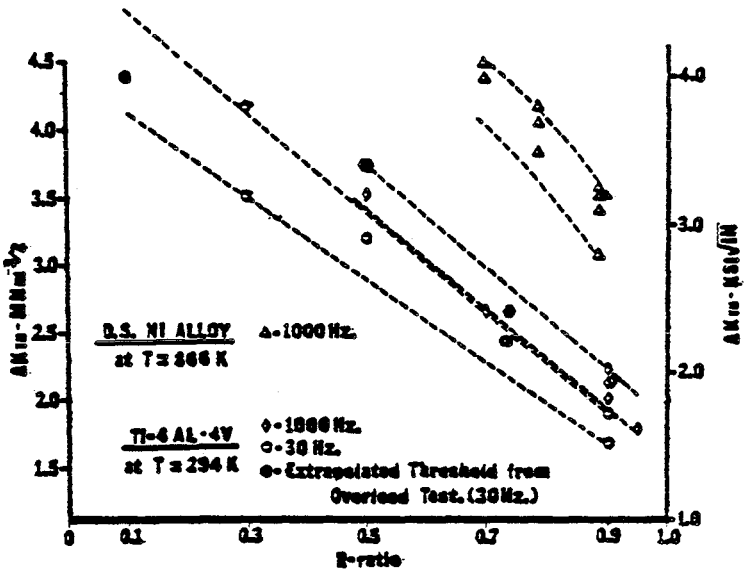

Figure 3-6. Influence of R-Ratio on Threshold ΔK for Ti-6Al-4V and Nickel Alloy Showing Linear Decrease in ΔK_{TN} With Increasing R (Data of Hopkins, et al [3-16]).

Table 3-1
Summary of Differences Between Growth of Short and Long Cracks [3-20]

DIFFERENCE BETWEEN THE GROWTH OF

		MICRO CRACKS	MACRO CRACKS
Aspects of mechanisms			
crack front length / grain diam.		small	large
restraint on slip		low 	high 
number of active slip systems		1 can be sufficient	≥2 (usually)
slip band cracking		possible	difficult
crack growth by	• shear decohesion • tensile decohesion • environmentally assisted decohesion	different mechanisms can apply	
striations		no (?)	yes
plasticity in wake of crack		limited	evident
fracture surface topography		?	not flat on micro level
Aspects of material inhomogeneity		MICRO CRACKS	MACRO CRACKS
elastic anisotropy		can be significant	averaged effect
inclusions		can start micro cracks	small effect (sometimes retarding)
grain boundaries		can be significant	average effect
material surface layer	examples: nitriding decarburizing shot peening rough surface	large effect (local properties)	negligible effect (bulk properties)

Although the mechanics of short crack behavior is still largely undefined, a few empirical models have been developed in regards to threshold conditions for design application. Romaniv, et al., [3-21] investigated short crack behavior in specimens of mild steel, aluminum alloy and austenitic steel. They found that in mild steel and aluminum initial fatigue crack length reduction resulted in a significant decrease in ΔK_{th}. These two materials also exhibited evidence of a critical initial crack length above which ΔK_{th} is independent of crack length. Through analysis of experimental data, Romaniv derived a relationship between the threshold stress intensity factor range for short cracks, ΔK_{th}^{SH}, and that for long cracks, ΔK_{th}. This relationship is presented in the following equation:

$$\Delta K_{th}^{SH} = \Delta K_{th} \left(\frac{a_s}{a_s^o} \right)^r \qquad (3\text{-}15)$$

where a_s is the short-crack length, a_s^o is the critical crack length above which crack length effect on ΔK_{th} is not observed, and r is an experimentally determined exponent dependent upon the material structure. Figure 3-7 shows the data used by Romaniv and the values of the terms defined above which fit Equation 3-15 to the data. Although the mechanics of the short crack phenomena are not identified, the empirical relation proposed by Romaniv is a good start to the characterization of short crack behavior.

Many problems and wide discrepancies exist in the experimental methods used to measure ultra-low fatigue crack growth rates and the definition of threshold stress intensity range. The most widely used method for experimental determination of fatigue threshold is "down-loading," as shown in Figure 3-8 [3-22]. This method involves propagating a fatigue crack at

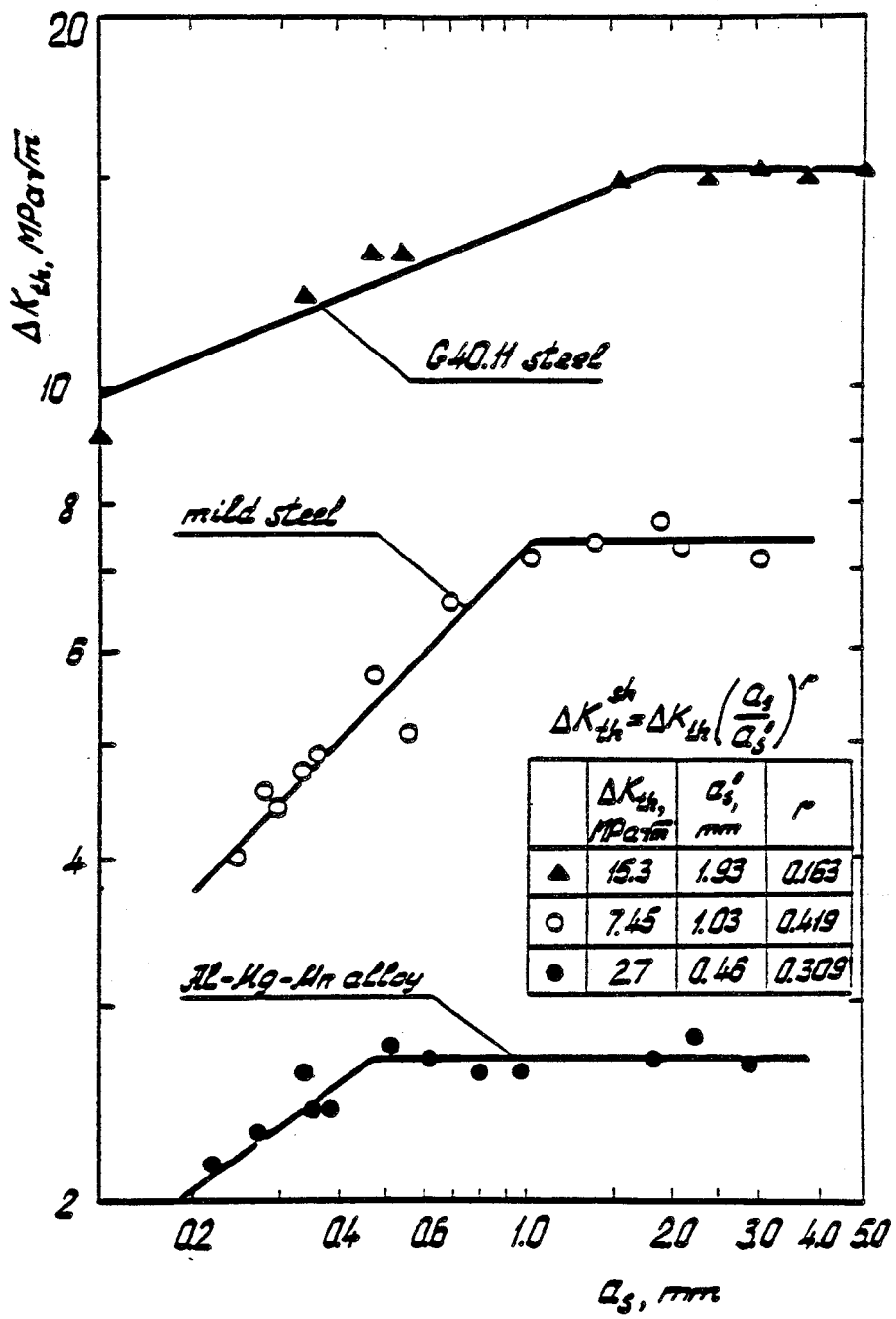

Figure 3-7. Data of Romaniv, et al [3-21] Showing the Influence of Crack Length on Threshold ΔK.

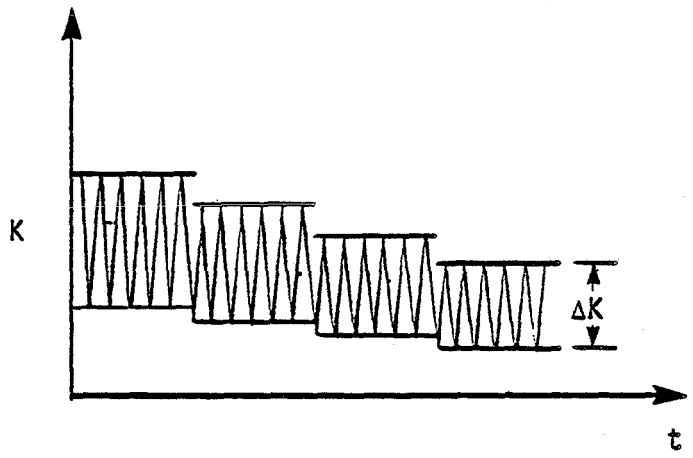

Figure 3-8. Schematic Representation of the "Down-Loading" Technique for Experimental Determination of Threshold ΔK.

successively decreased values of ΔK at a given stress ratio until no further propagation is observed. Although this general method is widely used, and has been proposed as an ASTM standard, a great deal of controversy persists over the associated requirements to prevent any effect of prior crack-tip plasticity on the value of ΔK_{th}. The ASTM proposed method requires that load-range reductions be no more than 10% of the previous range, and that crack advance between successive load-range reductions be no less than 0.5 mm. Cadman, et al., [3-13] have shown that these requirements may make the determination of very low threshold values at low crack growth rates difficult using standard specimen sizes due to the increase in ΔK with crack length. They have also observed increases in threshold with decreases in the rate of reduction of ΔK. This is contrary to the rationale on which the ASTM requirements are based.

Another method for experimental determination of fatigue threshold is "up-loading," as shown in Figure 3-9. One advantage to this method is that the crack-tip does not feel any overload effects from previous K_{max} values exceeding the K_{max} of the threshold, however, it can be difficult to obtain a valid precrack at low stress ratios. Hopkins, et al., [3-16] used this method in research of overload effects on threshold in commercial nickel-base and titanium-base alloy. As shown in Figures 3-10 and 3-11, they found that the threshold increased exponentially with the magnitude of a prior overload. This effect could be of great significance in certain cases of mixed low and high cycle fatigue. More detailed discussion of the influence of overloads on fatigue crack growth in general, as well as mixed low and high cycle fatigue, are included in the following sections. Additionally, Section 3.5.2 discusses the influence of various environments on fatigue crack growth thresholds.

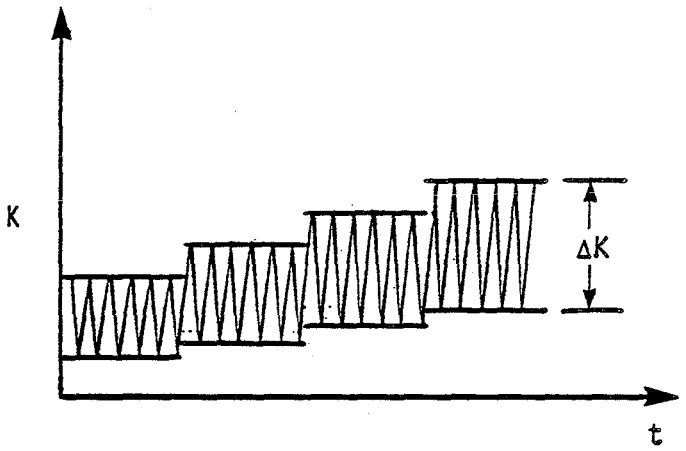

Figure 3-9. Schematic Representation of the "Up-Loading" Technique for Experimental Determination of Threshold ΔK.

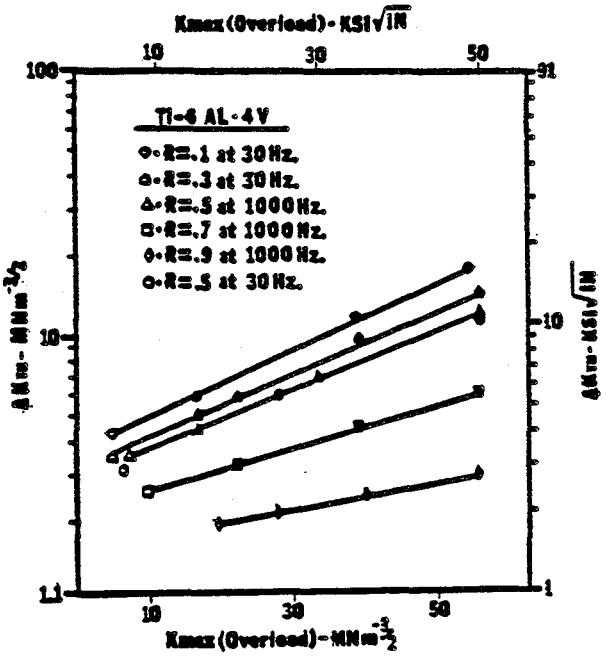

Figure 3-10. Overload Modified Threshold Stress Intensity Factor as a Function of the Maximum Single Cycle Overload Stress Intensity Factor for Ti-6Al-4V at 294 K and at both 1000 and 30 Hz [3-16].

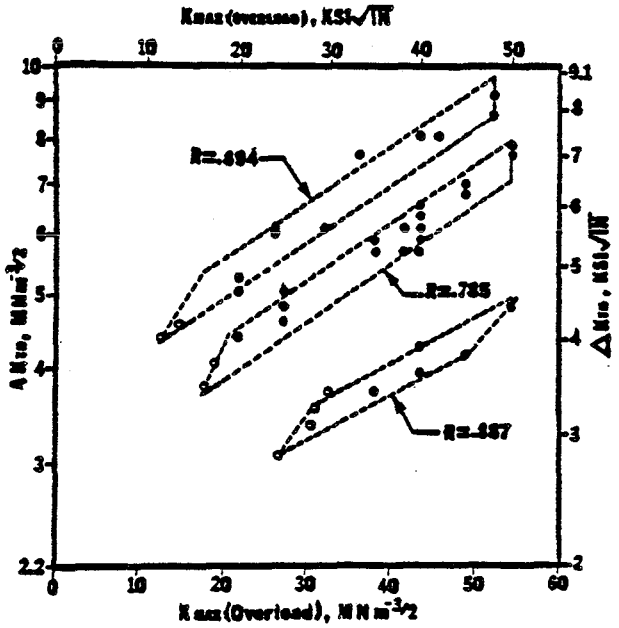

Figure 3-11. Overload Modified Threshold Stress Intensity Factor for the DS Nickel Alloy at 1000 Hz and 866 K After Single Cycle Overloads to Various K_{max} (Open Symbols Represent ΔK_{th} Without Overload) [3-16].

3.4 SUBCRITICAL GROWTH UNDER VARIABLE AMPLITUDE LOADING

Cyclic stresses that vary from cycle-to-cycle can produce fatigue crack growth that differs markedly from predictions made using crack growth characteristics from tests performed using constant cyclic stress. Such variable amplitude loading is often referred to as load interaction, and may retard crack growth.

3.4.1 Types of Variable Amplitude Loadings

The term variable-amplitude loading covers a wide range of loading types. The following five general categories have been used [3-23] to classify these different loading types:

1) Overloads

- single or repeated overloads/underloads in constant amplitude fatigue
- blocks of overloads (Figure 3-12a)

2) Step loading

- hi-lo sequences, lo-hi sequences (Figure 3-12b)

3) Programmed block loading

- sequences of various constant amplitude blocks (Figure 3-12c)

4) Flight-simulation loading

- sequences of various constant amplitude blocks with occasional overloads and underloads (Figure 3-12d)

5) Random loading

- random sequences of cycles of various amplitudes; often characterized by unimodal distributions (Figure 3-12e)

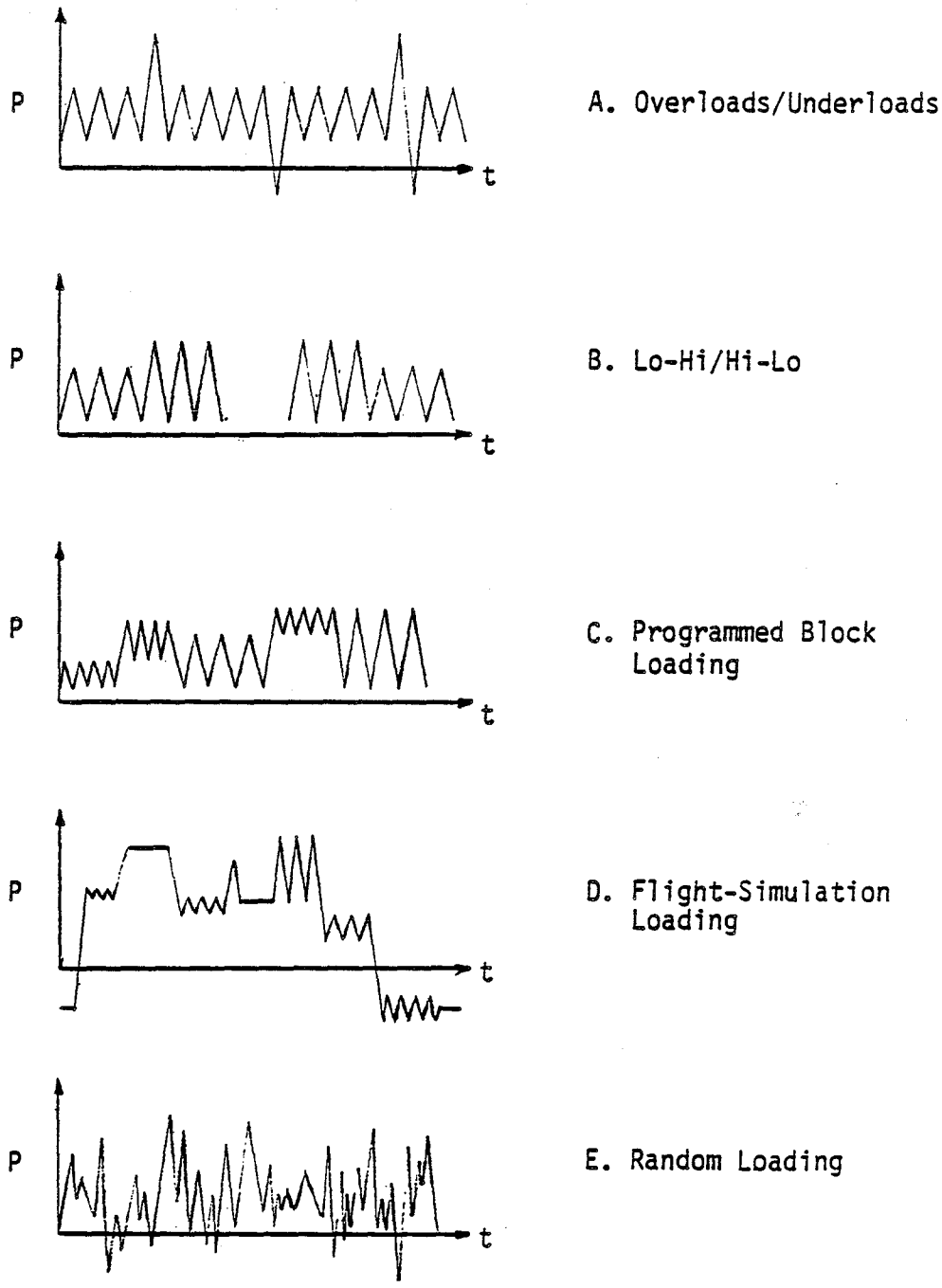

Figure 3-12. Types of Variable Amplitude Loading.

In addition to the variety of loading types, variables such as material, load frequency, mean stress, and environment can significantly affect the rate of fatigue crack growth under variable-amplitude loading.

Variable amplitude loading can also be divided on the basis of relative crack-tip plasticity and the resulting mascroscopic crack growth phenomena. Elber [3-24] makes the distinction between "long" and "short" spectra in variable amplitude fatigue. He considers "short" spectra to be those in which the amount of crack propagation during a repeating sequence, or block, is less than the size of the crack-tip plastic zone resulting from the maximum load in the sequence. Conversely, "long" spectra produce sufficient crack propagation during a repeating sequence to allow the crack-tip to propagate out of the region of influence of the plastic zone resulting from the maximum load in the sequence.

The important mechanistic variable involved in the distinction between short and long spectra is the crack opening stress, which is the stress level at which the crack first begins to open. Elber [3-25], in the late 1960's, was one of the first investigators to identify crack closure, resulting from residual plastic deformations in the wake of an advancing fatigue crack, as an important mechanism in fatigue crack growth. Prior to Elber's work, it was generally assumed that, under cyclic loading, the tip of a fatigue crack would open at the instant a tensile load was applied and close again at zero load. The crack closure concept has been utilized in extensive research during the 1970's and early 1980's to explain load interaction effects such as retardation and acceleration, stress ratio or mean stress effects, and environmental

effects on threshold. Each of these effects will be discussed in greater detail after the following brief discussion on cycle counting.

The definition of what constitutes a stress cycle becomes less clear as load histories other than constant amplitude cyclic loading are considered. This is especially obvious when considering random load histories, such as are shown schematically in Figure 3-12e. The convention for defining a cycle can have a marked influence on calculated extent of fatigue crack extension. Various schemes for counting load cycles have been suggested, with the range-pair and rainflow techniques being commonly used. References 3-26 and 3-27 provide reviews of the procedures involved.

3.4.2 Load Interaction

Load interaction is a term which describes the observed phenomenon that an increment of fatigue crack growth, Δa, is a function of the preceding cyclic load history rather than solely dependent on the present crack size and load cycle. Table 3-2 illustrates the concept of load interaction and highlights various phenomena which contribute to the coupling of present crack growth to previous load history [3-23].

In this section, experimental findings of overload and underload sequences and their retardation and acceleration effects on subsequent fatigue crack growth under constant amplitude (CA) loading are discussed. Figure 3-13 illustrates a general overload/underload sequence and defines parameters used in the following discussion.

Table 3-2
Factors Which Influence Crack Growth,
Δa, During a Load Cycle [3-23]

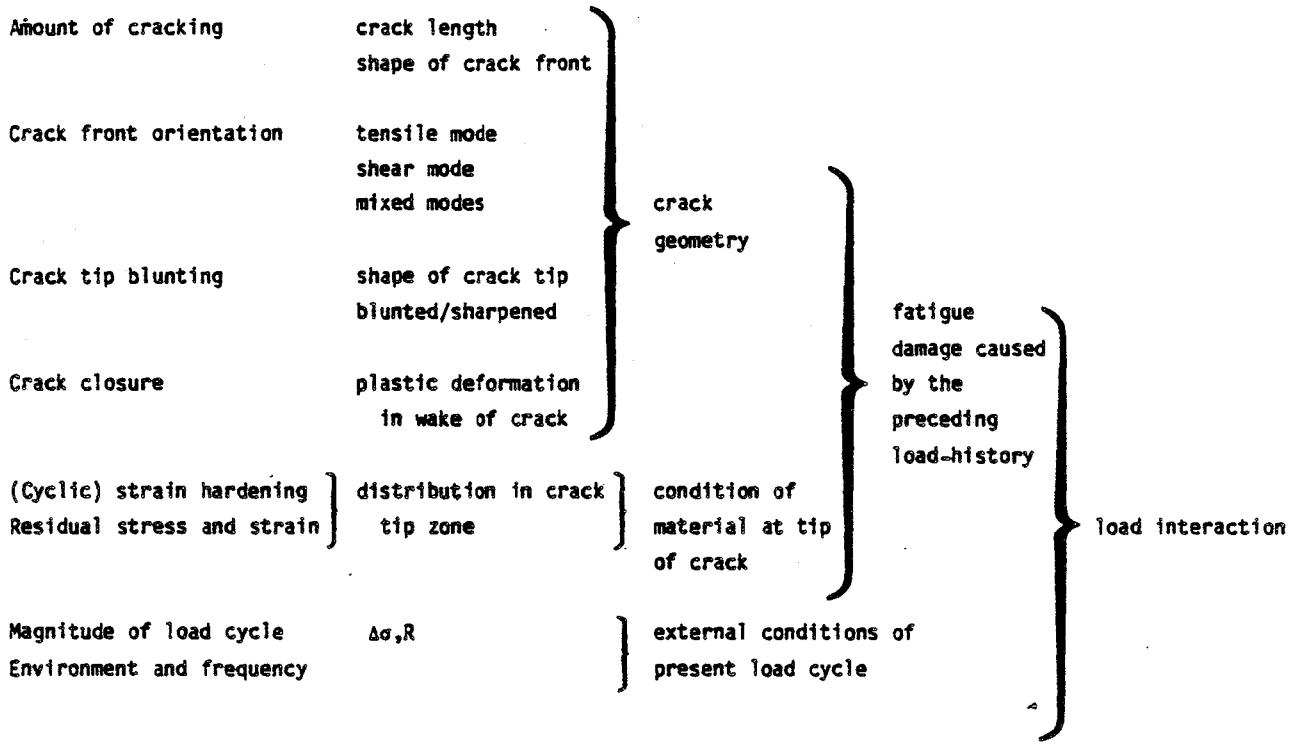

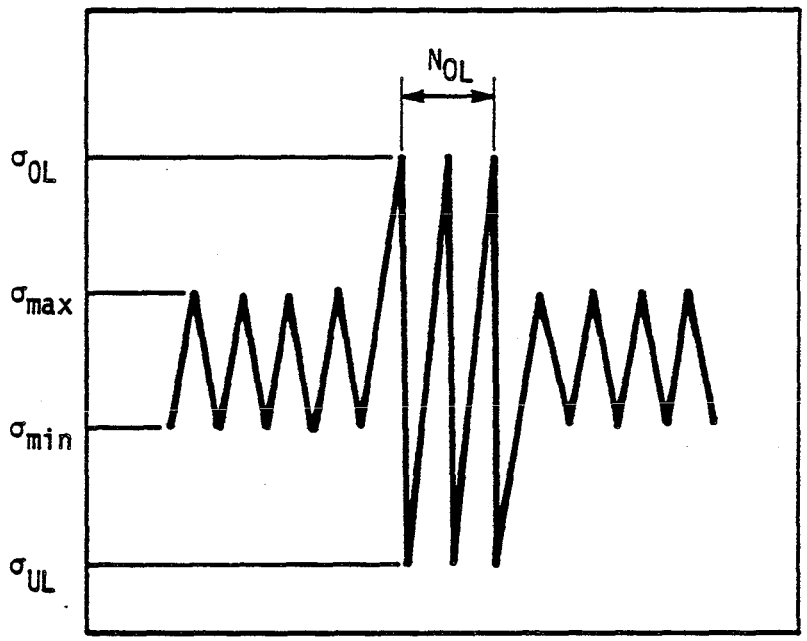

λ = Overload Ratio = σ_{OL}/σ_{max}

$R_{OL} = \sigma_{UL}/\sigma_{OL}$

$R_{CA} = \sigma_{min}/\sigma_{max}$

$\Delta\sigma_{OL} = \sigma_{OL} - \sigma_{UL}$

$\Delta\sigma_{CA} = \sigma_{max} - \sigma_{min}$

N_{OL} = Number of Overload Cycles

Figure 3-13. Definition of Parameters Used to Characterize Overload/Underload Sequence.

Tensile Overloads ($\sigma_{OL} > \sigma_{max}$): Retardation

It has been well known since the early 1960's that the occurrence of an overload during constant amplitude cycling will produce retardation (or delay) of the crack growth rate following the overload. Figure 3-14 illustrates crack growth retardation due to tensile overloads and defines retardation as the period (cycles, time) of abnormally low rate, or zero rate, of fatigue crack growth between a decrease in load level and the establishment of a crack growth rate commensurate with that for constant amplitude loading at the lower load. In the current literature, three crack-tip phenomena are used separately or in combination to explain retardation and correlate prediction models with experimental findings. The phenomena are (a) compressive residual stresses in front of the crack-tip due to unloading from a high tensile peak, (b) compressive residual stresses in the wake of a crack-tip passing through the overload-affected zone (Elber's crack closure concept [3-6]) and, (c) crack-tip blunting during overload application. Figure 3-15 illustrates these three crack retardation mechanisms.

Extensive test programs were conducted predominantly by the aircraft industry in the early and mid-1970's to assess and quantify the effect of retardation on crack growth in aircraft structures and gas turbines. Useful summaries of the experimental findings which are generally agreed upon as being generic to the tensile overload delay phenomenon have been published by Corbly and Packman [3-28], Schijve [3-23], and Nelson [3-29]. The following list of retardation phenomenon are highlights of summaries:

1) Tensile overloads introduce crack growth delay which can vary from no retardation to complete crack growth arrest. The extent of crack growth delay, as measured

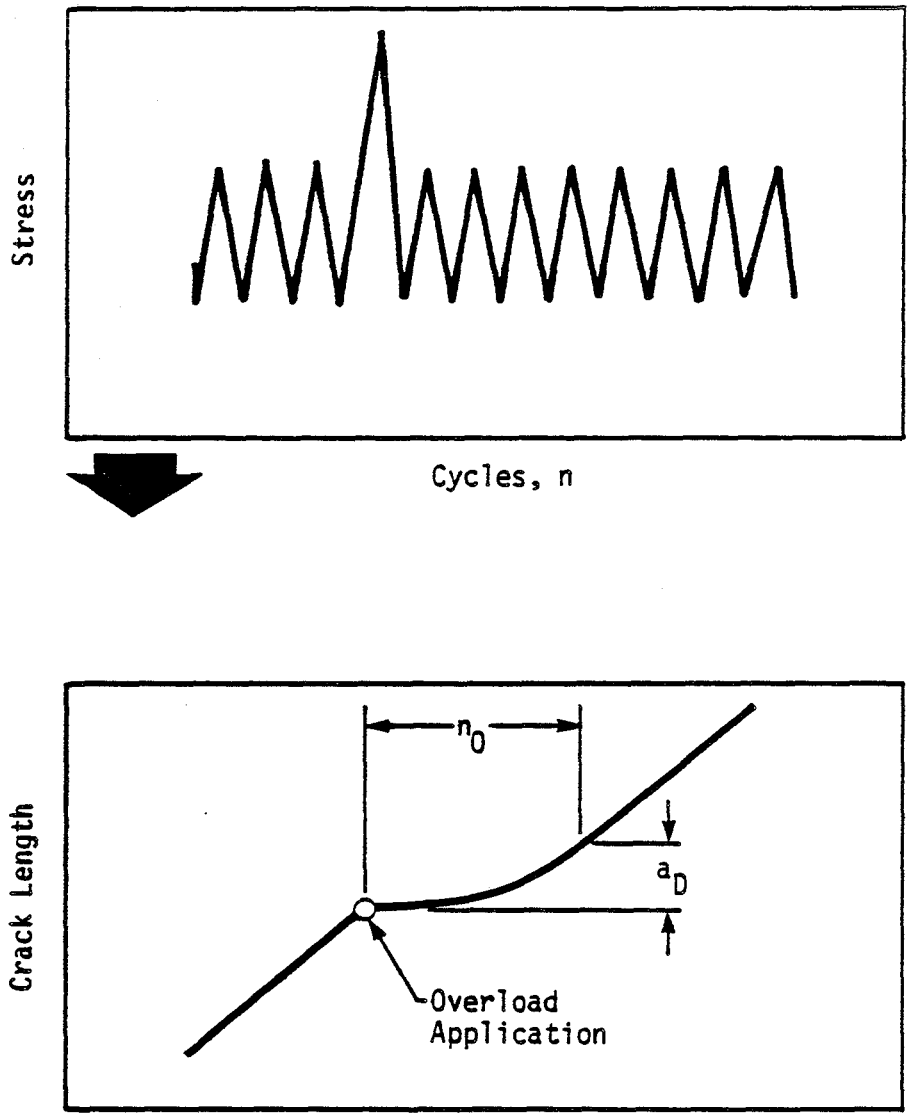

Figure 3-14. Illustration of Crack Growth Retardation Following a Tensile Overload.

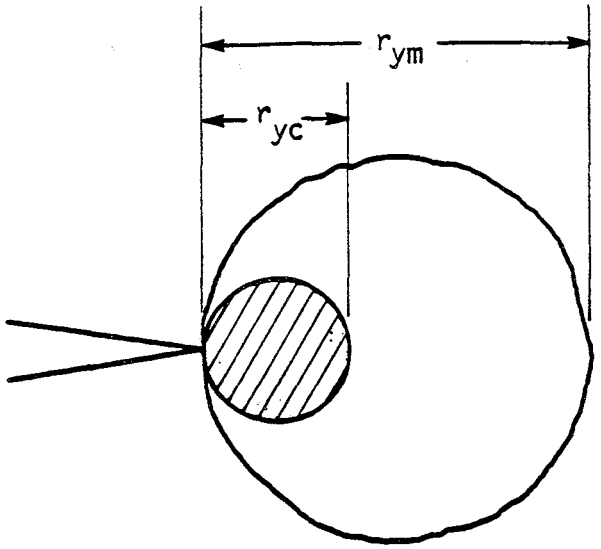

r_{ym} = Monotonic Plastic Zone Distance

$$= \frac{1}{\beta\pi}\left[\frac{K}{\sigma_{ys}}\right]^2$$

β = 2 (Plane Stress) = 6 (Plane Strain)

r_{yc} = Cyclic Plastic Zone Distance

= 1/4 r_{ym}

(a) Crack Tip Plasticity: Residual Stress Ahead of Crack Tip.

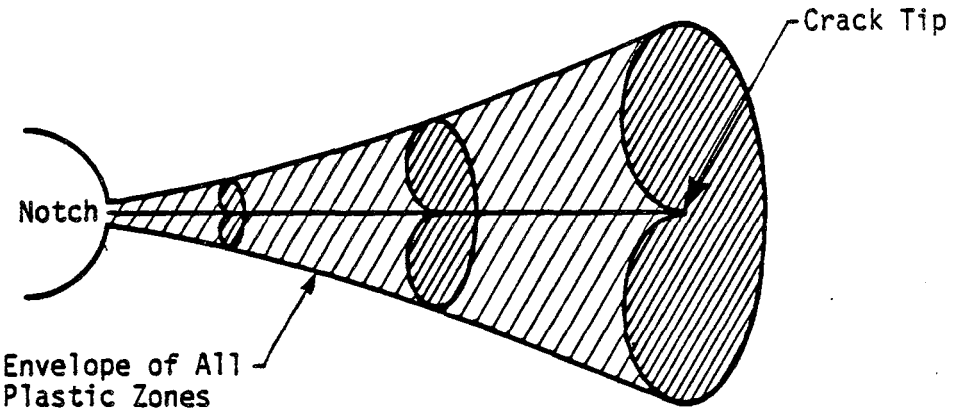

(b) Crack Closure: Residual Stresses Ahead of and In Wake of Crack Tip.

(c) Crack Tip Blunting.

Figure 3-15. Three Crack Retardation Mechanisms Used to Explain Observed Load Interactions.

by delay cycles, is dependent upon the stress intensity parameters associated with the overload and subsequent constant amplitude load cycles, (e.g., ΔK_{OL}, ΔK_{CA}, R_{OL}, R_{CA}. Retardation has been observed in various materials -- titanium alloys, high strength steels, mild steels, aluminum alloys -- and it appears that similar results may be expected for materials with similar (cyclic) strain behavior. Delay depends directly on the extent of crack-tip plasticity -- the larger the plastic zone in front of or surrounding the crack, the longer the retardation. Crack tip plastic zone size, r_p, can be expressed as $r_p = 2\ r_y = \frac{1}{\beta\pi}\left(\frac{K}{\sigma_{ys}}\right)^2$ where $\beta = 2$ (plane stress), $= 6$ (plane strain), and σ_{ys} is the material yield strength [3-30]. Consequently, as the relationship for r_p indicates, retardation is larger for a) low yield strength materials, b) thin specimens ($\beta \to 2$), and c) for conditions which effectively reduce material yield strength (e.g., high temperature).

2) For a given material, the overload ratio, $\lambda = K_{OL}/K_{max}$, approaches a threshold value below which no significant retardation is observed. Of course, for every material constant amplitude cycling is reached as $\lambda \to 1$ and no retardation occurs. Threshold values of λ are sensitive to various parameters including material type, R-ratios of both the overload and constant amplitude cycles, and specimen thickness. Literature values range between 1.0 and 1.5 [3-31, 3-32] for most materials.

3) Retardation increases with higher values of overload for a given value of constant amplitude loading. References to this phenomenon are numerous [3-28, 3-33 through 3-48]. The magnitude of overloads can produce delay effects which result in crack growth arrest. Table 3-3 illustrates overload ratios $\lambda = \sigma_{OL}/\sigma_{CA}$, at which crack growth arrest has been observed in various materials for particular types of specimen geometries and loading conditions. References are provided to identify specific test conditions and specimen geometries for which the tabulated overload ratios apply.

4) For constant values of $\Delta K_{OL}/\Delta K_{CA}$, delay decreases with increasing ΔK_{CA} [3-36].

Table 3-3
TENSILE OVERLOAD RATIOS PRODUCING CRACK GROWTH ARREST IN VARIOUS MATERIALS

Metal	Overload Ratio ($\lambda = K_{OL}/K_{CA}$)	Reference*
Ti-6Aℓ-4V	2.7	[3-44]
1020 CR Steel	2.5	[3-45]
Austenitic Mang. Steel	2.3	[3-46]
2024-T3 Aluminum	2.0 - 2.5	[3-41, 3-43, 3-47]
7075-T6 Aluminum	2.3 - 2.5	[3-28, 3-48]
4340 Steel	2.4 (Est)	[3-42]

*References are included for obtaining specific loading conditions and specimen geomeries for which crack arrest overload ratios apply.

5) For fixed values of ΔK_{OL} and ΔK_{CA}, delay decreases with increasing R_{CA}. In the limit, when K_{max} equals K_{OL}, no delay is experienced [3-36].

6) Delay increases with the number of repeated overload excursions, N_{OL} (see Figure 3-13), up to a limiting "saturation" value of overload cycles [3-28, 3-41, 3-45 through 3-48].

7) Retardation occurs for crack growth through the crack-tip plastic zone created by the tensile overload. The extent of the plastic zone over which retarded crack growth occurs is not generally agreed upon. Von Euw, et al. [3-41], observed that more than 80% of retardation occurs over less than one quarter of the overload plastic zone, r_p, where $r_p = 2r_y = 2\left[\frac{1}{\beta\pi}\left(\frac{K_{OL}}{\sigma_{ys}}\right)^2\right]$, and r_y is the crack-tip yield zone radius, $\beta = 2$ (plane stress), $= 6$ (plane strain). By comparison, Wei, et al. [3-44] observed that retarded crack growth can continue well after the crack has grown through the overload plastic zone, r_p.

8) Crack growth rate does not immediately reach its minimum value after the overload application. The minimum crack growth rate occurs after the crack has grown some distance, d, into the plastic zone as illustrated in Figure 3-16. This distance of delayed retardation has been measured by various investigators and varies between 7.5% to 25% of the overload plastic zone, r_p. Crack closure arguments have been employed to explain delayed retardation [3-27, 3-47]. The application of an overload produces residual compressive strains in the plastically deformed region ahead of the crack-tip. As long as the plastic zone is ahead of the crack-tip, the clamping action of the compressive residual stresses does not influence the crack opening. As the crack propagates into the plastic zone, the clamping action will act on the new fracture surfaces. This clamping action, which builds up as the crack propagates into the plastic zone, requires a larger applied stress to open the crack; hence, the crack propagates at a decreasing rate into the plastic zone.

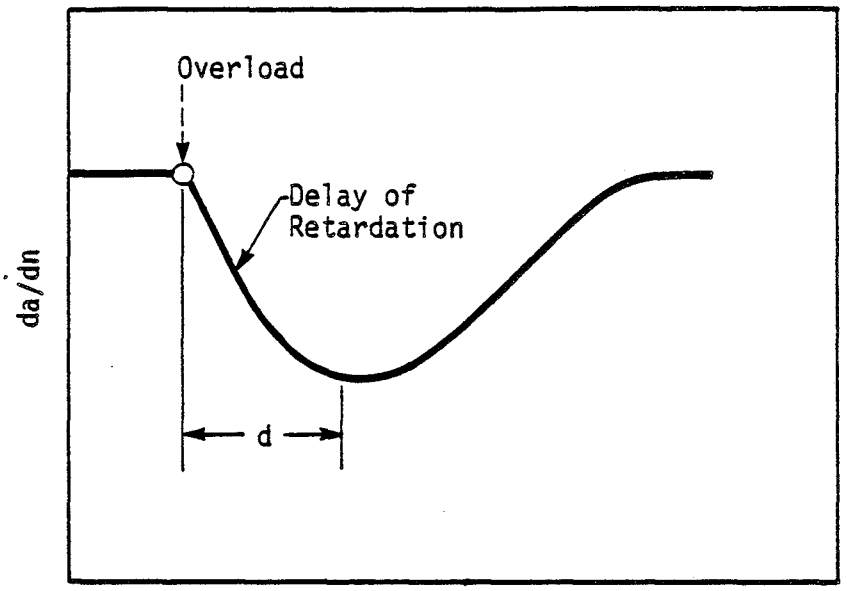

d = Percent of Plastic Zone Size, r_p

$$r_p = 2r_y = 2\left[\frac{1}{\beta\pi}\left(\frac{K_{OL}}{\sigma_{ys}}\right)^2\right]$$

β = 2 (Plane Stress) = 6 (Plane Strain)

d = 7.5% [3-46], 10-25% [3-41], 16-25% [3-42]

Figure 3-16. Delayed Retardation Phenomenon Observed Immediately After Application of Tensile Overload.

Tensile Overloads ($\sigma_{OL} > \sigma_{max}$): Acceleration

Crack growth during an overload cycle (see Figure 3-17) has been observed to be larger than expected from constant amplitude data for the same load level [3-28, 3-41, 3-44 through 3-50]. This phenomenon is referred to as crack growth acceleration. Crack growth is accelerated during the overload, but fortunately stabilizes within the first few cycles of the higher load sequence.

Possible explanations attribute acceleration to the crack and crack-tip plastic zone growing into an area with less residual stress than that of an equivalent constant amplitude case. Consequently, the crack growth is less inhibited. Elber [3-6], using crack closure arguments, purports that the first few cycles of the overload have a greater effective stress intensity range than subsequent (> 10^{th} cycle) cycles, causing an initial crack propagation rate larger than the equilibrium rate reached at the 10^{th} cycle.

Underloads ($\sigma_{UL} < \sigma_{min}$): Reduced Retardation

Underloads are defined as compressive or tensile loads that are lower in magnitude than subsequent constant amplitude loads. Figure 3-18 illustrates three general types of underloads which have been investigated in the literature for their effects on subsequent crack propagation. The following list highlights the results of the investigations:

1) An underload immediately following a tensile overload (Type I) will reduce the effect of retardation due to the overload. Hillberry, et al. [3-51], have performed extensive studies on 2024-T3 aluminum to assess the reduction of retardation as a function of magnitude of the underload immediately following the overload. This

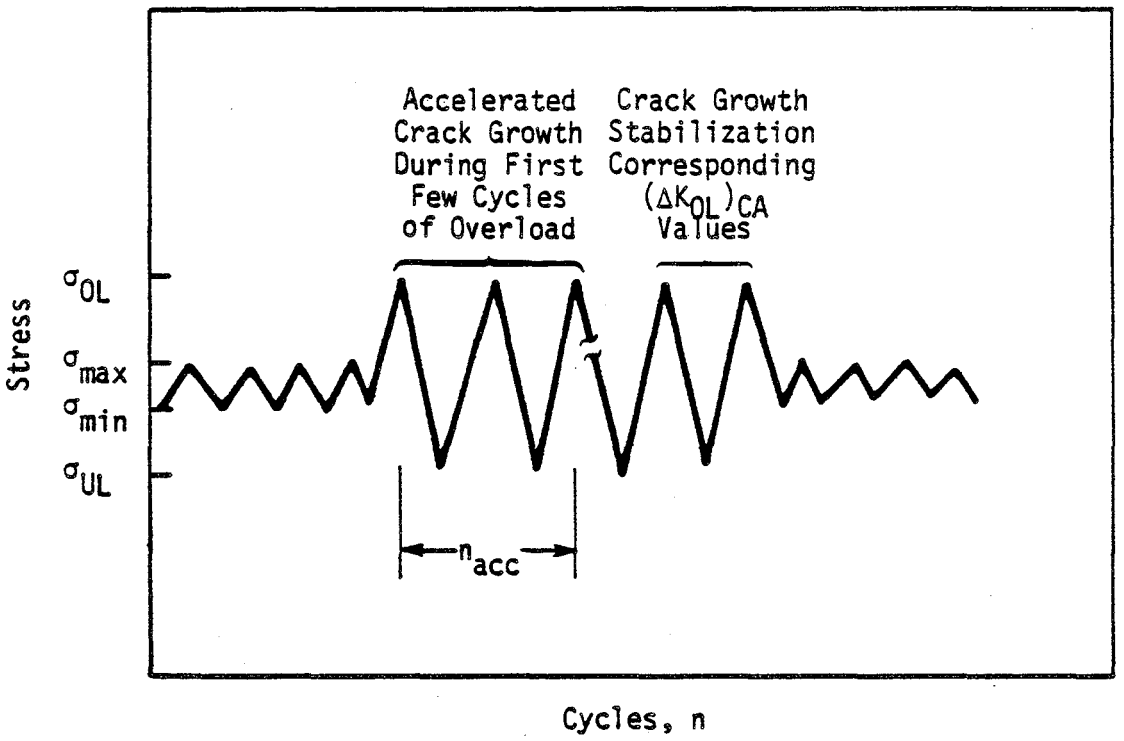

Accelerated Crack Growth Region, n_{acc}

$(da/dn)_{\Delta K_{OL}} > (da/dn)_{CA} @ \Delta K_{OL}$

$n = n_{acc}$

Figure 3-17. Schematic of Accelerated Crack Growth During First Few Cycles of Applied Overload.

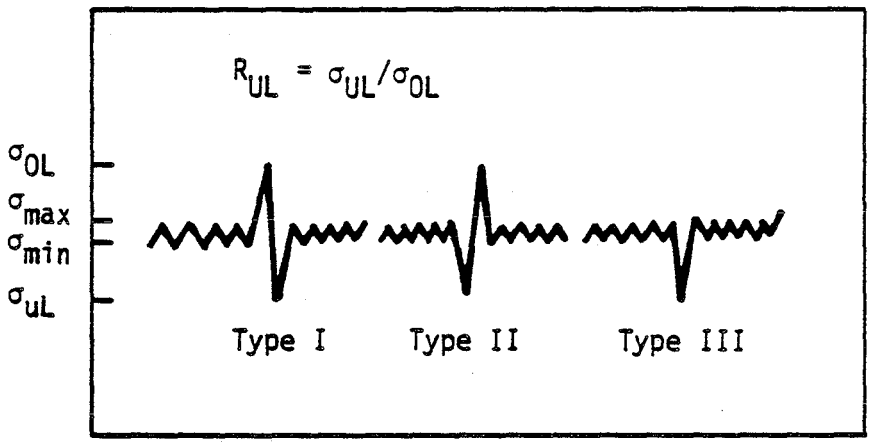

Underloads:

Type I - Underload Immediately Follows Overload

Type II - Underload Immediately Precedes Overload

Type III - Underload, No Overload

Figure 3-18. Underload Spectra Analyzed for Effects on Subsequent Fatigue Crack Growth.

magnitude is reflected by the overload R-ratio, $R_{OL} = \sigma_{UL}/\sigma_{OL}$ from $R_{OL} = -1$ (compressive fully reversed overload) to $R_{OL} = 0.3$ (tensile underload) and indicated that the reduction in crack growth delay increases as R_{OL} decreases (i.e., as R_{OL} goes from 0.3 to -1.0. Stephens, et al. [3-52], found that the beneficial effect of retardation due to an overload can in some cases be completely eliminated by repeated compressive constant amplitude loading where $R_{CA} < 0$ and $\sigma_{min} = \sigma_{UL}$. Hsu and Lassiter [3-53] observed a 5 to 40% reduction in retardation when tensile overload was followed by an equal compressive load ($R_{OL} = -1.0$).

2) If an underload immediately precedes the overload (Type II), the reduction in delay is much smaller than if an underload follows the overload. Stephens [3-52] found that underload-overload crack growth life was only slightly less than overload-only life. Hsu and Lassiter [3-53] observed that compressive underloads ($R_{UL} = -1.0$) preceding overloads produced less than 10% reduction of retardation in subsequent constant amplitude cycling at $R_{CA} = 0.0$.

3) The effect of compressive underloads (Type III, $R_{UL} < 0$) on constant amplitude fatigue crack growth is to shorten crack propagation times. As reported by Hsu and Lassiter [3-53] the degree of shortening varies for different materials. For example, no decrease in fatigue crack propagation times were observed for Ti-6Al-4V while a maximum of 15% decreases was observed for 7075-T73 aluminum. The authors' experience indicates that much greater crack growth acceleration could be caused by compressive underloads of small cracks emanating from large notches due to the large notch plastic zone of tensile residual stress created by the compressive underload. However, no published data was found on this notch case. The lack of large accelerations due to compressive underloads in a cracked, unnotched geometry is due to the contact of crack faces which prevent large compressive excursions and tensile residuals ahead of the crack tip.

Summary

The following paragraphs highlight the experimental observations on load interaction effects.

Large tensile overloads can cause large increases in crack growth life. If sufficiently large overloads are applied, crack arrest may occur. Retardation effects are diminished if subsequent constant amplitude loading is applied at high R-ratio values.

Crack retardation following a single tensile overload does not occur immediately after the overload but reaches a minimum value after a finite change in crack length. This phenomenon is termed delay of retardation.

A change from a lower level to higher level of constant amplitude cycling causes crack growth acceleration. However, this effect is confined to the first few cycles of higher load and its effect is thought to be small compared to crack retardation.

Underloads following overloads reduce the beneficial effect of the overload retardation. If compressive underloads are applied in the absence of overloads and notches, crack propagation times are shortened by 0 to 15%, depending on material type. Much larger accelerations are expected if compressive underloads are applied to cracked notch geometries and such testing is recommended.

As indicated by Schijve [3-23], most interaction effects were first evaluated for aluminum alloys. Subsequently, similar investigations were conducted on titanium, mild steels and high-strength steels. The retardation/

acceleration behavior of these materials were not identical, but apparently similar interaction effects may be expected for materials with similar (cyclic) strain behavior. This expectation follows from the concept of crack-tip plasticity being a dominant mechanism involved with crack growth retardation/acceleration.

3.4.3 Mixed Low and High Cycle Fatigue

Mixed low and high cycle fatigue spectra in variable amplitude loading include significant amounts of both 1) low cycle fatigue (LCF) consisting of relatively infrequent intermediate-to-high amplitude cycles, and 2) high cycle fatigue (HCF) consisting of high frequency low-to-intermediate amplitude cycles. In space shuttle main engine (SSME) environments, LCF often results from thermal, rotational, or pressure loading, and HCF from vibrational loading. The main injector LOX-posts experience LCF thermal cycles associated with the dramatic temperature gradients across tube walls separating hot hydrogen gases and cold liquid oxygen. Superimposed on the thermal LCF are flow-induced, vibrational HCF cycles. LCF in turbopump turbine blades results from centrifugal loads and the vibrational HCF may again be flow-induced. Duct welds experience LCF from high mean pressures and HCF from rapid pressure fluctuations or acoustic vibration. These represent only a few examples of SSME components which are subjected to mixed HCF/LCF variable-amplitude spectra.

It is generally agreed [3-16, 3-54, 3-55] that one of the most significant cases in which mixed LCF/HCF effects are important is in situations where LCF produces crack initiation and initial growth and HCF causes crack accel-

eration. Fatigue damage in structures exposed to mixed HCF/LCF loading often begins with high cyclic plasticity resulting from low-frequency, high-amplitude loads in areas of stress concentration such as fillet radii, weld defects, or notches. The cyclic plasticity associated with the LCF cycles enlarges micro defects through decohesion mechanisms usually associated with single active slip systems [3-20]. During this fatigue crack initiation phase, the LCF cycles dominate. The LCF cycles will also dominate the early stages of fatigue crack propagation as long as the crack-tip stress intensity range, ΔK, for the HCF cycles is less than the threshold values, ΔK_{th}. (Threshold effects were discussed in Section 3.3.) As the crack length, a, increases, ΔK increases for the given applied stress provided the stress gradient in the direction of crack propagation is not severe enough to dominate the K dependence on a. When the HCF ΔK exceeds the threshold value (ΔK_{th}), the crack growth will accelerate due to the much higher number of HCF cycles relative to the LCF cycles.

LCF cycles in which K_{max} exceeds the K_{max} of the superimposed HCF cycles may act as overloads which increase the value of ΔK_{th}. In cases such as this, it may be important to include the overload effect on threshold. Hopkins, et al. [3-16], have identified the overload effect on threshold and developed a test method to determine the effect experimentally. No data specifically addressing this phenomenon in mixed HCF/LCF environments has been found; however, Hopkins' data is significant and identifies the need for further experimental investigations. When the K_{max} of the LCF cycles is roughly equivalent to that of the HCF cycles, as in the superposition of vibrational cycles on an LCF dwell, Powell, et al. [3-54], have shown that simple linear

summation of fatigue crack growth rates can provide a reasonable approximation to test data (Figure 3-19).

The fatigue threshold for newly initiated cracks in mixed HCF/LCF environments, in many instances, will lie in the short crack regime. In cases where the HCF amplitudes are large enough to accelerate crack growth soon after a fatigue crack is initiated by the LCF cycles, the crack length at the onset of HCF damage may fall in the short crack regime. Consequently, the actual fatigue threshold may be lower than that predicted by long-crack tests [3-21].

3.4.4 High Compressive Load Effects

High compressive load effects result from the part of the fatigue loading cycle during which the crack is closed and the crack surfaces are in compression. This section deals with only cases of remotely applied compressive loads normal to the crack surfaces. Compressive stresses resulting from contact between bearing surfaces and the associated shear stress reversals are discussed as a part of multiaxial stress problems in another section. Compressive loads in the presence of a notch are discussed under the residual stress heading.

Compressive loads applied normal to a propagating fatigue crack can result in reversed yielding at the crack-tip and crack surface plastic zones and thereby increase the crack growth rate relative to that for constant amplitude, tension-tension fatigue with an equivalent tensile ΔK. Yuen, et al. [3-4], obtained crack growth rate data for Ti-6Al-4V at stress ratios ranging from -5.0 to 0.7. Figure 3-1 shows a plot of crack growth rate as a

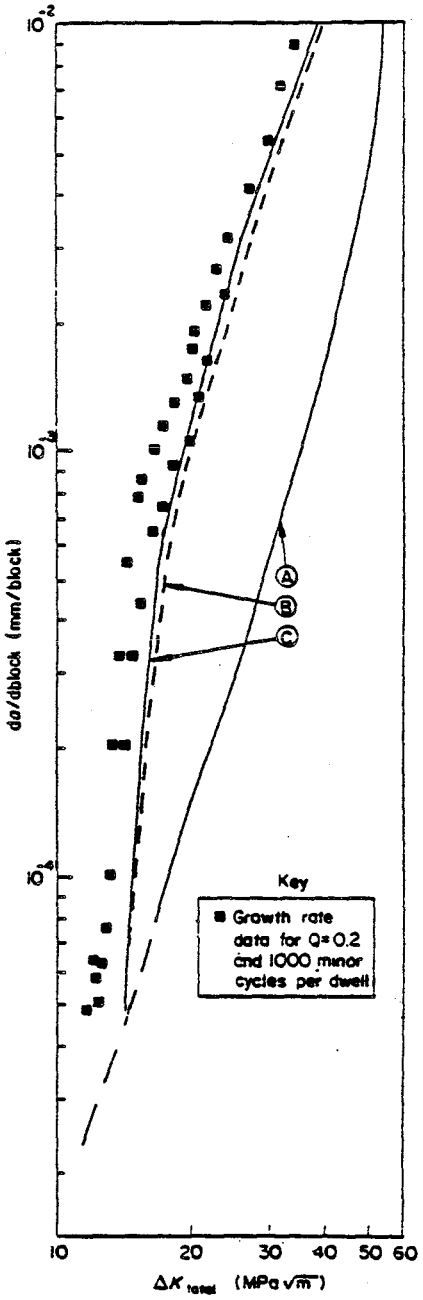

Figure 3-19. Linear Summation of FCG Rates (Damage: A - Associated with Applied Major Cycle; B - Associated with Applied Minor Cycles; C - Given by Summation of Major and Minor Cycle Damage) [3-54].

function of the full stress intensity range, $K_{max} - K_{min}$, where K_{min}, for computational purposes, is negative for negative R-ratios. The growth rates for $R < 0$ are seen to be much lower than for $R = 0$ because of the smaller stress range over which the crack is open. In Figure 3-20, the same data are plotted relative to the positive portion of ΔK, and negative R data tends to fall above the $R = 0$ data showing slightly higher growth rates. The accelerated growth associated with negative R-ratios did not exceed 10% on an average, and was found to reach saturation at low negative R. In accordance with Equation 3-11, Yuen, et al., used a generalized form of Forman's equation in which ΔK_{eff} was taken to be:

$$\Delta K_{eff} = \frac{C_1}{C_2 - R} \Delta K_{total}$$

For the data analyzed, the values of the constants C_1 and C_2 were determined to be 1.63 and 1.73 respectively. In Figure 3-2 the data from Figures 3-1 and 3-20 are plotted against ΔK_{eff}, showing a much better fit for all values of R between -5.0 and 0.7.

Experiments in aluminum conducted by Hsu and McGee [3-56] on the effects of compressive overloads revealed that fully compressive cycles imposed on blocked constant amplitude tests produced a maximum of 15% increase in crack growth rates and that increases in both magnitude and number of blocked compressive-compressive cycles had a negligible effect. These results were supported by tests in both aluminum and titanium conducted by Hsu and Lassiter [3-53]. It was therefore concluded that for the materials studied that moderate increases in crack growth rate can be expected for negative stress ratios relative to rates predicted for equivalent tensile-only stress inten-

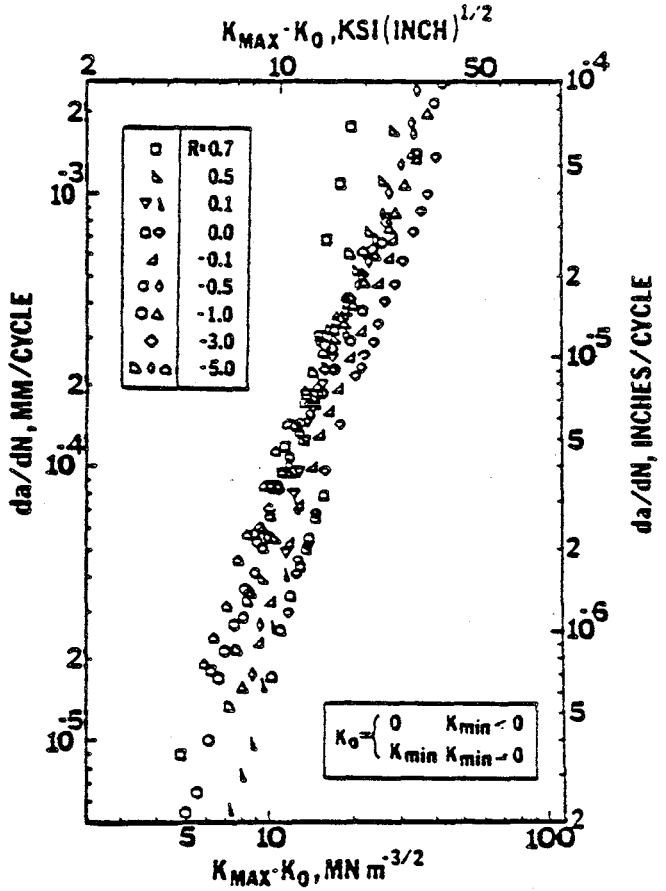

Figure 3-20. Crack Growth Rate as a Function of $K_{max} - K_0$ for the Various R-Ratios [3-4].

sity ranges. It was further concluded that increases in magnitude of compressive cycles beyond the saturation level produce no change in crack growth rate, and one compressive-compressive cycle is equivalent to many from a modeling standpoint. These two conclusions would not apply to cracked notch geometries for reasons given in Section 3.4.2.

3.4.5 Predictive Methods for Variable-Amplitude Fatigue

Fatigue crack growth under conditions where the cyclic stress is not of constant amplitude can be a complex phenomenon; as has already been discussed in earlier sections. Variable amplitude loading, such as mixed high cycle and low cycle fatigue discussed in Section 3.4.3 can produce complex effects that are often referred to as load interactions (see Section 3.4.2). These complications lead to the need for relatively complex procedures for analytically predicting fatigue crack growth under variable amplitude loading conditions. Such procedures will be reviewed in this section.

Predictive methods for variable-amplitude fatigue are analytical and empirical models developed to aid in fatigue life prediction estimates for components subject to variable amplitude load sequences. Many of these models are based on the Paris-type crack growth rate equation

$$\frac{da}{dn} = C\ \Delta K^m$$

A more general approach is often employed that uses a basic form such as

$$\frac{da}{dn} = C\ F\ (\Delta K_{eff})$$

with C and/or ΔK_{eff} being modified to account for variable amplitude loading. Such modifications are made to account for the effects of stress ratio, overloads, underloads, and load sequences, and yet still be able to use the vast amounts of constant amplitude fatigue data already in existence. The predictive models may be divided into three general categories based on the mechanism(s) assumed to be dominant:

1) Statistical models - in which crack growth rate is governed by statistical parameters such as ΔK_{RMS}, the root-mean-square stress intensity range, and R_{RMS}, the root-mean-square stress ratio;

2) Crack closure models - in which crack growth rate is governed by the difference between K_{max}, the maximum stress intensity, and K_{op}, the stress intensity at which the crack-tip opens and closes; and

3) Crack-tip plastic zone size models - in which variations in crack growth rate depend on the relative sizes of crack-tip plastic zones.

Statistical Models

Statistical crack growth models characterize a random amplitude stress history by the root-mean-square of the stress intensity range, ΔK_{RMS}, and assume that the fatigue crack growth rate can then be predicted using constant amplitude data. Because these models take no account of load sequence effects such as retardation and acceleration, they have been shown to be applicable only to short spectra, in which load sequence effects are minimized. Chang, et al., [3-57] studied fatigue life prediction methods with and without accounting for load interaction effects. They found that without considering load interaction, fatigue life predictions were highly conservative for random spectra consisting of predominantly tension-tension cycles ($R > 0$), and

predictions were nonconservative for spectra consisting of predominantly tension-compression cycles ($R < 0$).

The variable amplitude fatigue behavior of ASTM 514-B steel was studied by Barsom [3-58]. He found that for random load spectra represented by unimodal distributions such as Rayleigh, normal, or log-normal distributions, the average fatigue crack growth rates can be represented by the equation

$$\frac{da}{dn} = A\,(\Delta K_{RMS})^m \tag{3-16}$$

where A and m are constants, dependent upon material and environment, which can be obtained from constant amplitude data. Figure 3-21 is a plot of Barsom's data for three ratios of standard deviation, σ_{rd}, to nodal peak value, σ_{rm}, showing good correlation.

A study of the random amplitude fatigue behavior of 2219-T851 aluminum alloy as conducted by Hudson [3-59] as part of an ASTM round-robin analysis of variable amplitude prediction systems. Hudson extended Barsom's work by not only calculating the root-mean-square value of ΔK, but also the root-mean-square stress ratio, R_{RMS}. These statistical variables were then applied to Forman's equation for crack growth as a function of R to obtain

$$\frac{da}{dn} = \frac{C\,\Delta K_{RMS}^{\,m}}{(1 - R_{RMS})\,K_{Ic} - \Delta K_{RMS}} \tag{3-17}$$

where C and m are constants determined from constant amplitude tests. Analyses of eleven different aircraft random load histories and the tests performed using these histories resulted in an average ratio of predicted life to test

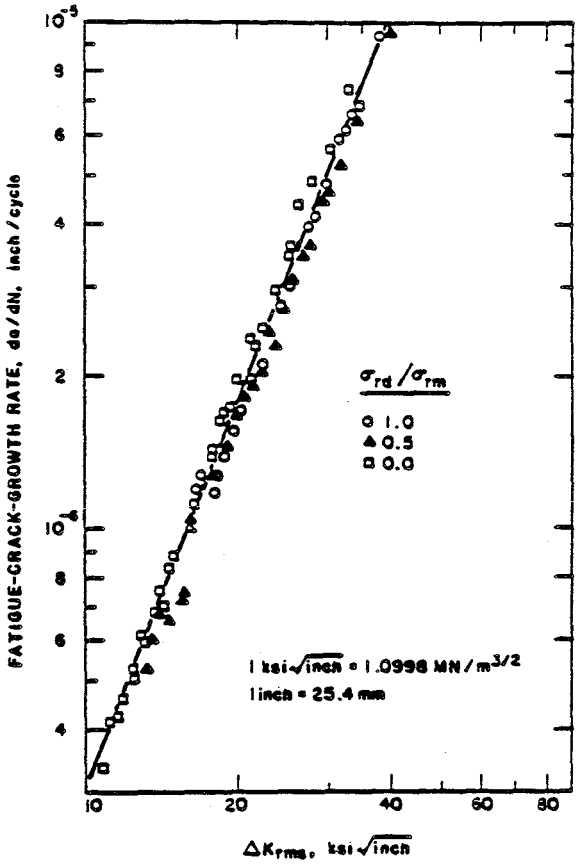

Figure 3-21. Barson's Data for 3 Ratios of σ_{rd} to σ_{rm}.

life of 1.38 with a standard deviation of 0.42. Although Hudson attributed the non-conservatism of the average prediction to normal scatter, he did state that the RMS approach is probably not applicable to non-random load sequences with relatively few overload or underload cycles due to the load interaction effects of retardation and acceleration.

Crack Closure Models

Crack closure models account for load interaction effects in variable-amplitude fatigue through the calculation of a crack opening stress, S_{op}, and the resulting $\Delta K_{eff} (= K_{max} - K_{op})$. Closure models, unlike statistical models, must compute fatigue crack propagation life on a cycle-by-cycle basis because single load excursions can have a significant effect on the crack opening stress.

The development of crack closure-based load interaction models began with the identification of the closure mechanism by Elber [3-6, 3-24]. In his early work, Elber developed a model only for the stress ratio effect on constant amplitude fatigue; however, he did point out the applicability of the closure concept to variable amplitude load interaction effects and conducted experiments to demonstrate closure stress variations with maximum stress [3-6]. Through his experiments, Elber was able to explain delayed retardation following an overload and acceleration resulting from a lo-hi step change in loading using closure arguments.

In the mid 1970's, Elber developed a closure-based method [3-24] for converting a random load sequence to an equivalent constant amplitude sequence for the purpose of variable amplitude fatigue life prediction under short-

spectrum loading. The method involves the calculation of an equivalent number of constant amplitude cycles with the same maximum stress, S_{max}, and crack opening stress, S_{op}, as the random sequence (Figure 3-22), using the equation

$$N_{eq} = \sum \frac{(S_i - \hat{S}_i)^m}{(1 - \alpha)^m (S_{max} - S_B)^m} \qquad (3\text{-}18)$$

where: S_i = maximum stress for the i^{th} cycle

$\hat{S}_i$ = effective minimum stress for the i^{th} cycle

S_{max} = maximum stress for the sequence

S_B = minimum stress for the sequence

m = material crack growth exponent

and

$$\alpha = \frac{S_{op} - S_B}{S_{max} - S_B}$$

It should be noted that the expression above for N_{eq} represents an extension of the Palmgren-Miner hypothesis, for linear summation of blocked constant amplitude fatigue, modified to include the effects of crack closure. The method does not account for load interaction effects and is therefore applicable only to short-spectrum variable amplitude sequences in which load interaction effects are minimized.

A closure-based model was developed by Dill and Saff [3-60] using crack surface displacements and contact stresses. Utilizing the Dugdale plastic zone model and a superposition of Westergaard's near-crack-tip elastic displacement solution and the displacements due to a constant-stress yield zone, Dill and Saff developed a weight function model accounting for residual plasticity, crack surface interference, and contact stresses behind the crack-tip

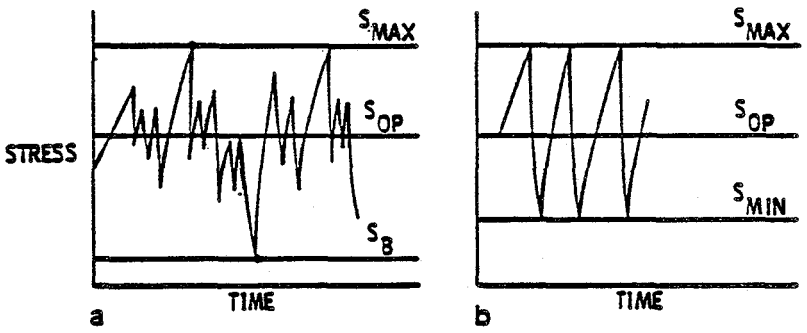

Figure 3-22. Definition of Stress Parameters: a) Spectrum Load Sequence, and b) Equivalent Constant Amplitude [3-24].

(Figure 3-23). The model has been shown to predict delayed retardation, overload cycle acceleration, and stress ratio effects; however, the model currently cannot account for negative stress ratio fatigue crack acceleration.

Newman [3-61] developed a crack closure model for fatigue crack growth using a Dugdale-type, strip-yielding concept modified to include residual plastic deformation in the wake of an advancing crack-tip (Figure 3-24). Calculated crack opening stresses were used to compute effective stress intensity ranges for use in the crack growth equation

$$\frac{da}{dn} = C\,\Delta K_{eff}^{m} \left[\frac{1 - \left(\frac{\Delta K_o}{\Delta K_{eff}}\right)^2}{1 - \left(\frac{K_{max}}{K_c}\right)^2} \right]$$

where ΔK_o is an effective threshold given by

$$\Delta K_o = \frac{1 - \left(\frac{S_o}{S_{max}}\right)}{1 - R}\,\Delta K_{th}$$

S_o represents the crack opening stress, and C and m are constants determined experimentally. The parameter ΔK_{eff} is given by

$$\Delta K_{eff} = K_{max} - K_{op}$$

where K_{op} is the stress intensity factor at which the crack opens. Figure 3-25 shows that the relation provides good correlation with constant amplitude data for aluminum over a wide range of stress ratio. Figures 3-26 and 3-27 show fairly good correlation between predicted and test lives for spectrum

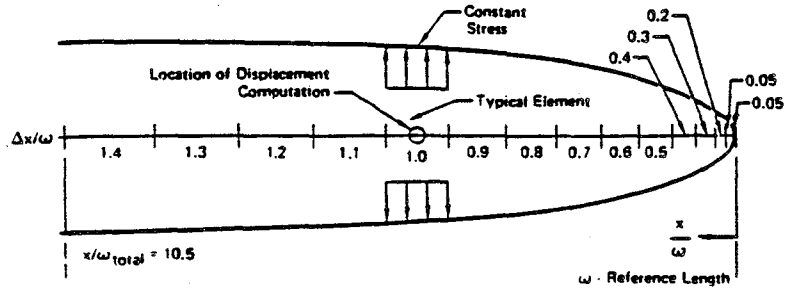

- 25 x 25 Influence Coefficient Matrix Derived Through Bueckner's Weight Function Approach
- Maximum Stress Limited to Yield
- No Tensile Stresses
- Displacements and Stress Intensity Computed for Input Values of K_{max}, K_{app}, E, and f.

Contact stress model of closure.

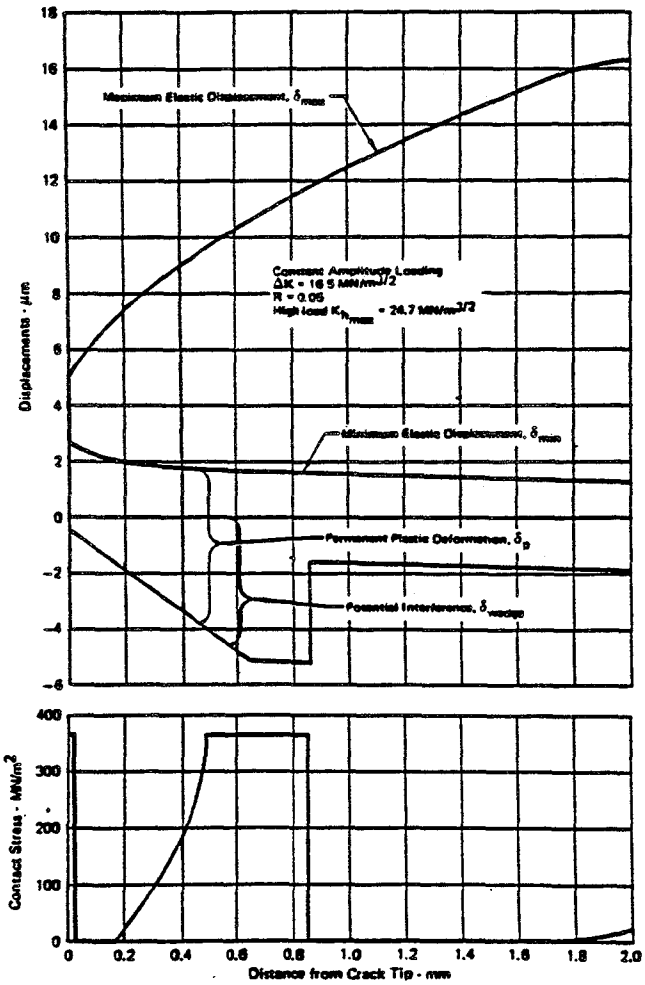

Crack surface displacements and stresses 0.635 mm after a single high load.

Figure 3-23. Summary of Dill and Saff's Model for Prediction of Crack Closure Effects in Variable Amplitude Fatigue [3-60].

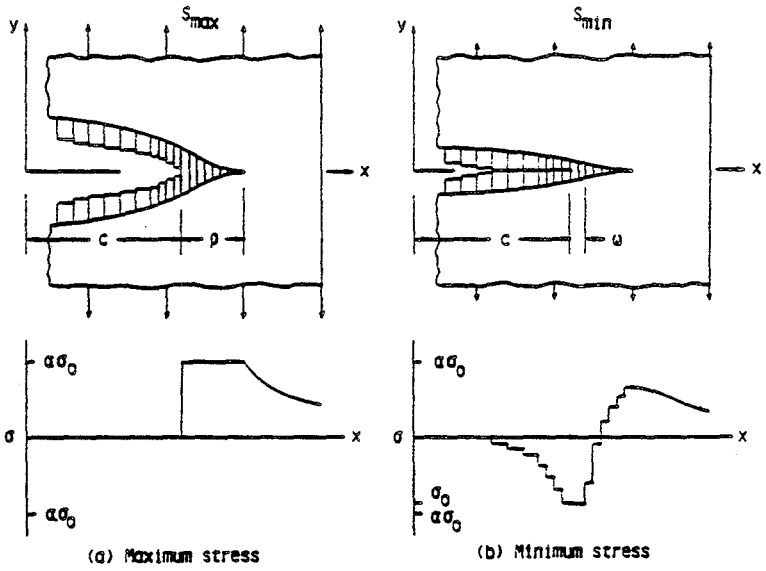

Figure 3-24. Crack-Surface Displacements and Stress Distributions Along Crack Line [3-61].

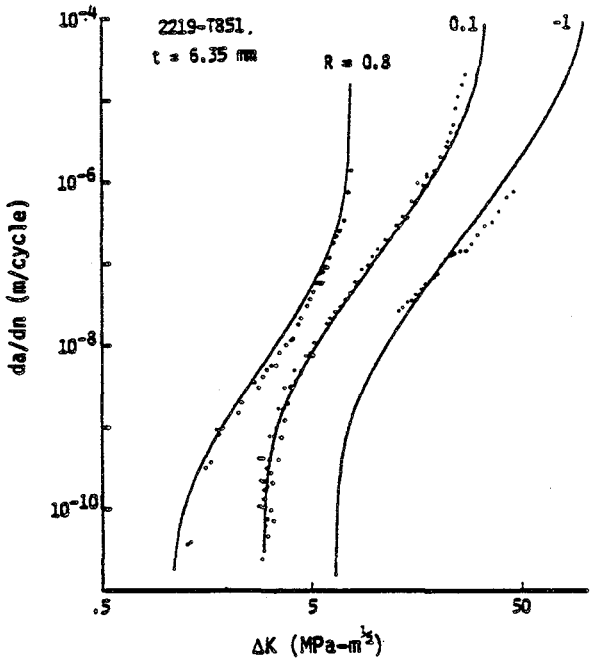

Figure 3-25. Comparison of Experimental Crack Growth Rates and Rate Equations for 2219-T851 Aluminum Alloy at Various R-Ratios [3-61].

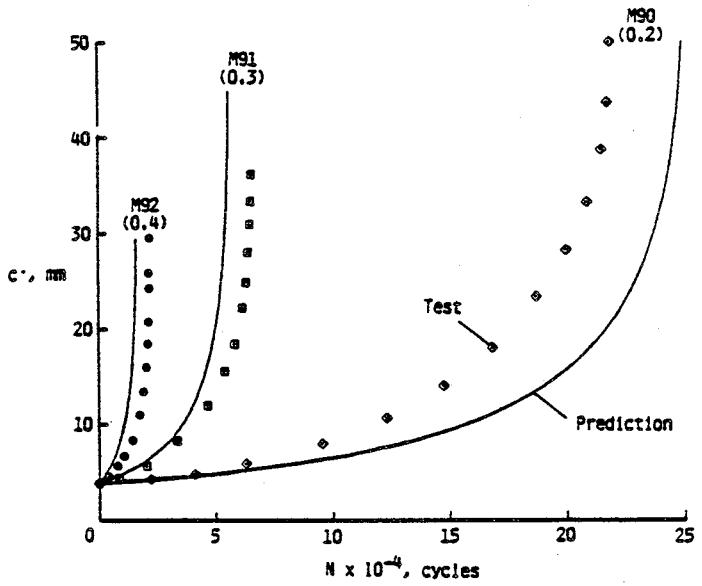

Figure 3-26. Comparison of Experimental and Predicted Crack-Length-Against-Cycles Curves for Spectrum Loading [3-61].

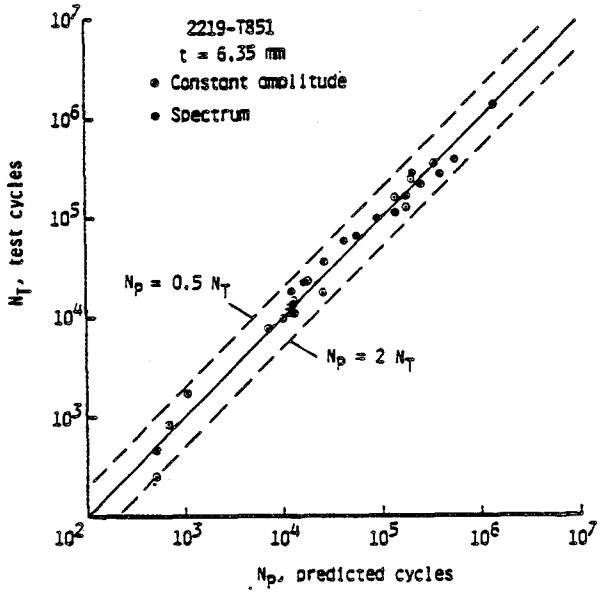

Figure 3-27. Comparison of Experimental (N_T) and Predicted (N_p) Cycles to Failure for 2219-T851 Aluminum Alloy Under Contant-Amplitude and Spectrum Loading [3-61].

loading. These comparisons with spectrum loading tests do not adequately test Newman's model, however, due to the lack of dominant retardation or acceleration effects, as evidenced by the fact that linear cumulative damage predictions offered nearly as good correlation.

One of the major disadvantages of the cycle-by-cycle fatigue crack life predictions models is the large number of computations required. Computer time can be much higher for crack closure models than for statistical models such as the RMS approach and linear summation models such as Elber's equivalent-constant-amplitude technique. Solution time is not the only consideration, however. The spectrum type being analyzed has been shown to affect the applicability of certain models. In cases involving significant load interaction effects, closure models can be far superior to models which cannot account for such effects as retardation and acceleration.

Crack-Tip Plastic Zone Size Models

Crack-tip plastic zone size models assume that the retarded/accelerated crack growth during variable amplitude loading can be related to the relative sizes and interaction of the crack-tip plastic zones. In the early 1970's, several empirical prediction models were developed incorporating plastic zone size concepts. The most publicized of these models were the Wheeler Model [3-62], and the Willenborg Model [3-63]. Both employed plastic zone sizes as indicated in Figure 3-28, but concepts for calculating retarded crack growth rate, $(da/dn)_{ret}$, were different.

The Wheeler model assumes that constant amplitude crack growth can be represented as $da/dn = f(\Delta K)$, i.e., $da/dn = C(\Delta K)^m$. The model sums crack

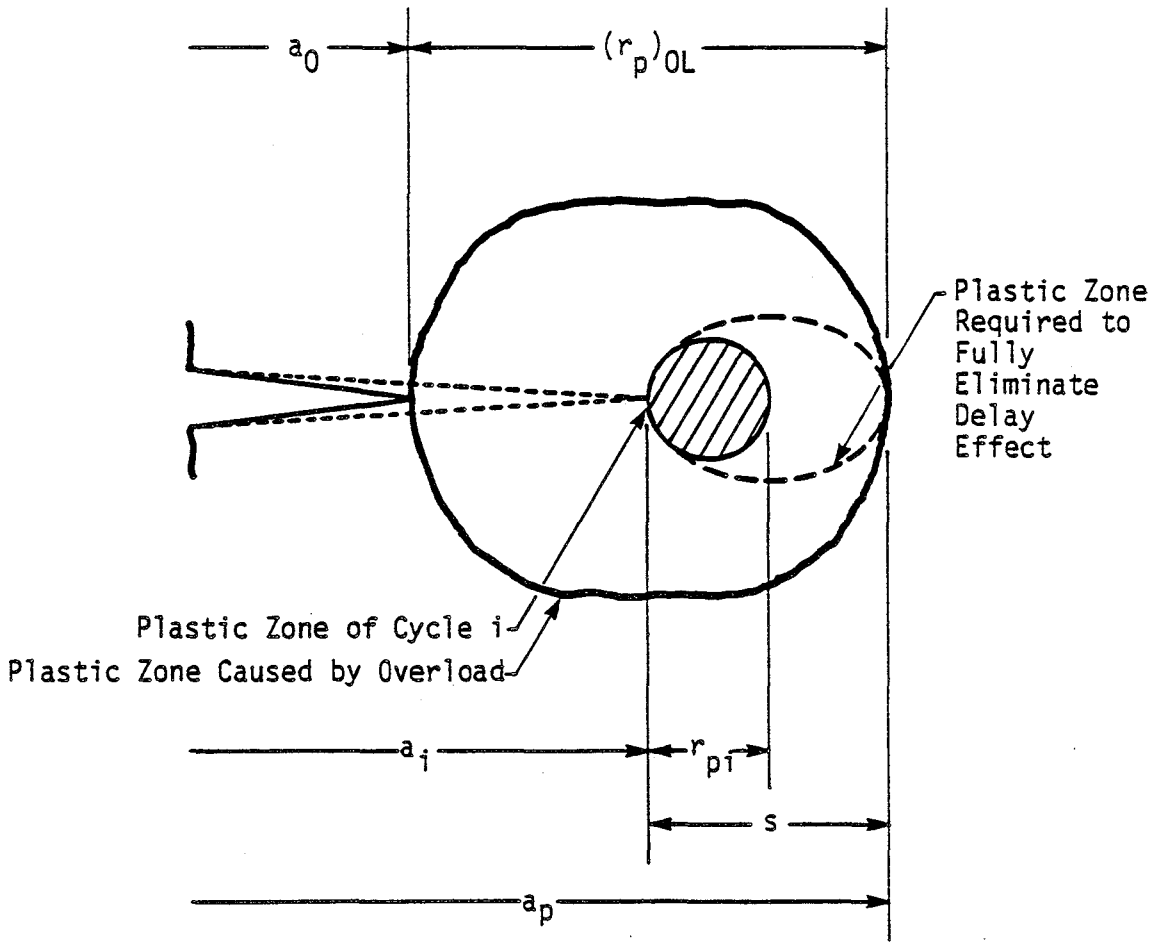

$$r_p = \frac{1}{\beta\pi}\left(\frac{K}{\sigma_{ys}}\right)^2$$

β = Parameter Reflecting Plane Strain, Plane Stress Conditions

Figure 3-28. Plastic Zone Size Concepts Employed in Wheeler and Willenborg Variable Amplitude (Retardation) Models [3-62, 3-63].

growth according to $a_r = a_o + \sum_{i=1}^{r} (da/dn)_i$ where a_o = initial crack length, a_r = crack length after r cycles, and $(da/dn)_i$ = crack growth rate during i^{th} cycle. To account for reduced crack growth behavior following a tensile overload, a retarded crack growth rate expression is used where

$$[(da/dn)_i]_{ret} = (C_p)_i \; [C \; (\Delta K)_i^m]$$

where $(C_p)_i$ is a retardation parameter bounded by values of 0.0 (crack arrest) and 1.0 (no retardation). Wheeler postulated that $(C_p)_i$ was a function of the ratio of the current plastic zone size, r_{p_i}, to the plastic zone size created by the overload. Using the notation of Figure 3-28, Wheeler's retardation parameter is defined as $(C_p)_i = (r_{p_i}/s)^p$ where r_{p_i} = plane strain yield zone size = $1/4\sqrt{2\pi}\,(K_{max}/\sigma_{ys})^2$ [3-62], s = distance from current crack-tip to yield zone boundary produced by last tensile overload, and p = "shaping parameter". Retardation ceases when the plastic zone of the current cycle, r_{p_i}, reaches the overload plastic zone.

Wheeler was able to make successful predictions of cracks in specimens subjected to six different spectra, having three different configurations, and made of two materials (D6AC steel and Ti-6Aℓ-4V). Trial and error was used to obtain values of p which correlated the predicted crack growth to the experimental data. Figure 3-29 shows some of Wheeler's correlations. However, even through the correlation is good, the shaping exponent is the key drawback to this model. There is no method except experimentation that can be used to determine the value of p.

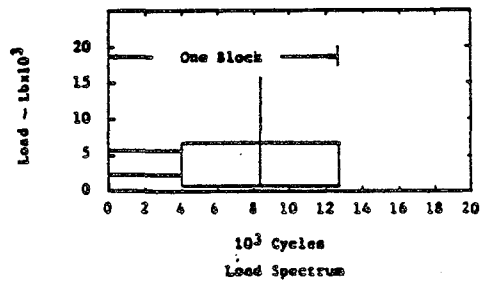

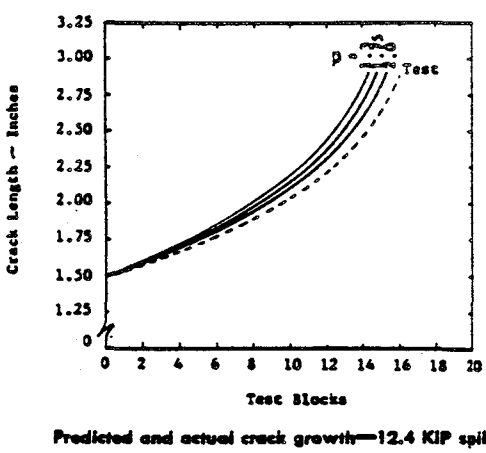

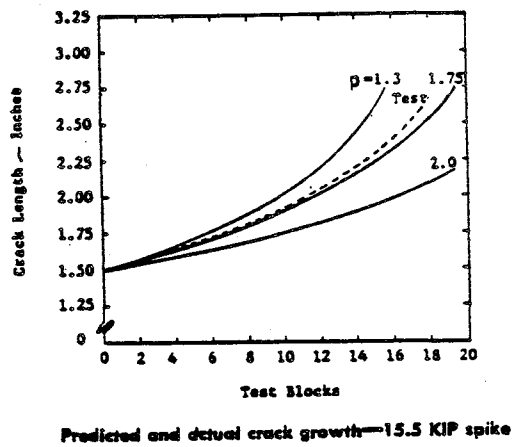

Figure 3-29. Examples of Wheeler's [3-62] Correlation Between Predicted and Experimental Crack Growth Under Variable Amplitude Loading.

In contrast to multiplying the constant amplitude crack growth expression $C\Delta K^m$ by a retardation parameter, $(C_p)_i$, Willenborg [3-63] modeled reduced crack growth rates through the overload plastic zone using an effective stress and operating directly on the crack growth stress intensity factors. The crack growth retardation is developed by changing the magnitude of ΔK or $(\Delta\sigma)$ to ΔK_{eff} (or $\Delta\sigma_{eff}$) in the crack growth rate expression, such as the relation $C\Delta K^m$. Simultaneously R-ratio is modified to $R_{eff} = (K_{min})_{eff}/(K_{max})_{eff}$.

Using the overload spectrum load definitions in Figure 3-13 and the plastic zone definitions in Figure 3-28, the plastic zone size corresponding to the overload conditions is first calculated

$$(r_p)_{OL} = \frac{1}{\beta\pi}\left(\frac{K_{OL}}{\sigma_{ys}}\right)^2$$

Taking the stress intensity relationship to be

$$K = \sigma\,(\pi a)^{1/2}\,Y$$

this can be written as

$$(r_p)_{OL} = \frac{\sigma_{OL}^{\,2}\,Y^2\,a}{\beta\,\sigma_{ys}^{\,2}}$$

This is added onto the physical crack length to give the "plastically corrected" crack length

$$a_p = a_o + r_p$$

Retardation will occur during subsequent loading until the "plastically corrected" crack length corresponding to the current conditions is equal to a_p.

Taking a_i to be the physical crack length at the "i-th" cycle, the first step is to calculate the applied stress that would be required to have (a_i + r_{p_i}) equal to a_p. This stress is denoted as σ' and is found from the relation

$$a_i + \frac{\sigma'^2 \, a_i \, Y^2}{\beta \, \sigma_{ys}^{\,2}} = a_p$$

This results in

$$\sigma' = \frac{\sigma_{ys}}{Y} \left[\beta \, \frac{a_p + a_i}{a_i}\right]^{1/2}$$

The next step is to determine a "reduction" stress, σ_{red}, according to

$$\sigma_{red,i} = \sigma' - \sigma_{max,i}$$

The actual maximum and minimum stresses in cycle "i" are then reduced by this amount to provide an "effective" stress

$$\sigma^{(e)}_{max,i} = \sigma_{max,i} - \sigma_{red,i} = 2\sigma_{max,i} - \sigma'$$

$$\sigma^{(e)}_{min,i} = \sigma_{min,i} - \sigma_{red,i} = \sigma_{max,i} + \sigma_{min,i} - \sigma'$$

If either of these effective stresses is less than zero, it is set equal to zero, and the value of $\Delta\sigma^{(e)}$ and $R^{(e)}$ then calculated. These values are then used in the constant amplitude crack growth "law" to find Δa_i -- the

crack extension during the "i-th" cycle. A new value of σ' is then calculated, from which follows the value of Δa for the next cycle. Alternatively, if another high stress cycle occurs, a new value of $(r_p)_{OL}$ is calculated.

Retardation due to an overload persists until the far edge of the plastic zone evaluated using current conditions reaches the far edge of the plastic zone corresponding to previous overload conditions. The procedure developed by Willenborg, et al. [3-63] provides procedures for estimating the extent of the retardation.

Figure 3-30 shows representative samples of the correlation Willenborg [3-63] obtained with test data. Note in this figure that Willenborg also compares Wheeler's model to the experimental results.

While both Wheeler [3-62] and Willenborg [3-63] reported good correlation between predicted and observed crack growth under spectrum loading in their respective publications, both models have been checked by various authors [3-31, 3-64 through 3-67], as reported by Schijve [3-23], but systematic agreement with test results was rarely found. The most significant difference between the two models is that the Willenborg model uses only constant amplitude crack growth data and does not require additional experimental test data to predict growth retardation -- as does the Wheeler model by including the shaping parameter, p. Both models cannot account for the following physical observations:

(1) The increase in retardation due to multiple overloads.

(2) Delay of retardation after overload application. Both models predict maximum retardation immediately after the overload.

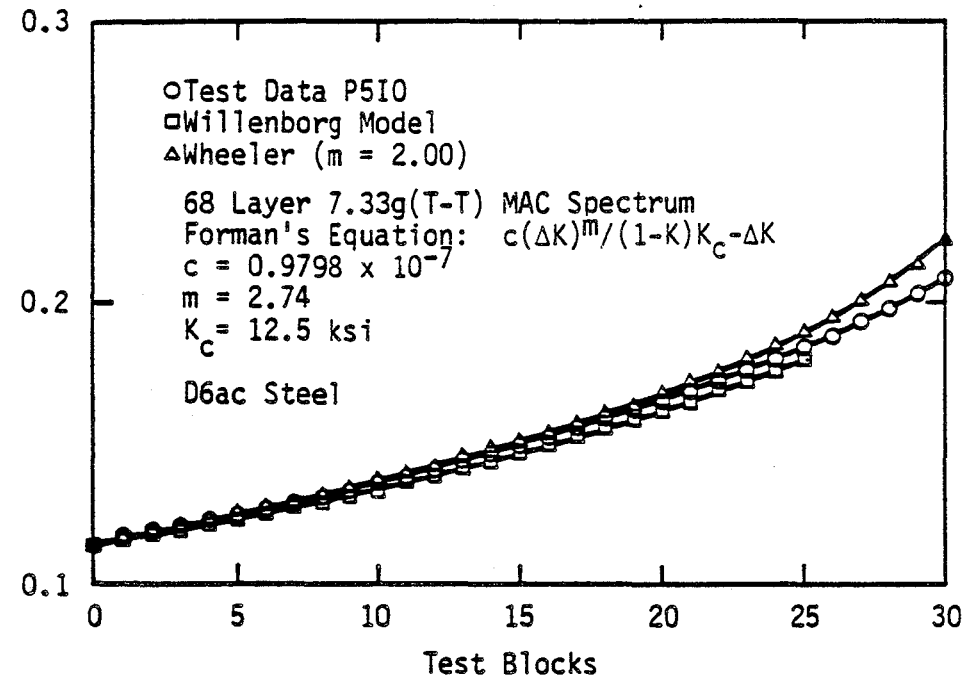

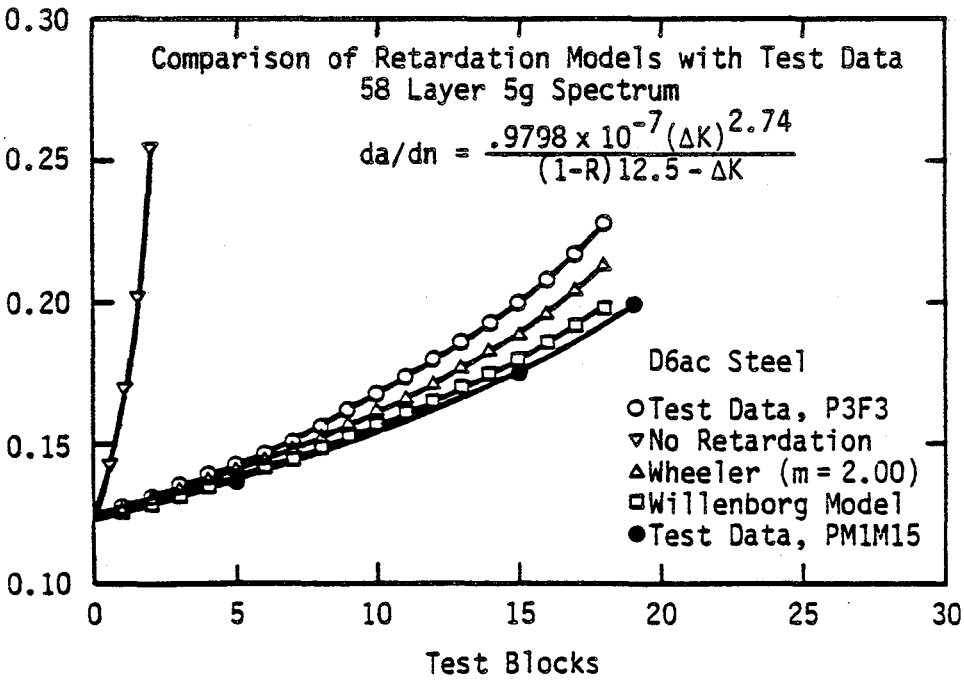

Figure 3-30. Examples of Willenborg's [3-63] Correlations Between Predicted and Experimental Crack Growth Under Variable Amplitude Loading. Note that Willenborg Includes Results by Wheeler [3-62] for Comparison.

(3) Crack growth acceleration due to up-loading of higher stress level.

(4) Threshold values of $\lambda = \sigma_{OL}/\sigma_{max} > 1.0$ which produces no crack growth retardation.

(5) Decrease in retardation due to underloads.

During the early and mid-1970's after the Wheeler and Willenborg models were suggested, analytical models based on crack-tip plasticity for predicting crack growth under spectrum loading focused on reformulating and adding to the basic concepts of the Willenborg model. As model development evolved during this period, attention was focused on expanding the crack models to account for the above-mentioned deficiencies inherent to the original model.

Gallagher [3-68, 3-69] reformulated the Willenborg model and in addition, added an empirical parameter, ϕ, to account for overload crack arrest values greater than 2.0 (as originally formulated). Gallagher's "effective" stress intensity factors were defined as:

$$K_{eff} = K_{max} - \phi K^{W}_{red}$$

where K^{W}_{red} is the reformulation of Willenborg's model expressed as (see Figure 3-28 for $r_{p(OL)}$ and s)

$$K^{W}_{red} = K_{OL}\left[1 - \frac{s}{(r_p)_{OL}}\right]^{1/2} - K_{max}$$

and

$$\phi = \frac{K_{max} - (K_{max})_{th}}{K_{OL} - K_{max}}$$

where $(K_{max})_{th}$ = threshold stress intensity at R = 0.0

The value of ϕ is determined by experiments which provide values of the shut-off (crack arrest) ratio $(K_{OL}/K_{max})_{shut\text{-}off}$ (see Probst and Hillberry [3-43]) and the threshold stress intensity, K_{th}, of the particular material. In Gallagher's expression, the parameter, ϕ, requires $K_{eff} = K_{th}$ when an overload ratio equal to the shut-off ratio is applied.

Using values of $(K_{OL}/K_{max})_{shut\text{-}off} = 2.3$ and $K_{th} = 6.0$ ksi-in$^{1/2}$ for 4340 steel of two different yield strengths, Gallagher [3-69] found that the model predicted to within 10% of the cycles requried for crack growth through the overload affected region but was not accurate in predicting the crack growth rate through the overload zone. Figure 3-31 summarizes these findings. Gallagher noted from Figure 3-31 (b) that his model was "conservative" since steady state crack growth rates were predicted sooner than observed. However, as shown in the table in Figure 3-31 (a), the predicted number of cycles to grow through the overload-affected region was not conservative.

An in-house load interaction model developed by Chang [3-57] at Rockwell/NAAD combined the generalized Willenborg model with a method to account for negative values of $(K_{min})_{eff}$ and R_{eff}. In the original Willenborg model, negative values of $(K_{min})_{eff}$ were reset to zero. Using the modified Walker Equation [3-70], Chang modeled crack growth during the overload-affected region as:

$$\frac{da}{dn} = C[K_{eff}/(1 - \bar{R}_{eff})^{1 - p}]^m$$

for $0 < \bar{R}_{eff} < R^{+}_{cut}$, $\bar{R}_{eff} = R_{eff}$

COMPARISON OF PREDICTED AND MEASURED DELAY PARAMETERS

Yield Strength Level σ KSI	Overload Affected Crack Length (a^*) mils	Measured Cycles to Achieve a^* (N^*)	Overload Yield Zone Radius ($r_{y_{OL}}$) mils	Measured Cycles to Achieve $r_{y_{OL}}$ (N^{**})	Predicted Cycles to Achieve $r_{y_{OL}}$	
					Willenborg et al (N_W)	New Model (N_M)
120	16.6	33,100	17.7	35,600	-	31,750
220	4.6	4,100	5.3	4,180.	-	3,780

$$z_{OL} = r_{y_{OL}} = \frac{1}{2\pi}\left[\frac{K^{OL}_{max}}{\sigma_{ys}}\right]^2$$

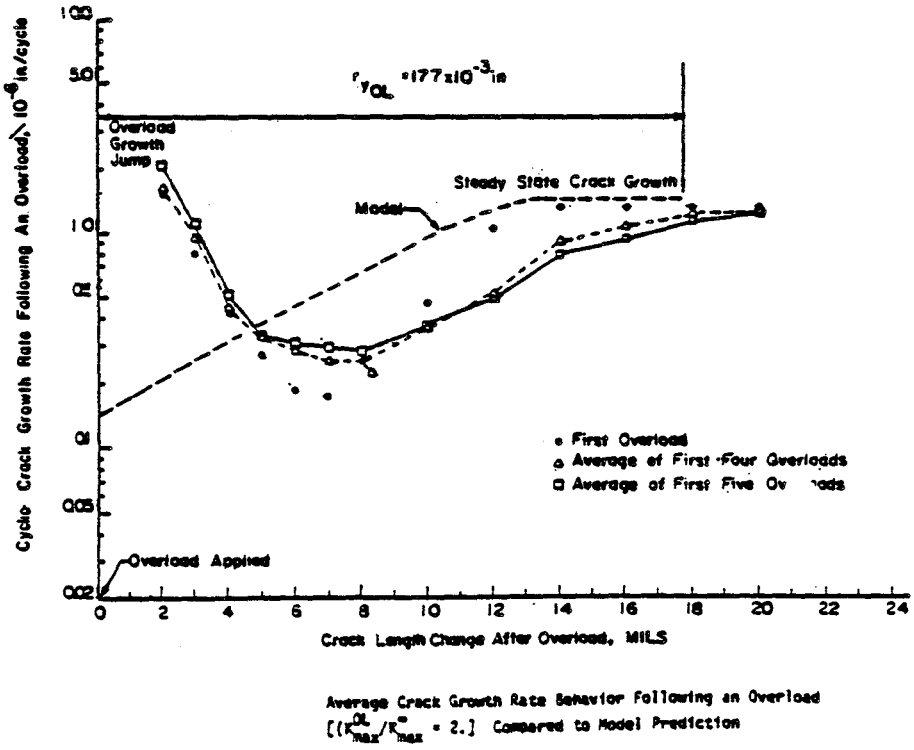

Average Crack Growth Rate Behavior Following an Overload $[(K^{OL}_{max}/K^{*}_{max} = 2.]$ Compared to Model Prediction

Figure 3-31. Correlation of Gallagher's Generalized Willenborg Model [3-69] with Experimental Data for a) Several Delay Parameters and b) Crack Growth Rates in Overload-Affected Region.

$$0 < \overline{R}_{eff} > R^{+}_{cut},\ \overline{R}_{eff} = R^{+}_{cut}$$

and

$$\frac{da}{dn} = C[(1 - R_{eff})^{q} (K_{max})_{eff}]^{m}$$

for $R_{eff} < 0$

where R^{+}_{cut} is the cut-off stress ratio above which da/dn $\neq$ f(R), p is the Walker "collapsing" factor, q is the negative stress ratio index expressed as

$$q = [\ln(r)/\ln(1 - R)]/n,\ R < 0$$

r is the ratio of crack growth rate at a specific negative R value to its counterpart at R = 0, and n is the fatigue crack growth rate exponent determined from R = 0 crack growth data.

Chang also included in his model an effective overload retardation zone size, $(r_{OL})_{eff}$, to account for reduced retardation due to an underload following an overload. The effective overload retardation zone size is defined as:

$$(Z_{OL})_{eff} = (1 - R_{eff})(Z_{OL}),\ R_{eff} < 0$$

where Z_{OL} is the plastic zone size produced by the tensile overload.

Chang's model was used to predict fatigue crack growth under spectrum loading in a recent ASTM round-robin analysis [3-71]. Chang was able to show good correlation with the experimental results as indicated in Table 3-4. As

Table 3-4
Results of Willenborg/Chang Retardation Model [3-57] Used to Predict Crack Growth Under Spectrum Loading in ASTM Task Group Round-Robin

—Comparison of analytical predictions with different overload shut-off ratios.

Test No.	Mission Type	Test Life, cycles	N_{pred}/N_{test}	
			$R_{SO} = 3.0$	$R_{SO} = 2.3$
M-81	Fighter (A-A)[a] DLS[b] = 20 ksi[c]	115 700	1.46	1.46
M-82	Fighter (A-A) DLS = 30 ksi	58 585	0.91	1.04
M-83	Fighter (A-A) DLS = 40 ksi	18 612	0.93	1.07
M-84	Fighter (A-G)[d] DLS = 20 ksi	268 908	1.37	1.37
M-85	Fighter (A-G) DLS = 30 ksi	95 642	0.96	1.11
M-86	Fighter (A-G) DLS = 40 ksi	36 367	0.80	0.93
M-88	Fighter (I-N)[e] DLS = 30 ksi	380 443	1.39	2.22
M-89	Fighter (I-N) DLS = 40 ksi	164 738	1.12	1.82
M-90	Fighter Composite DLS = 20 ksi	218 151	1.33	1.55
M-91	Fighter Composite DLS = 30 ksi	65 627	1.01	1.17
M-92	Fighter Composite DLS = 40 ksi	22 182	0.98	1.12
M-93	Transport MSS[f] = 14 ksi	1 359 000	1.31	1.36
M-94	Transport MSS = 19.6 ksi	279 000	1.14	1.18
Average			1.13	1.34
Standard deviation			0.22	0.29

[a] A-A = Air-to-Air.
[b] DLS = Design limit stress.
[c] 1 ksi = 6.9 MPa.
[d] A-G = Air-to-Ground.
[e] I-N = Instrumentation and Navigation.
[f] MSS = Maximum spectrum stress.

indicated in this table, the overload shut-off ratio was found to be an important factor in his model for predicting crack growth lives.

Johnson [3-72] formulated a phenomenological multi-parameter yield zone (MPYZ) model based on the Willenborg model to account for:

a) overload retardation shut-off (similar to Gallagher's model [3-68]),

b) overload retardation threshold,

c) multiple overload retardation,

d) acceleration due to low-high sequences, and

e) reduced retardation due to underloads.

As in the Willenborg model, the MPYZ model utilizes a residual stress intensity (K_R) concept. The above phenomena are accounted for by decreasing or increasing the effective stress ratio, R_{eff}, which is a function of K_R. The effective stress range used to calculate crack growth is equal to the applied constant amplitude stress range, but the mean of the stress range is altered by K_R to account for the appropriate load interaction effect. The basic relationships contained in the MPYZ model are as follows:

$$(K_{max})_{eff} = K_{max} - \phi_R K_R^W$$

$$(K_{min})_{eff} = K_{min} - \phi_R K_R^W$$

$$K_R = \phi_R K_R^W$$

$$(\Delta K)_{eff} = (K_{max})_{eff} - (K_{min})_{eff} = (\Delta K)_{CA}$$

$$R_{eff} = \frac{K_{min} - K_R}{K_{max} - K_R} = \frac{(K_{min})_{eff}}{(K_{max})_{eff}}$$

$$K_R^w = K_{OL}\left[1 - \frac{s}{(r_p)_{OL}}\right]^{1/2} - K_{max}$$

$$(r_p)_{OL} = \text{Plastic Zone Diameter} = \frac{1}{\gamma\pi}\left(\frac{K_{OL}}{\sigma_{ys}}\right) \quad \begin{pmatrix}\gamma = 3, \text{ plane strain} \\ \gamma = 1, \text{ plane stress}\end{pmatrix}$$

$$\phi_R = [1.0 - K_{th}/K_{max}]/[(\psi - 1.0) \times (1.0 - R_L)]$$

Overload retardation effects are accounted for in the parameter, ϕ_R. In the expression for ϕ_R, $\psi = B/A$ [A = retardation threshold parameter of the ratio of K_{OL} to K_{max} (no retardation effect), B = shut-off ratio K_{OL} to K_{max} (crack arrest)], and $R_L = \sigma_{UL}/\sigma_{OL}$ (ratio of underload to overload stress). To account for multiple overloads which tend to increase retardation (up to a saturation point), Johnson substituted B' for B, where $B' = [(B - 2.0)/N_{OL}] + 2.0$ and N_{OL} = number of successive overloads. In this expression, the value 2.0 was considered to be a lower bound for B' at the saturated number of overloads for 2219 aluminum alloy.

Parameters A and B are considered to be material parameters. Systematic single-overload tests, similar to tests conducted by Probst and Hillberry [3-43] are required to determine these parameters. Johnson found in the literature that typical values of A and B range from 1.0 to 1.5 and 1.8 to 2.5, respectively, for various materials.

Acceleration effects during application of the overload(s) was modeled by Johnson [3-72] using

$$K_R = \phi_A K_R^W \qquad \text{for } K_R^W < 0$$

where $\phi_A = (1.0 - R_L)$ and adjusts the amount of acceleration depending on the ratio, R_L, of the underload stress to the overload stress.

Underload effects (decreasing retardation) were modeled into the MPYZ model using an "effective" overload stress intensity factor K'_{OL} where

$$K'_{OL} = \frac{K_{eff}^{OL}}{Z - Y} (Z - \beta) + K_{max}$$

and

$$K_{eff}^{OL} = K^{OL} \left(1 - \frac{s}{(r_p)_{OL}}\right)^{1/2}$$

$$\beta = \frac{K_{pr} - K_{UL}}{K_{eff}^{OL} - K_{UL}}$$

where K_{pr} = minimum value of stress intensity before overload, Z = value of β above which K'_{OL} is K_{max}, and Y is the value of β below which K'_{OL} equals K_{eff}^{OL}. The relationship among these variables is shown in Figure 3-32 and illustrates that Y determines when the underload does not reduce the amount of retardation, and Z determines when no retardation occurs. As similar to the A and B parameters, Y and Z must be experimentally determined for the particular material.

In the ASTM round-robin analysis [3-71] the MPYZ model coupled with a Forman crack growth expression gave the results shown in Figure 3-33. As indicted, correlation was bounded by N_{pred}/N_{test} = 0.5 and 2.0 for the thirteen spectrum load tests conducted.

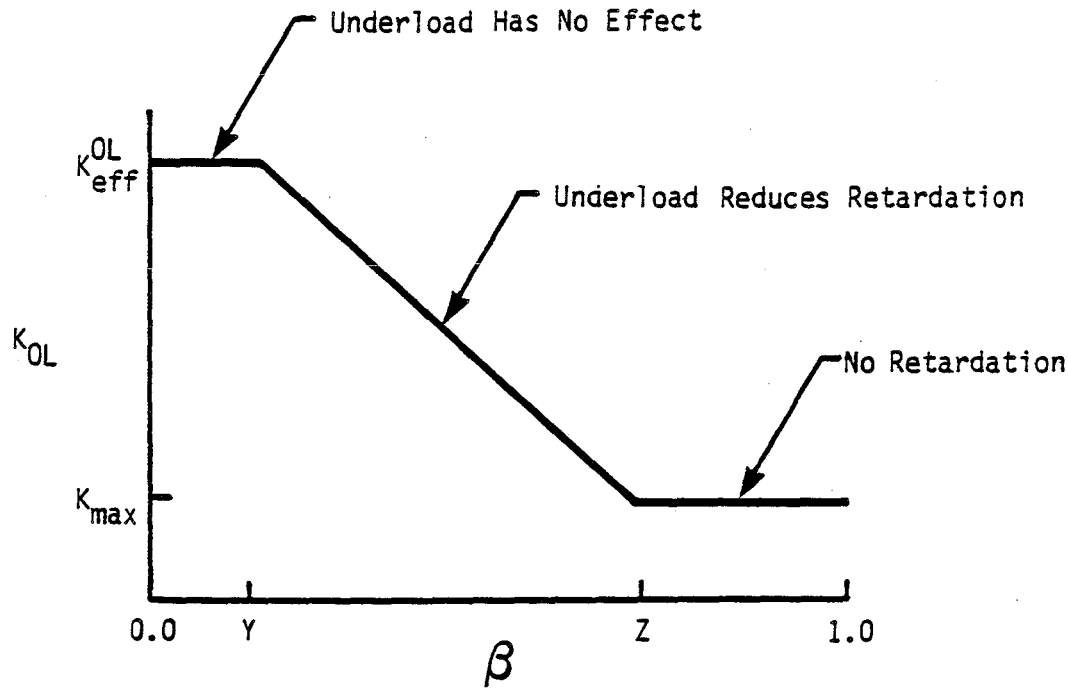

Figure 3-32. Schematic Illustration of Relationship Between Underload Parameters in Johnson's MPYZ Load Interaction Model [3-72].

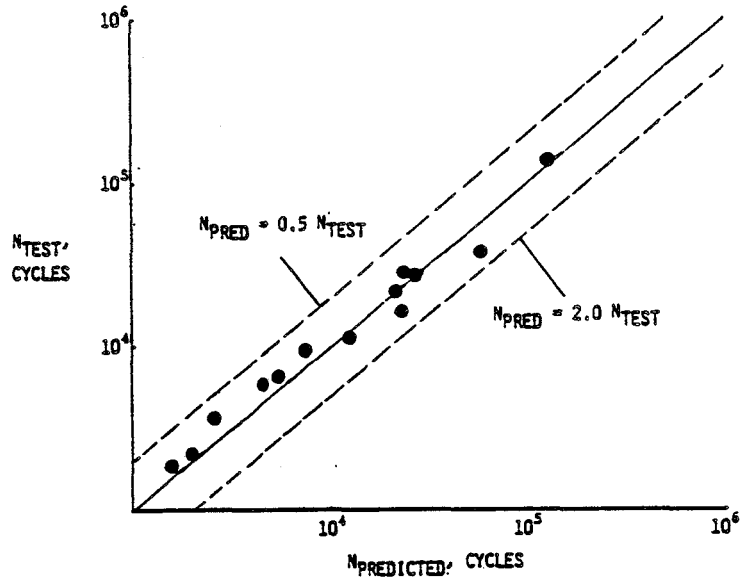

Correlation of predicted life (N_{pred}) to test life (N_{test}).

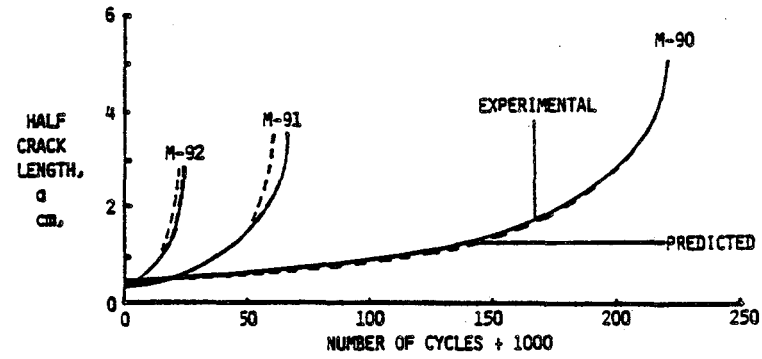

Sample crack growth predictions for the fighter composite mission spectra.

Figure 3-33. Predictions of Johnson's MPYZ Model [3-72] in the ASTM Round Robin Spectrum Loading Program.

3.5 ENVIRONMENTAL AND FREQUENCY EFFECTS

The environment can have a substantial influence on the nucleation and propagation of cracks in solids. Studies on the influence of environment on fatigue crack growth began in the mid-1960s [3-73, 3-74]. The early work was mainly concerned with characterizing the fatigue crack growth response and recording the influence of different variables on environmentally enhanced crack growth. The problem is one of immense complexity due to the large number of mechanical, metallurgical and environment variables involved. In fact, many of the observed effects of loading variables can be traced directly to environmental interactions. The development of a mechanistic understanding was essentially by inference and was often incidental to the earlier studies [3-75].

The application of linear elastic fracture mechanics to the study of stress corrosion cracking and corrosion fatigue has had considerable success. One would expect that environmental attack would most likely occur at the highly stressed region in the vicinity of the crack-tip, and would be dependent on the magnitude of the stresses near the crack tip. Hence, the stress intensity factor K_I seems the logical candidate to control stress corrosion cracking and fatigue.

In Section 3.5.1 a brief overview of the influence of environment on fracture properties is given while noting the rate dependence of stress corrosion cracking. Section 3.5.2 treats environmentally assisted fatigue. A summary of the basic phenomenological observations regarding corrosion fatigue is given first. The effects of frequency, temperature and pressure on sub-critical crack growth are then considered. "Classical" fracture mechanics

mechanisms do not appear to be able to fully explain the environmental effects on near-threshold crack growth -- this is examined in a separate subsection. A selection of mechanisms and models for crack growth in gaseous and high temperature environments is dealt with in Section 3.5.3.

3.5.1 Influence of Environment on Fracture Properties

The fracture properties of certain materials can be altered substantially in an aggressive environment. Stress corrosion cracking (SCC) is a fracture phenomenon resulting from the conjoint action of tensile stress and corrosion -- if either component is removed cracking will stop. Stress corrosion cracking depends in a complex way on a large number of mechanical, metallurgical and environmental parameters.

Speidel [3-76] presents a schematic representation of the effect of loading rate on the fracture resistance of solids in inert and aggressive environments (Figure 3-34). He emphasizes that, in general, fracture toughness tests (K_{Ic}) are performed at loading rates where the effects of all but the most aggressive environments is hardly measurable. As indicated in the figure, at sufficiently low loading rates a large difference may be apparent between the fracture toughness (K_{Ic}) and threshold value of K for stress corrosion crack growth (K_{ISCC}). This implies that environmental attack is strongly rate dependent. It has been suggested that K_{ISCC} should be the value of K corresponding to a crack growth of 3×10^{-11}m/s [3-76]. K_{ISCC} may be influenced by temperature, pressure of gaseous environments and microstructure.

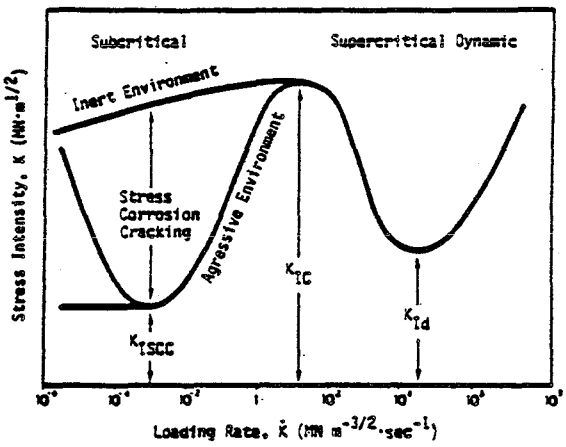

Figure 3-34. Schematic Representation of the Effect of Loading Rate on Stress Intensity at Which Crack Propagation Begins [3-76].

Fracture mechanics properties for the SSME materials and environments are investigated in References 3-77 through 3-82. Campbell [3-83] reviewed the fracture toughness of high strength alloys at low temperatures. He found that for many aluminum alloys, the fracture toughness increases or remains generally constant as temperature is lowered. Titanium alloys tended to have lower toughness as the testing temperature is decreased, but the effect is influenced by the alloy content and heat treatment. The fracture toughness of Inconel 718 was not affected at low temperatures [3-84].

3.5.2 Environmentally Assisted Fatigue

K_{ISCC} for an environment-material system defines the plane strain stress intensity below which stress corrosion crack growth will not occur under static loads. A number of investigators [3-75, 3-85, 3-86] suggest that the corrosion-fatigue behavior for the environment-material system could be altered when the maximum stress intensity in the load cycle (K_{max}) becomes greater than K_{ISCC}. This would imply that the corrosion-fatigue behavior should be divided into the below K_{ISCC} and above K_{ISCC} behavior. These two types of behavior have been named "true corrosion fatigue" for K_{max} less than K_{ISCC} and "stress corrosion fatigue" for those above K_{ISCC}. Austin [3-86] indicates that in true corrosion fatigue a joint action of both fatigue cycling and environmental attack is required for enhanced crack growth rates -- Type A behavior in Figure 3-35. Stress corrosion fatigue is the result of stress corrosion under cyclic loading with no interaction effects -- Type B. Type C behavior is typical of materials that exhibit true corrosion fatigue at all stress intensities and also suffer stress corrosion above K_{ISCC}.

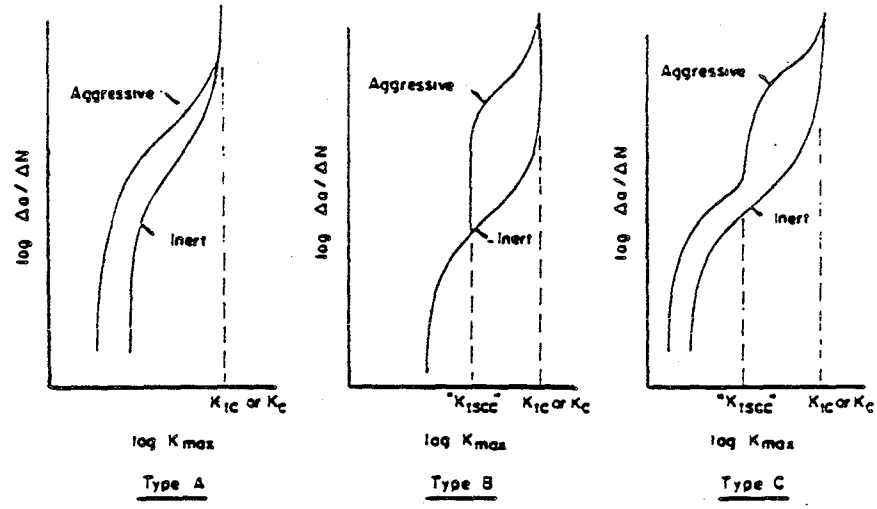

Figure 3-35. Types of Fatigue Crack Growth Behavior [3-75].

Wei [3-75] associates Type A behavior with aluminum alloys. The environmental effect is a function of thickness or state of stress and a small effect of frequency in fully saturated and aqueous environments. Partially saturated environments enhance the frequency effects and is related to the partial pressure of water vapor [3-87 through 3-89]. Type B fatigue crack growth behavior in aggressive environments depends on frequency, stress intensity level, stress ratio and waveform [3-86, 3-87, 3-90].

Actual situations may not always fit into the scheme shown in Figure 3-35. As exemplified by discussions by Gerberich and Yu [3-91], an abrupt increase in da/dn, such as occurs in Type B behavior, does not necessarily occur at the conventionally defined value of K_{ISCC}. The types of behavior shown in Figure 3-35 provide indications of general trends and the current state-of-the-art is such that specific tests on the material/environment system of concern must be performed in order to allow reliable and accurate crack growth calculations to be performed.

Frequency Effects

Fatigue crack growth rates in an inert environment at room temperature are independent of the cyclic load frequency. However, if a material is subject to fatigue in an adverse environment, a strong effect of cyclic frequency on crack growth rates may be observed. A dramatic example is given in Figure 3-36 for a high strength steel in water. The strong frequency dependence of the corrosion fatigue crack growth rate is attributed to the superposition of the cycle dependent fatigue crack growth and the time dependent stress corrosion cracking during each load cycle [3-92]. Environ-

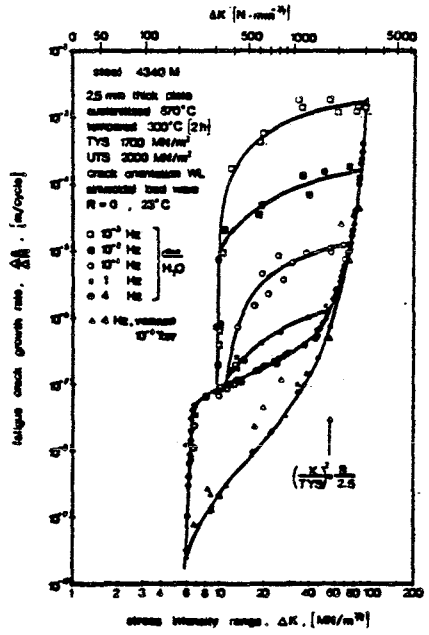

Figure 3-36. The Effect of Stress Intensity and Cyclic Frequency on the Crack Growth Rate of a High Strength Steel [3-76].

mental frequency effects are found to be negligible at high frequencies and reach a maximum at intermediate frequencies. Lower frequencies may produce a slight decrease or no change in the environmental effect. The magnitude of the variation from fatigue crack growth in an inert environment depends strongly on the material-environment system.

In Figure 3-37, the effect of cyclic load frequency on the fatigue crack growth rate of Inconel 718 in 10,000psi hydrogen is demonstrated. The stress intensity range is 54MPa-$m^{1/2}$ (50ksi-$in^{1/2}$). The crack growth rate in 5,000psi helium at a similar stress intensity range is included to represent an inert environment. From the figure it is evident that crack growth rate (per cycle) increases with cycle duration. Further, the cyclic crack growth would most likely approach the rate of helium at cyclic rates greater than 1 cycle per second (see also Figure 3-37b). Jewett et al. [3-79], notes that at 1Hz, where the influence of hydrogen was slight, the fracture was transgranular and ductile. The fracture at 0.1Hz was mainly intergranular. They concluded that the increase in crack growth rate and change of fracture mode to intergranular fracture at longer cycle durations indicates that the effect of cycle duration on cyclic crack growth is due to a superimposed sustained load crack growth.

Speidel [3-76] suggests that at low frequencies the time-dependent crack growth dominates and corrosion fatigue crack growth rates can be predicted from the known stress corrosion crack growth rate. An example of a situation where such linear superposition is applicable is shown in Figure 3-38. The prediction is indicated by the dashed line SCC. Rolfe and Barsom [3-85] note that a K_{ISCC} test may be considered a corrosion fatigue test at extremely low

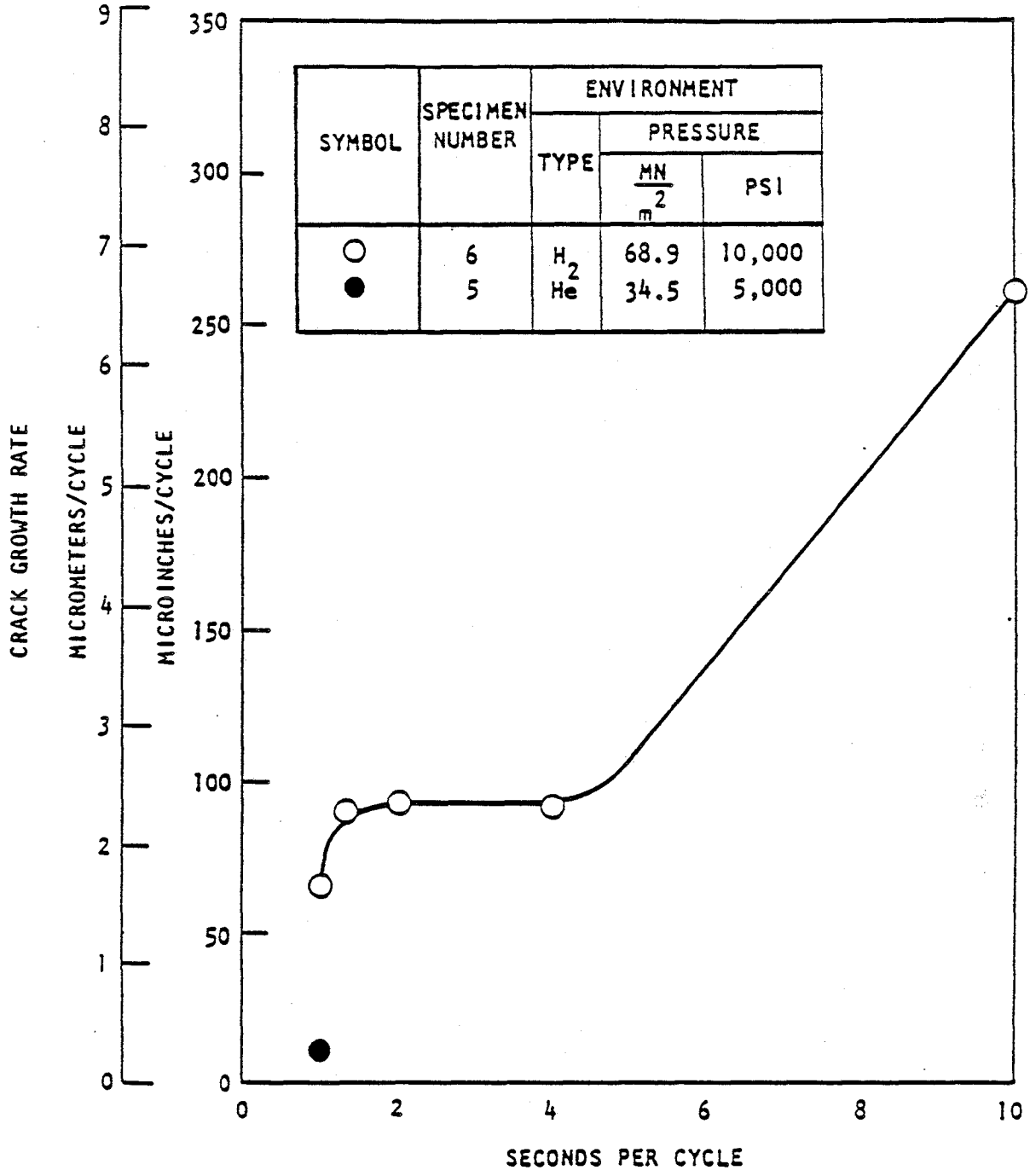

Figure 3-37a. Ambient Temperature Cyclic Crack Growth Rate as a Function of Cyclic Rate for Inconel 718 Specimen No. 6 Exposed to 68.9 MN/m^2 (10,000 psi) Hydrogen at Stress Intensity Range of 54.7 $MN/m^2 \sqrt{m}$ (50.0 ksi $\sqrt{in}$) [3-78].

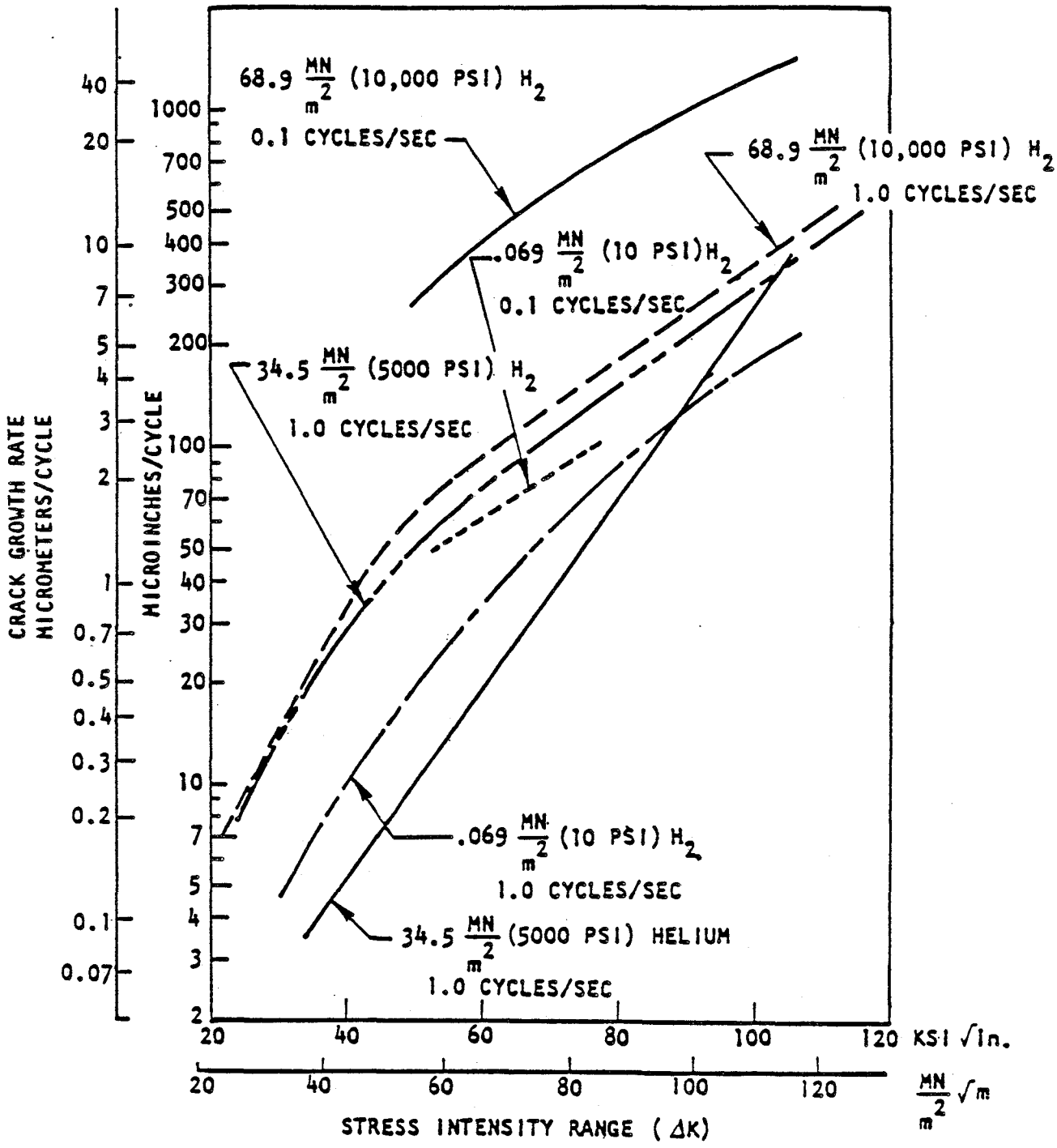

Figure 3-37b. Cyclic Crack Growth Rate as a Function of Stress Intensity Range for Inconel 718 Exposed to 34.5 MN/m^2 (5000 psi), and 68.9 MN/m^2 (10,000 psi) Hydrogen Ambient Temperature Environments [3-78].

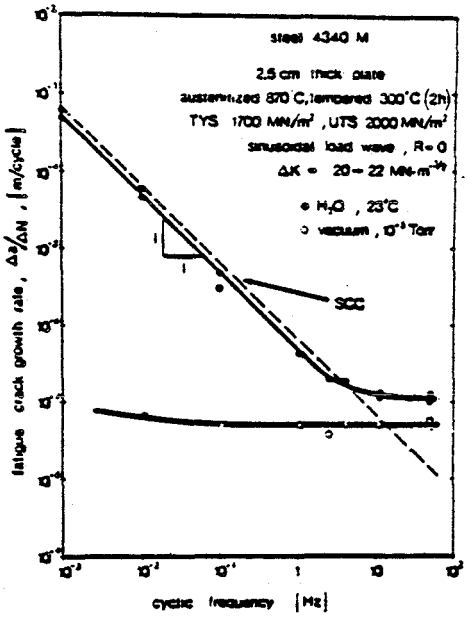

Figure 3-38. The Effect of Water and Vapor on the Frequency Dependence of Fatigue Crack Growth Rates in a High Strength Steel.

frequency. One may infer then, at very low cyclic load frequencies, $\Delta K_{th} = K_{ISCC}$. Based on this observation a schematic representation of the corrosion fatigue behavior of steels subjected to different cyclic load frequencies has been constructed by Rolfe and Barsom [3-85] and reproduced in Figure 3-39. Figure 3-40 indicates that the fatigue crack growth of 1% Cr-Mo-V steel at 550°C in air does appear to follow the idealized behavior shown in Figure 3-39. In Figure 3-41, the crack growth rate for wrought Inconel 718 in air and 5,000psi hydrogen is presented. These tests were performed utilizing a cycle of approximately 9 minutes in duration in order to simulate the SSME operating cycle [3-79]. The da/dn data for 5,000psi hydrogen was extrapolated to obtain an apparent 40ksi-in$^{1/2}$ threshold stress intensity for environmental effects. Data presented in Figure 3-37b suggests a significantly lower threshold stress intensity for Inconel 718 in 5,000psi hydrogen cycled at 1.0 cycles per second. Because of the long cycle duration (the majority of the cycle being at sustained load) used for the tests depicted in Figure 3-41, it is most likely that stress corrosion cracking was the dominant mechanism in promoting crack growth and that the apparent threshold of 40ksi-in$^{1/2}$ should correspond closely to K_{ISCC}. Schmidt and Paris [3-94] also observed a lowering of the threshold for 2024-T3 aluminum with increasing cyclic frequency from 342 to 1,000Hz. They suggested that localized heating at the crack-tip as the possible mechanism. However, Hopkins et al. [3-16] observed a slight increase in ΔK_{th} with increased frequency (30Hz to 1,000Hz) when testing Ti-6Al-4V at 294K. This effect was explained by less plasticity at the crack-tip and less time for environmental interaction.

Takezono and Satoh [3-95] investigated the effect of material viscosity in the plastic region on the fatigue crack propagation in 99.5% pure titanium

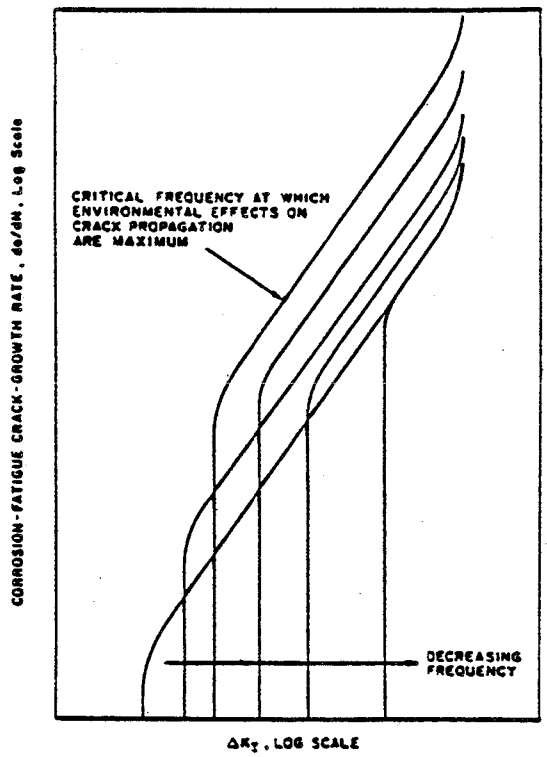

Figure 3-39. Schematic of Idealized Corrosion-Fatigue Behavior as a Function of Cyclic-Load Frequency [3-85].

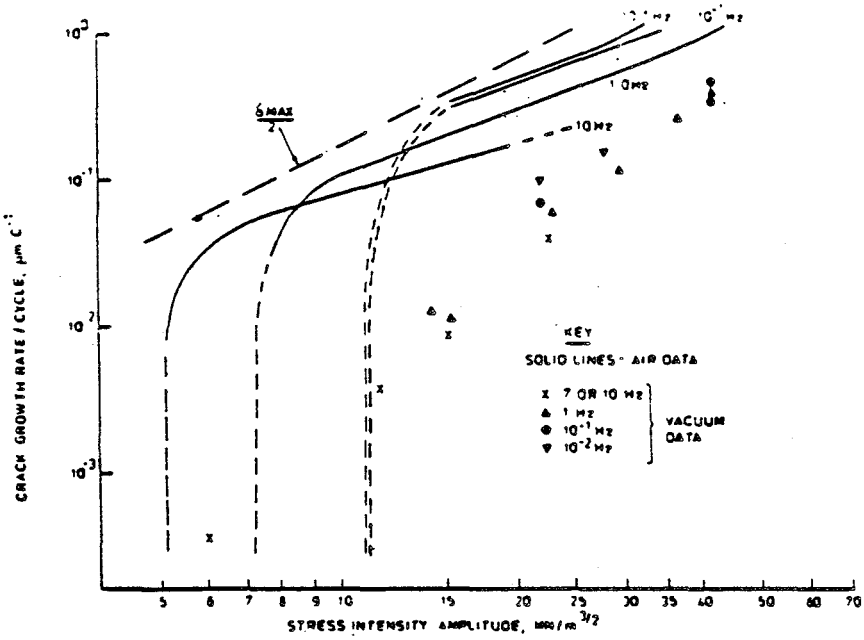

Figure 3-40. Effect of Environment on Fatigue Crack Growth Rate in a 1% Cr-Mo-V Steel at 550° C [3-93].

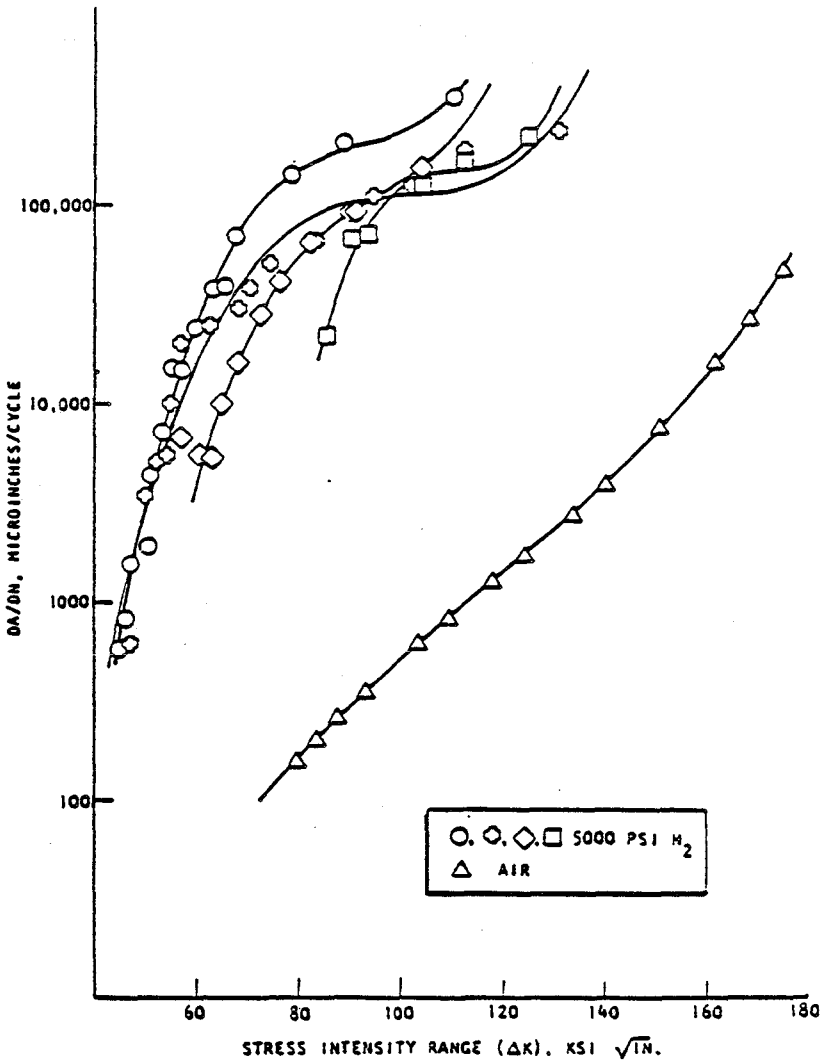

Figure 3-41. da/dn versus ΔK for Inconel 718 in Air and 5000 psi (34.5 MN/m^2) Hydrogen at Ambient Temperature. Specimen Thickness = 1 in., and R = 0.01. [3-79].

-- a material which has a substantial strain rate dependency in the plastic region. The crack propagation rate da/dn was approximately proportional to f^{-n} ($n > 0$), where f is the frequency. Experimental results were compared to an elasto/visco plastic FEM analysis.

Temperature Effects

The effect of temperature on fatigue crack growth can be significant as most materials exhibit reduced cycles to crack initation and failure with increased temperature [3-96 through 3-99]. The behavior of several high temperature alloys is similar to that of Inconel X-750 tested at various temperatures and as shown in Figure 3-42. Between 24° and 593°C crack growth rates steadily increase with temperature; however, a marked increase in crack growth rate occurs at a temperature of 704°C. Tomkins [3-96] believes that the steep slope at 704°C indicates a change from pure fatigue to static load crack mode, (i.e., creep crack growth).

At elevated temperatures, time-dependent processes are enhanced and reduction in cyclic load frequency may produce significant acceleration of the fatigue crack growth rate. Such phenomena are due to an interaction between fatigue crack growth due to cyclic loading and creep crack growth that can occur under sustained load. A thorough review of the rapidly evolving field of creep crack growth will not be attempted. Reference 3-100 provides a comprehensive review of this topic. James [3-101] investigated the effect of frequency upon the fatigue crack growth of 304 stainless steel at 1,000°F. His test results are summarized in Figure 3-43 which shows the dependence on frequency discussed above. If creep periods are introduced into the cycle

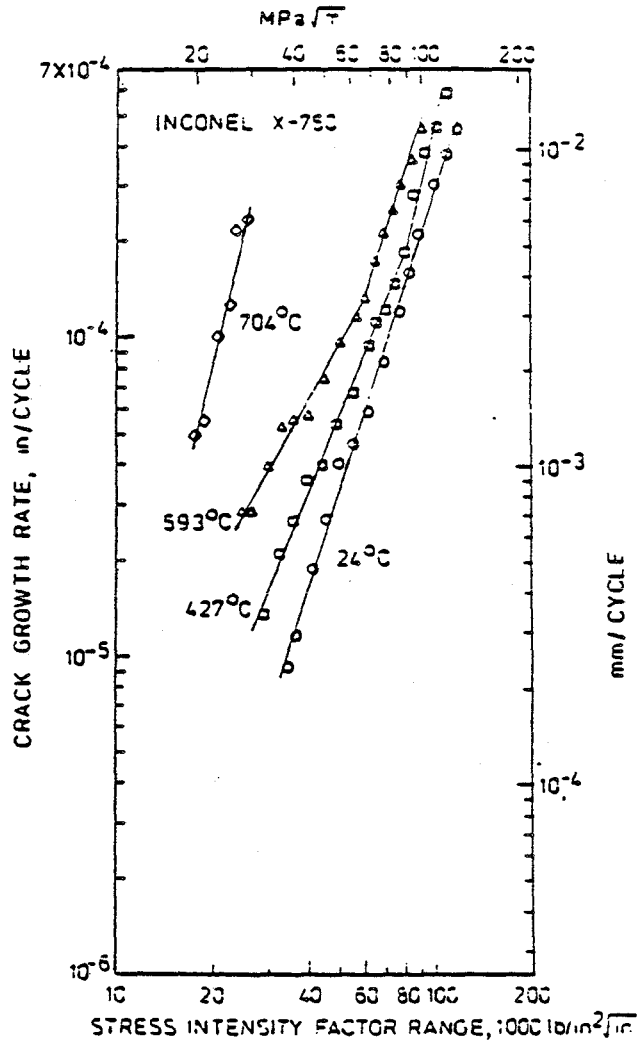

Figure 3-42. Fatigue Crack Growth Rates in Inconel X-750 as a Function of the Stress Intensity Factor Range (ν = 0.17 Hz).

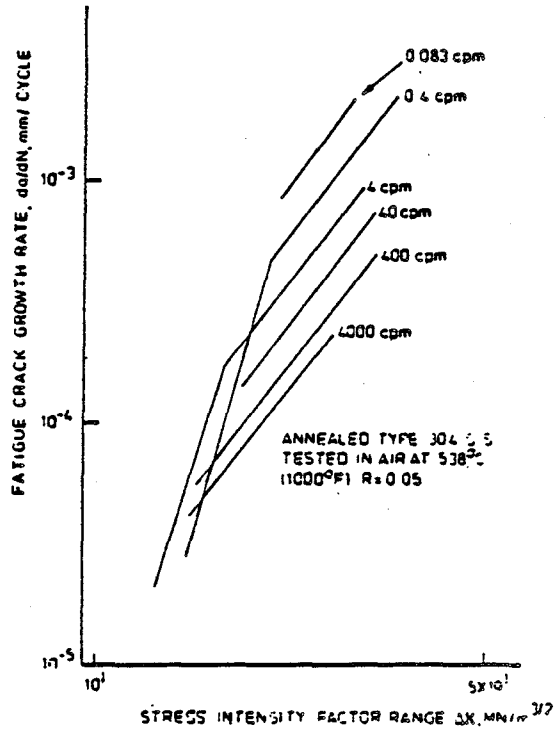

Figure 3-43. The Effect of Cyclic Frequency upon the Fatugue Crack Growth Behavior of Type 304 Stainless Steel Tested in an Air Environment at 538° C (1000° F) [3-101].

through tensile dwell loads, crack growth rates may be substantially increased. Figure 3-44 shows data for 20% cold worked 316 stainless steel at 593°C [3-101]. If the material is unaged, then an order of magnitude acceleration in growth rate is apparent when a 1 minute tensile dwell period is included. The effect is reduced significantly in the aged material indicating the existence of microstructural effects. The influence of different miscrostructures on high temperature fatigue of a nickel-based superalloy waspaloy was investigated by Runkle and Pelloux [3-102].

As with fatigue at ambient temperatures, environment can have a strong influence on crack growth rate at elevated temperatures. Several investigators [3-73, 3-103, 3-104] have showed that, in general, crack growth rates are reduced in a vacuum. Also, oxide products are nearly always found in fatigue cracks produced at low frequencies at elevated temperatures [3-97, 3-105]. Ericsson [3-105] provides a review of the effect of an oxidizing environment at elevated temperatures on the fatigue crack growth in steels, nickel and superalloys. He concludes that a number of effects were apparent:

(1) The crack growth in air is an order of magnitude faster than in vacuum;

(2) There is a stepwise or gradual transition from vacuum behavior to air behavior between approximately 10^{-6} to 1 torr;

(3) The apparent activation energy for the oxidation effect on crack growth rate is small, less than 10 kcal/mole;

(4) Oxidation promotes intergranular cracking but also accelerates transgranular cracking;

(5) The frequency dependence is stronger in oxidation environments than in a vacuum, but is also present in a vacuum; and

(6) The oxidation effect disappears at high strain amplitudes $N_f < 10^2$.

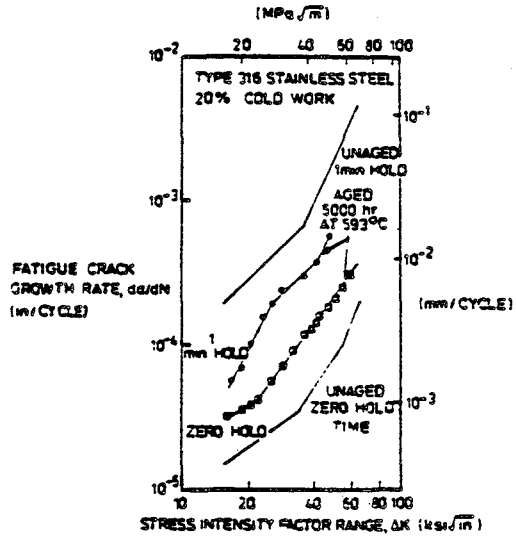

Figure 3-44. Effect of Hold Time on Fatigue Crack Growth for Cold Worked Type 316 Stainless Steel at 593° C [3-101].

Reference 3-73 shows that temperature effects on crack growth rates may change for different temperature ranges. Smith and Stewart [3-106] found that for 23° - 95°C the temperature dependence of the corrosion fatigue crack growth rates in hydrogen and water for 2Ni-Cr-Mo-V rotor steel were reversed. That is, the rates decreased with increasing temperature in hydrogen but increased with temperature in water. The reduction in crack growth rates in the hydrogen environment was explained by a change in the thermodynamic stability of hydrogen adsorbed at the crack-tip. Vroman et al. [3-82], also reported a decrease in crack growth rate in Inconel 718 in a 5,000psi hydrogen environment when the temperature was increased from 70° to 750°F. In fact, the embrittlement due to hydrogen was most severe at room temperature and drops off sharply as the temperature is increased or decreased [3-77].

Birnbaum [3-107] also reports that Stage II crack growth rates of a hydrogen embrittled material may depend in a complex manner on temperature, as is further discussed in References 3-108 and 3-109. For maraging steels and $T < 273K$ da/dt increased with temperature and was proportional to $P_{Hz}^{1/2}$ (Note, Sievert's Law: hydrogen solute concentration is proportional to $(\text{fugacity})^{1/2}$). However, for temperatures above 300K da/dt decreases with temperature and the hydrogen pressure dependence increased from $P_{Hz}^{1/2}$ to approximately P_{Hz}^{15}. At this time the mechanisms are not fully understood.

Strafford and Dalta [3-99] note that in high temperature-gaseous environments the corrosion fatigue behavior of most commercial alloys may be complicated by selective attack of one or more alloy components. Internal degradation processes such as internal oxide, nitride, sulphide or hydride formation may significantly affect crack initiation and growth. The morphologies

of these internally formed corrosion products are almost infinitely variable and little is known about their influence on mechanical properties. Puls, et al. [3-110] have examined the hydride-induced crack growth in zirconium alloys and present a quantitative model based on the growth of hydride platelets at crack-tips due to the diffusion of hydrogen resulting from the stress gradient.

The applicability of linear elastic fracture mechanics to characterize thermal mechanical fatigue crack propagation in nickel and cobalt-based superalloys was evaluated by Rau et al. [3-111]. Crack growth rates under different strain ranges, or for various crack lengths, were found to depend on the strain intensity factor range [3-111] over the range of crack growth rates of most practical importance.

At low temperatures, large changes in frequency generally have little or no effect on fatigue properties except at frequencies approaching ultrasonic [3-112]. Pittinato [3-84] evaluated the effect of hydrogen on crack growth rates in Ti-6Al-4V alloy. In inert environments the crack growth rate decreased slightly as the temperature was dropped. The effect of hydrogen environment is decreased as the temperature is decreased. This phenomenon was also reported for SSME relevant materials in high pressure hydrogen at cryogenic temperatures [3-79, 3-82]. However, Jewett et al. [3-79] were surprised that waspaloy was significantly embrittled by hydrogen at -300°F. This behavior is shown in Figure 3-45. Note that the specimens were subjected to the SSME load cycle of approximately nine minutes duration.

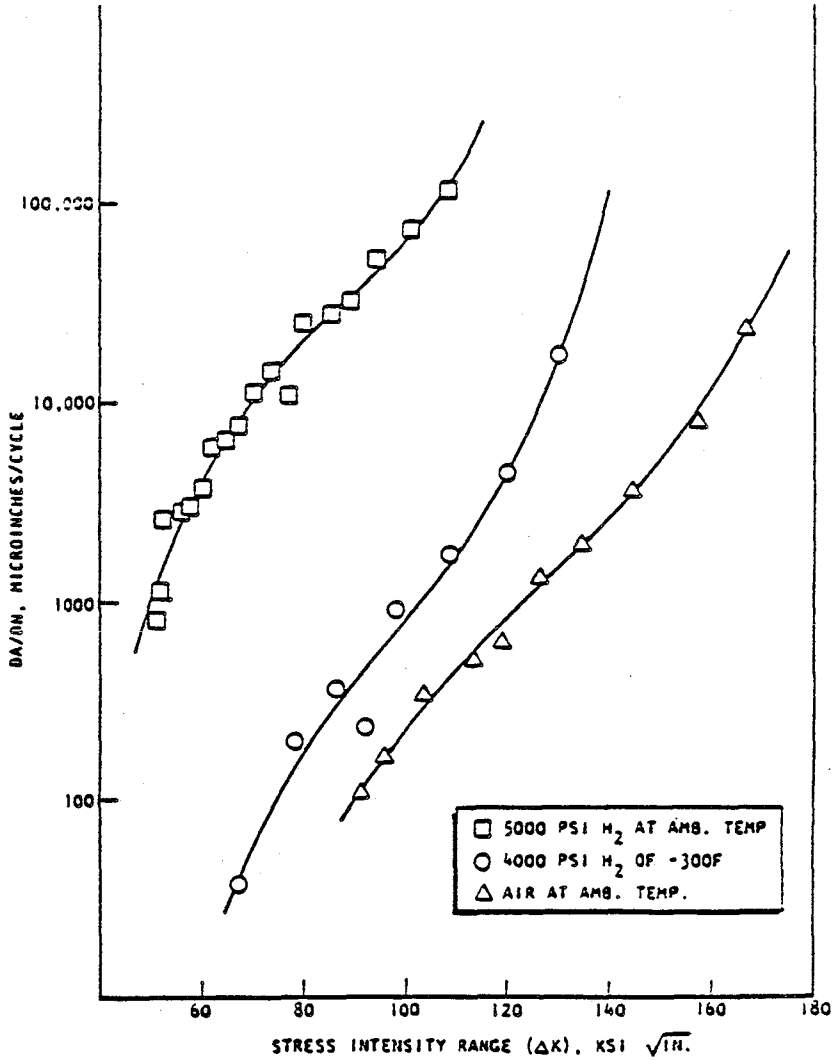

Figure 3-45. da/dn versus ΔK for Waspaloy in High Pressure Hydrogen at Various Temperatures. Specimen Thickness = 1 in., and R = 0.01 [3-79].

Pressure Effects

The partial pressure of a gaseous environment is an important variable for corrosion fatigue behavior [3-75, 3-113, 3-114]. Figure 3-46 shows the effect of oxygen pressure on crack growth rates in 316 stainless steel at 500°C and a frequency of 10Hz. The "S" shaped curves are typical and indicate a critical partial pressure of oxygen, below which crack growth rate is virtually independent of the environment as well as another critical pressure, above which increasing partial pressures do not further increase crack growth rates. Wei [3-115] also reported a critical water vapor pressure above which, no further environmental acceleration in the fatigue crack growth rate of 2219-T851 aluminum alloy. This behavior may be explained by a consideration of the rate of transport of the environment to the crack-tip as compared to the generation of new surface at the crack-tip and its propagation velocity [3-75, 3-113].

The variation of cyclic load crack growth rate in hydrogen for HY100 at constant stress intensity range is given in Figure 3-47. Acceleration in crack growth rate is apparent even at low pressures.

Environmental Effects on Near-Threshold Fatigue

As discussed in Section 3.3, the threshold stress intensity ΔK_{th} below which a crack will not grow when subjected to repeated cyclic loading can be of particular importance in engineering applications. Furthermore, ΔK_{th} may be strongly dependent on the environment, either increasing or decreasing depending on the particular material-environment couple. A comprehensive review of near-threshold fatigue behavior is given in Reference 3-116.

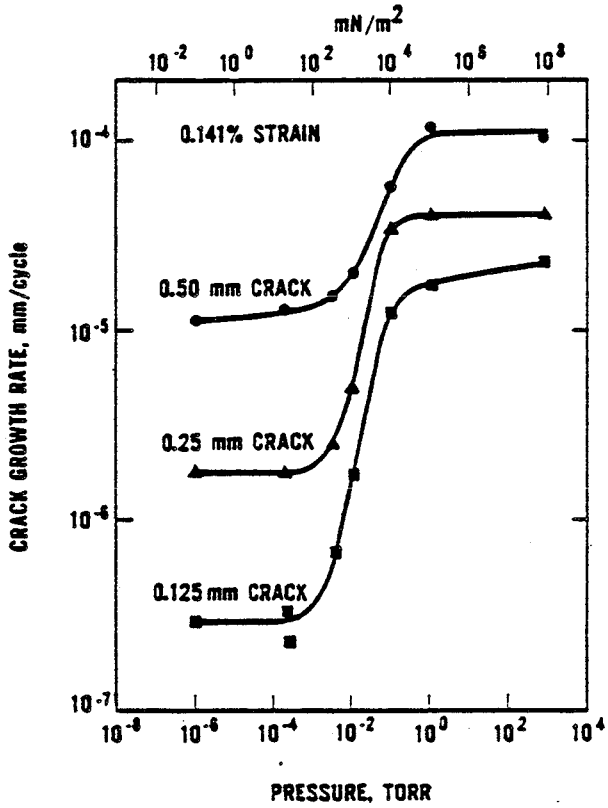

Figure 3-46. Effect of Oxygen Pressure on Crack Growth Rate in 316 Stainless Steel at 500° C (After Smith et al [3-114]).

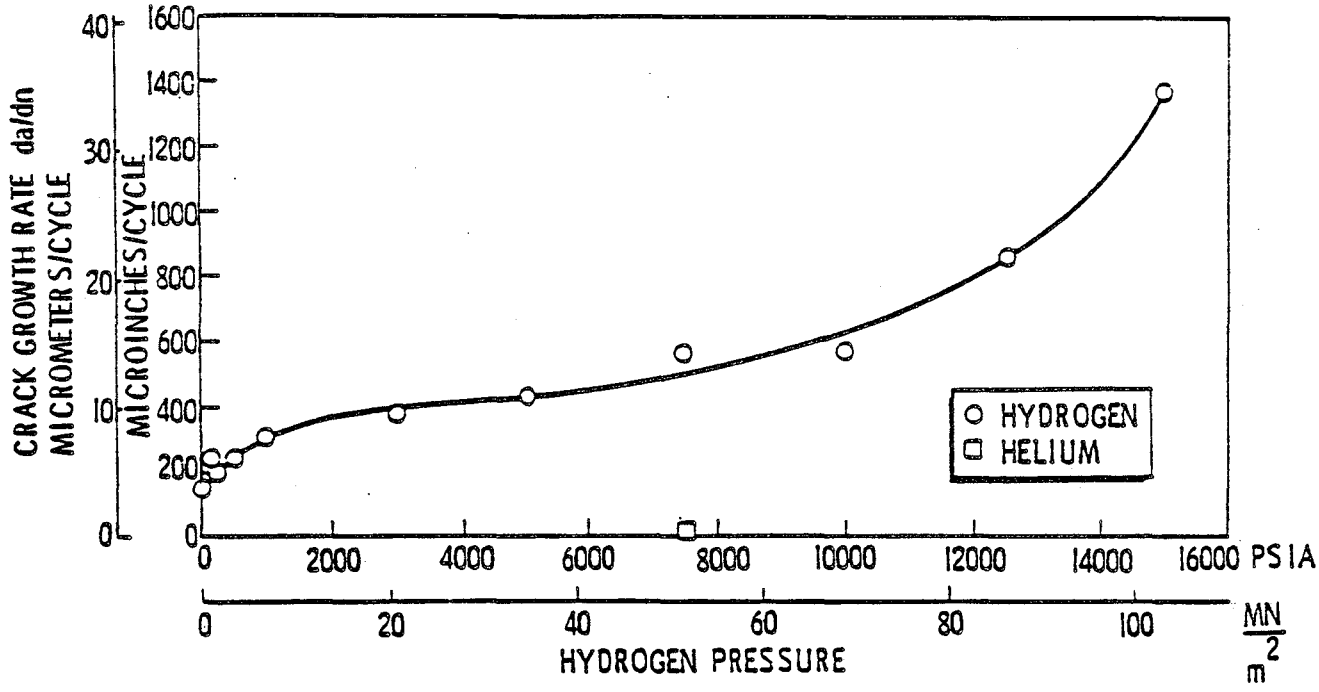

Figure 3-47. Ambient Temperature Cyclic Load Crack Growth Rate in Hydrogen for HY 100 at Stress Intensity Range of 54.7 $MN/m^2\sqrt{m}$ (49.7 $ksi\sqrt{in}$). (Cyclic Rate = 1.0 Cycle/sec) [3-77].

However, Ritchie [3-117] makes the point that at low, near-threshold growth rates (~ 10^{-6}mm/cycle) little is known about the crack propagation mechanisms although growth rates are strongly sensitive to microstructure, stress ratio and environment.

The effect of environment on ΔK_{th} for steels has been investigated by Ritchie and his co-workers [3-117, 3-118, 3-119]. They observed that environment had most effect at low R-ratios. For low strength steels thresholds were lower in dry inert atmospheres and higher in water than in room air (Figure 3-48). However, in ultra-high strength steels ΔK_{th} was higher in hydrogen gas compared to air (Figure 3-49). For low strength steels Ritchie concludes that at near-threshold levels the crack-tip displacements are small and the behavior is controlled by crack closure resulting from enhanced corrosion deposits within the crack which in turn lowers the effective cyclic stress intensity ΔK_{eff}. Crack growth rates in dry hydrogen or any reducing or inert environment at low load ratio will exceed those in room air or moist environment due to less oxide formation resulting in lower closure stress intensities and larger ΔK_{eff} (Figure 3-48). At high load ratios plastically induced closure is insignificant and oxide formation is not enhanced. Thus crack growth rates in all environments are similar. The mechanisms associated with environmenal attack in high and ultra-high strength steels are more complex and appear not to be consistent with either hydrogen embrittlement or crack closure.

Beevers [3-120] documents the variation of ΔK_{th} with load ratio for high strength aluminum alloys and En 24 steel in air and vacuum environments. The results indicate that ΔK_{th} is independent of R-ratio in the inert environment

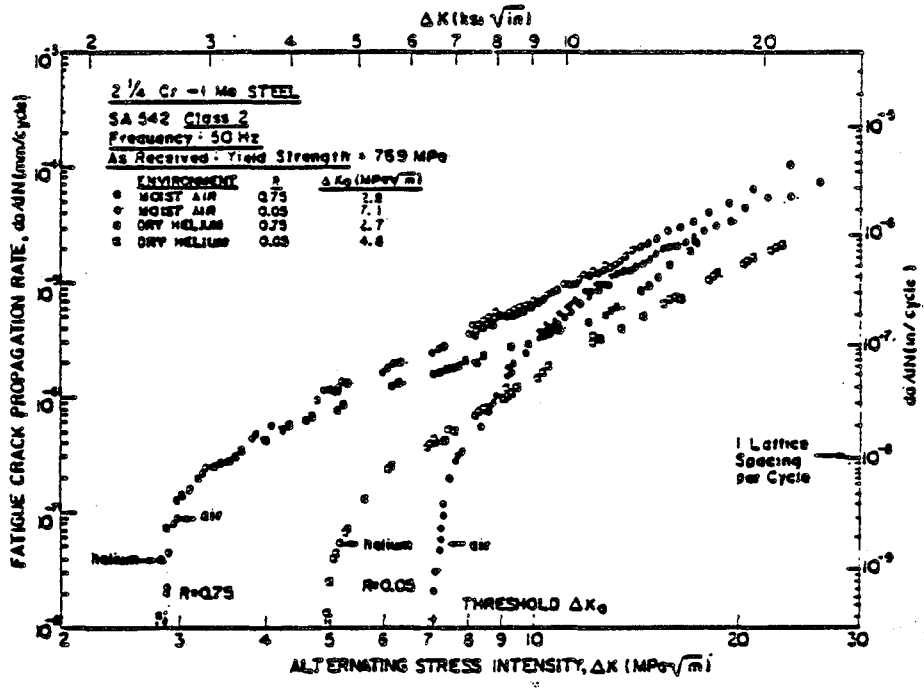

Figure 3-48. Fatigue Crack Growth in Martensitic SA542-2 Steel Tested in Moist Air and Dry Helium Gas, Showing Faster Near-Threshold Growth Rates in Helium at R = 0.05 [3-118].

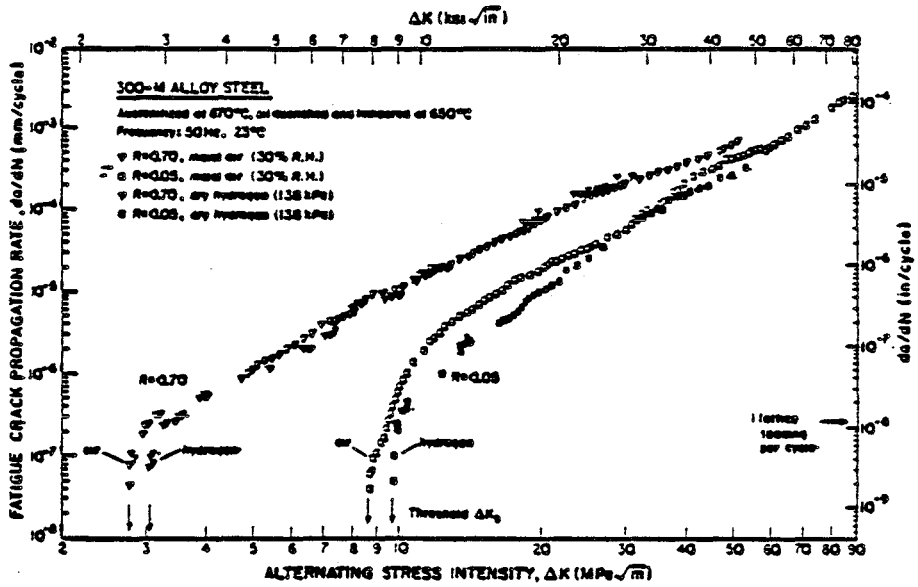

Figure 3-49. Fatigue Crack Growth in 300 M Showing Deceleration in Near-Threshold Growth Rates in Hydrogen Gas, Compared to Air, at Both High and Low Load Ratios [3-119].

and also the environmental effects are most significant at high load ratios (Figure 3-50). Speidel [3-76] uses the example of two nickel-based alloys to demonstrate possible dependences of ΔK_{th} on environment, temperature and load ratio (Figure 3-51). Note that at high temperatures the presence of air is more beneficial than a vacuum while at 23°C the reverse holds. The higher threshold values in air at 850°C may be due to crack branching, or to the buildup of an oxide layer or to crack-tip blunting by oxidation and thus reducing ΔK_{eff} [3-75].

3.5.3 Mechanisms and Models for Environmentally-Assisted Fatigue

Speidel [3-76] suggests that three theoretical concepts have been formulated to explain environmental effects on fracture:

1. film rupture and anodic dissolution,
2. hydrogen embrittlement, and
3. absorption of specific ions or molecules.

He goes on to state that so many convincing arguments have been presented in recent years for each of these mechanisms that it is highly probable that all of them are operative, albeit under different mechanical, metallurgical and environmental conditions. For the purposes of this review, mechanisms associated with gaseous environments will be discussed with particular attention being paid to hydrogen-environment embrittlement.

An extensive volume of literature is available that addresses the problem of hydrogen embrittlement in metals [3-121]. However, as Birnbaum [3-107] points out, no single failure mechanism appears to be able to account for all

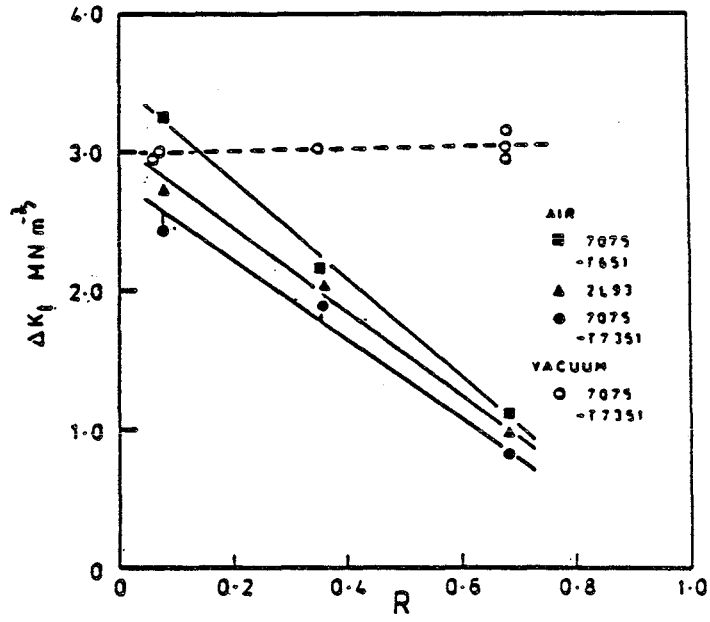

Figure 3-50. The Influence of R Ratio on the ΔK Threshold Values for High Strength Aluminum Alloys in Air and Vacuum [3-120].

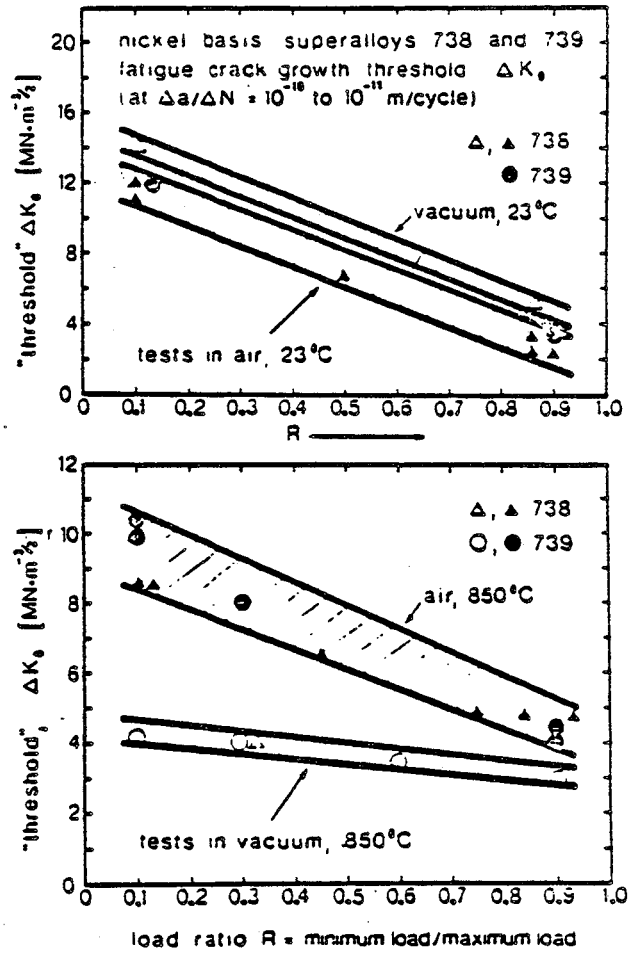

Figure 3-51. Fatigue Crack Growth Rate Threshold Stress Intensities of Cast Nickel Based Superalloys 738 and 739.

the observed behavior, although the "classical" hydrogen embrittlement failure mode is a change from ductile to brittle or cleavage failure resulting from hydrogen in the solution or in the environment. The mechanisms of hydrogen-embrittlement appear to be independent of the source. The reaction kinetics are affected, however, by the transport processes involved which provide the fundamental difference between internal and external hydrogen embrittlement. Walter, et al. [3-122] notes that there appears little correlation between the susceptibilities of various metals to internal or external hydrogen embrittlement. This point is demonstrated by high strength nickel-based alloys which are markedly embrittled by 10,000 psi gaseous hydrogen, but are essentially uneffected by electolytic charging. The difference may be due to the low mobility of the solute hydrogen as a result of trapping and the high hydrogen fugacity at the crack-tip [3-107].

In References 3-107 and 3-123 the authors suggest a possible breakdown for the sequential processes involved in the embrittlement by external gasous environments:

1. diffusion of hydrogen to the crack surface,
2. dissociation to atomic hydrogen,
3. adsorption into the metal matrix, and
4. diffusion through the lattice to the region of embrittlement.

Birnbaum [3-107] believes the kinetics of transfer of hydrogen across the solid-gaseous interface and the pressure which determines the hydrogen concentration are of primary importance.

Titanium alloys, particularly those having acicular α-β microstructure are embrittled by hydrogen gas over a wide range of pressures with fracture occurring along the α-β interfaces [3-123]. Nelson [3-124] reported severe embrittlement of titanium in gaseous hydrogen due to localized surface, or near surface, precipitation of brittle hydride phase. Mechanisms involving formation of hydrides have been proposed in References 3-125 though 3-128 -- the most general formulation being the latter. Birnbaum [3-107] presents a comprehensive review of the role of precipitated and stress induced hydrides on fracture mechanics. Nickel alloys such as Inconel 718 are severely embrittled in gaseous hydrogen atmospheres as demonstrated in previous sections.

If one removes the kinetic factors, then hydrogen embrittlement can be characterized into:

1. hydride forming systems,
2. systems in which hydrides are not stable,
3. systems in which unstable hydrides may be stabilized by applied stress [3-122].

In hydride forming systems the fracture mechanism is stress induced hydride formation and clearage. The degree to which the hydride is stable relative to the solid solution is a function of applied stress and the hydrogen chemical potential at the crack-tip. If hydrides are stabilized at the crack-tip then stress induced precipitation and fracture may apply. In non-hydride forming systems the fracture mechanism is not well understood. The reduction of surface energy by adsorbed hydrogen [3-107, 3-129, 3-130] does not account for the experimental observations as does hydrogen effects on the plastic proper-

ties of metals [3-130]. The decohesion mechanism, originally postulated by Troiano [3-131, 3-132] and expanded by Oriani and Josephic [3-133 through 3-135] seems to have the most promise, however, many questions remained unanswered [3-107]. The decohesion mechanism stipulates that when the load stress exceeds the atomic bond strength which can be reduced by the presence of hydrogen solute, brittle fracture occurs.

The mechanisms assocated with fatigue crack growth at elevated temperatures have been summarized in several review papers [3-105, 3-113, 3-136]. If environmental effects are neglected then fatigue crack propagation at high temperature is controlled by strain and diffusion mechanisms. For example, the effect of frequency shown in Figure 3-44 can be explained by a decrease in the range of crack-tip displacement with frequency due to higher effective flow stress at higher strain rate [3-136]. Several authors [3-137 through 3-139] have developed quantitative models to treat this effect of time and temperature. The formation and growth of cavities remote from the crack-tip as a result of diffusion effects is discussed by Wells [3-136]. It is noted that in order for there to be any significant effect on the crack growth rate the crack-tip opening displacement must be in the same order as the cavity spacing.

As mentioned earlier, the effect of environment on high temperature fatigue can be significant, as added to the above mechanisms is the effect of diffusion of a gaseous species. In his review of the effects of oxidization at high temperature on fatigue crack growth, Ericsson [3-105] reports a lack of a unifying mechanistic theory to describe the observations. The factors he believes to be important include; chemisorption of oxygen and oxidation at the

crack-tip, segregation of oxygen to grain boundaries ahead of the crack-tip, cracking of the crack-tip oxide and oxidation of fresh metal and inhibited reversal of slip at the crack-tip. Wells [3-136] suggests that the formation and properties of films at the crack-tip appear to be the fundamental problems to be addressed.

In some material environment systems the combined influence of the fatigue induced subcritical crack growth and stress corrosion cracking above K_{ISCC} appears to be the sum of the two processes acting independently with no synergistic effect. Wei and Landes [3-92] postulated a model to account for the effect of water vapor on the corrosion fatigue of steels above K_{ISCC} which was based on the superposition of time-dependent slow crack growth and the mechanical cyclic component. The model appeared to predict crack growths reasonably well in some instances and Nelson [3-124] indicated its applicability to a titanium alloy in a gaseous hydrogen environment. However, Walter and Chandler [3-78] found that this model did not appear to hold true for Inconel 718 in hydrogen.

Recently, considerable progress has been made concerning the rate limiting steps in the sequence of events that lead to environment induced failure. Coordinated fracture mechanics and surface chemistry studies are leading to an understanding of the chemical processes that control crack growth rates. The influence of the environment on the transport processes are measured and compared with the environmental effects on subcritical crack growth rates.

Wei [3-75, 3-140] found that the rate controlling process for sustained load crack growth for a high strength steel in water/water vapor was the

nucleation and growth of oxide on the surface and the concomitant production of hydrogen which leads to embrittlement at the crack-tip. Fatigue crack growth in an aggressive environment both above and below K_{ISCC} is the sum of three components, such that

$$\left(\frac{da}{dn}\right)_{CF} = \left(\frac{da}{dn}\right)_{i} + \left(\frac{da}{dn}\right)_{cf} + \left(\frac{da}{dn}\right)_{SCC}$$

where the following definitions apply

- $\left(\frac{da}{dn}\right)_{i}$ is the fatigue crack growth rate in an inert environment
- $\left(\frac{da}{dn}\right)_{SCC}$ is the amount of crack growth due to stress corrosion cracking during the time occupied by a single load cycle. This growth is considered to occur under sustained loads and can be evaluated from knowledge of the SCC crack growth relation between K and da/dt. By definition, this contribution will be zero for values of K below K_{ISCC}.
- $\left(\frac{da}{dn}\right)_{cf}$ is the cycle-dependent component that accounts for synergistic interaction between fatigue and environmental attack. This term accounts for environmental influences that are observed below K_{ISCC}.

The modeling effort concentrated on establishing an analytical expression for estimating the dependence of $(da/dn)_{cf}$ with pressure and frequency in gaseous environment. Correlation was obtained between model and experimental results for fatigue crack growth below K_{ISCC} for varying frequency and pressure for different alloy-environment systems (aluminum-water vapor, steel-water vapor, steel-hydrogen sulphide).

It is apparent from this review that the environment can have a dramatic effect on subcritical crack growth rates and that reliability of service life predictions must necessarily depend critically on the proper accounting of

environmentally induced effects. Wei and Simons [3-140] remark that these effects have not been fully appreciated by a large sector of the engineering community. They substantiate this by the "indiscriminate" use of "accelerated" tests and a disregard of cyclic load frequency as a significant variable in design.

To date the phenomenological aspects of environment enhanced fatigue crack growth are fairly well documented in voluminous literature. However, as Speidel [3-76] points out, on an atomistic level, the important steps involved in the material environment interaction resulting in crack growth have, in most cases, not been identified. Many mechanisms have been postulated, however most are limited in their application and relevant for a small class of material-environment systems.

Obviously, a better understanding of the basic mechanisms involved in corrosion fatigue is required in order that interpolation from limited data can be made with any confidence. The interdisciplinary approach adopted by Wei [3-75, 3-140] to establish the rate limiting steps in the fracture process appears to have promise and has been applied to a range of material-environment systems.

Additionally, the work of Ford as reported in Reference 3-141 and 3-142, summarizes recent advances in gaining a better understanding of stress corrosion cracking and corrosion fatigue in material environmental systems of interest in the power generating industry.

3.6 TRANSITION CRITERIA

Cracks and defects in aerospace components generally are initially part-through cracks that are open to the surface. This is especially true of pressurized components, because the presence of a through-wall crack would result in a leak. Part-through surface cracks can grow in a subcritical manner due to cyclic loading and/or stress corrosion cracking or hydrogen induced crack growth. If left unchecked, this subcritical crack growth will most often eventually produce a through-wall crack. During this period, the behavior of that crack changes from that of a semi-elliptic surface flaw to that of a through crack. The transition region may be defined as that region between well defined part-through crack behavior and well defined through crack behavior as shown schematically in Figure 3-52. Local plasticity, shear lips, ligament behavior, geometric non-linearities, breakthrough, stress intensity variation, as well as the parameters of part-through and through cracks are all significant components of transition criteria.

For analytical purposes, a slightly more precise definition of transition is possible. Within an analytical model, the transition region begins at the point that the surface flaw model ceases to adequately model actual crack growth. The region ends at the point that the through crack model adequately models crack behavior. The transition region must, therefore, be defined in the context of the overall analytical model, as most investigators have done.

Experimentally, transition may be defined as that range of behavior where back face effects play a significant role in crack behavior. A great portion of behavior thus defined may be accurately incorporated into the part-through crack model, leaving only a small fraction to be defined by transition

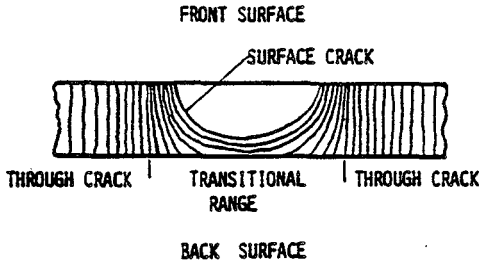

Figure 3-52. Typical Surface Flaw Growth Behavior.

criteria. In reality, stable crack growth is a continuum, and it is not always possible to discriminate between discrete regions under test conditions. Breakthrough may also be narrowly defined both analytically and experimentally as the initial rupture of the ligament allowing the passage of fluid.

Motivation for the understanding of transition behavior comes almost exclusively from pressure vessel and piping applications although it is applicable in certain other areas for fracture mechanics. For most piping or pressure vessel applications leakage and/or rupture are the modes of failure of primary concern. Accurate understanding of transitioning is necessary to accurately predict the life to breakthrough or leakage (assuming stable crack growth). Once breakthrough has occurred the leakage rate may be of concern and detailed description of crack growth and opening becomes necessary. The third concern is stable versus unstable crack growth within the transition region. It has generally been assumed that if the subsequent through-crack is stable, unstable crack growth in the transition region need not be considered. This criterion is the foundation of all widely used leak before break criteria. In certain applications crack arrest of unstable crack growth must be investigated to assess overall damage and safety.

The topic of transitioning may be conveniently broken down into three subareas, 1) analytical techniques, 2) experimental techniques and data, and 3) available data. Fracture studies have been included because various aspects of fracture of part-through crack specimens have provided some insight into various analytical techniques that have been adopted for fatigue life

prediction and transition criteria. Notation of flaw geometry is shown in Figure 3-53.

3.6.1 Analytical Techniques

For most fracture mechanics problems involving surface flaws, transition and breakthrough criteria are not addressed explicitly. Rather, a leak-before-break (LBB) criterion is employed as an upper bound on transition behavior. The maximum stress intensity is calculated for a through crack of length 2t, and if it is less than K_{Ic}, the LBB criterion is satisfied. This approach presumes that the initial crack surface length (2c) is less than 2t, and that the maximum K does not exceed K_{Ic} at any point prior to the through crack condition, or that the arrest value of K (K_{Ia}) equals K_{Ic}. In general terms both test results and in-service performance records indicate that the leak-before-break approach produces satisfactory, and possibly conservative, designs for materials typically employed in pressure vessel applications. Since the universal applicability of this approach is uncertain, in critical applications, to account for the possibility of more rapid or critical crack growth during transition than after transition, the limiting K may be taken as K_{Ia}, the crack arrest threshold. Both criteria are satisfactory for engineering applications where safety is the paramount concern. They are inadequate where more detailed assessment is required.

State of the art techniques for detailed analysis of transition behavior in the aerospace industry are presented in a collection of symposium papers published in ASTM Special Technical Publication 687, "Part-through Crack Fatigue Life Prediction" [3-143]. Various researchers participated in a round

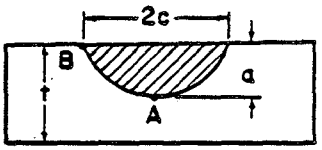

Figure 3-53. Surface Flaw Geometry.

robin study to assess the accuracy of currently available fatigue life prediction codes. (Some of these codes are reviewed in Section 3.7.) Each investigator was supplied with basic material properties derived from compact test specimens. They were also given information on part-through crack test specimen configurations, loading, and environments. Each researcher made a prediction of the specimen life until breakthrough and/or failure for a limited number of specimens. While the overall objective of this study was not assessment of transition criteria as such, all authors report on the transition and breakthrough criteria contained within the code they were using.

Three different approaches to transition were reported: "transition point," "lower bound," and "upper bound". The transition point criterion presumes that breakthrough and transition occur simultaneously when the depth of the semi-elliptic surface crack becomes equal to the wall thickness. With the lower bound approach, transition begins with the onset of back face yielding (which occurs prior to breakthrough). The upper bound approach assumes semi-elliptic crack growth until the back face crack length is 90% of the front face crack length. All three approaches are reportedly based upon observed behavior and consistent with limited test data.

Three authors used the transition point approach of abrupt transition from part-through to through crack behavior [3-144 through 3-146]. When the calculated depth of the semi-elliptic part-through crack is equal to the wall thickness ($a/t = 1$), both breakthrough and transition are deemed to have occurred and a model for a through crack of length 2c is adopted (Figure 3-54).

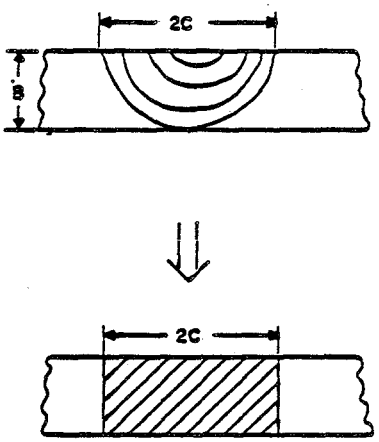

Figure 3-54. Basic Transition Criteria [3-144].

The "lower bound" approach is contained in the code developed for analysis of the SSME used by Peterson and Vroman [3-147] in the round-robin study. This approach employs separate criteria for transition and breakthrough. The development of this approach is based on crack growth patterns observed in laboratory tests.

Transition begins with the onset of back face yielding, calculated as follows:

$$\frac{\sigma}{\sigma_{ys}} = 1 - \frac{\pi a}{4t} + \left(1 - \frac{a}{t}\right)\left(\frac{a}{t}\right)\left(\frac{a}{c}\right) \qquad (3\text{-}19)$$

where:

σ = Imposed net section stress

σ_{ys} = Material yield stress

when the equality is satisfied, the surface crack length continues to grow but growth in the crack depth is inhibited until breakthrough. Equation 3-19 is a simplified approach, based on limited test data that is in good agreement with a model prepared by Kobayashi and Moss [3-148] as shown in Figure 3-55. This approach is in close agreement with available test data.

Breakthrough is defined to occur when Equation 3-20 is satisfied.

$$\frac{2c}{t} = \left[0.860\left(\frac{a}{2c}\right)\right]^{-0.821} \qquad (3\text{-}20)$$

This is a purely empirical approach derived initially from limited test data and refined using the data from Reference 3-149.

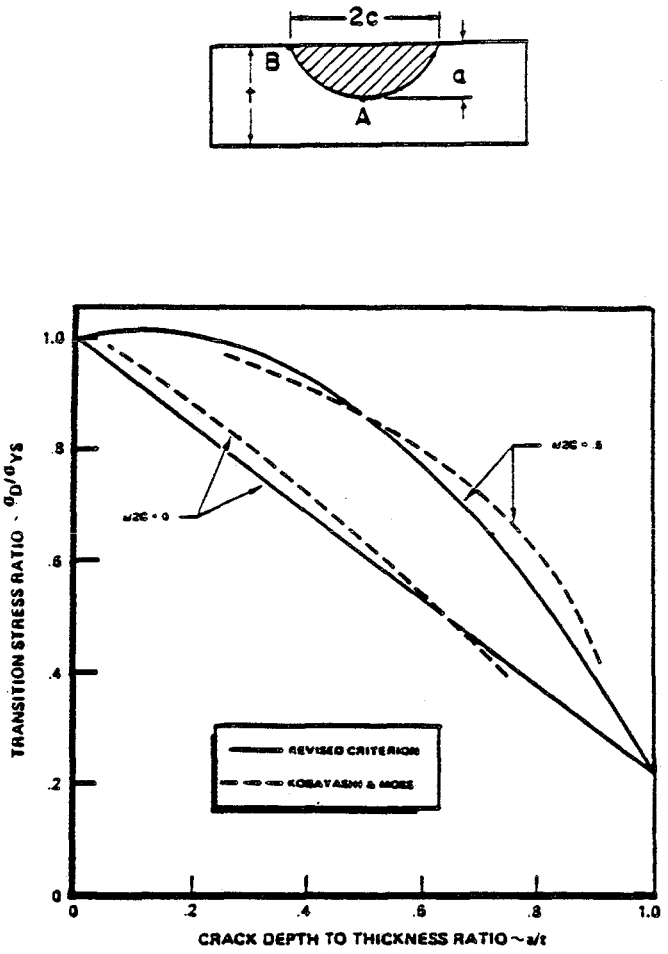

Figure 3-55. Backface Yielding Criteria [3-147].

The overall predictive accuracy of the code employed by Peterson & Vroman [3-147] is indicated by the results of predictions for ten test samples. The average ratio of (predicted cycles/test cycles) to breakthrough was 0.95 with a standard statistical deviation of 0.14.

Johnson [3-150] reports on the techniques employed in General Dynamic's crack growth program, CGR-GD which employs an upper bound transition criterion. He uses separate criteria for breakthrough and transitioning. Apparently the breakthrough criterion is that when the calculated crack depth, a, is equal to the specimen thickness, t, breakthrough has occurred. This marks the start of the transition region. The crack is assumed to continue to grow through the transition region in elliptical shape as shown in Figure 3-56 according to the following equation:

$$\frac{c'^2}{c^2} + \frac{t^2}{a'^2} = 1$$

where

a' = imaginary crack depth if a > t

c'= back face surface length

When c' = 0.9c through crack criteria are then employed. During transition the stress intensity factor is:

$$K = 1.12\ \sigma\ M_k\ (\pi a/Q)^{1/2}$$

where:

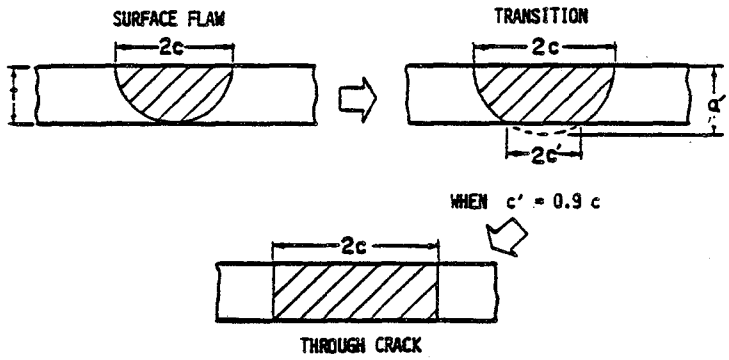

Figure 3-56. Surface Flaw Transition Criteria [3-150].

M_k = Back face correction factor for a/t = 1

Q = Flaw shape parameter

Reportedly, this approach agrees well with the trend of experimental data at General Dynamics.

It is very difficult to explicitly assess the accuracy of the various breakthrough or transition criteria employed by various investigators given the complex interaction of various program assumptions. However, the accuracy of the various life prediction codes may be assessed. In summary, Vroman reports overall average predicted to test ratios (N_{pred}/N_{test}) very close to 1. The range of prediction ratios for a specific sample (averaged among all investigators) ranged from 0.454 (with a standard deviation, s, equal to 0.099) to 2.186 (s = 1.390). These results are based on individual sample test results so it is quite likely that material variability or specimen variability play a large part in the observed errors. The standard statistical deviations associated with the above ratios give an indication of the variation among researchers with s = 0.099 representing a high degree of agreement among the various researchers and the s = 1.390 representing the maximum disagreement among various researchers.

A qualitative assessment of the transition point criteria employed by three of the participants in the comparisons reported in Reference 3-143 is possible by examination of a figure presented by Rudd [3-144]. Two plots of crack length versus cycles are shown; Figure 3-57, which shows an unconservative life estimate, and Figure 3-58, which shows a conservative prediction. While significant errors exist in the overall accuracy of both predictions, it

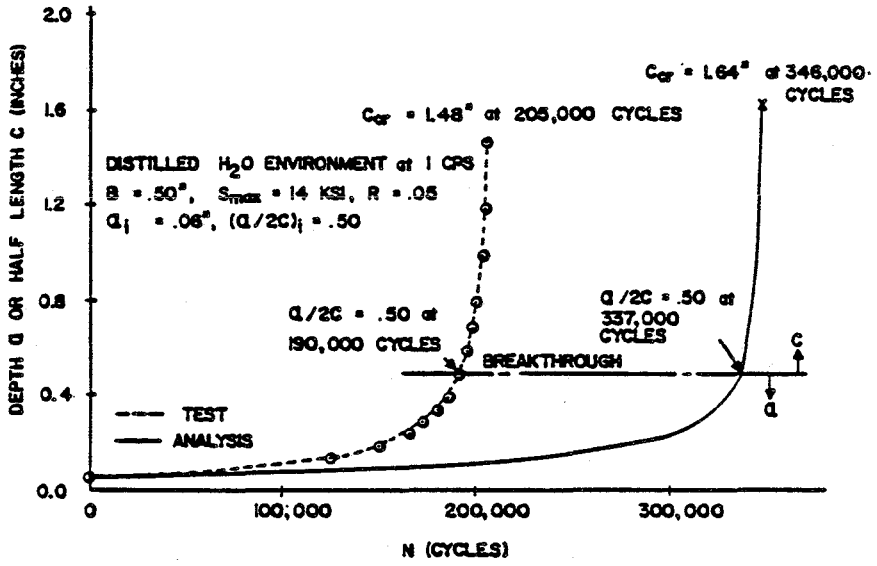

Figure 3-57. Crack Growth Prediction and Test Results; Unconservative Overall, but Conservative After Breakthrough [3-144].

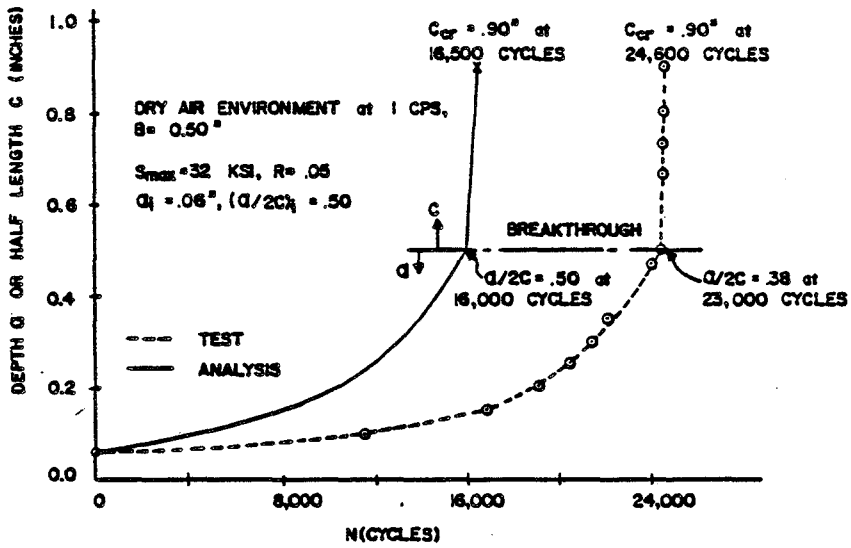

Figure 3-58. Crack Growth Prediction and Test Results; Conservative [3-144].

is apparent that the majority of the error accumulated at the early stages of crack growth. In the vicinity of breakthrough, there is close agreement between the analytical prediction and the experimental data within the scales shown on the figures. This indicates the adequacy of a very simple transition criterion in this particular case, and suggests the need for refinement of the part-through crack model. Since the number of cycles spent in the transition stage was small relative to the number of cycles to failure, inaccuracies in the transition stage predictions have only a small influence on the overall predicted lifetime.

Scott and Thorpe report on the development of part-through fatigue life prediction techniques by the UK Atomic Energy Authority [3-151]. They present an assessment of the accuracy of currently available (1981) stress intensity factors and crack growth criteria for semi-elliptic cracks. Scott and Thrope employ Newman's stress intensity formulation modified by back face yielding criteria (i.e., when the plastic zone radius exceeds the uncracked ligament thickness at its deepest point, the crack is treated as a through thickness crack).

A problem closely related to transition criteria is determination of stress intensity factors along the crack front of a part-through crack. This topic is covered in detail elsewhere (see Section 2). Only a few comments or areas of overlap will be made here. Numerous stress intensity formulations for part-through cracks have been proposed which in some way include the back face proximity correction factor. Newman [3-152] and Scott and Thorpe [3-151] provide reviews and comparisons of a number of techniques. While most formulations are limited to a/t ratio of something less than 1, several are

explicitly applicable for a/t → 1 [3-153]. Newman compared model predictions with fracture test results on brittle epoxy specimens and found correlation of ± 10% for 95% of the data for several solutions. The test was designed specifically to minimize placticity effects so the results are not directly applicable to ductile materials. A formulation proposed by Newman provides good correlation up to and including a/t = 1. The formulation has a further appeal in that for a/t = 1 and a uniform for field stress (σ_m) it reduces to

$$K = \sigma_m (\pi c)^{1/2}$$

which is the solution for a through-crack of length 2c. This formulation provides a rational procedure for cracks which grow stably from part-through to through-cracks. Transition occurs abruptly at breakthrough when a/t = 1.

All other solutions reviewed by Newman do not reduce to the through crack solution, but require some transition criteria to eliminate the analytical discontinuity at a/t = 1.

3.6.2 Experimental Work

Initial results of experimental work conducted in the United Kingdom at Berkeley Nuclear Laboratories are reported by Darlaston and others [3-154, 3-155]. Initial results have shown the widely used equivalent through-crack criteria to be overly conservative in certain situations, such as long cracks. Figure 3-59 shows the defect profile just after breakthrough of a surface flaw that was classified as a sudden rupture defect by the equivalent through crack approach. It was found that an initial long surface crack did not grow

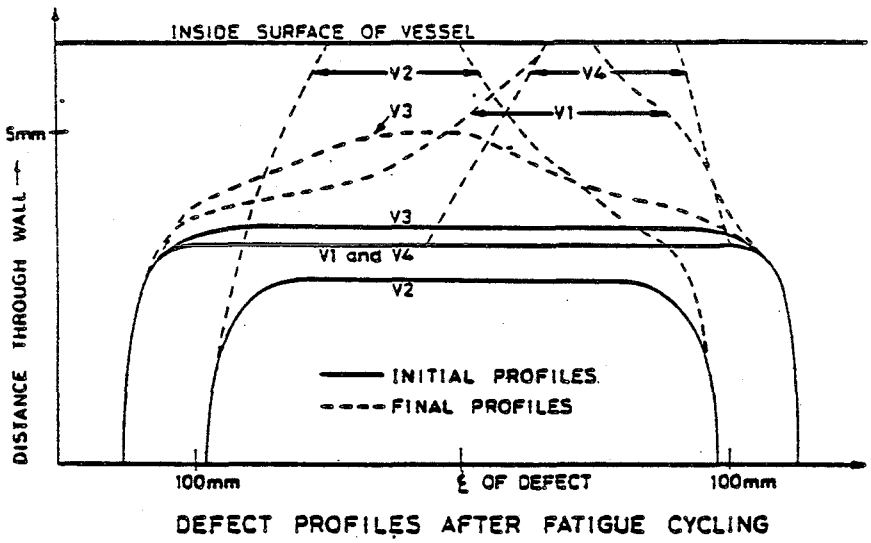

Figure 3-59. Tunneling Behavior in Specimens with Long Surface Flaws [3-154].

uniformly in depth to a through crack but tended to tunnel through the wall over a short portion of the crack length. The result in all test cases was a leak-before-break failure rather than the expected rupture. Such results are consistent with studies of shorter surface defects that indicated a preferred aspect ratio of $a/c \sim 0.8 -- 1.0$. Tests were conducted on a very limited number of sample types and are not necessarily generally applicable. A simple empirical model to predict leak or break behavior was presented. The continuing research objective is to characterize leak before burst behavior of pressure vessels and associated equipment. They appear to consider more details than most authors regarding the phenomena involved in breakthrough (e.g., dynamic effects due to breakthrough, fatigue versus stress corrosion, crack arrest, leak rates, plastic behavior of the ligament). Reportedly, research is in progress which may yield excellent data on transition behavior.

Several NASA studies (with more general objectives) have generated an experimental data base which has proved useful to several investigators in deriving expression for behavior in the transition region [3-149, 3-153, 3-156, 3-157]. Typical data available in these studies include the number of cycles to breakthrough for a variety of crack and specimen geometries, onset of back face yielding, variety of materials and basic material properties, and in some cases correlation of tensile specimens and prototype pressure vessels. Little detailed information is available on progress of the crack through the transition region.

With a few notable exceptions, the problems of transition and breakthrough have been addressed with simple bounding criteria (e.g. equivalent part-through crack) or equally simple analytical techniques [3-85, 3-140,

3-145, 3-146]. Such criteria have proven to be quite satisfactory for most engineering applications. Several empirical improvements have been suggested and incorporated into crack growth models [3-147, 3-150, 3-151]. Given the dependency of transition criteria on the overall modeling technique, it is difficult to assess the accuracy of improved breakthrough criteria from the literature, although it appears to be on par with the overall accuracy of crack growth models.

3.7 AUTOMATED FLAW GROWTH COMPUTER PROGRAMS

The design and safety analysis of cyclically loaded light-weight structures, such as often encountered in aerospace applications, often involves considerations of fatigue crack growth. In a manner similar to that outlined in Section 3.1, subcritical crack growth characteristics are combined with stress histories and stress intensity factor solutions to calculate how hypothesized cracks would behave in service. Due to various complexities in the analysis and to the large number of analyses often required, numerical calculations on a computer are usually employed. This section will review some of the more widely known computer programs for evaluation of flaw growth. Such programs are often combined with automated means of calculating stress intensity factors and therefore are closedly related to the computer programs reviewed in Section 2.3.

Several state-of-the-art automated flaw growth programs were identified and reviewed. Automated flaw growth programs are defined as computer algorithms which use input or previously calculated stress intensity factors and figuratively grow the flaw through a structure to compute such parameters as

fatigue life, residual static strength, and flaw shape change as a function of time or number of applied load cycles. These algorithms typically output tables and/or plots showing crack growth as a function of cycles (fatigue) or time (stress corrosion, creep).

In practice, automated stress intensity programs and flaw growth computer programs are rarely developed as separate entities, but are rather coupled together to form one convenient computer algorithm. Typically, the flaw growth computer programs include a subroutine or series of subroutines which contain previously generated or input-determined stress intensity solutions (i.e., automated stress intensity routines) and which are called during execution for the user-specified geometry and loading conditions to be used for the crack growth solution.

Table 2-2 lists the automated crack growth programs -- each containing its own internal automated stress intensity algorithms -- which were reviewed in Section 2.3. These codes also have capabilities for analysis of crack growth. These capabilities will be reviewed here. This list is by no means complete since most private companies and university researchers involved in crack growth prediction have developed their own in-house, unpublished algorithms to suit their particular applications. The programs shown in Table 2-2 were selected on the basis of:

1. "Automated" Stress Intensities
2. "Automated" Crack Growth
3. Availability to NASA-MSFC
4. Applicability to NASA-MSFC Needs

Availability of the algorithms to NASA-MSFC requires that the algorithm (source deck and documentation) be available at no charge from the developer or that the program can be purchased from the developer through the sponsoring agency. The programs listed in Table 2-2 are of general nature in that loading and crack geometry are not tailored to a specific industry or component(s) within an industry, and consequently, are versatile for anticipated NASA-MSFC applications. For reference purposes, several application programs and brief abstracts are provided in Table 2-3. These programs were not reviewed in the current project.

Section 3.7.1 addresses how available algorithms in general reflect the current state-of-the-art fracture mechanics life technology. Section 3.7.2 provides brief excerpts from published code abstracts which describe in general the options of each program. Also included in this section is a convenient tabular summary of the important options/features of each program.

3.7.1 Computer Modeling of Fracture Mechanics Life Technology

Ideally, a flaw growth computer program should be a repository for most or all fracture mechanics life technology. In addition, it should be efficient and reasonably "user friendly." Several composite categories which reflect current fracture mechanics life technology are presented in this section and are used as criteria for evaluation of the computer codes listed in Table 2-2. The composite categories are:

- Flaw Geometries and Loading
- Crack Growth Material Models

- Variable Amplitude Loading
- Special Crack Growth Models
- Efficiency

Flaw Geometries and Loading

For ongoing fracture mechanics life technology projects, the ability to have an efficient and accurate library of stress intensity factors for a wide variety of loadings and geometries is obviously important.

Crack Growth Material Models

The programs surveyed typically contained one or more crack growth models which provided the analyst with options as to which relationship is best suited to accept his inputs of da/dn versus ΔK. The most frequently encountered crack growth models were the following (or modifications thereof):

Paris: $da/dn = C(\Delta K)^m$

Forman: $da/dn = \dfrac{C\ (\Delta K)^m}{(1 - R)\ K_c - \Delta K}$

Walker: $da/dn = C \left\{ \dfrac{\Delta K}{(1 - R)^{1-s}} \right\}^m$

Tabular: Point by Point Input of da/dn, ΔK

Several other less well known crack growth relations were found in these programs. In fact, it frequently appears that each program has its own "more

realistic" crack growth model. Several examples of these models are the Collipriest-Ehret found in MSFC-2 [3-158], the Hopkins-Rau [3-16] in BIGIF, the inverse-hyperbolic-tangent in BEWICH, and the completely-general model developed in FATPAC. It is not the intent of this section to discuss in detail the applicability, merits, or validity of these various material "models" which, for the most part, are nothing but regression equations used to fit reduced crack growth data from the laboratory. It is, however, important that as future algorithms are developed, they consider the importance of such parameters as R-ratio, K_{max}, and threshold intensities, $\Delta K_{th}(R)$, on fatigue crack growth rate. The model available in FATPAC illustrates a complex attempt at including these various parameters simultaneously:

$$\frac{da}{dn} = A \left\{ \frac{\Delta K^{\alpha} (\Delta K^{\beta} - [\Delta K_{th}(o)\ (1 - R)^{\gamma}]^{\beta})^{\delta}}{(1 - R)^{\tau}\ \sigma_{UTS}^{\varepsilon}\ (K_{Ic}^{\rho} - K_{max}^{\rho})^{\sigma}} \right\}^{m}$$

where $\Delta K_{th}(R)$ is the threshold value of ΔK below which no growth occurs and is assumed to depend on R through the equation

$$\Delta K_{th}(R) = \Delta K_{th}(o)\ (1 - R)^{\gamma}$$

where $\Delta K_{th}(o)$ is threshold at R = 0, σ_{UTS} is the ultimate tensile stress, K_{Ic} is the fracture toughness and A, α, β, γ, δ, ε, ρ, σ and τ are regression (i.e., data fitting) constants. Implicit in the use of this crack growth equation is the assumption that besides effects on threshold, the only other

explicit dependence on R is represented by the $(1 - R)^{\tau}$ term in the denominator. For positive values of R the dependences on R are reasonable in certain circumstances. However the onus of establishing their applicability to cases of negative R must rest with the user.

The most direct and general method to model the crack growth rate as a function of these various parameters is to give the various regression equations and to input in tabular form da/dn versus ΔK where ΔK has been parametrically varied to include R-ratio, K_{max}, and $\Delta K_{th}(R)$ effects. Two programs which currently include this option of multivariate, generalized da/dn, (ΔK, R, ΔK_{th}) tabular input and use various interpolation techniques for obtaining continuous values of da/dn are MSFC-2 and BIGIF. Extreme caution must be used by the analyst in that he must be aware of how a specific algorithm -- whether using tabular or equational material models -- performs interpolations and especially extrapolations from input values of da/dn as a function of ΔK (R, ΔK_{th}, K_{max}).

Variable Amplitude Loading

Fatigue crack propagation under variable amplitude loading and the associated load interaction effects (described in Section 3.4) have been of primary concern to aircraft and gas turbine manufactureres since the late 1960s and early 1970s. The implementation of a fracture control plan on airframe structures -- as specified in MIL-STD-1530A -- reflects this concerted effort to be able to accurately predict crack growth under flight loading conditions. Aircraft manufacturers realize that to neglect crack growth retardation caused by tensile overloads could lead to unnecessary

weight increases and cost penalties. On the other hand, an unsafe design could result if acceleration effects and reduction of retardation effects caused by underloads, creep, etc. are not accounted for in the analysis.

As a consequence of this commitment to modeling variable amplitude fatigue crack growth, all of the flaw growth programs listed in Table 2-2 which are or have been associated with the aerospace industry (FATPAC being the exception) are capable of accepting, in increasing order of complexity, overloads, step loading, programmed block loading, and flight-simulation loading (see Figure 3-60). FATPAC, although not aerospace associated, has this capacity, too. Crack growth is accounted for on a cycle-by-cycle basis in these programs. Each code has specific limits on the number of allowable blocks, number of allowable steps within a block, and the number of allowable cycles within a step. These limits usually are determined by computer storage capacities and typically can be increased without much effort. One program in particular, EFFGRO, contains great flexibility in spectrum definitions by setting up working blocks through the use of dummy steps and "rotated groups" to insure that fractions of cycles are included in the analysis.

All of the programs reviewed contained load interaction models except BIGIF and FATPAC. In fact, one of the codes contained multiple interaction models and allows the user to select the most appropriate model -- or no retardation model at all. The following retardation/acceleration models were found in these programs (see Section 3.4 for a discussion of these retardation models):

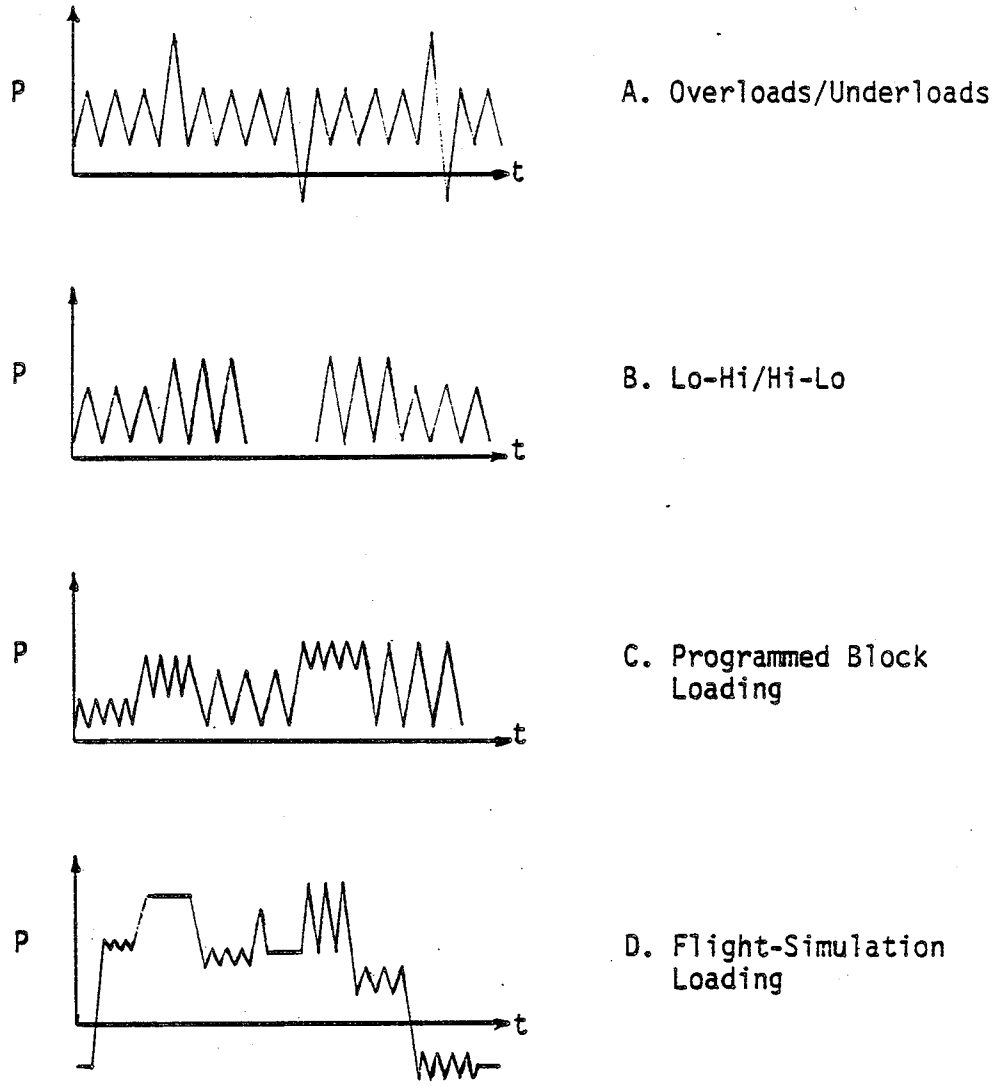

Figure 3-60. Loading Conditions Capable of Being Input into Surveyed Automated Crack Growth Programs.

Retardation Model	Code
Wheeler [3-62]	BEWICH, MSFC-2
Willenborg (modified) [3-63]	FLAGRO-4, MSFC-2
Multi Parameter Yield Zone (MPYZ) [3-72]	CGR-LaRC
Willenborg/Chang [3-57]	EFFGRO
Modified Elber [3-61]	FAST-2
Grumman Closure Model [3-159]	MSFC-2

Several of the programs and interaction models were used recently in a round robin analysis conducted by ASTM Task Group E24.06.01 [3-71] for predicting fatigue crack growth behavior under random loading sequences. Although reasonably accurate predictions were achieved, it is not clear whether the load spectra adequately test these models due to the lack of dominant retardation or acceleration effects, as evidenced by the fact that linear cumulative damage predictions offered nearly as good correlation.

Special Crack Growth Models

A crack growth model for the transition of a surface flaw or corner crack to a through-thickness crack is available in three of the programs surveyed. Figure 3-61 illustrates transition criteria for several of the programs. Note that the sister program of CGR-LaRC, CGR-GD, developed at General Dynamics contains the upgraded feature of the transition model. A survey of breakthrough (transition region) criteria -- including experimental results and analytical modeling -- is included in Section 3.6.

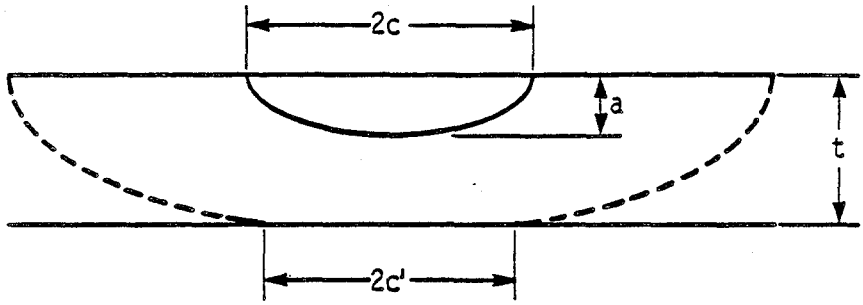

Surface Flaw

Code:	BEWICH	2-87
	CGR-GD*	2-88
	EFFGRO**	2-91
	MSFC-2	2-95

* General Dynamics version of CGR-LaRC
**Original version. Updated version developed at Rocketdyne not available at time of review.

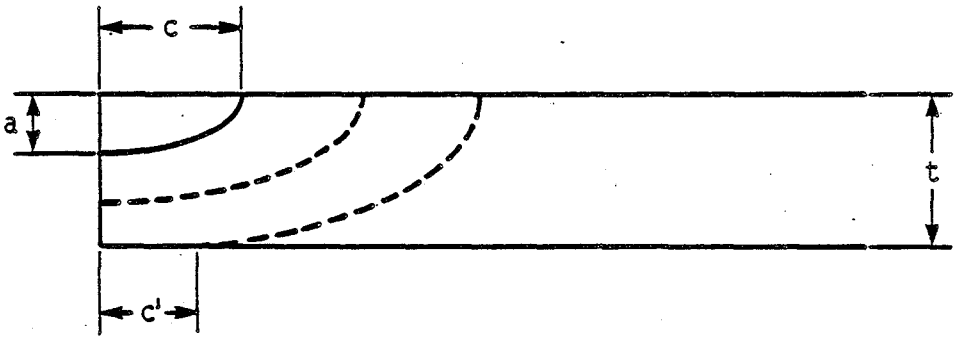

Corner Crack

Transition Criteria to Through Crack:

$a > t$

$c' > 0.9c$

$a > (1-\sigma_{tr}/\sigma_{ys}) \frac{4}{\pi} t_{equiv}$

$a = t$ (Start Transition)

$c' > 0.95c$ (Complete Transition)

Figure 3-61. Various Transition Models for Surface or Corner Cracks Propagating to Through-Thickness Cracks.

Each program surveyed in Table 2-2 contained one or several "special" crack growth features. For example, BEWICH contains special checks on validity of user-input plane stress or plane strain conditions, and validity of linear elastic fracture mechanics by comparing σ with σ_{ys}. BIGIF likewise contains special options on variable thickness used frequently to model after-the-fact crack propagation of surface flaws from measured benchmarks, and special options on inputting the critical stress intensity factor, K_{Ic}, as a function of crack depth. Because of the large number of these "special" techniques, each one cannot be discussed in detail for the programs listed in Table 2-2. However, the summary table presented in Section 3.7.2 will provide a list of the important salient features. The reader is referred to references at the end of this chapter if more detailed information is desired.

Efficiency

By definition, optimum state-of-the-art stress intensity and flaw growth programs should a) accurately utilize current fracture mechanics technology, b) be efficient in terms of computer storage and execution time, and c) be reasonably "user friendly". The previous paragraphs addressed current fracture mechanics technology while the following paragraphs address efficiency. No comments will be made on the degree of user friendliness, since this judgement cannot be made from reviewing program manuals, but must come from users who are able to make comparisons as a result of executing the codes.

Most computation time in a flaw growth program is consumed during the integration of the first order differential equation, $da/dn = f(a)$, where $f(a)$ can be one of several relationships, e.g., the Paris formulation $f(a) =$

$C(\Delta K)^m$. As three-dimensional, multi-degree freedom crack geometries are evaluated for stress intensities and crack growth at several locations around the crack front, numerical techniques become more involved since they must now handle the solution of a set of coupled differential equations of the following form:

$$da_1/dn = F_1(a_1, a_2, \ldots, a_n)$$
$$da_2/dn = F_2(a_1, a_2, \ldots, a_n)$$
$$\vdots$$
$$da_n/dn = F_n(a_1, a_2, \ldots, a_n)$$

Computer execution time is also directly proportional to the number of load blocks, load steps within a block, and load cycles within a step. Consequently, computer execution time becomes of more concern when extensive variable amplitude cycling is modelled (e.g., flight by flight execution of aircraft).

The best available reference to data which describes and compares the relative efficiency of the most popular numerical techniques for crack growth applications is an article by Chang et al. [3-160]. In this article a review and evaluation of the state-of-the-art numerical techniques was conducted to select a cost-effective method for incorporation into an improved crack growth algorithm developed at Rockwell. The numerical techniques reviewed were common methods of solving two categories of crack growth analyses. In mathematical form,

Category 1:

$$n = \sum_{i=1}^{m-1} \Delta n_i = \sum_{i=1}^{m-1} \int_{a_o}^{a_f} \frac{da}{F(\Delta K, R...)}\Bigg|_i$$

Category 2:

$$\Delta a = a_f - a_o = \sum_{i=1}^{m} da/dn\Big|_i$$

The numerical methods selected for Chang's et al. review were the closed-form solution, mean value and Runge-Kutta, Taylor series expansion, and linear approximation. Details are provided on each of these methods in [3-160]. The results of Chang's survey indicated that the Runge-Kutta and linear approximations were most frequently used in crack growth programs. Selecting these two methods for evaluation, Chang et al. executed CRACKS [2-89] and EFFGRO [2-91] which contained Runge-Kutta and linear approximation algorithms, respectively.

Briefly, the Runge-Kutta integration technique calculates the increment of crack size, Δa, from the current crack size, a_i, within Δn cycles as follows:

$$\Delta a = a_{n+1} - a_n = 1/6\ (k_o + 2k_1 + 2k_2 + k_3)$$

where

$$k_0 = \Delta n \left.\frac{da}{dn}\right|_{a_n}$$

$$k_1 = \Delta n \left.\frac{da}{dn}\right|_{a_n + k_0/2}$$

$$k_2 = \Delta n \left.\frac{da}{dn}\right| a_n + k_1/2$$

$$k_3 = \Delta n \left.\frac{da}{dn}\right| a_n + k_2$$

All four k-values represent slopes at various points. k_0 is the slope of the starting point; k_3 is the slope at the right-hand point whose ordinate is $a_n + k_2\ (\Delta n)$; k_2 is one of the two slopes considered at the midpoint with ordinate $(a_n + 1/2\ k_1 \Delta n)$; and, finally, k_1 is the second slope at the midpoint whose ordinate is $(a_n + 1/2 k_0 \Delta n)$.

The Vroman method [2-87] assumes that the growth rate is constant throughout a load step so that the crack size is a linear relationship with the number of load cycles. The method proceeds by considering a load step, i, and taking the values of $(\sigma_{max})_i$ and $(\sigma_{min})_i$ to compute the crack growth rate, da/dn. The value of $(\delta a)/(da/dn)$ is then compared to n_i, where "a" is the crack size. If $(\delta a)/(da/dn)$ is greater than n_i, then the crack growth for that particular load step is $\Delta a = n_i x\ (da/dn)_i$; "a" is increased by Δa, and the program proceeds to the next load step, (i + 1). If $(\delta a)/(da/dn)$ is less than or equal to n_i, the number of cycles to grow (δa) is $(\delta a)/(da/dn)$. This value is subtracted from n_i, the crack size "a" is increased by (δa), and this load step is reconsidered. This process continues with $(\delta a)/(da/dn)$ being compared to the remaining cycles in this load step. When all the load steps in a block are exhausted, the program proceeds to the first load step of the next block.

Chang's results for various types of loading are reproduced in Table 3-5. Chang concluded that fatigue crack growth predictions were very close. The

Table 3-5
Results of Chang's et al. [3-160] Survey and Evaluation
of Efficiency of Popular Crack Growth Numerical Procedures

Loading Type	CRACKS		EFFGRO		
	Predicted Life Cycles	CPU	Predicted Life Cycles	CPU	$\frac{\text{CPU(CRACKS)}}{\text{CPU(EFFGRO)}}$
Constant Amplitude	1,009,500 2,199,750	0.1352	1,004,270 2,184,830	0.0260	5.2
	1,010,325 150,000	1.0023	1,001,420 150,000	0.0683	14.7
	11,325 24,675	0.0177	11,310 24,630	0.0098	1.8
Single Overload	14,105 14,105	0.0390	14,105 12,860	0.0370	1.05
	40,015 12,505	0.0092	12,515 12,505	0.0067	1.37
	35,010 25,010	0.0235	35,010 25,010	0.0068	3.45
Block Loading	11,500 9,250 17,620 25,500	0.0218	10,885 8,560 17,705 23,080	0.0260	0.84
	10,485 8,000 17,620 23,000	0.0237	10,495 6,850 17,470 22,135	0.0250	0.95
	74,750 8,800 102,000 12,050	0.0308	74,625 8,210 101,760 10,970	0.0177	1.74
	65,750 6,550 95,750 9,900	0.0128	65,625 6,000 95,760 9,850	0.0177	0.72
Random cycle-by-cycle flight spectrum	156,650 90,070	2.6667 0.4998	155,290 90,500	0.4598 0.2267	5.8 2.2

linear approximation appears to be more efficient for constant amplitude and flight-by-flight spectrum loading. For block loading, computer costs for the two methods were identical.

3.7.2 Program Abstracts

This section contains selected excerpts from the abstracts (if available at time of report issue) of the manuals for the computer codes listed in Table 2-2. Brief background material on the program is provided when possible.

Computer Code: BEWICH

Computer code BEWICH was developed by Imtiaz [2-87] in a joint effort with Beech Aircraft Corporation and Wichita State University. No acronym was assigned to the code in [2-87], so the indicated acronym was assigned for purposes of reference within this document. Excerpts from the introduction follow:

> This program has the capability of analyzing growing of most common types of cracks (edge cracks, center cracks, corner cracks, and surface cracks) as well as accounting for the transition from a corner or surface crack to a completely thru-the-thickness crack. The input loading may be a "mission profile" type of stresses with or without concentrated loads. This mission profile may be repeated a number of times. The stresses may be applied in cyclic block-increments or in individual cycles. For each cycle or block-cycle, crack growth rate and the new crack length is calculated. The user has the option to use either Walker's equation or Jaske-Feddersons's inverse-hyperbolic-tangent equation for the crack growth rate calculations. Material constants for Walker's equation are input by the user while for Jaske-Federsons's they are stored within the program. (At present constants for only 2024-T3, 7075-T6, 7075-T7351, 300M, and Ti-6Aℓ-4V are stored).
>
> For each loading there are built-in checks and corrections for plastic zone size, finite width, plane stress versus plane strain, applicability of linear elastic fracture mechanics, and failure of

the specimen. In case of corner crack, the depth of the crack grows proportional to the length and when the crack grows completely through the thickness of the material, the problem is reformulated as a thru-crack problem.

Wheeler's model is used for crack growth retardation. The use of retardation and plastic-zone correction are optional to the user and go hand-in-hand.

The output data contains all the input parameters, a complete description of input problem, and most of the useful intermediate calculations used in finding the new crack length. More than one problem may be stacked back-to-back in one computer run.

Computer Code: BIGIF

BIGIF [2-17] was developed at Failure Analysis Associates under funding from several sources, most notably the Electric Power Research Institute. Salient features and options are noted in the following excerpts from the summary [2-17]:

The fracture mechanics approach to structural reliability accepts that some flaws will be present, but that conditions can be established to assure that flaws do not grow to an unacceptable size during the life of the structure. Fracture mechanics life prediction requires calculation of crack tip stress intensity factors (K) to quantify both stable crack growth and the conditions of unstable fracture in complex geometries under complex elastic loading conditions which lead to high stress gradients. The Influence Function (IF) technique for general fracture mechanics-based fracture, fatigue, and stress-corrosion cracking analysis has been incorporated into an efficient computer program called BIGIF, an acronym for Boundary-Integral-equation-Generated Influence Functions. The BIGIF computer code has been developed to perform accurately and inexpensively these life predictions for a wide range of two- and three-dimensional stress fields and cracks and structural geometries, given that the elastic stress solution for the uncracked structure is available from another independent source.

BIGIF has four advantages over other publicly available fracture mechanics programs. The most important advantage is that the program accurately accounts for general tensile elastic stress gradients due to notches, holes, temperature gradients, or residual stress fields in the vicinity of the crack and maintains accuracy

even for very severe stress gradients. The second advantage is that the program is very efficient (inexpensive to operate) for both two- and three-dimensional problem models with stress gradients, some of which simulate the changing shape of a growing crack. The third advantage is the program's capability to model the simultaneous effects of many cyclic load transients with different stress fields, each specified in any of several ways. The fourth advantage is that BIGIF can account for first order plasticity effects on subcritical crack growth provided that the inelastic deformation is contained enough to provide a near-linear load-displacement curve. All of these capabilities, particularly the capability of modelling accurately the nonlinear stress gradients, make BIGIF a suitable alternative technique for the non-mandatory flaw evaluation procedure in the ASME Boiler and Pressure Vessel Code, Section XI, Appendix A, whenever the Code procedure is judged to be inadequate.

For a broad class of three-dimensional elastic crack problems in which a stress analysis is available for the uncracked structure, BIGIF is at least one hundred times less costly to use than generally available direct finite element (FE) method computer solutions which include the crack in the idealization. Furthermore, the accuracy of IF-calculated K values is nearly independent of the severity of the stress gradients, while the cost and error of FE analyses can increase rapidly with the gradient of stress. The accuracy of the IF solutions have been verified by both the present investigators and others by comparison with other analytical solutions, experimental structural simulation, and crack growth rates observed on structures in the field.

The IF method has been used extensively by Failure Analysis Associates to solve a variety of fracture mechanics-based subcritical crack growth problems involving fatigue, corrosion-assisted fatigue, and stress-corrosion cracking. Electric utility applications include postulated pressure vessel beltline weld and nozzle cracks, cracks in steam turbine rotors, shafts, and blades, pipe cracks, and cracks in steel beams in the nuclear containment structure. By December 1980, over fifty electric utilities, corporate, and individual users in the energy industry had acquired the BIGIF program. Non-utility applications are numerous and include evaluation of the significance of cracks in auto components, bridge structures, supertanker welds, wind tunnel pressure boundaries, valves in cryogenic LNG systems, toilet tanks, and critical gas turbine and helicopter components. In addition, the three-dimensional IF method used in BIGIF is a key element in the current design analysis systems at the Pratt & Whitney Aircraft Division of United Technologies Corp., where it was initially developed to analyze aircraft gas turbine engine structures.

. . . To use BIGIF, the user inputs the general material crack growth properties, the uncracked structure's stress field, and certain other parameters for each cyclic load transient. The BIGIF

computer program allows the user to model multiple load transients on a structure which can be assembled into one time or cyclic block which is applied repeatedly to the structure. He also chooses, from a library of seventeen flaw models, the crack geometry model that simulates the actual structure being analyzed. Each of these models has been evaluated and verified with test cases. The present investigators are continuing to develop and incorporate new influence function solutions into BIGIF to expand the program's library of geometries.

Besides standard fatigue analysis, BIGIF can be applied to predict stable crack growth by stress-corrosion or creep cracking which crack growth rate on a per-time basis can be specified in the crack growth relation instead of on a per-cycle basis. Using other straightforward transformations of input data and minor program modifications, the program can even be used to compute changes in strain energy, structural stiffness, and natural vibrational frequency caused by the growing crack.

Computer Code: CGR-LaRC

CGR-LaRC was developed by Johnson [2-88] and is currently available at NASA Langley. The version, CGR-GD, is currently used at General Dynamics and contains the through-crack transition model, but was not made available for a complete review in this survey. The function of CGR-LaRC is to predict crack length versus cycles (or time) from an initial crack size to final flaw size. Embedded in this program is the Multi-Parameter Field Zone Model developed by Johnson [3-72] to analyze variable amplitude loading. The program contains several special checks including $\sigma_{ligament} < \sigma_{ULT}$ and da/dn less than the value input by the user of da/dn for fast fracture. No published abstracts, introductions, or summaries were available for inclusion in this section.

Computer Code: CRACKS IV

CRACKS IV is the latest version of the general fracture mechanics crack growth program, CRACKS, and was developed by Engle [2-86] at Wright-Patterson Air Force Base.

Computer Code: CRACKGRO

CRACKGRO [2-90] is currently being constructed by Rockwell under funding of Wright-Patterson Flight Dynamics Laboratory (WPFDL). CRACKGRO is a combination of the current versions of CRACKS and EFFGRO.

Computer Code: EFFGRO

EFFGRO [2-91] was developed at Rockwell International in the early 1970's and was based on Vroman's Crack Growth Method [unpublished] of linear approximation. The features available within the original EFFGRO program [2-91] are described in the following excerpt from the Introduction:

> This summary presents the necessary information for the usage of the program "EFFGRO", available under the auspices of North American Rockwell, Los Angeles Division, from Structures Analysis, Fatigue and Fracture Mechanics Group.
>
> The program predicts crack propagation based on G. Vroman's, Crack Growth Method. The method utilizes the fact that small changes in crack length have a minimal effect on the crack growth rate, and therefore, is able to calculate crack propagation histories efficiently. The program uses Forman's equation for part through cracks and/or through cracks. The crack(s) may emanate from a hole.
>
> The loading spectrum or loading block may be in form of percent bending moment, percent stress, bending moment, or stress. The spectrum or block may be permutated according to sets of randomized steps. It also may have groups of steps which are rotated among themselves at given intervals, it may also have groups of special steps which are applied only at given intervals.
>
> Crack growth may be analyzed with or without the effects of retardation due to overloads. Both part through and through the thickness cracks may be considered. Part-through cracks may transition and become through-thickness cracks. The analysis is ended when instability occurs or when the transition requirements are not satisfied.

Computer Code: FAST-2

FAST-2 was developed by Newman [2-92] at NASA-Langley Research Center. Newman's closure model [3-61] is coded into this program which is described by the following excerpt:

> FAST (Fatigue-Crack Growth Analysis of Structure -- A Closure Model) [2-92] is a program to predict crack length against cycles from an initial crack size to failure for various crack configurations. The applied cyclic loads can be constant or variable amplitude. The program uses the crack-closure concept to account for load-interaction effects (acceleration and retardation). Either tensile or compressive loads can be applied to the crack configurations. The crack-opening stresses (S_0) are calculated from crack-surface displacement equations and the effective stress-intensity factor range is elastic. Many of the variables used in the program are defined in the comment section at the beginning of the main program (FAST-2).

Computer Code: FATPAC

FATPAC was developed by Chell [2-93] at the Central Electricity Research Laboratories in England. FATPAC is jointly executed with FRAPAC, an algorithm which computes the stress intensity factors for use in life calculations. The FATPAC program is based on the weight function (on influence function) method. The program's options and capabilities are best summarized by the following excerpts from the summary [2-93]:

> The computer program FATPAC calculates the growth of a defect by fatigue using the stress intensity factor subroutine incorporated in the computer program FRACPAC. To aid failure assessments many facilities have been written into FATPAC. Up to 80 different load transients can be specified, either in terms of the stress distribution in the uncracked structure, or as stress intensity factors, or as combinations of other transients. Stress gradients can be taken into account if these vary only in one direction. Growth can be calculated for up to 40 periods and within each period up to 80 loading blocks can be applied. A total of 35 crack and structural

geometries can be handled, ranging from extended and elliptical embedded and surface defects in infinite bodies, to the same defects in structures of finite dimensions. Elliptic defects have up to three-degrees-of-freedom which means that in stress gradients not only is the size and shape of the growing defect predicted but also the position of the centre of the defect which may display an apparent movement from its original position.

To describe growth a generalized fatigue law may be used or one based upon the Paris-Erdogan equation. In the latter case the fatigue law constants can be made to depend on both R and ΔK so that a piecewise description is possible of a wide range of fatigue behavior. If, for example, frequency or wave form are important, specific loading blocks may require their own set of fatigue laws. In FATPAC this is accommodated by using range numbers which can be assigned to each loading block, allowing identification of the set of fatigue law constants to be used for the block.

Fatigue growth can be either forward or backward, that is with increasing or decreasing crack size, thus enabling the determination of tolerable defect sizes from critical data. Although severe stress gradients can be catered for, the facility exists whereby the stress is linearized over the crack and this modified stress used in the calculation. The program can also be used to estimate growth by stress corrosion or creep mechanisms provided these can be expressed in a form relating the growth rate to the stress intensity. . .

Computer Code: FLAGRO-4

FLAGRO-4 [2-94] was developed by Rockwell International Corporation and is currently used at NASA-Johnson Space Center. The following abstract describes its options:

Structural flaws and cracks may grow under fatigue inducing loads and, upon reaching a critical size, cause structural failure to occur. The growth of these flaws and cracks may occur at load levels well below the ultimate load bearing capability of the structure. The Advanced Crack Propagation Predictive Analysis Program, FLAGRO-4, was developed as an aid in predicting the growth of pre-existing flaws and cracks in structural components. FLAGRO-4 provides the fracture mechanics analysts with a computerized method of evaluating the "safe crack growth life" capabilities of structural components. FLAGRO-4 could also be used to evaluate the damage tolerance aspects of a given structural design.

The propagation of an existing crack is governed by the stress field in the vicinity of the crack tip. The stress intensity factor is defined in terms of the relationship between the stress field magnitude and the crack size. The propagation of the crack becomes catastrophic when the local stress intensity factor reaches the fracture toughness of the material. FLAGRO-4 predicts crack growth using a two-dimensional model which independently predicts flaw growth in two directions based on the calculation of stress intensity factors. The analyst may specify that the growth rate be controlled by Collipriest's equation, Forman's equation, Paries' equation, or by tabulated, user-supplied data. FLAGRO-4 can model part-through, through, and corner cracks located on panels, on panel edges, at open holes, at pin loaded holes, at pin loaded lugs, and on tube or bar surfaces. The modeling of the crack growth may be continued until propagation becomes catastrophic. FALGRO-4 can accommodate part-through to through crack transitions, stress gradients across the width and thickness, cold worked hole residual stresses, material property variations due to environmental changes, and Willenberg retardation.

Input to FLAGRO-4 consists of initial crack definition (which can be defined automatically), rate solution type, flaw type and geometry, material properties (if they are not in the built-in material table), load spectrum data, load-stress functions, and design limit stress levels. FLAGRO-4 output includes an echo of the input with any error or warning messages and a life history profile of the crack propagation. . .

Computer Code: MSFC-2

MSFC-2 [2-95] is the current crack growth analysis program used at NASA-Marshall Space Flight Center. No acronym was assigned to the code in [2-95], so the above acronym was assigned for purposes of reference within this report. Excerpts from the user's manual introduction follow:

The MSFC crack growth computer program calculates crack growth for part-through cracks, through-thickness cracks and cracks which are transitioning from part-through cracks to through-thickness cracks. The computer program has been written to be flexible in its operation and to be easily adapted and changed as fracture mechanics technology changes and/or the design usage of the program changes.

The computer program is essentially an integration routine which calculates crack growth from an initial defect size and terminates calculation when the crack is sufficiently large for a critical

condition (instability or rapid growth) to be reached. The initial defect size may be designated by the user or established by the computer program on the basis of proof test logic. In addition, if a design life is not met for a particular structure, the program has the capability of varying the thickness of the structure or initial defect size so as to establish the geometry which will meet the design requirements.

During the period when a crack is a part-through crack, crack growth in the depth and surface directions may be different due to variations in stress intensity factors and/or directional dependence of material properties. The MSFC computer program considers both of these effects and hence incorporates realistic crack shape changes. During the period when a crack is transitioning from a part-through crack to a through-thickness crack, the crack lengths on the backside and the frontside are different. The MSFC computer program tracks the growth of these two dimensions separately; evaluating the stress intensity factors at each surface until these dimensions are the same and the crack has completed its transition to a through-thickness crack.

The computer program allows two different methods of load input. For each step in the loading block, the user specifies either: (1) Maximum Stress, Minimum Stress, Number of Cycles or (2) Maximum Stress, Stress Ratio, Number of Cycles. It should be noted that if crack growth mechanisms other than fatigue are being considered (e.g., static stress corrosion) the appropriate rate variable can be used instead of cycles (e.g., time at load) in conjunction with appropriate material constants as described below to perform a wide range of phenomenological studies.

The use of a limit load (a load which may be higher than any load in the actual spectrum) to determine the end of design life is a common practice. The MSFC computer program has therefore been written to consider a separate limit load (apart from those in the spectrum) and to determine when it causes failure. However, after failure due to limit load occurs, the crack growth calculation continues. The limit load failure information is included in the output.

The crack growth rate material properties may presently be input into the program in any of four formats: (1) Paris equation with upper and lower cutoffs in stress intensity factor; (2) Forman equation with upper and lower cutoffs in stress intensity factor; (3) Collipriest-Ehret equation with additional upper and lower cutoffs in stress intensity factor; (4) tabulated as a function of stress intensity range and stress ratio. An important feature of the material property description is that different material properties (crack growth equations, fracture properties, yield stress, etc.) may be designated for each step in the loading spectrum. Thus varying temperatures and environments may be considered.

The MSFC crack growth computer program has the capability of utilizing any one of three crack growth retardation models. Of course, the effects of retardation on crack growth will not be considered if the user does not request it. The three models presently available are: (1) Willenborg; (2) Wheeler; (3) Grumman Closure Model.

Table 3-6 is a summary of the most salient features of the programs surveyed in the current project. More detailed explanations of any option/method can be obtained from the user manuals.

3.8 FATIGUE CRACK GROWTH UNDER COMPLEX STRESS CONDITIONS

The vast majority of fatigue crack growth problems encountered in the aerospace industry involve cyclic loading of cracks in the opening mode (Mode I). Situations occur in which fatigue cracks can nucleate and grow in other modes of loading. Such situations result from complex stress systems, such as are produced by Hertzian contact. Ball and roller bearings and train wheels on rails are familiar examples.

Several criteria are available for combining component stresses into a single "effective" stress term which simplifies prediction of fatigue of crack growth under combined stresses [3-4, 3-161, 3-162]. Such formulations are intended to unify and extend fatigue and crack growth data obtained with simple laboratory specimens to define fatigue and crack growth in structures subjected to complex stress fields. The choice of formulation to use will depend on:

1. the mechanics of flaw initiation and growth as to the local stresses and their distribution which are required to force the material to form and extend a crack,

Table 3-6
Automated Stress Intensity and Crack Growth Programs

*Acronym for reference only
(N/A): Information not available
(N/L): No fixed limit

CODE HISTORY		FLAW GEOMETRIES AND LOADING CONDITIONS			VARIABLE AMPLITUDE CAPABILITIES	
Code Name [Reference]	Sponsor (Developer) [Reference]	Available K-solutions (Method)	Applied Stress Distributions	Plasticity Options	Cycle Input Format (Capacities)	Load Interaction Models
BEWICH*	Beech Aircraft (S. Imitiaz) [2-87]	9 (Handbook, Closed-Form)	Uniform, Pin Loading	Crack Tip Plastic Zone	Blocks (N/A) Steps (N/A) Cycles (N/A)	Wheeler
BIGIF	Failure Analysis Assoc. (P. Besuner) [2-17]	17 (Closed-Form, Weight Functions)	General Stress Distributions	Contained Plasticity -Notches, Holes, K_T's-	Blocks (N/L) Steps (20) Cycles (N/L)	None
CGR-LaRC	NASA-Langley R.C. (S. Johnson) [2-88]	10 (Handbook, Closed-Form)	Uniform, Pin Loading	None	Blocks (N/A) Steps (N/A) Cycles (N/A)	Multi Parameter Yield Zone (MPYZ)
EFFGRO	Rockwell Int. (NAAD) (M. Szamossi) [2-91]	10 (Handbook, Closed-Form, Tabular)	Uniform	Crack Tip Plastic Zone (plane strain)	Blocks (N/A) Steps (N/A) Cycles (N/A)	Vroman (unpublished) Similar to Willenborg Model
FAST-2	NASA-Langley R.C. (J. Newman) [2-92]	9 (Handbook, Closed-Form)	Uniform, Bending (surface crack only)	None	Blocks (N/L) Steps (50) Cycles (N/L)	Newman's Closure Model
FATPAC	Central Electricity Research Labs (G. Chell) [2-93]	35 (Closed-Form, Weight Functions)	General Stress Distribution	Crack Tip Plastic Zone (35 Geometries) Contained Plasticity, COD (12 Geometries)	Blocks (40) Steps (80) Cycles (N/L)	None
FLAGRO-4	NASA-JSC (A. Liu) [2-94]	13 (Handbook, Closed-Form)	Uniform, Bending, Pin Loading	None	Blocks (N/A) Steps (250) Cycles (N/L)	Willenborg
MSFC-2*	NASA-MSFC (M. Creager) [2-95]	30 (Handbook, Closed-Form, Tabular)	Uniform, Pin Loading	None	Blocks (N/A) Steps (N/A) Cycles (N/A)	Willenborg Wheeler Grumman Closure

CODE NAME	CRACK GROWTH MODELS				INTEGRATION TECHNIQUE	ADDITIONAL FEATURES
	da/dn vs. ΔK (options)	K_{Ic}, K_c	K_{th}	Breakthrough (Transition from part-through to through crack)		
BEWICH	Walker Jaske-Federson Inverse-Hyperbolic Tangent Function (5 Materials)	K_{Ic},K_c = Constant	Embedded in Inverse-Hyperbolic Tangent Function ΔK_{th} = constant	c > t	N/A	Check for applicability (σ/σ_{ys} limits) Finite Width/Thickness Effects
BIGIF	Paris (2) Forman (2) Tabular (2)	K_{Ic},K_c=f(crack depth)	ΔK_{th} = constant ΔK_{th} = f(R-ratio)	None	Modified rectangular (similar to linear approximation) Runge-Kutta (weight functions)	Plotting Variable Thickness (8 geometries) Finite Width/Thickness Effects
CGR-LaRC	Paris Modified Forman	K_{Ic},K_c = Constant	ΔK_{th} = f(R-ratio)	None	N/A	Finite Width/Thickness Effects Check for $\sigma_{ligament} > \sigma_{ult}$ Check for da/dn < $[(da)dn]_{fast}$
EFFGRO	Modified Forman	K_{Ic},K_c = Constant	None	$a > 1 - \frac{\sigma_{trans}}{\sigma_{ys}} \frac{4}{\pi} t_{equiv}$	Linear Approximation	Finite Width/Thickness Effects Flexibility in Load Spectrum Specification
FAST-2	Modified Power Law (Elber) (Effective Crack Opening Stress Intensities) Tabular	$K_{max} > K_{Ic}$ $K_{max} > K_{IE}$ K_{IE} = f(K_c,$\sigma_{nom}/\sigma_{ult}$)	ΔK_{th} = f(R) 3 options (N/A)	None	Crack Growth (N/A) Gauss-Seidel (Crack Closure Stresses)	Finite Width/Thickness Effects Option to grow from starter notch to specified initial crack size
FATPAC	Paris General Power Law (Chell)	K_{Ic},K_c = Constant	ΔK_{th} = f(R) (Embedded in Crack Growth Law)	None	Trapezoidal Incremental Scheme	Various crack growth models through use of generalized power law. 'Reverse' crack growth (a_f a_{init}) Finite width/Thickness Effects
FLAGRO-4	Paris Forman Collipriest-Ehret Tabular	K_{Ic},K_c=f(Cracking Directions, monotonic or cyclic loading, crack geometry)	ΔK_{th} = constant	Yes (Details N/A)	Incremental Scheme (Details N/A)	Cold-worked hole model Finite Width/Thickness Effects
MSFC-2	Paris Forman Collipriest-Ehret Tabular	K_{Ic},K_c = f (Cracking Direction, load spectrum)	ΔK_{th} = Constant (used for cutoff values in material crack growth laws)	a = t (start transition) c' > 0.95C (Complete transition)	Linear Approximation	Built-in thickness and initial flaw size combinations for specified design requirements Limit Load Analysis Material Properties designated for each load step

2. the magnitudes of stress components in the structure considered (whether stresses are triaxial, biaxial, or uniaxial),

3. the relative orders of magnitude of stresses across the face of a flaw compared to stresses carried around the end of a flaw due to its presence, and

4. the corresponding stress situations represented by the available fatigue and crack growth data.

One summary of descriptions, references and fractographs for crack growth mechanisms is given by Fowler [3-163]. While written with special reference to pearlitic rail steels, Fowler provides information of a general nature on crack growth. For example, the reference shows how shear stresses are necessary to form striations to extend a crack in Mode I. Other references on the role of shear in various mechanisms for crack extension include the work of Parker [3-164] and Kitajima and Futagami [3-165] on cleavage, Forsyth [3-166] and Lin [3-167, 3-168] on intrusion-extrusion and gating, Sines [3-169, 3-170] on combined stresses and Low [3-171] on fracture. Hertzberg and Mills [3-172] use electron fractograph studies to illustrate the commonality of crack extension mechanisms over several different metal alloys (see also Beevers, et al. [3-173]). Clark [3-174] and Lindley and Richards [3-175] provide further discussions on mechanisms related to crack growth.

The stress fields induced in a ball bearing system, for example, can vary from highly triaxial to nearly uniaxial during passage of a ball bearing over a given point depending on its location. Stresses in the inner bearing race may arise from cyclic and moving loads imposed through the ball bearings on the race and residual stresses from the interference fit of the race on the shaft. The ball bearings are loaded by shaft side, axial and bending loads and by whirl mode response of the shaft due to mass imbalance. The bearings

induce both triaxial contact stresses under the ball and indirectly produce tensile, shear or compressive stresses through transfer of bearing loads across the race to the shaft.

The problem of flaw growth in wheel loaded rails is another example of complex stresses. While the part size and loading frequencies are different from those of the ball bearing situation, the essential combined stress cycle experienced by a small flaw is the same. Consequently, the example of wheel loaded rails will be discussed and used to illustrate the problem of flaw growth in constrained parts under cyclic contact loadings. The stress fields induced by wheel on rail loadings and other sources of stress vary from highly triaxial to nearly uniaxial during a typical cycle. For example, in the rail head, the vertical loading from a wheel contributes

1. negative bending stress under the wheel and a lesser positive bending stress away from the wheel, and

2. high triaxial negative contact stresses which peak under the wheel and whose principal directions rotate enough for a moderate transverse shear to peak under the edge of the wheel rail contact zone and to reverse upon passage of the wheel.

Horizontal wheel loadings arise from

3. longitudinal wheel rail traction to produce axial rail stresses

4. lateral and longitudinal wheel-rail sliding for friction contact stresses, and

5. lateral flange impact and slifing on the gage side of the rail head.

In addition, the rail head also experiences

6. axial thermal stresses due to daily and seasonal temperature changes, and

7. residual stresses arising from past loadings and fabrication.

Thus, directly under a wheel, the dominant contact stresses will produce high compressive stresses (vertical stresses on the order of 100 to 150 ksi with longitudinal and transverse stresses between 30 and 75 ksi at 0.1 to 0.14 inches below the rail running surface under 20 to 30 kip wheel loadings). Six feet from such a wheel, a uniaxial tensile stress of from 4 to 12 ksi may be experienced in the rail head due to reversed bending. As a consequence, for tranvserse flaws, the compressive stresses across the face of a flaw under a wheel can be of the same order of magnitude as tensile stresses at 1-10 microns beyond the edge of a crack when the wheel is six feet away. Under these circumstances, the rates of crack growth for transverse flaws may not be predictable if stress intensity factors are used alone with the unmagnified compressive stresses ignored.

Metallic materials including aluminum, steel and titanium have been subjected to cyclic loading in the laboratory to determine fatigue lives, crack growth rates, and fracture strengths. Most of these tests have been conducted on uniaxial, rotating bend, or other simple loaded coupon specimens. These tests have included both positive and negative stress ratios, R (e.g., some as low as R = -5 on titanium by Yuen, Hopkins et al. [3-4]). Some tests have been conducted on full scale structural systems or, in this example, full size wheels and rails. However, full scale tests are expensive and, hence, few.

Nevertheless, it is possible to ascertain the formulation of combined stresses affecting crack growth by observing the direction and rate of crack

extension when loadings are applied at an inclined angle with respect to the line of a starting crack [3-161, 3-162, 3-176]. Some cyclic loading tests on an inclined angle have been conducted by Iida and Kobayashi [3-177], Yokobori [3-178], and Allison [3-179]. However, crack direction data for inclined angle loading is essentially limited to static fracture tests [3-162, 3-176, 3-180, 3-181]. Moreover, for some test cases necessary to confirm combined stress formulations for crack extension, even the static fracture data is insufficient. As a consequence, the action of combined stresses is difficult to evaluate from experiments available to date, since direction of crack extension is sensitive to minor variations of stress and, at values of Poisson's ratio represented in the data, only small differences in direction of crack extension among alternative theories can be expected. Thus, the intent of an any more definitive experimental program should be to provide the key combinations of Poisson's ratio, inclined angle, and stress ratio necessary to discriminate between the leading suggested formulations governing crack growth under combined stress conditions.

In predicting crack growth, it may be possible to define an effective stress term to produce the same crack growth rate for all combinations of component stresses among those anticipated. In addition, the lowest gradient of the same term with respect to direction should define the direction of crack extension. Under any given load, the local elastic stresses σ_{ij}, which are added by the presence of a crack are given by [3-161]

$$\begin{Bmatrix} \sigma_{11} \\ \sigma_{22} \\ \sigma_{33} \\ \sigma_{12} \\ \sigma_{23} \\ \sigma_{31} \end{Bmatrix} = \frac{1}{\sqrt{2\pi}} \frac{1}{\sqrt{r}} \begin{bmatrix} U_c - U_{cs} & 2U_s - U_{sc} & 0 \\ U_c + U_{cs} & U_{sc} & 0 \\ 2\nu U_c & 2\nu U_s & 0 \\ U_{sc} & U_c - U_{cs} & 0 \\ 0 & 0 & U_c \\ 0 & 0 & U_s \end{bmatrix} \begin{Bmatrix} K_I \\ K_{II} \\ K_{III} \end{Bmatrix} \tag{3-21}$$

where
$\sigma_{ij} = \sigma_{ij}(r,\theta)$
$U_s = \sin \theta/2$
$U_{sc} = \sin \theta/2 \cos \theta/2 \cos 3\theta/2$
$U_c = \cos \theta/2$
$U_{cs} = \cos \theta/2 \sin \theta/2 \sin 3\theta/2$

and K_I, K_{II} and K_{III} are the stress intensity factors for opening, shear, and tearing modes of crack loading, respectively.

Some of the combined stress terms $f(\sigma_{ij})$ to be entertained include:

1. stress normal to direction from crack-tip (Figure 3-62a)

$$f_t(\sigma_{ij}) = \cos^2\theta\sigma_{22}(r, \theta) + 2\cos\theta \sin\theta\sigma_{12}(r,\theta) + \sin^2\theta \sigma_{11}(r,\theta) \tag{3-22}$$

2. shear along direction from crack-tip (Figure 3-62b)

$$f_v(\sigma_{ij}) = \sigma_{12}(r,\theta)(\cos^2\theta - \sin^2\theta) + \cos\theta \sin\theta (\sigma_{11}(r,\theta) + \sigma_{22}(r,\theta)) \tag{3-23}$$

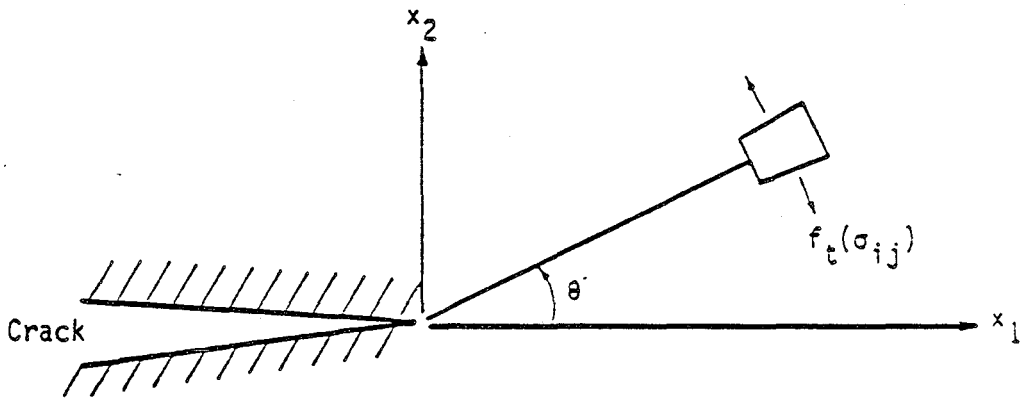

a) Stress Normal to Direction From Crack Tip.

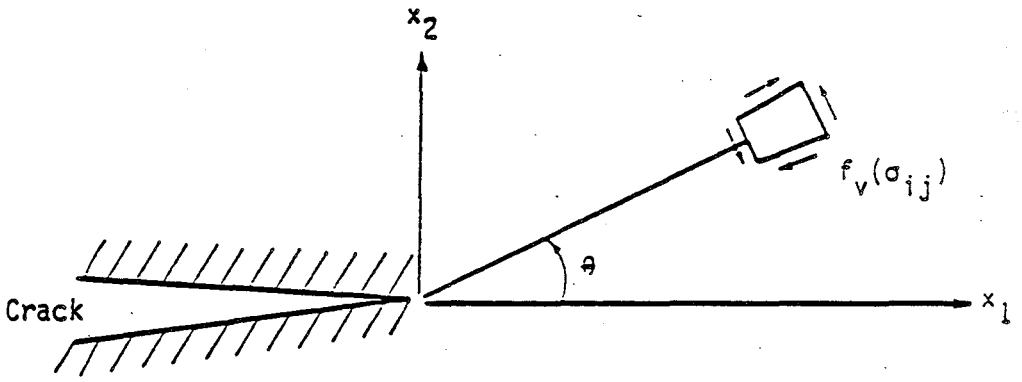

b) Shear Along Direction From Crack Tip.

Figure 3-62. Stress Element Rotated to Line From Crack Tip.

3. shear at 45° to crack-tip

$$f_{45}(\sigma_{ij}) = [\sigma_{22}(r,\theta) - \sigma_{11}(r,\theta)](\cos^2\theta - \sin^2\theta) + \sigma_{12}(r,\theta)\cos\theta\sin\theta \quad (3\text{-}24)$$

4. octahedral shear (distortion energy)

$$f_d(\sigma_{ij}) = (\sigma_{11} - \sigma_{22})^2 + (\sigma_{22} - \sigma_{33})^2 (\sigma_{33} - \sigma_{11})^2 + 6(\sigma_{12}^2 + \sigma_{23}^2 + \sigma_{31}^2) \quad (3\text{-}25)$$

5. strain energy density [3-161]

$$f_s(\sigma_{ij}) = C_1 f_d(\sigma_{ij}) + C_2 (\sigma_{11} + \sigma_{22} + \sigma_{33})^2 \quad (3\text{-}26)$$

where C_1 and C_2 are related to the elastic constants [3-161]. Whichever term or combination $f(\sigma_{ij})$ governs crack growth will also predict the direction, θ, of crack growth. That is, for a given configuration of specimen, crack and loading, K_I, K_{II}, K_{III}, the governing $f(\sigma_{ij})$ will show an extreme for values of θ that match experimentally measured directions of crack growth.

As an example, let a plate with a center-through-crack be uniaxially loaded at various angles β between the crack plane and direction of stress. Here, we not that σ_{ij} in Equations 3-21 to 3-26 are functions of $\vec{K} = \{K_I, K_{II}, K_{III}\}$ as well as of r and θ. As a consequence, with $\vec{K}$ a function of load and specimen configuration which in this case means load to crack line angle, β, as well as of r and θ it is clear that $f(\sigma_{ij})$ is a function of β. Thus, if the normal stress term and the strain energy density term are to be compared, the predicted directions, θ, of crack extension may be plotted against load angle, β (Figure 3-63). With Poisson's ratio $\nu = 0.33$, the

predicted directions are the same for $\beta = 90°$ and $\beta = 45°$. However, at $\beta = 60°$ or $\beta \leq 20°$, the predicted directions do show a difference. Moveover, if Poisson's ratio is changed, the cracked direction will change if strain energy density governs but not if maximum principal tension governs crack growth. Thus, by appropriate choices of crack line versus load angle and Poisson's ratio, the effective stress term affecting the direction of crack growth can be experimentally selected. Such tests would provide guidance in the selection of appropriate criteria governing crack growth under complex stress conditions. However, knowledge of the exact direction of crack growth under complex stress conditions is usually not required in order to make accurate predictions of structural life.

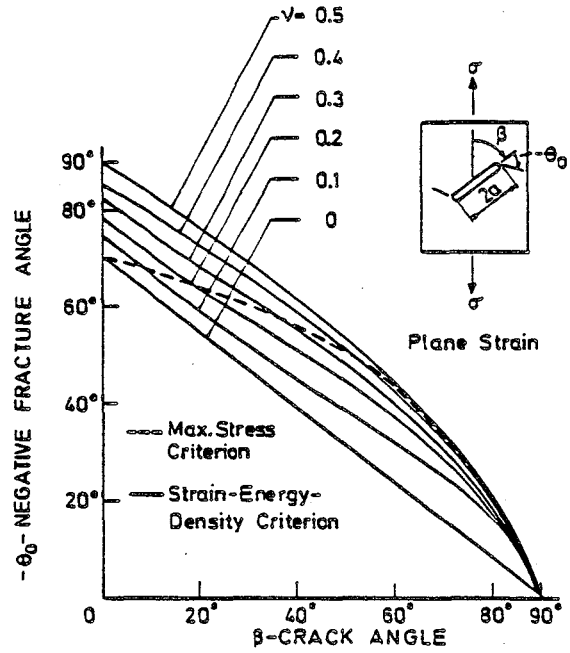

Figure 3-63. Crack Angle Versus Fracture Angle in Tension [3-161].

3.9 REFERENCES

3-1. Johnson, H.H., and Paris, P.C., "Subcritical Flaw Growth," Engineering Fracture Mechanics, Vol. 1, No. 1, pages 3-45, June 1968.

3-2. Paris, P.C., Gomez, M.P., and Anderson, W.E., "A Rational Analytic Theory of Fatigue," The Trend in Engineering, Vol. 13, No. 1, University of Washington, January 1961.

3-3. Tada, H., Paris, P.C., and Irwin, G.R., Stress Analysis of Cracks Handbooks, Del Research Corporation, Hellertown, Pennsylvania, 1973.

3-4. Yuen, A., Hopkins, S.W., Leverant, G.R., and Rau, C.A., "Correlations Between Fracture Surface Appearance and Fracture Mechanics Parameters for Stage II Fatigue Crack Propagation in Ti-6Aℓ-4V," Metallurgical Transactions, Vol. 5, pages 1833-1842, August 1974.

3-5. Forman, R.G., Kearney, V.E., and Engle, R.M., "Numerical Analysis of Crack Propagation in a Cyclic-Loaded Structure," Journal of Basic Engineering, Transactions of the ASME, Vol. 89, Series D, No. 3, pages 459-464, 1967.

3-6. Elber, W., "The Significance of Fatigue Crack Closure," Damage Tolerance in Aircraft Structures, ASTM Special Technical Publication 486, pages 230-242, 1971.

3-7. Radon, J.C., "Fatigue Crack Growth in the Threshold Region," Fatigue Thresholds, Vol. I, edited by Bäcklund, Blom, and Beevers, Engineering Materials Advisory Services LTD., West Midlands, UK, pages 113-132, 1982.

3-8. Shih, T.T. and Wei, R.P., "A Study on Crack Closure in Fatigue," NASA CR-2319, October 1973.

3-9. James, L.A., "Some Questions Regarding the Interaction of Creep and Fatigue," Journal of Engineering Materials and Technology, ASME paper 75-WA/Mat-6, 1975.

3-10. Musuva, J.K. and Radon, J.C., "The Effect of Stress Ratio and Frequency on Fatigue Crack Growth," Fatigue of Engineering Materials and Structures, Vol. 1, pages 457-470, 1979.

3-11. Backlund, J., Blom, A.F., Beevers, J.C., editors, Fatigue Thresholds, Fundamentals and Engineering Applications, Volumes I and II, Engineering Materials Advisory Services LTD., West Midlands, UK, 1982.

3-12. Smith, R.A., "Fatigue Thresholds - A Design Engineer's Guide through the Jungle," Fatigue Thresholds, Vol. I, Bäcklund, Blom, Beevers, Editors, Engineering Materials Advisory Services LTD., West Midlands, UK, pages 33-44, 1982.

3-13. Cadman, A.J., Brook, R., and Nicholson, C.E., "Effect of Test Technique on the Fatigue Threshold ΔK_{th}," Fatigue Thresholds, Vol. 1, edited by Bäcklund, Blom, and Beevers, Engineering Materials Advisory Services LTD., West Midlands, UK, pages 59-75, 1982.

3-14. Rolfe, S.T., and Barsom, J.M., Fracture and Fatigue Control in Structures, Section 7.6 Nonpropagating Fatigue Cracks, Prentice-Hall Inc., Englewood Cliffs, New Jersey, pages 224-225, 1977.

3-15. Chalant, G., and Remy, L., "A Tentative Rationale of the Threshold Behavior Obtained from Strain Distribution at the Crack Tip," Fatigue Thresholds, Vol. I, edited by Bäcklund, Blom, and Beevers, Engineering Materials Advisory Services LTD., West Midlands, UK, pages 33-44, 1982.

3-16. Hopkins, S.W., Rau, C.A., Leverant, G.R., and Yuen, A., "Effect of Various Programmed Overloads on the Threshold for High-Frequency Fatigue Crack Growth," Fatigue Crack Growth Under Spectrum Loads, ASTM Special Technical Publication 595, pages 125-141. 1976.

3-17. El Haddad, M.H., Smith, K.N., and Topper, T.H., "Fatigue Crack Propagation of Short Cracks," Journal of Engineering Materials and Technology, Vol. 101, pages 42-46, 1979.

3-18. Leis, B.N., et al., "A Critical Review of the Short Crack Problem in Fatigue," Air Force Wright Aeronautical Laboratories Report AFWAL-TR-83-4019, Wright-Patterson Air Force Base, Ohio, January 1983.

3-19. Newman, J.C., Jr., "A Nonlinear Fracture Mechanics Approach to the Growth of Small Cracks," presented at AGARD Specialists Meeting on Behavior of Short Cracks in Airframe Components, Toronto, Canada, September 1982.

3-20. Schijve, J., "Differences Between the Growth of Small and Large Fatigue Cracks in Relation to Threshold K Values," Fatigue Thresholds, Vol. II, edited by Bäcklund, Blom, and Beevers, Engineering Materials Advisory Services LTD., West Midlands, UK, pages 881-908, 1982.

3-21. Romaniv, O.N., Siminkovich, V.N., and Tkach, A.N., "Near Threshold Short Fatigue Crack Growth," Fatigue Thresholds, Vol. II, Bäcklund, Blom, Beevers, Editors, Engineering Materials Advisory Services LTD., West Midlands, UK, pages 799-807, 1982.

3-22. Döker, H., Bachmann, V., and Marci, G., "A Comparison of Different Methods of Determination of the Threshold for Fatigue Crack Propagation," Fatigue Thresholds, Vol. I, edited by Bäcklund, Blom, and Beevers, Engineering Materials Advisory Services LTD., West Midlands, UK, pages 45-57, 1982.

3-23. Schijve, J., "Observations on the Prediction of Fatigue Crack Growth Propagation Under Variable-Amplitude Loading," Fatigue Crack Growth Under Spectrum Loads, ASTM Special Technical Publication 595, pages 3-23, 1976.

3-24. Elber, W., "Equivalent Constant-Amplitude Concept for Crack Growth Under Spectrum Loading," Fatigue Crack Growth Under Spectrum Loads, ASTM Special Technical Publication 595, pages 236-250, 1976.

3-25. Elber, W., "Fatigue Crack Propagation," Ph.D. Thesis, University of New South Wales, Australia, 1968.

3-26. Dowling, N.E., "Fatigue Failure Predictions for Complicated Stress-Strain Histories," Journal of Materials, Vol. 7, No. 1, pages 71-87, March 1972.

3-27. Nelson, D.V., and Fuchs, H.O., "Predictions of Cumulative Damage Using Condensed Load Histories," Paper 750045, presented at SAE Automotive Engineering Congress and Exposition, February 1975.

3-28. Corbly, D.M., and Packman, P.F., "On the Influence of Single and Multiple Peak Overloads on Fatigue Crack Propagation in 7075-T6511 Aluminum," Engineering Fracture Mechanics, Vol. 5, pages 479-497, 1973.

3-29. Nelson, D.V., "Review of Fatigue-Crack-Growth Prediction Methods," Experimental Mechanics, Vol. 17, No. 2, pages 41-49, February 1977.

3-30. Irwin, G., "Plastic Zone Near a Crack and Fracture Toughness," Proceedings of the Seventh Sagamore Conference, page IV-63, 1960.

3-31. Jones, R.E., "Fatigue Crack Growth Retardation After Single-Cycle Peak Overload in Ti-6Aℓ-4V Titanium Alloy," Engineering Fracture Mechanics, Vol. 5, pages 585-604, 1973.

3-32. Jonas, O., and Wei, R.P., "An Exploratory Study of Delay in Fatigue-Crack Growth," International Journal of Fracture Mechanics, Vol. 7, No. 1, pages 116-118, March 1971.

3-33. Schijve, J., "Fatigue Crack Propagation in Light Alloy Sheet Material and Structures," Report MP-195, National Aerospace Lab, The Netherlands, August 1960.

3-34. Hudson, C.M., and Hardrath, H.F., "Investigation of the Effects of Variable Amplitude on the Rate of Fatigue Crack Propagation Patterns," NASA TN-D-1803, 1963.

3-35. Hudson, C.M., and Hardrath, H.F., "Effects of Changing Stress Amplitude on the Rate of Fatigue Crack Propagation in Two Aluminum Alloys," NASA TN-D-960, 1961.

3-36. Wei, R.P., and Shih, T.T., "Delay in Fatigue Crack Growth," International Journal of Fracture Mechanics, Vol. 10, No. 1, pages 77-85, March 1974.

3-37. Shih, T.T., "Fatigue Crack Growth Under Variable Amplitude Loading," Ph.D. Thesis, Lehigh University, Bethlehem, Pennsylvania, 1974.

3-38. Shih, T.T., and Wei, R.P., "The Influence of Chemical and Thermal Environments on Delay in a Ti-6Aℓ-4V Alloy," Fatigue Crack Growth Under Spectrum Loads, ASTM Special Technical Publication 595, pages 113-124, 1976.

3-39. Alzos, W.X., Skat, A.C., and Hillberry, B.M., "Effect of Single Overload/Underload Cycles on Fatigue Crack Propagation," Fatigue Crack Growth Under Spectrum Loads, ASTM Special Technical Publication 595, pages 41-60, 1976.

3-40. Schijve, J., and Broek, D., "Crack Propagation Under Variable Amplitude Loading," NLR Report M2094, January 1962.

3-41. Von Euw, E.F., Hertzberg, R.W., and Roberts, R., "Delay Effects in Fatigue Crack Propagation," Stress Analysis and Growth of Cracks, ASTM Special Technical Publication 513, pages 230-259, 1972.

3-42. Gallagher, J.P., and Hughes, T.F., "Influence of Yield Strength on Overload Affected Crack Growth Behavior in 4340 Steel," AFFDL-TR-74-27, July 1974.

3-43. Probst, E.P. , and Hillberry, B.M., "Fatigue Crack Delay and Arrest Due to Single Peak Tensile Overloads," AIAA Journal, Vol. 12, No. 3, pages 330-335, March 1974.

3-44. Wei, R.P., Shih, T.T., and Fitzgerald, J.H., "Load Interaction Effects on Fatigue Crack Growth in Ti-6Aℓ-4V Alloy," NASA CR-2239, April 1973.

3-45. Vargas, L.G., and Stephens, R.I., "Subcritical Crack Growth Under Over-Loading in Cold Rolled Steel," Proceedings of Third International Conference on Fracture, Munich, April 1973.

3-46. Rice, R.C., and Stephens, R.I., "Overload Effects on Subcritical Crack Growth in Austenitic Manganese Steel," Progress in Flaw Growth and Fracture Toughness Testing, ASTM Special Technical Publication 536, pages 95-114, 1973.

3-47. Trebules, V.W., Roberts, R., and Hertzberg, R.W., "Effects of Multiple Overloads on Fatigue Crack Propagation in 2024-T3 Aluminum Alloy," Progress in Flaw Growth and Fracture Toughness Testing, ASTM Special Technical Publication 536, pages 115-146, 1973.

3-48. Hudson, C.M., and Raju, K.N., "Investigation of Fatigue Crack Growth Under Simple Variable Amplitude Loading," NASA TN-D-5702, 1970.

3-49. McMillan, J.C., and Pelloux, R.M., "Fatigue Crack Propagation Under Program and Random Loads," Fatigue Crack Propagation, ASTM Special Technical Publication 415, pages 550-535, 1967.

3-50. Hall, L.R., Shah, R.C., and Engstrom, W.L., "Fracture and Fatigue Crack Growth Behavior of Surface Flaws and Flaws Originating at Fastener Holes," AFFDL-TR-74-47, May 1974.

3-51. Hillberry, B.M., Alzos, W.X., and Skat, A.C., "The Fatigue Crack Propagation Behavior in 2024-T3 Aluminum Alloy Due to Single Overload/Underload Sequences," AFFDL:AD-A018-860, August 1975.

3-52. Stephens, R.I., Chen, D.K., and Hom, B.W., "Fatigue Crack Growth with Negative Stress Ratio Following Single Overloads in 2024-T3 and 7075-T6 Aluminum Alloys," Fatigue Crack Growth Under Spectrum Loads, ASTM Special Technical Publication 595, pages 27-40, 1976.

3-53. Hsu, T.M., and Lassiter, L.W., "Effects of Compressive Overloads on Fatigue Crack Growth," AIAA Structures, Structural Dynamics and Materials Conference, No. 74-365, April 1974.

3-54. Powell, B.E., Duggan, T.V., and Jeal, R., "The Influence of Minor Cycles on Low Cycle Fatigue Crack Propagation," International Journal of Fatigue, Vol. 4, No. 1, pages 4-14, January 1982.

3-55. Carlson, J., Erickson, S., and Sundstrand, A., "Fatigue Cracks in Electric Generator Rotors - A Case Study," Fatigue Thresholds, Vol. II, edited by Bäcklund, Blom, and Beevers, Engineering Materials Advisory Services LTD., West Midlands, UK, pages 989-1005, 1982.

3-56. Hsu, T.M., and McGee, W.M., "Effects of Compressive Loads on Spectrum Fatigue Crack Growth Rate," Effect of Load Spectrum Variables on Fatigue Crack Initiation and Propagation, ASTM Special Technical Publication 714, pages 79-90, 1980.

3-57. Chang, J.B., Szamossi, M., and Liu, K-W., " Random Spectrum Fatigue Crack Life Predictions With or Without Considering Load Interactions," Methods and Models for Predicting Fatigue Crack Growth Under Random Loading, ASTM Special Technical Publication 748, pages 115-132, 1981.

3-58. Barsom, J.M., "Fatigue Crack Growth Under Variable Amplitude Loading in ASTM 514-B Steel," Progress in Flaw Growth and Fracture Toughness Testing, ASTM Special Technical Publication 536, pages 147-167, 1973.

3-59. Hudson, C.M., "A Root-Mean-Square Approach for Predicting Fatigue Crack Growth Under Random Loading," Methods and Models for Predicting Fatigue Crack Growth Under Random Loading, ASTM Special Technical Publication 748, pages 41-52, 1981.

3-60. Dill, H.D., and Saff, C.R., "Spectrum Crack Growth Prediction Method Based on Crack Surface Displacement and Contact Analyses," Fatigue

Crack Growth Under Spectrum Loads, ASTM Special Technical Publication 595, pages 306-319, 1976.

3-61. Newman, J.C., Jr., "A Crack-Closure Model for Predicting Fatigue Crack Growth under Aircraft Spectrum Loading," Methods and Models for Predicting Fatigue Crack Growth Under Random Loading, ASTM Special Technical Publication 748, pages 53-84, 1981.

3-62. Wheeler, O.E., "Spectrum Loading and Crack Growth," Journal of Basic Engineering, Transactions of the ASME, Vol. 94, Series D, No. 1, pages 181-186, March 1972.

3-63. Willenborg, J., Engle, R.M., and Wood, H.A., "A Crack Growth Retardation Model Using an Effective Stress Concept," AFFDL, TM-71-1-FBR, January 1971.

3-64. Wood, H.A., "Fatigue Life Prediction for Aircraft Structures and Materials," AGARD Section Series No. 62, 1973.

3-65. Gallagher, J.P., and Stalnaker, H.D., "Methods of Analyzing Fatigue Crack Growth Rate Behavior Associated with Flight-by-Flight Loading," AIAA Structures, Structural Dynamics and Materials Conference, AIAA Paper No. 74-367, April 1974.

3-66. Sayer, R.B., "Nonlinear Effects of Spectrum Loading on Fatigue Crack Growth in Transport Wings," AIAA Structures, Structural Dynamics and Materials Conference, AIAA Paper No. 74-984, August 1974.

3-67. Engle, R.M., and Rudd, J.L., "Analysis of Crack Propagation Under Variable Amplitude Loading Using the Willenberg Retardation Model," AIAA Structures, Structural Dynamics and Materials Conference, AIAA Paper No. 74-363, April 1974.

3-68. Gallagher, J.P., "A Generalized Development of Yield Zone Models," AFFDL-TM-74-28-FBR, January 1971.

3-69. Gallagher, J.P., "Influence of Yield Strength on Overload Affected Fatigue Crack Growth Behavior in 4340 Steel," AFFDL-TR-74-27, July 1974.

3-70. Walker, K., "The Effect of Stress Ratio During Crack Propagation and Fatigue for 2024-T3 and 7075-T6 Aluminum," Effects of Environment and Complex Load History on Fatigue Life, ASTM Special Technical Publication 462, pages 1-14, 1970.

3-71. Chang, J.B., and Hudson, C.M., editors, Methods and Models for Predicting Fatigue Crack Growth Under Random Loading, ASTM Special Technical Publication 748, 1981.

3-72. Johnson, W.S., "Multi-Parameter Yield Zone Model for Predicting Spectrum Crack Growth," Methods and Models for Predicting Fatigue

Crack Growth under Random Loading, ASTM Special Technical Publication 748, pages 85-102, 1981.

3-73. Achter, M.R., "Effect of Environment on Fatigue Cracks," Fatigue Crack Propagation, ASTM Special Technical Publication 415, pages 181-202, 1967.

3-74. Corrosion Fatigue: Chemistry, Mechanics and Microstructure, NACE-2, National Association of Corrosion Engineers, 1972.

3-75. Wei, R.P., "On Understanding Environment-Enhanced Fatigue Crack Growth -- A Fundamental Approach," Fatigue Mechanisms, Proceedings of the ASTM-NBS-NSF Symposium, ASTM Special Technical Publication 675, pages 816-840, 1979.

3-76. Speidel, M.O., "Influence of Environment on Fracture," Advances in Fracture Research, edited by D. Francois, Fifth International Conference on Fracture, Cannes, France, March 29 - April 3, Vol. 6, pages 2685-2704, 1981.

3-77. Chandler, W.T., and Walter, R.J., "Hydrogen-Environment Embrittlement of Metals and its Control," Hydrogen Energy, Part B, Plenum Press, pages 1057-1078, 1975.

3-78. Walter, R.J., and Chandler, W.T., "Influence of Gaseous Hydrogen on Metals -- Final Report," NASA Report No. NAS8-25579, 1973.

3-79. Jewett, R.P., Walter, R.J., and Chandler, W.T., "Influence of High Pressure Hydrogen on Cyclic Load Crack Growth in Metals," Corrosion Fatigue Technology, ASTM Special Technical Publication 642, pages 243-263, 1978.

3-80. Harris, J.A., Jr., and Van Wanderham, M.C., "Properties of Materials in High Pressure Hydrogen at Cryogenic, Room and Elevated Temperatures -- Final Report," Pratt & Whitney Aircraft, Florida, NASA Contract No. NAS8-216191, 1973.

3-81. Walter, R.J., and Chandler, W.T., "Effect of Hydrogen Environment on Inconel 718 and Ti-6Aℓ-4V Under Simulated J-2 Engine Operating Conditions," NASA Contract No. NAS8-19C, 1969.

3-82. Vroman, G.A., Jewett, R.P., and Nathan, A., "Fracture Properties for SSME Life Predictions," Rockwell International, Rocketdyne Division, Report No. RSS-8637, 1980.

3-83. Campbell, J.E., "Fracture Toughness of High Strength Alloys at Low Temperature -- A Review," Fatigue and Fracture Toughness -- Cryogenic Behavior, ASTM Special Technical Publication 556, pages 3-25, 1974.

3-84. Pittinato, G.F., "Hydrogen-Enhanced Fatigue Crack Growth in Ti-6Aℓ-4V ELI Weldments," Metallurgical Transactions, Vol. 3, No. 1, pages 235-242, 1972.

3-85. Rolfe, S.T., and Barsom, J.M., Fracture and Fatigue Control in Structures - Applications of Fracture Mechanics, Prentice-Hall, 1977.

3-86. Austin, I.M., "Measurement of Crack Length and Data Analysis in Corrosion Fatigue," The Measurement of Crack Length and Shape During Fracture and Fatigue, EMAS, edited by J.C. Beevers, pages 164-189, 1980.

3-87. Wei, R.P., "Some Aspects of Environment-Enhanced Fatigue Crack Growth," Journal of Engineering Fracture Mechanics, Vol. 1, No. 4, pages 633-651, 1970.

3-88. Bradshaw, F.J., and Wheeler, C., "The Effect of Environment on Fatigue Crack Growth in Aluminum and Some Aluminum Alloys," Applied Materials Research, Vol. 5, No. 2, pages 112-120, April 1966.

3-89. Hartman, A., "On the Effect of Oxygen and Water Vapor on the Propagation of Fatigue Cracks in 2024-T3 Alcald Sheet," International Journal of Fracture Mechanics, Vol. 1, pages 167-188, 1965.

3-90. Landes, J.D., and Wei, R.P., "Kinetics of Subcritical Crack Growth and Deformation in a High Strength Steel," Journal of Engineering Materials and Technology, Transactions of the ASME, Vol. 95, Series H, pages 2-9, 1973.

3-91. Gerberich, W.W., and Yu, W., "Hydrogen Interactions in Fatigue Crack Thresholds," Fracture Problems and Solutions in the Energy Industry, Proceedings of the Fifth Canadian Fracture Conference, September 3-4, 1981, pages 39-51, 1982.

3-92. Wei, R.P., and Landes, J.D., "Correlation Between Sustained-Load and Fatigue Crack Growth in High Strength Steels," Materials Research and Standards, Vol. 9, No. 7, pages 25-27, July 1969.

3-93. Haigh, J.R., Skelton, R.P., and Richards, C.E., "Oxidation-Assisted Crack Growth During High Cycle Fatigue of a 1% Cr-Mo-V Steel at 550°C," Journal of Material Science and Engineering, Vol. 26, No. 2, pages 167-174, 1976.

3-94. Schmidt, R.A., and Paris, P.C., "Threshold for Fatigue Crack Propagation and the Effects of Load Ratio and Frequency," Progress in Flaw Growth and Fracture Toughness Testing, ASTM Special Technical Publication 536, pages 79-94, 1973.

3-95. Takezono, S., and Satoh, M., "Effect of Stress Frequency on Fatigue Crack Propagation in Titanium," Journal of Engineering Materials and Technology, Vol. 104, pages 257-261, 1982.

3-96. Tomkins, B., "Fatigue: Introduction and Phenomenology," Creep and Fatigue in High Temperature Alloys, Applied Science Publishers, Ltd., London, 1981.

3-97. Coffin, L.F., Jr., "Fatigue at High Temperature," Fatigue at Elevated Temperatures, ASTM Special Technical Publication 520, pages 5-34, 1973.

3-98. Gell, M., and Leverant, G.R., "Mechanisms of High Temperature Fatigue," Fatigue at Elevated Temperatures, ASTM Special Technical Publication 520, pages 37-67, 1973.

3-99. Strafford, K.N., and Datta, P.K., "High Temperature Corrosion, Creep and Fracture Processes, and Their Interaction," Behavior of High Temperature Alloys in Aggressive Environments, Proceedings of the Petten International Conference, Metals Society of London, page 945, 1979.

3-100. Sandananda, K., and Shahinian, P., "Creep-Fatigue Crack Growth," Cavities and Cracks in Creep and Fatigue, edited by J. Gittus, Applied Science Publishers, London, pages 109-196, 1981.

3-101. James, L.A., "The Effect of Frequency Upon the Fatigue Crack Growth of Type 304 Stainless Steel at 1,000°F," Stress Analysis and Growth of Cracks, Part 1, ASTM Special Technical Publication 513, pages 218-229, 1972.

3-102. Runkle, J.C., and Pelloux, R.M., "Micromechanisms of Low-Cycle Fatigue in Nickel-Based Superalloys at Elevated Temperatures," Fatigue Mechanisms, Proceedings of a ASTM-NTB-NSF Symposium, May 1978, ASTM Special Technical Publication 675, pages 501-527, 1979.

3-103. White, D.J., Proceedings of the Institute of Mechanical Engineering, Applied Mechanics Group, Vol. 184, page 223, 1969-1970.

3-104. Nachtigall, A.J., Klima, S.J., Freche, J.C., and Hoffman, C.A., "The Effects of Vacuum on Fatigue and Stress Rupture Properties of S-B16 and Inconel 550 at 1500°F," NASA TN-D2898, June 1965.

3-105. Ericsson, T., "Review of Oxidation Effects on Cyce Life at Elevated Temperatures," Canadian Metallurgy Quarter, Vol. 18, pages 177-195, 1975.

3-106. Smith, P., and Stewart, A.T., "Effect of Aqueous and Hydrogen Environments on Fatigue Crack Growth in 2Ni-Cr-Mo-V Rotor Steel," Metal Science, Vol. 13, No. 7, pages 429-435, July 1979.

3-107. Birnbaum, H.K., "Hydrogen Related Failure Mechanisms in Metals," Environment-Sensitive Fracture of Engineering Materials, edited by Z.A. Foroullis, AIME, 1977.

3-108. Gangloft, R.P., and Wei, R.P. "Gaseous Hydrogen Embrittlement of High Strength Steels," Metallurgical Transactions A, Vol. 8A, No. 7, pages 1043-1053, July 1977.

3-109. Williams, D.P.,and Nelson, H.G., "Gaseous Hydrogen-Induced CRacking of Ti-5Al-2.5Sn," Metal Transactions, Vol. 3, No. 5, pages 2107-2113, May 1972.

3-110. Puls, M.P., Simpson, L.A., and Dutton, R., "Hydride-Induced Crack Growth in Zirconium Alloys," Fracture Problems and Solutions in the Energy Industry, Proceeding of the Fifth Canadian Fracture Conference, September 3-4, 1981, Pergamon Press, England, 1982.

3-111. Rau, C.A., Jr., Gemma, A.E., and Leverant, G.R., "Thermal-Mechanical Fatigue Crack Propagation in Nickel and Cobalt-Based Superalloys Under Various Strain-Temperature Cycles," Fatigue at Elevated Temperatures, ASTM Special Technical Publication 520, pages 166-178, 1973.

3-112. Stephenson, N., Memorandum No. M320, National Gas Turbine Est. Pyestock, Hants, England, June 1958.

3-113. Duquette, D.J., "A Mechanistic Understanding of the Effects of Environment on Fatigue Crack Initiation and Propagation," Environment-Sensitive Fracture of Engineering Materials, Metallurgical Society of AIME, pages 521-537, 1977.

3-114. Smith, H.H., Shahinian, P., and Achter, M.R., "Fatigue Crack Growth Rates in Type 316 Stainless Steel at Elevated Temperatures as a Function of Oxygen Pressure," Transactions of the Metallurgical Society of AIME, Vol. 245, page 947, 1969.

3-115. Wei, R.P., Simons, G.W., Hart, R.G., Pao, P.S., and Wei, T.W., "Fracture Mechanics and Surface Chemistry Studies of Fatigue Crack Growth in an Aluminum Alloy," to be published in the Metallurgical Transactions A.

3-116. Backlund, Blom, and Beevers, editors, Fatigue Thresholds, Engineering Materials Advisory Services, LTD., West Midlands, UK, 1982.

3-117. Ritchie, R.O., "Environmental Effects on Near-Threshold Fatigue Crack Propagation in Steels: A Re-Assessment," Fatigue Thresholds, edited by Backlund, Blom, and Beevers, Engineering Materials Advisor Services, LTD., West Midlands, UK, 1982.

3-118. Suresh, S., Zamiski, G.F., and Ritchie, R.O., "Oxide-Induced Crack Closure: An Explanation for Near-Threshold Corrosion Fatigue Crack Growth Behavior," Metallurgical Transactions A, Vol. 12A, No. 8, pages 1435-1443, August 1981.

3-119. Toplosky, J., and Ritchie, R.O., "On the Influence of Gaseous Hydrogen in Decelerating Fatigue Crack Growth Rates in Ultrahigh Strength Steels," Scripta Metallurgica, Vol. 15, No. 8, pages 905-908, August 1981.

3-120. Beevers, C.J., "Some Aspects of the Influence of Microstructure and Environment on ΔK Thresholds," Fatigue Thresholds-Fundamentals and Engineering Applications, Proceedings of the International Conference in Stockholm, June 1-3, 1981, EMAS, page 257, 1981.

3-121. For recent review see the conference proceedings: Hydrogen in Metals, The Metallurgical Society AIME, edited by I.M. Berstein and A.W. Thompson, 1974; Effect of Hydrogen on Behavior of Materials, AIME, New York, edited by A.W. Thompson and I.M. Berstein, 1976, 1980; Hydrogen in Metals, Pergamon Press, Oxford, England, 1978; Mechanisms of Environment Sensitive Cracking of Materials, The Metal Society, London, 1977.

3-122. Walter, R.J., Jewett, R.P., and Chandler, W.T., "On the Mechanism of Hydrogen-Environment Embrittlement of Iron- and Nickel-Based Alloys," Material Science and Engineering, Vol. 5, No. 2, pages 99-110, 1969/70.

3-123. Blackburn, M.J., and Smyrl, W.H., "Critical Review - Stress Corrosion and Hydrogen Embrittlement," Titanium Science and Technology, Vol. IV, edited by Jaffee and Burte, Plenum Press, New York, pages 2577-2609, 1973.

3-124. Nelson, H.G., "Kinetic and Mechanical Aspects of Hydrogen-Induced Failure in Metals," NASA, Washington, D.C., Report No. NASA TN-D-6691, 1972.

3-125. Wood, R.W., and Daniels, R.D., "The Influence of Hydrogen on the Tensile Properties of Columbium," Metal Society of AIME Transactions, Vol. 233, pages 898-903, May 1965.

3-126. Westlake, D.G., "Hydrogen Embrittlement: A Resistometric Study of Niobium (Columbium) - Hydrogen Alloys," Metal Society of AIME Transactions, Vol. 245, pages 287-292, February 1969.

3-127. Huber, O.J., Gates, J.E., Young, A.P., Pobersekin, M., and Frost, P.D., "Hydrogen Distribution in Heat-Treated Titanium as Established by Autoradiography," Journal of Metals, Transactions, AIME, Vol. 9, pages 918-923, July 1957.

3-128. Westlake, D.G., "A Generalized Model for Hydrogen Embrittlement," Transaction ASM, Vol. 62, pages 1000-1006, 1969.

3-129. Petch, N.J. and Stables, P., "Delayed Fracture of Metals Under Static Load," Nature, Vol. 169, pages 842-843, 1952.

3-130. Petch, N.J., "The Lowering of Fracture Stress Due to Surface Adsorption," Philosophical Magazine, 8th Series, Vol. 1, pages 331-337, 1956.

3-131. Troiano, A.R., "BISRA," The Iron and Steel Institute, Hamogate Conference, page 1, 1961.

3-132. Steigerwald, E.A., Schaller, F.W., and Troiano, A.R., "Role of Stress in Hydrogen Induced Delayed Failure," Transactions of the Metallurgical Society of AIME, Vol. 218, No. 5, pages 832-841, October 1960.

3-133. Oriani, R.A., and Josephic, P.H., "Equilibruim Aspects of Hydrogen-Induced Cracking of Steels," Acta Metallurgica, Vol. 22, No. 9, pages 1065-1074, September 1974.

3-134. Oriani, R.A., "A Decohesion Theory for Hydrogen-Induced Crack Propagation," Proceedings of the International Conference on Stress Corrosion Cracking and Hydrogen Embrittlement of Iron-Based Alloys, Unieux-Firming, pages 351-357, June 1973.

3-135. Oriani, R.A., and Josephic, P.H., "Equilibrium and Kinetic Studies of the Hydrogen-Induced Cracking of Steels," Acta Metallurgica, Vol. 25, No. 9, pages 979-988, September 1977.

3-136. Wells, C.H., "High Temperature Fatigue," Fatigue and Microstructure, Material Division ASM, 1979.

3-137. Vitek, V., "A Theory of the Initiation of Creep Crack Growth," International Journal of Fracture, Vol. 13, No. 1, pages 39-50, February 1977.

3-138. Riedel, H., "A Dugdale Model for Crack Opening and Crack Growth Under Creep Conditions," Materials Science and Engineering, Vol. 30, 1977.

3-139. Evans, J.T., "Time-Dependent Plastic Relaxation at a Crack Tip," Acta Metallurgica, Vol. 25, No. 7, pages 805-808, July 1977.

3-140. Wei, R.P., and Simmons, G.W., "Recent Progress in Understanding Environment-Assisted Fatigue Crack Growth," International Journal of Fracture, Vol. 17, No. 2, pages 235-247, 1981.

3-141. Ford, F.P., "Mechanisms of Environmental Cracking in Systems Peculiar to the Power Generation Industry," Electric Power Research Institute Report EPRI NP-2589, Palo Alto, California, September 1982.

3-142. Ford, F.P., "Mechanisms of Stress Corrosion Cracking," Aspects of Fracture Mechanics in Pressure Vessels and Piping, ASME-PVP-Vol. 58, pages 229-269, New York, 1982.

3-143. Chang, J.B., editor, Part-Through Crack Fatigue Life Prediction, ASTM Special Technical Publication 687, 1979.

3-144. Rudd, J.L., "Part-Through Crack Growth Predictions Using Compact Tension Crack Growth Rate Data," Part-Through Crack Fatigue Life Prediction, ASTM Special Technical Publication 687, pages 96-112, 1979.

3-145. Hudson, C.M., and Lewis, P.E., "NASA-Langley Research Center's Participation in a Round-Robin Comparison Between Some Current Crack-Propagation Prediction Methods," Part-Through Crack Fatigue Life Prediction, ASTM Special Technical Publication 687, pages 113-128, 1979.

3-146. Chang, J.B., "Assessment of the Sensitivity of Crack Growth Rate Constants to Predictive Accuracy of Part-Through Crack Fatigue Life Predictions," Part-Through Crack Fatigue Life Prediction, ASTM Special Technical Publication 687, pages 156-167, 1979.

3-147. Peterson, D.E., and Vroman, G.A., "Computer-Aided Fracture Mechanics Life Prediction Analysis," Part-Through Crack Fatigue Life Prediction, ASTM Special Technical Publication 687, pages 129-142, 1979.

3-148. Kobayashi, A.S., and Moss, W.L., "Stress Intensity Magnification Factors for Surface-Flawed Tension Plate and Notched Round Tension Bar," Proceedings of the Second International Conference on Fracture, Brighton, England, pages 31-45, 1969.

3-149. Masters, J.N., Engstrom, W.L., and Bixler, W.D., "Deep Flaws in Weldments of Aluminum and Titanium," NASA CR-134649, 1974.

3-150. Johnson, W.S., "Prediction of Constant Amplitude Fatigue Crack Propagation in Surface Flaws," Part-Through Crack Fatigue Life Prediction, ASTM Special Technical Publication 687, pages 143-155, 1979.

3-151. Scott, P.M., and Thorpe, T.W., "A Critical Review of Crack Tip Stress-Intensity Factors for Semi-Elliptical Cracks," Fatigue of Engineering Materials and Structures, Vol. 4, No. 4, pages 291-309, 1981.

3-152. Newman, J.C., Jr., "A Review and Assessment of the Stress-Intensity Factors for Surface Cracks," Part-Through Crack Fatigue Life Prediction, ASTM Special Technical Publication 687, pages 16-42, 1979.

3-153. Masters, J.N., Bixler, W.D., and Finger, R.W., "Fracture Characteristics of Structural Aerospace Alloys Containing Deep Surface Flaws," NASA CR-134587, 1973.

3-154. Darlaston, B.J.L., Connors, D.C., and Hellen, R.A.S., "Problems Identified in Quantifying Leak Before Break in Pressure Containing Structure," Fifth International Conference on Structural Mechanics in Reactor Technology, page F5.4, 1979.

3-155. Darlaston, B.J.L., and Harrison, R.P., "The Concept of Leak-Before-Break and Associated Safety Arguments for Pressure Vessels," Annual Conference of the Stress Analysis Group of the Institute of Physics, University of Sheffield, England, Sept. 14-16, 1976, Applied Science Publishers, England, pages 165-172, 1977.

3-156. Pettit, D.E., and Hoeppner, D.W., "Fatigue Flaw Growth and NDI Evaluation For Preventing Through Cracks in Spacecraft Tankage Structures," NASA CR-NAS9-11722 LR25387, 1972.

3-157. Bixler, W.D., "Fracture Control Method for Composite Tanks With Load Sharing Liners," NASA CR-134758, 1975.

3-158. Creager, M., "MSFC Crack Growth Analysis Computer Program, Version II User's Manual," NASA:MSFC, NASA CR-150153, 1976.

3-159. Bell, P.D., and Creager, M., "Crack Growth Analysis for Arbitrary Spectrum Loading," AFFDL-TR-74-129, Vol. 1, Final Report, June 1972 - October 1974.

3-160. Chang, J., Engle, R.M., and Szamossi, M., "Numerical Methods in Computer-Aided Fatigue Crack Growth Analysis," Proceedings of the Second International Conference on Numerical Methods in Fracture Mechanics, pages 631-643, July 1980.

3-161. Sih, G.C., "A Special Theory of Crack Propagation," Mechanics of Fracture, Vol. 1: Methods of Analysis and Solutions to Crack Problems, Noordhoff International Publishing, pages XXI-XLV, 1973.

3-162. Swedlow, J.L., "Criteria for Growth of the Angled Crack," Cracks and Fracture, ASTM Special Technical Publication 601, pages 506-521, 1976.

3-163. Fowler, G.F., "Fatigue Crack Initiation and Propagation in Pearlitic Rail Steels," Ph.D. dissertation, University of California, Los Angeles, 1976.

3-164. Parker, E.R., "Status of Ductile Ceramic Research," Properties of Crystalline Solids, ASTM Special Technical Publication 283, pages 40-65, 1961.

3-165. Kitajima, J., and Futagami, K., "Fractographic Studies on the Cleavage Fracture of Single Crystals of Iron," Electron Microfractography, ASTM Special Technical Publication 453, pages 33-59, 1969.

3-166. Forsyth, P.J.E., "Fatigue Damage and Crack Growth in Aluminum Alloys," Acta Metallurgica, Vol. 11, No. 7, pages 703-715, July 1963.

3-167. Lin, T.H., "Mechanics of a Fatigue Crack Nucleation Mechanism," Journal of the Mechanics and Physics of Solids, Vol. 17, pages 511-523, 1969.

3-168. Lin, T.H., "The Influence of Strain-Hardening and Grain Size on Early Fatigue Damage Based on a Micromechanics Theory," Journal of the Mechanics and Physics of Solids, Vol. 19, pages 31-38, 1971.

3-169. Sines, G., "The Prediction of Fatigue Fracture Under Combined Stresses at Stress Concentrations," Bulletin of the Japan Society for Mechanical Engineers, Vol. 4, No. 15, pages 443-453, 1961.

3-170. Sines, G., "Yielding and Plastic Instability Under Biaxial Stress in Design of Metal Pressure Vessels," Journal of Materials, Vol. 4, No. 2, pages 377-392, June 1969.

3-171. Low, J.R., Jr., "The Fracture of Metals," Progress in Materials Science, Vol. 12, No. 1, pages 1-96, 1963.

3-172. Hertzberg, R.W., and Mills, W.J., "Character of Fatigue Fracture Surface Micromorphology in the Ultra-Low Growth Rate Regime," Fractography-Microscopic Cracking Processes, ASTM Special Technical Publication 600, pages 220-234, 1976.

3-173. Beevers, C.J., Cooke, R.J., Knott, J.F., and Ritchie, R.O., "Some Considerations of the Influence of Subcritical Cleavage Growth During Fatigue-Crack Propagation in Steels," Metal Science, Vol. 9, pages 119-126, 1975.

3-174. Clark, W.G., Jr., "Subcritical Crack Growth and Its Effect Upon the Fatigue Characteristics of Structural Alloys," Engineering Fracture Mechanics, Vol. 1, pages 385-397, 1968.

3-175. Lindley, T.C., and Richards, C.E., "The Influence of Stress Intensity and Microstructure on Fatigue Crack Propagation in Ferritic Materials," RD-L-R 1804, Central Electricity Research Laboratories, Leatherhead, Surrey, England, July 1972.

3-176. Ewing, P.D., and Williams, J.G., "The Fracture of Spherical Shells Under Pressure and Circular Tubes with Angled Cracks in Torsion," International Journal of Fracture, Vol. 10, No. 4, pages 537-544, 1974.

3-177. Iida, S., and Kobayashi, A.S., "Crack-Propagation Rate in 7075-T6 Plates Under Cyclic Tensile and Transverse Shear Loadings," Journal of Basic Engineering, Transactions of the ASME, Series D, Vol. 91, No. 4, pages 765-769, December 1969.

3-178. Yokobori, T., Kamei, A., and Yokobori, A.T., "Fatigue Crack Propagation Under Mode II Loading," International Journal of Fracture, Vol. 12, pages 158-160, 1976.

3-179. Allison, D.E., "Fatigue Crack Propagation of Surface Flaw Rotated at Various Angles in a Biaxial Stress Field," M.S. Thesis, Pennsylvania State University, 1977.

3-180. Ewing, P.D., and Williams, J.G., "The Fracture of Spherical Shells under Pressure and Circular Tubes with Angled Cracks in Torsion," International Journal of Fracture, Vol. 10, No. 4, pages 537-544, December 1974.

3-181. Coughlan, J., and Barr, B.I.G., "Future Path Prediction," International Journal of Fracture, Vol. 10, pages 590-592, 1974.

Section 4

NONLINEAR FRACTURE MECHANICS

The increased use of tough materials in aerospace applications has led to a growing need for a means of accounting for nonlinear material behavior in the analysis of the subcritical and unstable growth of cracks. Linear elastic fracture mechanics (LEFM) concepts are often too conservative for predicting, or even bounding, the behavior of cracks in tough materials. Recently developed methods for including nonlinear material behavior (primarily plasticity) will be reviewed in this section. Attention will first be focussed on monotonically increasing load conditions, followed by consideration of cyclic plastic loading. This section will then conclude with a discussion of nonlinear structural response.

4.1 PLASTICITY UNDER MONOTONIC LOADING

Three main approaches are available for extending fracture mechanics beyond LEFM into regions of significant plasticity and which are sufficiently developed for ready engineering application. In addition, all three approaches provide, to a greater or lesser extent, methods for predicting instability under conditions where stable ductile tearing occurs. The main features of these three aproaches are briefly described below. The approaches are:

- J-integral estimation techniques, including extension to tearing instability.
- The design curve, originally developed at the Welding Institute, which utilizes a crack tip opening displacement.

The failure assessment diagram, originally developed at Central Electricity Generating Board, which incorporates a combination of LEFM and proximity of the net section to plastic collapse.

These procedures are aimed at defining loading and material property parameters that account for the reserve strength in materials beyond the initiation of a crack and for the transition between fully ductile and brittle modes of failure such as shown schematically in Figure 4-1. Each of the above approaches will be reviewed in the following portion of Section 4.1. A fourth approach has recently been suggested that holds promise of advancing nonlinear fracture mechanics and overcoming some of the current shortcomings. However, this approach, which is based on the T-integrals formulated by Atluri and his co-workers [4-1, 4-2], is in the early stages of development and will not be further discussed.

4.1.1 J-Integral Approaches

The J-integral proposed by Rice [4-3, 4-4] has emerged as an accepted parameter for predicting both crack initiation and stable extension, largely due to the experiments by Begley and Landes [4-5]. The J-integral concept was found to be applicable for either the occurance of small (contained) or large scale plasticity prior to fracture. More recent research by Battelle [4-6] and General Electric [4-7] under EPRI sponsorship [4-8] have further substantiated the applicability of the J-integral as a parameter than can predict plastic fracture.

The J-integral characterizes the crack tip singularity for nonlinear material behavior and is defined for two dimensional problems by a contour integral around the crack tip:

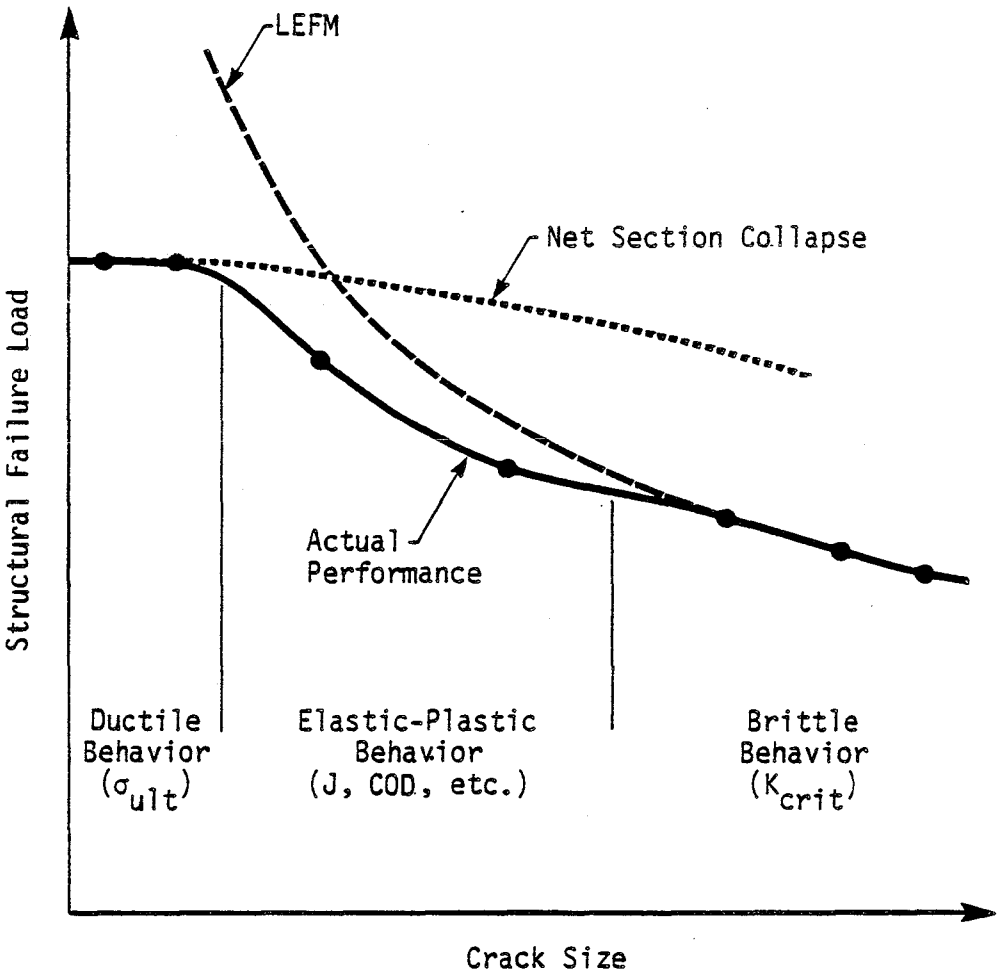

Figure 4-1. Schematic Representation of the Dependence of Failure Load on Crack Size.

$$J = \int_R W dy - T \cdot \frac{\partial u}{\partial x} ds \qquad (4\text{-}1)$$

where W is the strain energy density defined by

$$W = W(\varepsilon_{ij}) = \int_0^{\varepsilon_{ij}} \sigma_{pq} d\varepsilon_{pq} \qquad (4\text{-}2)$$

and R is any contour surrounding the crack tip, T is a traction vector defined by outward normal m along R, $T_i = \sigma_{ij} m_j$, u is the displacement vector, and s is arc length along R. For any elastic or elastic-plastic material treated by deformation theory of plasticity, Rice [4-4] has proven path independence of the J integral under monotonic loading. Other studies [4-9, 4-10] using incremental theory for finite element analysis also demonstrate an approximate path independence within the plastic region, although it is not clear that this prevails for contours immediately adjacent to the crack tip [4-11].

An alternate and equivalent interpretation [4-3] of J for elastic (linear or nonlinear) materials is that of a total strain energy difference for identically loaded configurations having neighboring crack sizes a and a + da. In particular

$$J = - \frac{\partial (U/B)}{\partial a} \qquad (4\text{-}3)$$

where U is the total strain energy, a is the crack length, and B is the specimen thickness.

The theoretical basis for use of J and the crack tip opening displacement as characterizing parameters derives from asymptotic crack-tip stress and strain field solutions. These are based on the work of Hutchinson [4-12] and Rice and Rosengren [4-13] and are referred to as the "HRR" field equations. For stationary cracks, they assume the form

$$\sigma_{ij} = \sigma_o \left(\frac{EJ}{\sigma_o^2 \, I_n r} \right)^{1/n+1} \tilde{\sigma}_{ij}(\theta, n) \tag{4-4}$$

$$\varepsilon_{ij} = \frac{\sigma_o}{E} \left(\frac{EJ}{\sigma_o^2 \, I_n r} \right)^{n/n+1} \tilde{\varepsilon}_{ij}(\theta, n) \tag{4-5}$$

where n and σ_o are the flow properties of a material described by the power law strain hardening exponent and yield stress, respectively ($\varepsilon \propto \sigma^n$); r and θ are polar coordinates centered at the crack-tip; I_n is an integration constant which is a function of n only; and $\tilde{\sigma}_{ij}$ and $\tilde{\varepsilon}_{ij}$ are dimensionless functions of θ and n only.

The above equations show that J is the amplitude of the crack tip singularity fields, thus the strain energy density, which is proportional to the product of stress and strain, has a 1/r singularity for the stationary crack (independently of the value of n). For power law hardening materials it can be shown that crack tip opening displacement δ is related to the J-integral by the following

$$\delta = d_n \frac{J}{\sigma_o} \tag{4-6}$$

where d_n is a function of the strain hardening exponent and the stress state (plane strain versus plane stress) and σ_o is the flow stress. Therefore, as described in more detail elsewhere, the crack tip opening displacement can be used as an analogous parameter for initiation of plastic fracture. For linear elastic materials J is identical to the elastic energy release rate G [4-2, 4-3]. Then the critical value of J (i.e. the crack initiation), J_{Ic} equals

$$J_{Ic} = \frac{K_{Ic}^2}{E'} \qquad (4\text{-}7)$$

where E' = E Young's modulus for plane stress, and $E' = E/(1-\nu^2)$ for plane strain, with ν denoting Poisson's ratio.

Crack growth initiation occurs when the applied value of J reaches the critical value, J_{Ic}. This is completely analogous to K and K_{Ic} for linear elastic materials, but provides an extension of the mechanics into the regime of nonlinear behavior. Once the applied value of J exceeds J_{Ic}, crack growth will begin to occur. However, such growth may not be sudden and catastrophic, because the material's resistance to crack extension can increase as the crack grows. If this resistance to crack growth increases faster (with increasing crack length) than the crack driving force (J-applied) then crack extension will remain stable. Hence, the use of J_{Ic} as a final failure criterion can be very conservative. Comparisons of crack growth resistance with applied driving force in analysis of crack instabilities is not restricted to elastic-plastic conditions. Such an approach is also applicable to nominally elastic conditions, in which case the stress intensity factor can be used as a measure of the driving force. Such procedures are referred to as the R-curve approach, which has found applicability for plane stress conditions.

The tearing instability theory of crack growth under elastic-plastic conditions has been devised to account for increasing material toughness with increasing crack extension [4-14]. The increased driving force required for crack extension can be measured experimentally with results such as shown in Figure 4-2 being obtained. Such results are referred to as J_R curves and are characteristic of the material. The slope of the J_R curve is called the tearing modulus, which is often idealized as being a constant once Δa exceeds some small amount.

Stable crack growth occurs when the applied value of the tearing modulus T [4-14], (which is proportional to dJ/da) is less than the material value of the tearing modulus obtained from the J_R resistance curve. The tearing modulus [4-14] is a dimensionless parameter proposed by Paris and co-workers characterizing stable crack growth using the J-resistance curve and given by

$$T = \frac{dJ}{da} \quad \frac{E}{\sigma_o^2} \tag{4-8}$$

where E is Young's modulus and σ_o is the material flow strength. There are size requirements for this theory to be valid. The first of these conditions requires that the amount of crack growth Δa be small compared to the characteristic radius R of the Hutchinson-Rice-Rosengren (HRR) singularity. The second condition requires that the ratio of J_{Ic} to the slope of the J_R curve be small compared to R. The two conditions are expressed as

$$\Delta a \ll R$$

$$\frac{J_{Ic}}{\frac{dJ}{da} R} \ll R \tag{4-9}$$

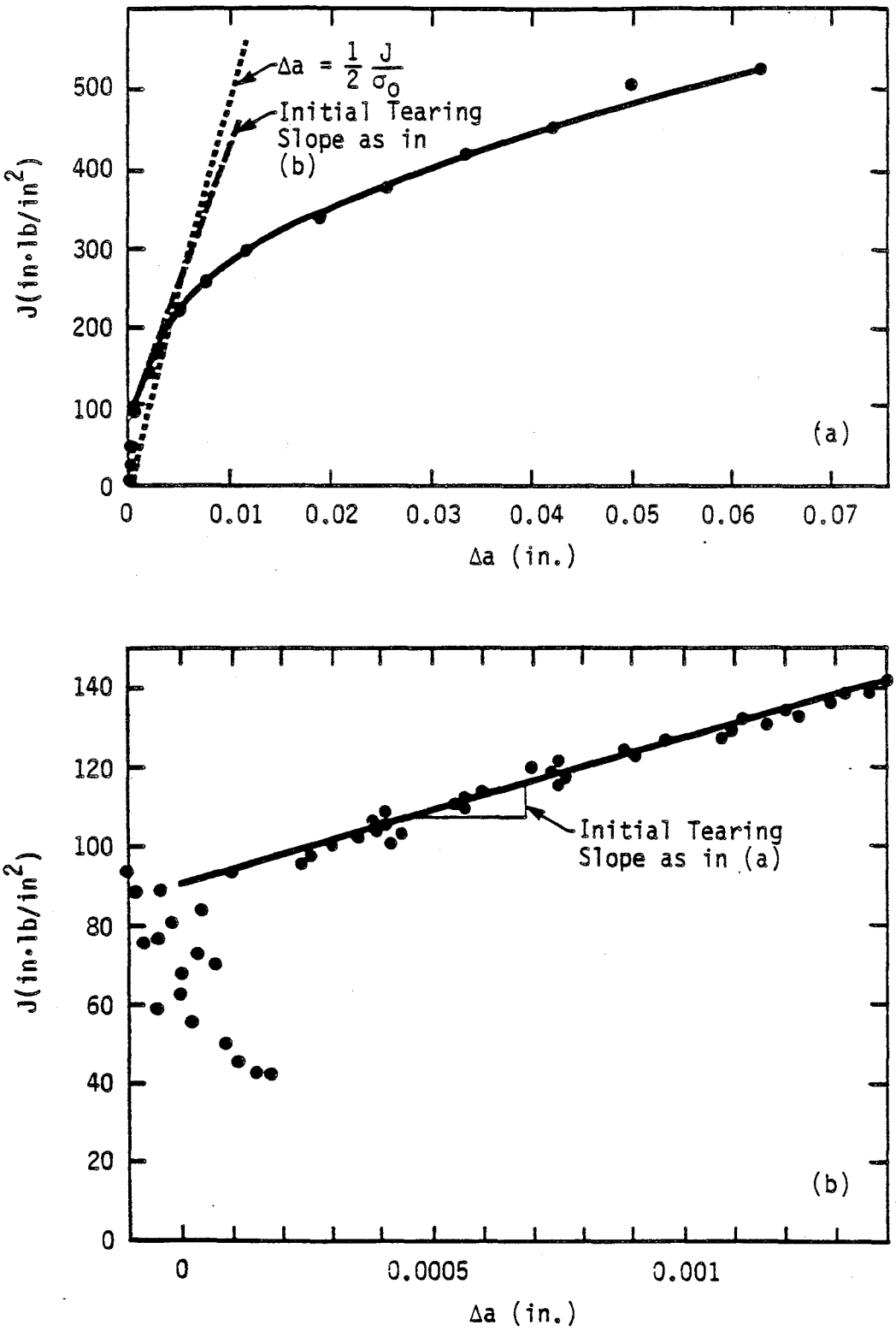

Figure 4-2. R-Curve for 5083 Aluminum Alloy: (a) Large Scale, (b) Small Scale [4-15].

A study of these conditions for problems involving bending loads showed that the above conditions can be expressed as

$$\Delta a < 0.6\, b$$

$$\omega = \frac{b}{J_{Ic}} (dJ_R/da) > 10 \qquad (4\text{-}10)$$

where b is the remaining ligament in the bend configuration. In addition, the ligament has to satisfy the condition

$$\rho = \frac{b}{(J_R/\sigma_o)} > 25 \qquad (4\text{-}11)$$

where J_R is the current value of J on the J-resistance curve.

The principle of J-controlled growth further requires that there be sufficient plane strain constraint. This can be met for bending problems by requiring the effective configuration width B to be sufficiently large; i.e.,

$$B > b \qquad (4\text{-}12)$$

The J-integral can be evaluated experimentally or be computed for contained or small scale plasticity by the formula that relates J or the strain energy release rate to the stress intensity factor (see Equation 4-7). With small amount of plasticity contained about the crack, the Irwin plastic zone correction can be used to approximately account for plasticity. An effective crack length is determined by adding a correction r_y to the actual crack size a. That is, [4-16]

$$a_{eff} = a + r_y \qquad (4\text{-}13)$$

where

$$r_y = \frac{1}{2\pi}\left(\frac{K}{\sigma_y}\right)^2 \qquad \text{for plane stress} \qquad (4\text{-}14)$$

$$r_y = \frac{1}{6\pi}\left(\frac{K}{\sigma_y}\right)^2 \qquad \text{for plane strain} \qquad (4\text{-}15)$$

and σ_y = yield stress.

Other techniques for determining the J-integral are the η factor [4-17], and the stiffness gradient methods used by Derbalian [4-18].

In the η factor method [4-17] of fracture analysis, the J-integral is defined to be proportional to the sum of an elastic $\eta_{e\ell}$ factor times the elastic work plus a plastic $\eta_{p\ell}$ times the plastic work. Specifically:

$$J = (\eta_{e\ell} W_{e\ell} + \eta_{p\ell} W_{p\ell})/Bb \qquad (4\text{-}16)$$

where b is the uncracked ligament width, and B is the thickness. In linear fracture mechanics this expression provides an exact relationship between the energy release rate, G, and the elastic work done, $W_{e\ell}$, in the form [4-19]

$$G = \eta_{e\ell} W_{e\ell}/Bb \qquad (4\text{-}17)$$

and

$$\eta_{e\ell} = \frac{b}{\phi}\frac{d\phi}{da} \qquad (4\text{-}18)$$

where ϕ is the compliance of the system.

The $\eta_{p\ell}$ term can be evaluated for plastic limit conditions and for simple geometries, such as deeply notched members in bending or tension. In such

cases $\eta_{p\ell} = 1$ for tension and 2 for the case of bending. Paris, et al., [4-20] provides additional discussion.

More recently, the J-integral for elastic-plastic loading has been defined [4-17, 4-21] in terms of a single combined η_o factor times the total work:

$$J = \eta_o W_t / Bb \tag{4-19}$$

This definition also bears resemblance to Derbalian's approximate J estimation method [4-18], whereby the J-integral is defined by:

$$J = -\frac{1}{B}\frac{1}{k}\frac{\partial k}{\partial a} W_t \tag{4-20}$$

Here k is the <u>elastic</u> stiffness (force per unit displacement) that depends on the crack length but not on the load. Since both the η factor method and the stiffness-gradient method of Derbalian are exact for linear load displacement situation, the combined η_o factor must degenerate to the elastic $\eta_{e\ell}$ factor, η_o is then related to stiffness-gradient method for linear elasticity by

$$\eta_o = -\frac{b}{k}\frac{dk}{da} \tag{4-21}$$

Conversely, the stiffness can be derived in terms of the η factor by solving the above first order differential equation* [4-22]

$$k = c \exp\left(-\int \frac{\eta}{b}\, da\right) \qquad (4\text{-}22)$$

where c is a constant.

The combined η_0 factor method and equivalently the stiffness-gradient methods are found to give good approximations for J for the 3 point bend specimen. Turner's finite element computation in plane strain indicates that η is nearly constant for several different crack sizes over a wide range of loading.

Qualitatively, the stiffness-gradient and η-factor methods provide good approximations to J for deep cracks where the plastic zone lies ahead of the crack. For these cases, Turner claims that η is approximately equal to 2 for bending and 1 for tension.

If the yield zone spreads away from the process zone near the notch, this would radically affect the relationship between the notch stress intensification as measured by J_I and the overall work. Therefore, the single η_0 approximation becomes less accurate in this instance. A practical way of examining if the stiffness-gradient method for a given problem is applicable is the shape of the global load-displacement relationship. If the force-displacement curves of two similarly cracked specimens, with crack lengths a

*Note that the total derivative was used in Equation 4-21 because the elastic stiffness k depends only on the configuration (i.e., crack length a).

and $a + \Delta a$, defined by f_1 and f_2 respectively, are such that the ratio f_1/f_2 remains constant then the stiffness gradient method becomes exact. Mathematically this means that the force is a separable function H of crack size and P of displacement, that is

$$F = H(a)P(\delta) \tag{4-23}$$

The stiffness-gradient method is shown to be exact if the global force-displacement curve is linear as well as in the situation of a rigid-plastic force displacement [4-17]. In many cases of contained yielding the force displacement curve remains linear in spite of appreciable local yielding. Then the stiffness-gradient method is exact in those situations.

Paris and co-workers [4-20] have concluded that for a power hardening material Ilyushin's theorem [4-23] may be invoked to show the conditions for existence of $n_{p\ell}$ for 2D crack configurations.

For fully plastic solutions General Electric [4-24] has developed a handbook of J-integral values for different crack geometries. This handbook contains fully plastic solutions based upon deformation plasticity for fracture mechanics specimens. A finite element deformation plasticity computer program developed by Needleman and Shih [4-25] was used to generate these fully plastic solutions. If a material can be represented by deformation plasticity theory and a power law hardening model, Ilyushin's principle [4-23] can be used to show that the resulting plasticity solutions are scaleable. Simple expressions for the J-integral can then be written in terms of the strain hardening exponent. By utilizing the functional forms of both the

fully plastic solution and the linear elastic solution, Shih and Hutchinson [4-26] first showed that a simple approximate estimate for the complete range of applied stress and strain on a structure can be formulated in terms of the total J-integral, which can be written as:

$$J = J^e(a_{eff}, P) + J^P(a,P,n) \qquad (4\text{-}23)$$

where J^e is the elastic contribution based on Irwin's plasticity adjusted crack length (a_{eff}) and J^P is the deformation plasticity solution in terms of the J-integral. J^e is available from elastic fracture handbooks and J^P for selected geometries is provided by Reference 4-24.

The estimation scheme of Shih and Hutchinson can be used to predict both the onset of crack growth and instability using the resistance curve approach [4-27], where:

$$J(a,P) = J_R(\Delta a) \qquad (4\text{-}24)$$

and $a = a_o + (\Delta a)$ is the current crack length and P is the remote, applied load. $J_R(\Delta a)$ is the crack growth resistance of the material, and J(a,P) the crack-driving force, if given by Equation 4-23.

Finally, for complicated geometries or those for which no prior J solution has been determined, the finite element analysis can be used that will directly compute J by methods such as the virtual crack extension of Parks [4-28].

4.1.2 Design Curve Approach

The design curve approach was originally developed at the Welding Institute in England using crack tip opening displacement (COD or CTOD) [4-29 through 4-32]. This approach is based on a curve of the type shown in Figure 4-3. This curve relates CTOD to the far-field applied stress or strain and the defect size. A critical value of CTOD for the material can be determined from experiments on testpieces, in accordance with the relevant British Standard [4-33]. This critical value of CTOD may be the value for crack initiation in the testpiece or may be the value of CTOD at maximum load (i.e. instability in load control). When the applied stress or strain in the structure exceeds that given by the design curve (for the critical CTOD for that material and thickness, and the particular defect dimensions), the structure is predicted to fail. Thus the curve can be used to define the maximum allowable stress or strain, or the critical defect size.

The design curve approach has been extended and formalized as a British Standards Institution Published Document [4-34] (note that issuance as a "Published Document" indicates that it does not have the status of a standard). This document presents the design curve (in equation rather than in graphical form) as part of an overall approach to determining acceptance levels for weld defects, including LEFM calculations for lower net section stress levels and for fatigue crack growth. It even includes limited material dealing with buckling, creep and other failure modes. The document is arranged to guide the user step by step through the assessment method and the approach is therefore straightforward to use. The analysis required is limited. The main experimentally-determined parameter needed to use the design curve portion of

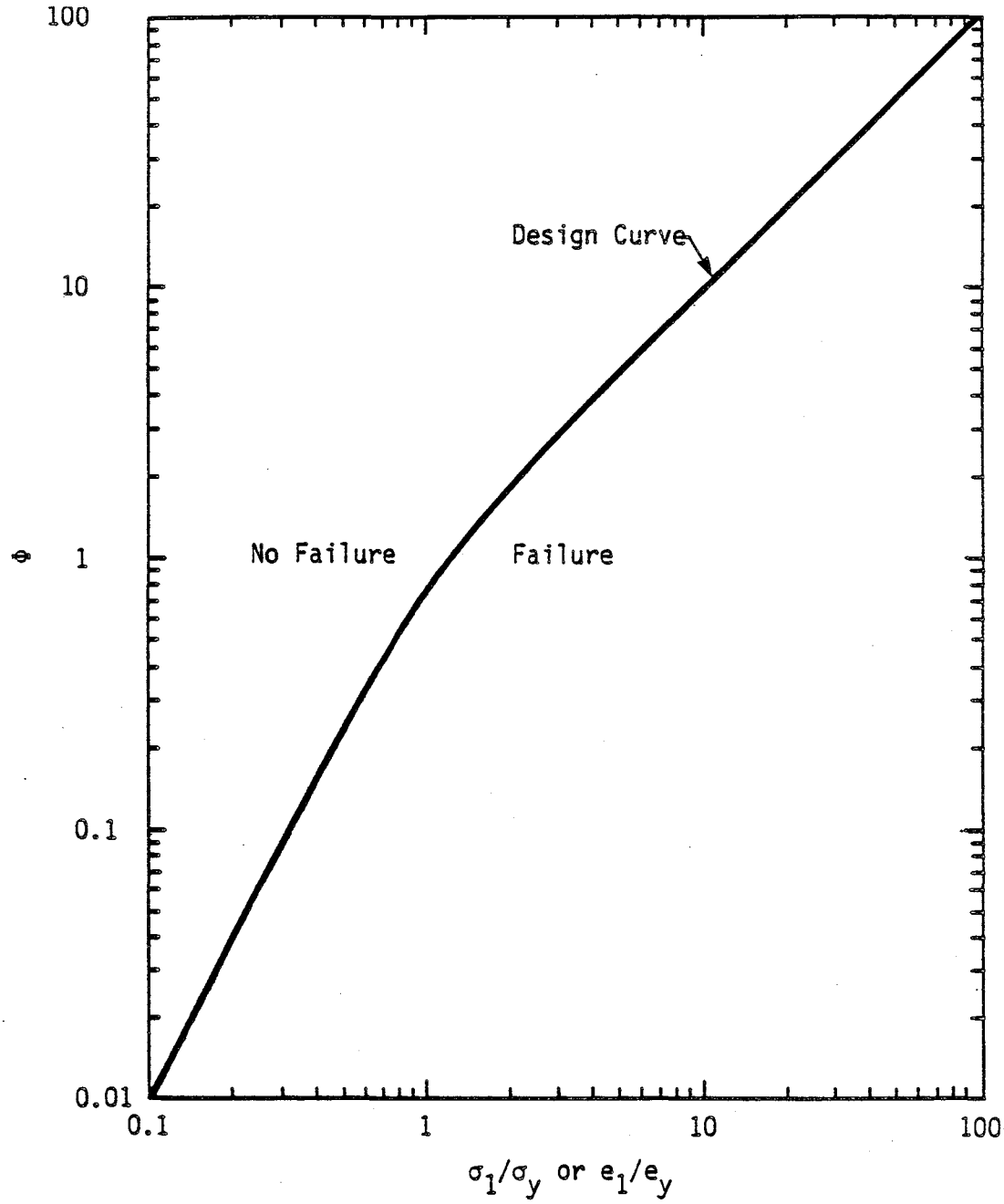

Φ is the "Non-Dimensional COD" = $\frac{\delta_c}{2\pi e_y \bar{a}}$

Where δ_c = Critical COD for the Material and Thickness

e_y = Yield Strain

$\bar{a}$ = Defect Dimension

Figure 4-3. CTOD Design Curve.

the document is a critical value of CTOD. Measurement of CTOD at maximum load is in general considerably easier and cheaper than measuring K_{IC}. Furthermore the approach can take into account residual stresses.

Stable ductile tearing can be taken into account by use of maximum load values of CTOD rather than using critical CTOD values measured at crack initiation. In ductile materials some considerable (but normally not measured) amount of stable crack growth will have occurred by the point of maximum load. Using maximum load CTOD, instead of initiation CTOD, allows this ductile tearing to be taken into account, at least in an approximate manner. Recent work at the Welding Institute has justified the use of maximum load CTOD with the design curve as conservative for assessing defect tolerability in applications showing fully ductile behavior [4-35, 4-36].

As noted above, the design curve approach requires only limited analysis and a readily-measured experimental parameter. It does however have significant disadvantages. The original design curve was based on a theoretical analysis by Burdekin and Stone [4-37]. However the experimental results proved a very poor fit to this analysis, see e.g. Reference 4-38, and the current design curve is essentially empirical. Even for this present curve the agreement with experiment is not close, with experimental results scattered over a significant range [4-38] (although some of the scatter there is a result of using differing definitions of the point of measurement of critical CTOD, uncertainty in residual stress values etc.). The approach in [4-34] yields "tolerable" defect sizes not critical defect sizes. These "tolerable" defect sizes include safety factors on defect dimension which are not generally explicit and can range from two to well over 20 [4-39]. The

results can be very over-conservative therefore. Another problem is that the amount of tearing and the degree of conservatism inherent in using maximum load CTOD to account for stable crack growth are also not explicit. To date, the approach has only been validated for ferritic steels, although there is no reason to believe that it is not valid for other materials.

For many applications the ease of use and comprehensive coverage of the approach are strong recommendations. It is less attractive when there are significant penalties associated with conservative design, because of e.g. increases in weight or in thermal stresses, or where resouces are available to provide more detailed analysis.

Turner [4-40, 4-41] has recently defined a J design curve approach using a parameter he refers to as EnJ (engineering J). This approach has yet to be validated experimentally. However, in its early form, a comparison with CTOD design curve methods and with the Failure Assessment Diagram (described in more detail below) indicated some similarity between all approaches when the different assumptions and recommendations were unified [4-42].

4.1.3 Failure Assessment Diagram

The Failure Assessment Diagram, originally developed at the Central Electricity Generating Board in England [4-43], is based on earlier work by Dowling and Townley [4-44]. This approach uses the LEFM stress intensity factor K and allows for plasticity effects by incorporating a factor based on the proximity of the net ligament to plastic collapse. Recently this approach has been validated by comparison with more rigorous J integral analyses, and

extended in a number of ways, by workers at General Electric and Babcock and Wilcox [4-24, 4-45].

Figure 4-4 presents the failure assessment diagram. On one axis are values of K_r, where

$$K_r = \frac{K_{applied}}{K_{Ic}}$$

On the other axis are values of S_r, where

$$S_r = \frac{\text{Applied load}}{\text{Plastic collapse load}}$$

Thus one axis represents pure LEFM and the other axis represents plastic collapse. The essence of the diagram is the interpolation between these two regimes. The interpolation curve was obtained from the Dugdale solution for the plane stress problem of a finite crack in an infinite sheet of elastic-perfectly plastic material. Any K_r, S_r point that lies within the region bounded by the curve is "safe". Points outside the curve may lead to failure. Methods for using the curve have been formalised and laid out for easy application in Reference 4-43. Where there are no secondary stresses (e.g. residual or thermal stresses), $K_{applied}$ is calculated using LEFM only, without it even being necessary to incorporate plastic zone correction factors. If secondary stresses are present then the analysis is somewhat more complex. Even then, however, the analysis is essentially straightforward. If a K_{IC} value is not available then it may be calculated from measurements of critical J or COD at crack initiation.

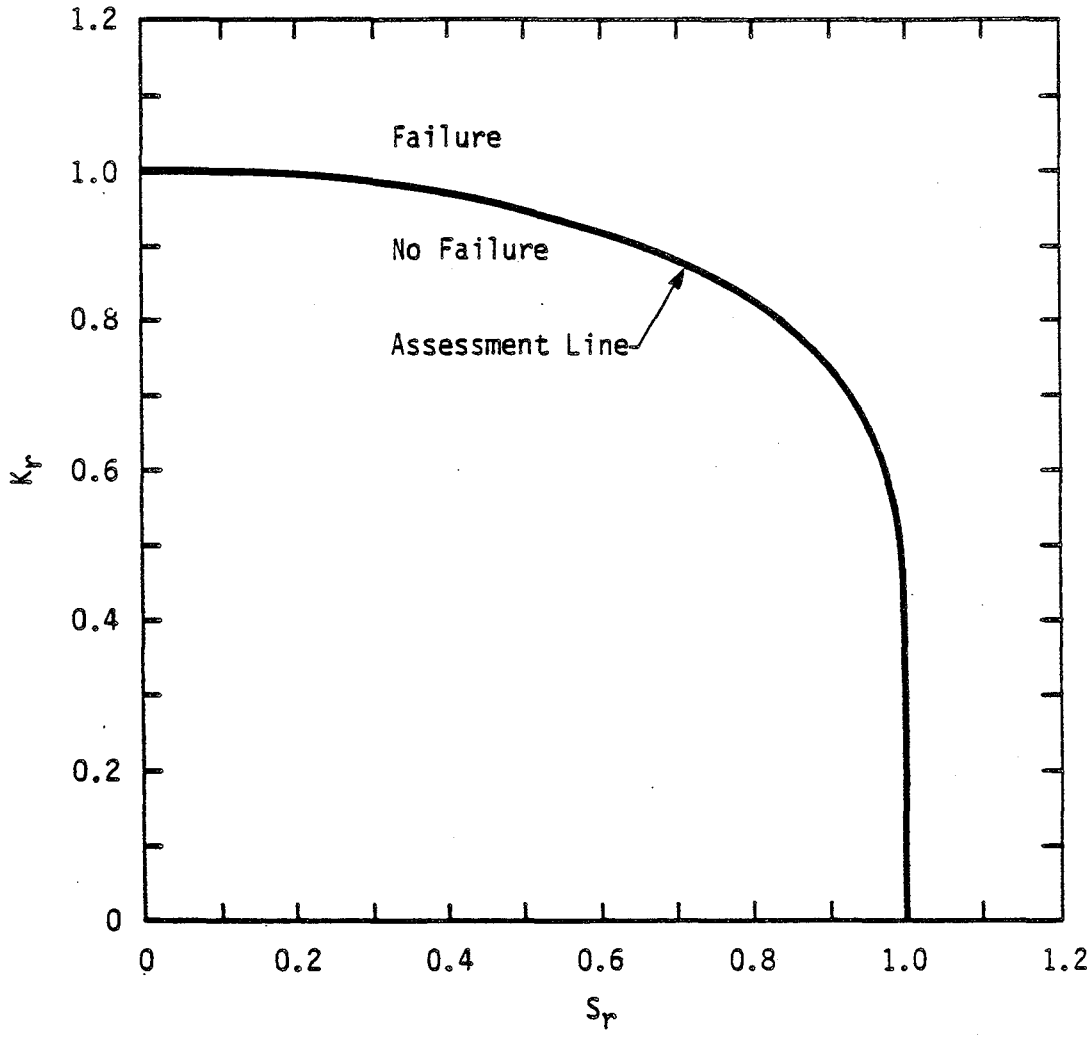

Figure 4-4. The Failure Assessment Diagram.

The Dugdale solution on which the FAD curve is based contains simplifications (e.g., assuming elastic-perfectly plastic material in infinite sheets). Bloom, and Shih and co-workers, compared the FAD curve with those obtained using a considerably more rigorous derivation, finite element analysis with a J integral fracture criterion [4-46 through 4-48]. The resulting curve shows some dependency on the geometry of the cracked body, the type of loading and the material work hardening properties. However the FAD is remarkably close to the curves and generally forms a lower bound on them. If greater accuracy is desired, particularly for strongly work hardening material, then it may be desirable to use the curves given in References 4-46 through 4-48. For most applications however the original FAD curve should be adequate. In Reference 4-49 the curve is compared with numerous experimental results on a variety of steels. With the exception of two failure points which fall just inside the curve, and which are stated in Reference 4-49 to be unreliable, all experimental failure points fall on the "failure" side of the curve. Significant scatter is evident, typically corresponding to a safety factor between 1 and 3 on defect size, and in a few cases more.

The scatter mentioned above is probably due, at least in part, to stable crack growth prior to failure. Reference 4-24 describes how the effect of stable crack growth can be taken into account by using the K or J resistance curve for the material. After each increment of crack growth the value of K_r is calculated taking account of the increased toughness with crack extension. S_r is also calculated using the new ligament, and a new point plotted. This procedure is repeated for further increments of crack growth. The crack growth behavior can thus be evaluated. Experimental use of this approach is reviewed in Reference 4-50. The procedure is shown to work satisfactorily for

materials with low to moderate strain hardening, but less well for materials with higher strain hardening. Overall, the failure analysis diagram is relatively easy to use without a great sacrifice in accuracy of predictions.

4.2 CRACK GROWTH DURING CYCLIC PLASTICITY

The application of fracture mechanics to fatigue crack growth, as discussed in Section 3, was based on linear elastic fracture mechanics. Therefore, such procedures are applicable only when the plastic zone at the crack tip is small relative to the crack size or remaining ligament. This is not always the case. Instances where net section yielding occurs during cyclic loading is an obvious case where nonlinear effects are important in fatigue crack growth. Another case is small cracks near notches where a plastic zone near the notch root is produced by the stress concentrating nature of the notch. Figure 4-5 shows a fatigue crack in the region of plasticity associated with a notch. The crack length, a, is of the same order of magnitude as the notch root radius, ρ. The local stress concentration effect may be large and cannot be evaluated by linear elasticity due to the fact that the plastic zone r_y is not small compared to other significant dimensions ρ and a. However, if the crack grows to a length that is large compared to the root radius of the notch, such that the crack tip plastic zone becomes small compared to the remaining ligament, b, and the effective crack length, than the elastic fracture mechanics techniques become valid. Other investigators who have studied FCGR behavior above the power law region of the FCGR-LEFM curve ($da/dn = C\Delta K^m$) have noted that FCGR behavior is not always uniquely related to the LEFM driving parameter. Frost, et al. [4-51] have presented previously published fatigue crack growth rate data as a function of ΔK, which

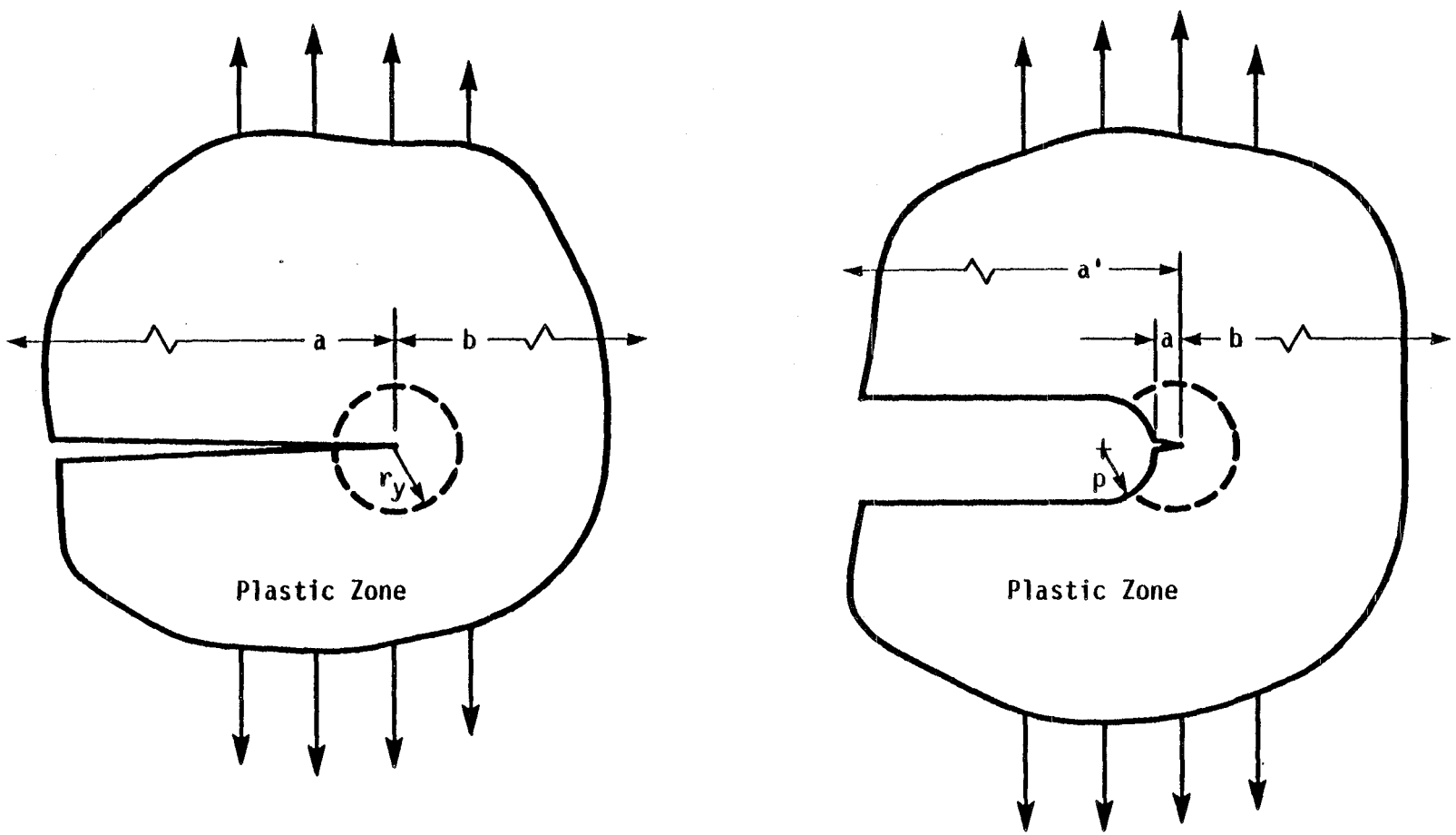

(a) Plastic Zone Small Compared to Both Crack Length and Ligament.

(b) Fatigue Crack in a Region of Plasticity Associated with a Notch.

Figure 4-5. Relative Dimensions Governing the Applicability of Linear Elastic Fracture Mechanics.

demonstrates that the maximum applied stress or net section stress will influence the fatigue crack growth rate behavior in the high fatigue crack growth rate region for some but not all metals studied. Similar conclusions were given by Dubensky [4-52] in his analysis of 7075 and 2024 aluminum alloys in the high FCGR region. Frost, et al. [4-51] attempted to qualify the usefulness of LEFM by studying a limit on the plastic zone size r_y in a center crack, CC, or edge crack, EC, test specimen.

$$r_y = \frac{1}{2\pi}\left(\frac{K_{max}}{\sigma_0}\right)^2 \leq \frac{a}{7} \qquad (4\text{-}25)$$

where σ_0 is the yield strength and a is the half crack length in the CC specimen and the crack length in the EC specimen. The correlation of FCGR with the single LEFM parameter appears to fail for those conditions in which the crack is either propagating into or through a zone of gross plastic yielding. When a crack is propagating through a material experiencing net section yielding, material ratcheting will further increase the levels of crack tip stress fields above that predicted by LEFM. In these cases, the crack no longer generates an elastic stress field which contains and controls the cycling behavior of the nonlinear material at the tip of the crack. To better describe FCGR response under loading conditions which induce nonlinear material behavior, investigators have suggested the use of elastic-plastic fracture mechanics parameters. These parameters are based on either the field approach or the crack tip approach. The field approach is similar to that of the LEFM in that a parameter is used such as the J integral measuring the elastic-plastic stress or strain field at the tip of the crack. The crack tip approach is based on directly computing the parameter at the crack tip which

is suspected of controlling the crack growth behavior. These include the near tip strain, crack tip opening displacement (CTOD), crack tip opening angle (CTOA), crack opening angle (COA), crack tip nodal force, and others based on energy, such as crack separation energy rate G_Δ, change in energy rate in process zone G_p, generalized energy release rate at the process zone, G which is equal to $G_\Delta + G_p$.

The J-integral has been used with success by Dowling and Begley [4-53] to relate fatigue crack growth rate to ΔJ. As described earlier, the J integral is defined for deformation plasticity and is path independent. In a review of Dowling and Begley's results obtained on compact type specimens, Parks [4-54] observed that objections to the operational use of the parameter ΔJ can be rationalized if one notes the fact that stable hysteresis (microscopic load displacements) are nearly symmetrical for reversed stressing. This observation implies that most material points have seen fully reversed loading (i.e., zero mean deviatoric stressing). The stable hysteresis loop hypothesis leads to a strain energy function W* approach such that $\Delta\sigma = \frac{\partial W^*}{\partial \Delta\varepsilon} = \Delta\sigma(\Delta\varepsilon)$ exists for all material points in the crack tip region. Much of the current research in modeling high fatigue crack growth rate behavior utilizes the assumption that the HRR equations are applicable to quasi-static moving cracks. Paris [4-55] has suggested an argument to justify J integral for FCGR studies based on the following logic. "For high rates of growth, the crack tip moves ahead during each cycle into relatively new material in terms of plastic deformation compared to the intense deformation it will sustain at the crack tip during the next cycle. Thus, during the next cycle, past history will not be significant compared to the loading which is then being sustained. As long as a moving crack is considered it may be possible to neglect past history including

unloading in a J integral analysis and characterization of material behavior." Rice [4-56] suggests that a crack tip integral similar to J can be defined for cyclic loadings if the alteration $\Delta\sigma_{ij}$ of stress (i.e., the stress range) following any load maximum or minimum is related to the corresponding alteration of strain $\Delta\varepsilon_{ij}$. Dowling's experiments showed excellent correlation between cyclic J and fatigue crack growth rates for the tests under deflection control. The test data fell near a single straight line for all six different specimens. Test results were obtained over approximately two orders of magnitude in crack growth rate. Thus, over a range of crack lengths in the single specimen geometry tested, the cyclic J criterion is independent of crack length. The data for tests under load control show significant deviation from the straight line behavior observed in the displacement control tests. Above a certain ΔJ value, crack growth rates increase without further increase in ΔJ. This behavior is related to the unstable increase in crack growth rate observed at the end of linear elastic crack growth tests on ductile materials. The ΔJ values determined differed significantly from the elastic strain energy release rate $G = K^2/E$ whenever appreciable plastic flow occurred. The effect of incremental plasticity should be viewed as an effect on mean J analogous to the effect of mean K in linear fracture mechanics. The crack growth behavior is then caused by an increasing mean J while ΔJ remains approximately constant. It is not surprising that, just as in linear elastic fracture mechanics, the range and the mean value of the controlling parameter must be known to predict the fatigue crack growth rate. Dowling and Begley conclude that microscopic crack closure during gross plasticity is an important effect and significantly influences the fatigue crack growth rate. Also, crack growth rates during incremental plastic deflection cannot be predicted by ΔJ

criterion alone and more general criteria that include the effect of the mean J level are needed.

More recent analyses by Dowling [4-57 through 4-58] and Brose and Dowling [4-59] do further confirm the validity of representing fatigue crack growth in terms of ΔJ. Fatigue data were collected from test results conducted on compact tension (CT) and center cracked panels (CC) of varying widths using A533 and 304SS materials. A plot of da/dn versus ΔJ is shown in Figure 4-6 for A533B CC specimens that Dowling and Begley [4-53] tested under displacement control. Values of ΔJ were experimentally determined from load-displacement records measured during cyclic loading. A least squares fit through the data of Figure 4-6 has the following equation

$$\frac{da}{dn} = 2.13 \times 10^{-8} (\Delta J)^{1.587}$$

Sadananda and Shahinian [4-60] have also conducted cyclic J-integral FCGR testing on Udimet 700 at high temperature and similarly concluded the validity of representing FCGR in terms of ΔJ. They have also shown that FCGR can be correlated by $\Delta J.E$ for cold worked type 316 SS at high temperature [4-61].

Besuner and Rau [4-62] have recently addressed the solution of a significant class of problems which are characterized by a state of "constrained or contained" plasticity. In such problems the plastic stress redistribution resulting from some significant geometrical feature, like a notch, or load component is constrained by the primarily elastic structure. However, the redistribution has a substantial effect on the subcritical growth rate of

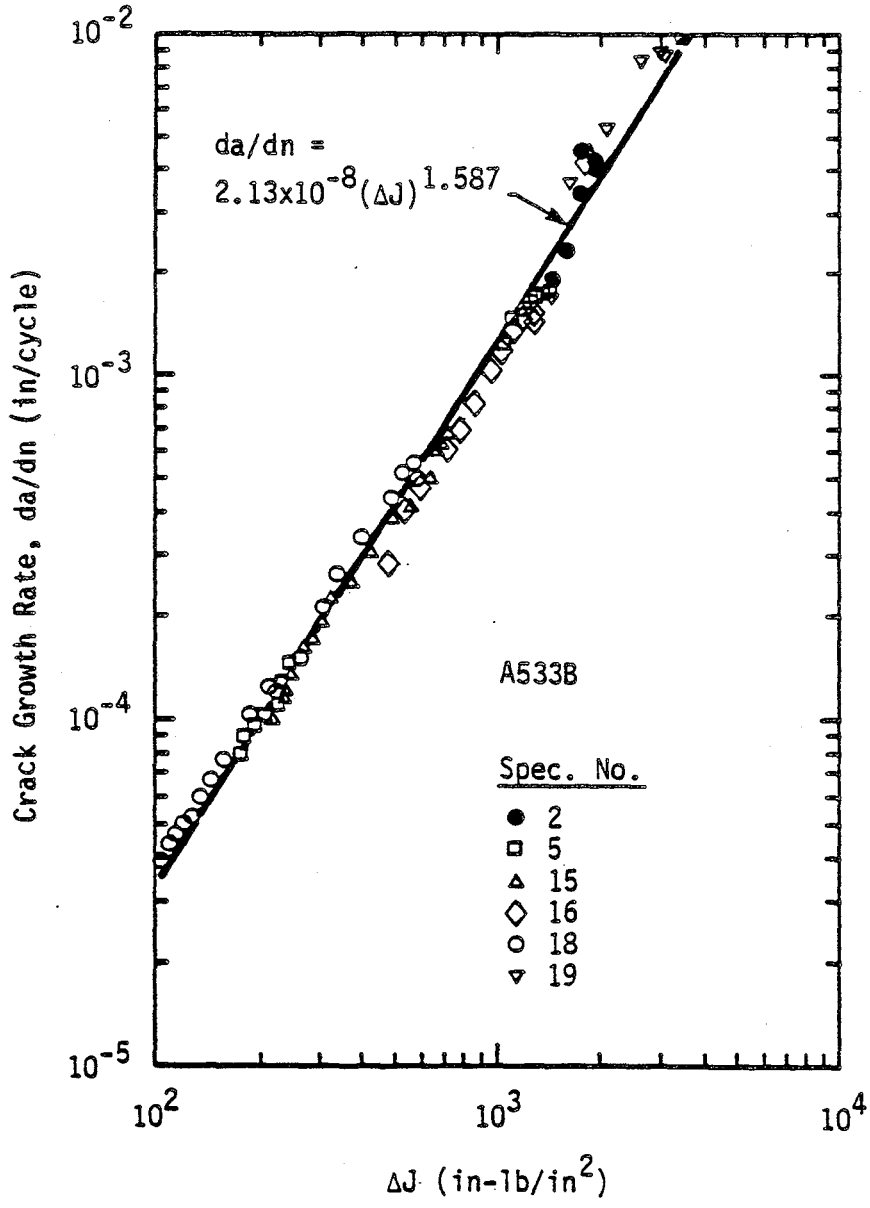

Figure 4-6. Fatigue Crack Growth Rate as a Function of J for Deflection Control [4-53].

cracks introduced or extended after the stress field "shakes down" to either an elastic state or a stable hysteresis loop.

A stress analysis technique has been developed for application to sub-critical crack growth problems. The technique has been programmed, documented in detail [4-62], and incorporated into the fracture mechanics program BIGIF [4-63]. This program performs rapid and accurate analysis of certain contained plasticity problems by computing the plastic redistribution of stress from a simple set of implicit equations, thereby eliminating the need for elastic-plastic finite element analysis. The technique is based on Neuber's rule [4-64].

The model for load-controlled problems satisfies the following conditions along a line perpendicular to the surface at the crack origin: 1) Neuber's rule [4-64] for elastic-plastic stress concentration factors; 2) The uniaxial stress-strain curve for the material as expressed by Ramberg-Osgood [4-65]; and 3) Force equilibrium in the "y-direction" perpendicular to the xz crack plane; defined by the line integral:

$$\int_L \sigma_{elas\text{-}plas}(x)dx = \int_L \sigma_{elas}(x)dx$$

Since satisfaction of the above three conditions does not provide a unique solution, a scheme for load redistribution must be specified. As described in [4-62], the $\sigma_{elas\text{-}plas}(x)$ solution is not heavily dependent upon which of several investigated schemes are employed.

A major feature of the model is the inclusion of all principal stress components in the shear-free crack plane. This was accomplished by the

iterative procedure outlined below: 1) Elastic values of σ_x and σ_y (and, for plane strain, $\sigma_z = \nu(\sigma_x + \sigma_y)$) are used to compute the effective uniaxial elastic stress σ_{elas} from the Von Mises yield condition; 2) Using this value of σ_{elas}, the equivalent uniaxial plastic stress $\bar{\sigma}$ is obtained from a relation derived by combining the Neuber and Ramberg-Osgood equations

$$\bar{\sigma}^2 + K \frac{\bar{\sigma}^{(n+1)}}{\sigma_{yield}^{(n-1)}} - \sigma_{elas}^2 = 0$$

where the values K, n, and σ_{yield} are curve-fitting coefficients for the stress-strain data for the material. For a monotonic loading, σ_{yield} is chosen only to provide an optimum curve fit and does not coincide with any particular yield-stress definition. For complex load reversal histories, best results are obtained by defining σ_{yield} as the stress needed to cause only 0.01% plastic strain; 3) For plane strain conditions, the value of $\bar{\sigma}$ is used to determine an effective Poisson's ratio (ν_{eff}) based on a weighted average of the elastic and plastic strains computed from the Ramberg-Osgood stress-strain relation

$$\varepsilon_{tot} = \frac{\bar{\sigma}}{E} \text{ (elastic part)} + K \frac{\sigma_{yield}}{E} \left(\frac{\bar{\sigma}}{\sigma_{yield}} \right)^n \text{ (plastic part)}$$

4) The value of ν_{eff} and $\bar{\sigma}$ are used as initial values in an iterative solution. The through-thickness stress σ_z is estimated by:

$$\sigma_z = \nu_{eff} (\sigma_x + \sigma_y)$$

and 5) A new value of σ_y is calculated from the Von Mises relation. This value of σ_y is then used in step 4 to recalculate σ_z, etc., until convergence. The technique outlined above is applicable to multiaxial, univariate stress fields on shear free planes; however, by modifying the force equilibrium requirement to a surface integration, viz.,

$$\iint_{R\ \text{elas-plas}} \sigma_y(x,z)dxdz = \iint_{R\ \text{elas}} \sigma_y(x,z)dxdz,$$

uniaxial (and, most recently, multiaxial) bivariate stress fields are analyzed.

Extension of the technique to analyze load reversal conditions was accomplished by ensuring that, for each analyzed location, the input cyclic stress-strain relationship is satisfied. The developed software can be used only for kinematic-hardening cyclic stress-strain curves with initial symmetry between the tensile and compressive portions. However, because matching the stress-strain curve involves no more than detailed numerical bookkeeping [4-62], any cyclic stress-strain relation may be modeled, including one with time-dependence. Therefore, for the subject class of problems, general load histories can be completely tracked and analyzed.

To verify the model's ability to predict the stress field resulting from contained plastic conditions, a finite element (FE) parametric study was conducted [4-62]. The items considered in the study included: 1) Geometry consisting of a large plate with a central circular hole (K_t = 3.0) or an elliptic edge notch (K_t = 5.61); 2) Loading conditions, uniaxial plane stress and plane strain for both geometries and biaxial plane strain for circular

hole geometry; 3) Two material stress-strain curves representing increased strain hardening; and 4) Load history involving yield-producing tension loading followed by unloading, yield-producing compression, a second unloading, and final tension. The finite element program MARC [4-66] was used to conduct the parametric study, by the use of four-noded isoparametric, quadrilateral, plane stress/strain elements. The cost of the study was significant and included $9,000 in direct computer charges. The high cost exemplified the need for simple and effective models of plasticity and other nonlinear effects. The model developed, when used to perform the same parametric study, required less than $10 in direct computer charges.

Comparisons of the simplified model with the finite element results have been provided [4-62] which show reasonable agreement for both the initial tension in the load history and for subsequent load reversals. Thus, it appears that model is capable of economically providing a means of predicting stress redistribution near notches subjected to cyclic plastic loading. Such results are of use in the analysis of cracks growing in such regions. Overall, it appears that suitable means are available for approximate prediction of fatigue crack growth under cyclic loading conditions, but these techniques are not near as advanced as the corresponding ones for nominally elastic conditions that were discussed in Section 3.

4.3 REFERENCES

4-1. Atluri, S.N., "Path-Independent Integrals in Finite Elasticity and Inelasticity, with Body Forces, Inertia, and Arbitrary Crack-Face Conditions," Engineering Fracture Mechanics, Vol. 16, No. 3, pages 341-364, 1982.

4-2. Nakagaki, M., and Atluri, S.N., "On a Study of the Use of the T-Integral in Fracture Analysis of Solids with Inelastic Rate-Constitutive Laws," Journal of Pressure Vessel Technology, Vol. 104, pages 331-337, 1982.

4-3. Rice, J.C., Fracture: An Advanced Treatise, Vol. II, Mathematical Fundamentals, Academic Press, New York, 1968.

4-4. Rice, J.R., "A Path Independent Integral and the Approximate Analysis of Strain Concentration by Notches and Cracks," Journal of Applied Mechanics, Transactions of the ASME, Vol. 35, Series E, No. 2, pages 379-386, June 1968.

4-5. Begley, J.A., and Landes, J.D., "The J Integral as a Fracture Criterion," and "The Effect of Specimen Geometry on J_{Ic}," Fracture Toughness, Proceedings of the 1971 National Symposium on Fracture Mechanics, ASTM Special Technical Publication 514, pages 1-20 and 24-39, 1972.

4-6. Kanninen, M.F., et al., "Development of a Plastic Fracture Methodology," Final Report to EPRI, Contract No. RP601-1, EPRI Report NP-1734, Battelle Columbus Laboratories, Columbus, Ohio, March 1981.

4-7. Shih, C.F., et al., "Methodology for Plastic Fracture," Final Report to EPRI, Contract No. RP601-2, General Electric Company, Schenectady, New York, August 1980.

4-8. EPRI Ductile Fracture Research Review Document NP-80-10-LD, WS 80-912, Workshop Report, December 1980.

4-9. Sumpter, J.D.G., and Turner, C.E., "Fracture Analysis in Areas of High Nominal Strain," Proceedings of the Second International Conference on Pressure Vessel Technology, ASME, pages 1095-1103, 1973.

4-10. Hayes, D.J., "Some Applications of Elastic-Plastic Analysis of Fracture Mechanics," Ph.D. dissertation, Imperial College, University of London, October 1970.

4-11. Levy, N., Marcal, P.V., Ostergren, W.J., and Rice, J.R., "Small Scale Yielding Near a Crack in Plane Strain: A Finite Element Analysis," International Journal of Fracture Mechanics, Vol. 7, No. 2, pages 143-156, 1971.

4-12. Hutchinson, J.W., "Singular Behaviour at the End of a Tensile Crack in a Hardening Material," and "Plastic Stress and Strain Fields at a Crack Tip," Journal of the Mechanics and Physics of Solids, Vol. 16, pages 13-31 and pages 337-347, 1968.

4-13. Rice, J.R., and Rosengren, G.F., "Plane Strain Deformation Near a Crack Tip in a Power-Law Hardening Material," Journal of the Mechanics and Physics of Solids, Vol. 16, pages 1-12, 1968.

4-14. Paris, P.C., Tada, H., Zahoor, A., and Ernst, H., "The Theory of Instability of the Tearing Mode of Elastic-Plastic Crack Growth," Elastic-Plastic Fracture, ASTM Special Technical Publication 668, pages 5-36, 1979.

4-15. Argy, G., Paris, P.C., and Shaw, F., "Fatigue Crack Growth and Fracture Toughness of 5083-0 Aluminum Alloy," Properties of Materials for Liquified Natural Gas Tankage, ASTM Special Technical Publication 579, pages 96-137, 1975.

4-16. McClintock, F.A., and Irwin, G.R., "Plasticity Aspects of Fracture Mechanics," Fracture Toughness Testing and Its Applications, ASTM Special Technical Publication 381, pages 84-113, 1965.

4-17. Turner, C.E., "The Ubiquitous η Factor," Fracture Mechanics, Proceedings of the Twelfth National Symposium on Fracture Mechanics, ASTM Special Technical Publication 700, pages 314-337, 1980.

4-18. Derbalian, G., "J-Integral Estimation Procedures," 1981 ASME Pressure Vessel and Piping Conference, Denver, Colorado, Paper No. 81-PVP-10, 1981.

4-19. Turner, C.E., "Fracture Toughness and Specific Fracture Energy: A Re-Analysis of Results," Materials Science and Engineering, Vol. 11, pages 275-282, 1973.

4-20. Paris, P.C., Ernst, H., and Turner, C.E., "A J-Integral Development of η-Factors," Fracture Mechanics, Proceedings of the Twelfth National Symposium on Fracture Mechanics, ASTM Special Technical Publication 700, pages 338-351, 1980.

4-21. Srawley, J.E., "On the Relation of J_I to Work Done per Unit Uncracked Area: 'Total,' or Component 'Due to Cracks'," International Journal of Fracture, Vol. 12, pages 470-474, 1976.

4-22. Rainvelle, E.D., and Bedient, P.E., Elementary Differential Equations, Fourth Edition, MacMillan, 1969.

4-23. Ilyushin, A.A., "The Theory of Small Elastic-Plastic Deformations," Prikladnaia Matematika i Mekhanika, Vol. 10, page 347, 1946.

4-24. Kumar, V., German, M.D., and Shih, C.F., "An Engineering Approach for Elastic-Plastic Fracture Analysis," EPRI Topical Report NP-1931, Research Project 1237-1, July 1981.

4-25. Needleman, A., and Shih, C.F., "A Finite Element Method for Plane Strain Deformations of Incompressible Solids," Computer Methods in Applied Mechanics and Engineering, Vol. 15, No. 2, pages 223-240, 1978.

4-26. Shih, C.F., and Hutchinson, J.W., "Fully Plastic Solutions and Large Scale Yielding Estimates for Plane Stress Crack Problems," Journal of Engineering Materials and Technology, Transactions of the ASME, Vol. 98, Series H, No. 4, pages 289-295, October 1976.

4-27. McCabe, D.E., editor, Fracture Toughness Evaluation by R-Curve Methods, ASTM Special Technical Publication 527, April 1973.

4-28. Parks, D.M., "The Virtual Crack Extension Method for Nonlinear Material Behavior," Computer Methods in Applied Mechanics and Engineering, Vol. 12, pages 353-364, 1977.

4-29. Burdekin, F.M., and Dawes, M.G., "Practical Use of Linear Elastic and Yielding Fracture Mechanics With Particular Reference to Pressure Vessels," Institute of Mechanical Engineers, Proceedings, London, page 28, May 1971.

4-30. Dawes, M.G., "The COD Design Curve," Advances in Elastic Plastic Fracture Mechanics, edited by L.H. Larsson, Applied Science Publishers, London, 1980.

4-31. Harrison, J.D., Dawes, M.G., Archer, G.L., and Kamath, M.S., "The COD Approach and its Application to Welded Structures," Elastic-Plastic Fracture, ASTM Special Technical Publication 668, pages 606-631, 1979.

4-32. Harrison, J.D., "The State of the Art in Crack Tip Opening Displacement (CTOD) Testing and Analysis," Metal Construction, Vol. 12, Nos. 9, 10, and 11, pages 415-422, 524-529, and 600-605, 1980.

4-33. British Standards Institution, "Methods for Crack Opening Displacement (COD) Testing," BS5762, 1979.

4-34. British Standards Institution, "Guidance on Some Methods for the Derivation of Acceptance Levels for Defects in Fusion Welded Joints," BS PD 6493, 1980.

4-35. Towers, O.L., and Garwood, S.J., "The Use of Maximum Load Toughness for Ductile Fracture Assessments," Welding Institute Members Report 157, 1981.

4-36. Garwood, S.J., Willoughby, A.A., and Rietjens, P., "The Application of CTOD Methods for Safety Assessment in Ductile Pipeline Steels,"

Fitness for Purpose Validation of Welded Constructions Conference, London, November 1981.

4-37. Burdekin, F.M., and Stone, D.E.W., "The Crack Opening Displacement Approach to Fracture Mechanics in Yielding," Journal of Strain Analysis, Vol. 1, pages 145-153, 1966.

4-38. Kamath, M.S., "The COD Design Curve: An Assessment of Validity Using Wide Plate Tests," International Journal of Vessels and Piping, Vol. 9, pages 79-105, 1981.

4-39. Garwood, S.J., private communication.

4-40. Turner, C.E., "A J Based Engineering Usage of Fracture Mechanics," Proc. of ICF-5, Cannes, Vol. 3, pages 1167-1192, March 1981, and Chapter 2 in Post Yield Fracture Mechanics, 1979.

4-41. Turner, C.E., "A J Based Engineering Procedure (En J) for Fracture Assessment," Nuclear Installations Inspectorate Seminars at EPRI, Palo Alto, July 1982 and MPA, Stuttgart, October 1982.

4-42. Burdekin, F.M., Cowan, A., Milne, I., and Turner, C.E., "Comparison of COD, R6 and J Contour Integral Methods of Defect Assessment, Modified to Give Critical Flaw Sizes," Fitness for Purpose Conference, London, November 1981.

4-43. Harrison, R.P., Loosemore, K., Milne, I., and Dowling, A.R., "Assessment of the Integrity of Structure Containing Defects," Central Electricity Generating Board, August 1976.

4-44. Dowling, A.R., and Townley, C.H.A., "The Effects of Defects on Structural Failures, a Two Criteria Approach," International Journal of Pressure Vessels and Piping, Vol. 3, No. 77, 1975.

4-45. Bloom, J.M., and Malik, S.N., "Procedure for the Assessment of the Integrity of Nuclear Pressure Vessels and Piping Containing Defects," Electric Power Research Institute Report NP-2431, Palo Alto, California, June 1982.

4-46. Bloom, J.M., "Prediction of Ductile Tearing Using a Proposed Strain Hardening Failure Assessment Diagram," International Journal of Fracture, Vol. 6, pages R73-R77, 1980.

4-47. Shih, C.F., German, M.D., and Kumar, V., "An Engineering Approach for Examining Crack Growth and Stability in Flawed Structures," General Electric Company TIS Report No. 80CRD205, International Journal of Pressure Vessels and Piping, September 1980.

4-48. Shih, C.F., Kumar, V., and German, M.D., "Studies on the Failure Assessment Diagram Using the Estimation Scheme and J-Controlled Crack Growth Approach," General Electric Company TIS Report, 1981.

4-49. Central Electricity Generating Board, "Assessment of the Integrity of Structures Containing Defects, Supplement 1 - Validation," Research Division, London Office, July 1979.

4-50. Milne, I., "An Experimental Validation of Resistance Curve Analysis," to be published in ASTM Special Technical Publication 803, 1983.

4-51. Frost, N.E., Marsh, K.J., and Pook, L.P., Metal Fatigue, Oxford University Press, Ley House, London, England, 1974.

4-52. Dubensky, R.G., Fatigue Crack Propagation in 2024-T3 and 7075-T6 Aluminum Alloys at High Stresses, NASA CR-1732, prepared by University of Akron, Ohio, March 1971.

4-53. Dowling, N.E., and Begley, J.A., "Fatigue Crack Growth During Gross Plasticity and the J-Integral," Mechanics of Crack Growth, ASTM Special Technical Publication 590, pages 82-103, 1976.

4-54. Parks, D.M., "Reversed Plasticity from Unloading," Remarks Conference on Elastic-Plastic Mechanics, Washington University, St. Louis, 31 May-2 June 1978.

4-55. Paris, P.C., "Fracture Mechanics in the Elastic-Plastic Regime," Flow Growth and Fracture, ASTM Special Technical Publication 631, pages 3-27, 1977.

4-56. Rice, J.R., "Elastic-Plastic Fracture Mechanics," The Mechanics of Fracture, F. Erdogen, Applied Mechanics Division, Vol. 19, pages 23-53, 1976.

4-57. Dowling, N.E., "Geometry Effects and the J-Integral Approach to Elastic Plastic Fatigue Crack Growth," Cracks and Fracture, ASTM Special Technical Publication 601, pages 19-32, 1976.

4-58. Dowling, N.E., "Crack Growth During Low-Cycle Fatigue of Smooth Axial Specimens Cyclic Stress Strain and Plastic Deformation Aspects of Fatigue Crack Growth," Fatigue Crack Growth, ASTM Special Technical Publication 637, pages 97-121, 1977.

4-59. Brose, W.R., and Dowling, N.E., "Side Effects on the Fatigue Crack Growth Rate of Type 304 Stainless Steel," Elastic-Plastic Fracture, ASTM Special Technical Publication 668, pages 720-735, 1979.

4-60. Sadananda, K., and Shahinian, P., "A Fracture Mechanics Approach to High Temperature Fatigue Crack Growth in Udimet 700," Engineering Fracture Mechanics, Vol. 11, pages 73-86, 1979.

4-61. Sadananda, K., and Shahinian, P., "Application of J-Integral to High Temperature Fatigure Crack Growth in Cold Worked Type 316 Stainless Steel," International Journal of Fracture, Vol. 15, pages R81-R83, 1979.

4-62. Besuner, P.M., and Rau, S.A., "Stress and Subcritical Crack Growth Analysis under Contained Plastic Conditions," EPRI NP-81-8-LD Key Phase Report, April 1981.

4-63. Besuner, P., et al., "BIGIF, Fracture Mechanics Code for Structures," EPRI NP-1830-CCM, Manuals 1, 2, and 3, December 1980.

4-64. Neuber, J., "Theory of Stress Concentration for Shear-Strained Prismatical Bodies with Arbitrary Nonlinear Stress-Strain Law," Journal of Applied Mechanics, Transactions of the ASME, pages 544-550, December 1961.

4-65. Ramberg, W., and Osgood, W.R., "Description of Stress-Strain Curves by Three Parameters," NACA-TN 902, July 1943.

4-66. MARC-CDC General Purpose Finite Element Analysis Program, developed by MARC Analysis Research Corporation, Palo Alto, California, Rev. J-2.

Section 5

SPECIAL TOPICS

Previous sections have detailed the current state-of-the-art for fracture mechanics. Linear elastic and nonlinear stress analysis of cracks have been presented along with a discussion of subcritical crack growth and criteria for final fracture. Therefore, the basic elements of fracture mechanics analysis of crack growth behavior have been covered. However, there are several additional topics of interest to SSME applications that have yet to be addressed. These include the treatment of thermal and residual stresses, probabilistic aspects, proof testing and weld defects. The purpose of this section is to review these special topics.

5.1 RESIDUAL STRESSES

Residual stresses are defined as self equilibrating internal stresses existing in a continuum body when no external tractions or body forces are applied. Residual stresses as treated in this report pertain to macrostress contained within a structural component or specimen. Residual stresses are formed when portions of a member undergo nonuniform permanent dimensional change. The permanent dimensional change usually occurs as plastic deformation, but may also be caused by localized expansion or contraction of the metal lattice as with nitriding, carburizing, or phase transformation.

Nonuniform plastic deformation is commonly the result of mechanical metal forming processes such as drawing, rolling, forging, and grinding. These stresses are usually detrimental but can be introduced as beneficial surface

compression stresses in components prone to fatigue failure. Shot-peening is the most versatile of the cold-working treatments, being applicable to virtually all metals and shapes. Mechanically induced misfit in parts is another source of residual stress. Pre-loading of bolts or autofrettaged concentric cylinders are often used to introduce stresses which are in the opposite direction to the service stresses.

The misfit required for residual stress can be caused by differential thermal expansions causing yielding in isolated portions of a structure. The heat treatment of steel takes advantage of introducing desirable compressive residual stresses at the surface of parts. Induction hardening and flame hardening are among the processes taking specific advantage of this principle. Flame cutting and most welding operations leave surfaces in residual tension.

Processes which change the volume of a material through phase transformation can produce residual stresses. When steel undergoes the austenite-to-martensite transformation, the crystal lattice structure becomes slightly less dense and occupies correspondingly greater volume. Volume changes can also be caused by phase precipitation. If the precipitate and matrix have differing densities, residual stresses are created.

It is widely known that residual stresses can affect fatigue crack initiation, crack propagation, brittle and ductile fracture, and time-dependent cracking in structures, and the inclusion of their effects in design is mandatory. A substantial literature has developed, primarily from the field of fracture mechanics, aimed at estimation of fatigue lives when residual stresses are present in components. Investigators in the field are well aware that if reliable estimates are to be made, however, both experimental and

analytical determinations of residual stress fields must be made. Therefore this review will consist of three areas of interest; experimental determination of residual stresses, analytical computation of residual stresses, and the effect of residual stress on fatigue life.

5.1.1 Measurement of Residual Stress

An in-depth review and evaluation has recently been published on non-destructive examination (NDE) methods of residual stress measurement [5-1]. This Electric Power Research Institute Report containing 135 references discusses nine generic types of stress measurements:

1) Ultrasonic
2) Electromagnetic (including Barkhausen)
3) Neutron Diffraction
4) X-ray Diffraction
5) Positron Annihilation
6) Nuclear Hyperfine
7) Chemical Etchant
8) Indentation (partially destructive)
9) Hole Drilling (partially destructive)

Reference 5-1 concluded that presently the most reliable methods (other than complete destructive sectioning procedures) are hole drilling and X-ray diffraction. The semi-destructive method of hole-drilling is capable of measuring stresses to a depth of a few millimeters into the specimen, and the associated instrumentation is portable and inexpensive. The state of the art is relatively highly developed compared to many completely NDE methods which require considerable research and development work to bring them beyond the stage of laboratory based methods.

The X-ray diffraction (XRD) technique is the only truly non-destructive method presently available that can be widely applied to the measurement of residual stress. Significant research efforts at The Pennsylvania State University (C. O. Ruud) and at Rockwell North America (M. R. James) are underway to develop increased portability, compactness and speed of operation for XRD equipment. A severe limitation is that it can only measure surface stress obtained from averaging stresses in the first 0.001 inch of material. This limitation is not severe for producing data required in fatigue crack initiation calculations but can severely restrict information required for crack propagation analysis. The method also suffers from sensitivity to texture, grain size, microstructure and surface condition.

The ultrasonic methods hold the greatest promise for practical application, especially for three-dimensional stress fields. However, their general implementation is by no means likely to evolve in the near future. Current research at Stanford University [5-2] uses sophisticated ultrasonic velocity measuring techniques to measure changes in internal stress fields due to changes in the applied stress. Rayleigh surface waves are being exploited to measure the residual stress gradient away from a butt-welded pipe. These surface waves are conceivably capable of penetrating the surface to a depth on the order of millimeters thus representing a possible improvement over XRD. Ultrasonic methods do suffer from sensitivity to texture, grain size, microstructure and surface condition.

Most of the other non-destructive methods that have been proposed are either of such limited use or in such an elementary state of development that

their practical application is likely to be further away than that of ultrasound.

The destructive methods of residual stress measurement monitor displacement or strain while physically relieving the locked-in stresses by saw cutting, slicing, drilling, or trepanning. Experimental procedure must insure that additional stresses are not introduced by the material removal process itself. The methods are at present highly developed and considered quite dependable.

Further discussions of the general research area of experimental determination of residual stresses are to be found in [5-3 to 5-7]. Among the highly specialized topics included is a technique for residual stress measurement in a metal matrix composite using XRD [5-6]. Standards for residual stress measurements are reviewed in [5-5].

5.1.2 Calculation of Residual Stress

Experimental methods are presently the only truly reliable technique for assessing residual stresses in structures. A well established empirically based literature exists for use by designers for determination of beneficial residual stresses induced by mechanical, thermal, and phase transformations [5-8 through 5-11].

The proceedings of a conference sponsored by the American Society for Metals [5-8] includes a comprehensive review of residual stresses arising from manufacturing processes including; carburizing, induction hardening, through hardening, casting, shot-peening, and machining. Analytical efforts based on

elastic-plastic finite element analysis to predict stress distributions in engineering parts are compared with experimental data. Shot-peening is the most versatile of the surface treatment methods. The paper by Brodrick [5-9] includes residual stress distributions as a function of shot size, intensity and hardness levels for steel, aluminum and titanium alloys. A very useful designers' guide with fifty complete references is the Metal's Handbook [5-10]. Since it is difficult (and often only of academic interest) to experimentally evaluate residual stresses, most of the available data for surface treatments pertain to the overall specimen strengthening process as a result of the presence of such stresses without necessarily determining their magnitude.

Perhaps the most often common example of a detrimental residual stress is the welding process. Much attention has been given to the development of analytical understanding of heat flow, transient temperatures and stresses during the welding process. The major centers of technical expertise in calculation of thermally induced weld residual stress are Masubuchi at MIT [5-12], Rybicki at the University of Tulsa (formerly of Battelle Memorial Institute) [5-13] and Tall at Lehigh [5-14].

In a study for the NASA G.C. Marshall Space Flight Center, Masubuchi, et al., [5-15] developed a FORTRAN IV computer program to analyze thermal stresses in the one-dimensional case. This study is presented in detail in Reference 5-15, and included linear strain hardening and temperature dependent material properties. A strain analysis was included for subsequent comparison to experimental results. Recently this program has undergone further development and can handle certain practical problems such as variable weld location

on strip, distortion analysis and multipass effect. One limitation is the assumption of a steady state temperature distribution, so the important effects of weld start/stop are not included.

Two dimensional finite element programs capable of computing stresses under plane stress and plane strain conditions in bead on plate and butt welds have been developed at MIT. These analyses included: account of stress free state in the molten zone, solidification of weld material, and moving boundary conditions during butt welding. Current research is being conducted to include effects of metallurgical transformation (dimensional changes) during welding.

Efforts have been made to extend the analysis into three dimensions making it possible to treat cases such as cylindrical shells and heavy weld units. The one dimensional welding thermal stress programs cost only a few dollars per calculation while the present two-dimensional programs cost hundreds of dollars per calculation. Three dimensional calculations would be prohibitively expensive and therefore techniques for using two-dimensional analysis in complicated structural geometries are being pursued vigorously.

NASA has sponsored much of the experimental verification work at MIT concerning aluminum alloys, tantalum and columbium. Comparison of analytical predictions at MIT with experimental data have led to the following conclusions:

1) The one-dimensional analysis is sufficiently accurate in predicting longitudinal strains produced during bead on plate welding. The experimental data and analytical predictions were in close agreement in most of the

materials studied, including low carbon steel, stainless steel, aluminum, titanium, columbium, and tantalum.

2) The two dimensional finite element program was successful in predicting longitudinal and transverse strains in butt welds on aluminum plate.

3) In HY-80 steel the inclusion of metallurgical transformation effects was necessary for correct analytical predictions.

Work by Rybicki [5-13] has involved computing residual stresses due to multi-pass welds in piping systems. Both a finite element heat transfer and stress analysis were performed including elastic-plastic material properties and unloading. Methods of combining weld passes in the analysis are presented which yield tolerable computing costs. A thermal analysis is performed for each pass, but an envelope of thermal responses is extracted for input into the stress analysis. The combining of individual passes before submittal to elastic-plastic finite-element analysis greatly reduces computer time.

In summary, it appears that significant break-throughs in the analytical prediction of residual stress in weldments are imminent. Success has been achieved in predicting residual stresses, strains, and distortions in simple weld geometries. With advances in computer technology and more efficient finite element solution algorithms it will be possible in the near future for design engineers to optimize welding procedures using analytical techniques. Until then, reasonable estimates of stress distributions must be assumed based on experience and a wealth of experimental data in the literature.

A somewhat related source of residual stress must not be overlooked. Repeated thermomechanical loads acting on mechanical components in service can generate significant residual stress fields. Here again, advanced elastic-

plastic finite element stress analysis in conjunction with heat transfer analysis is required. At high temperatures the creep response of material must be accounted for. Numerous publications are available on this subject, a review of which is available in [5-16].

5.1.3 Residual Stress Effects in Fatigue

A comprehensive collection of the latest observations and analysis including residual stress effects in fatigue is found in the recently published proceedings of a symposium sponsored by ASTM [5-17]. Local strain concepts are discussed with respect to estimation of fatigue crack initiation including effects of "fading" or "shakedown" during cyclic loading. Residual stresses near a notch surface may be relaxed by localized cyclic plastic straining, but the re-equilibrated distribution in depth may still have a significant influence on subsequent crack growth behavior. The use of superposition of elastic (or contained plastic) stress intensity factor relationships, including expressions that consider residual stress, has become widely accepted in recent years. Superposition allows the analytical estimation of fatigue life to include residual stress effects in fatigue crack propagation calculations. Another concentration of such information is found in the proceedings of the 28th Army Sagamore Conference [5-18].

The state-of-the-art approach for crack initiation life prediction and/or shakedown analysis is the "local strain approach" applied at a notch (e.g., weld toe) detail. Nueber's rule is typically used to track the cyclic stress-strain behavior. Lawrence, et al., [5-19] review well known closed form analytical expressions for computing fatigue crack initiation at weld details.

Such analyses are generally applicable to other structural details assuming the stress concentration factor is known. The computer program BIGIF is capable of predicting these mean stress shifts (shakedown) caused by applied loading acting in the same direction as the residual stresses [5-20]. The effect of multi-axial stress fields can be included, as was discussed in more detail in Section 4.2.

Most fatigue design rules for welded steel structures [5-21] are based purely on stress range regardless of mean stress in order to account for high tensile residual stresses. This accounts for the fact that fatigue cracks can develop under purely compressive applied loading superimposed on tensile residual stresses. The rationale for neglecting mean stress effects for tensile applied loading is that the residual stresses will relax out rapidly and not affect the initiation life. Maddox of the Welding Institute [5-22] has verified the validity of these approaches for certain steel alloys. However it is pointed out that caution must be used in extrapolating these results to other materials such as aluminum. Such design rules can be nonconservative for the combination of high tensile residual stresses and high tensile applied mean stress. Another factor which could make current rules nonconservative is the effect of tensile strength. Residual stress magnitude increases with tensile strength but not in proportion of yield strength. Satoh [5-23] has shown that in high strength steels yield level residual stresses will not occur, whereas in mild steels they do.

Nearly all fatigue crack propagation analysis account for pre-existing residual stress fields by calculating a stress intensity factor (K_{res}) for the residual field which is then superimposed on the applied stress intensity

factor. Some controversy exists over the mathematical validity of this approach in that the method may not properly account for the redistribution of residual stresses during crack growth.

Heaton [5-24] presents a mathematically rigorous proof of Bueckner's weight function approach to problems involving residual and thermal stress fields. Parker [5-25] further substantiates applicability of weight function techniques to residual stress crack problems. Parker has indicated procedures to include the nonlinear effect of crack surface "overlapping" on the computation of the stress intensity factor under highly compressive loadings resulting from residual stresses.

The weight function technique requires knowledge of the uncracked residual stress distribution. Closed form solutions are available for numerous crack geometries and simple loadings but the integration required when complex stress fields are present limit their use to cases of simplified stress distribution. The computer program BIGIF [5-20] computes stress intensity factors for arbitrary residual stress distributions including two-dimensional stress fields.

An experimental effort by Glinka [5-26] has recently received considerable attention. The research dealt with the effect of residual stresses on fatigue crack growth in medium strength low alloy steels. Specimens were tested under constant amplitude and variable amplitude load. Parker [5-25] has calculated the experimentally predicted crack growth with reasonable success using the weight function and superposition approach. Nelson [5-27] has also predicted the crack growth rates using a crude "crack closure" approach which accounts for crack generated residual stresses. Nelson places

some reservation on the ability of the weight function approach on accurately handling crack growth through the region where the residual stress changes sign. However, crack closure approaches are not fully developed as yet and the superposition continues to be considered the state-of-the-art. Details of the crack closure approaches are included in the variable amplitude loadings section of this report.

Residual stresses can play an important role in time dependent cracking phenomena as shown by Harris [5-28, 5-29]. A linear elastic fracture mechanics analysis which uses weight functions to compute the residual stress intensities is presented. Time dependent cracking is strongly dependent on the mean stress intensity factor and therefore strongly influenced by K_{res}. Here again the use of the superposition principle is the accepted method today for calculating K_{res} and therefore predicting stress corrosion cracking response.

In summary, the superposition approach has the distinct advantage for use in design analysis in that stress intensities can be calculated by established methods of linear elastic fracture mechanics. However since it is based on elastic analysis, it lacks the ability to account for the influence of crack induced residual stress effects. The crack closure approach provides the mechanics to account for such influences, but has not been used extensively in this regard. The primary limitation of the approach is the necessity of elastic-plastic finite element analysis, which must be repeated as the crack grows. Simple models, such as Dugdale's, reduce computational burdens but their usefulness is limited to simple crack geometries and loading conditions.

5.2 THERMAL STRESSES

Thermal stress fields pose particular problems for fracture mechanics technology because they usually are highly time dependent and possess severe gradients. Thermal stresses are also highly sensitive to boundary conditions and component geometries. Cracks subject to thermal stresses interact with the stress fields through several mechanisms. As a crack propagates through a body, it may relieve the thermal stresses by effectively increasing the compliance of the body, thereby decreasing the stress intensity at the crack tip. A crack may also disturb the heat flow in the body, acting as an insulating or semi-insulating inclusion. The resultant local perturbation in the temperature gradient can produce local stress fields with concentrations at the crack tip.

This section will review the means of including the influence of thermal stresses in a fracture mechanics analysis of crack behavior. The determination of stress intensity factors due to thermal stresses will be reviewed, along with procedures for predicting crack behavior under such situations. A general review of current thermal stress analysis techniques will not be provided. References 5-30 through 5-32 provides information in this area.

Methods such as finite element and finite difference analysis are commonly used to determine thermal stresses in complex structures subject to various thermal and mechanical boundary conditions. Thermal stress analysis therefore will be discussed only as it applies to determining stress fields due to the presence of a crack. This survey also considers the temperature dependence of materials properties which are involved in thermal stress

analysis of cracks only. The temperature dependence of other properties (da/dn (ΔK, R), K_c, etc.) are considered elsewhere in this report.

5.2.1 Thermal Stresses with Cracks

Special considerations of the analysis of thermal stresses when cracks are presented will be discussed here. Methods for determination of stress intensity factors for cracked bodies subjected to thermal stresses will be reviewed in Section 5.2.2.

Hasselman [5-33] and Chell and Ewing [5-34] have demonstrated the sensitivity of thermal stress fracture analysis to the boundary conditions involved in individual problems. In many instances, thermal stresses develop due to a displacement boundary condition on a body. If a crack propagates due to those stresses, the effective compliance of the body increases due to the presence of the crack. The stress intensity is therefore less than would result from pure traction loading boundary conditions. One implication of this behavior is that cracks growing either critically of subcritically may be arrested once they propagate sufficiently far to decrease stresses to the point were the crack's associated stress intensity falls below the material's K_c or ΔK_{th} value, respectively. Blauel [5-35] has demonstrated this behavior in glass specimens subjected to thermal shock. Chell and Ewing's example of this phenomenon is the simple case of a plate with a center crack held at its ends and cooled uniformly. Chell and Ewing, however, also offer a counter example in which stresses are not relieved by crack propagation, and the associated stress intensity factors are identical to those resulting from traction boun-

dary conditions which produce the same stress distribution. Chell and Ewing's conclusion is that,

> Unfortunately, there are no universal rules for dealing with thermal stress effects in fracture mechanics and therefore each case must be approached on its own merits.

They do find however that for many specimen geometries, the stress-relieving effect (fixed-grip, displacement-controlled analogy) of a thermal stress-induced crack does not become apparent until the crack penetrates more than 10 to 15 percent through the specimen width.

Another aspect of the problem of thermally stressed bodies with cracks involves the case of a crack influencing the flow of heat through a body. This was first considered by Florence and Goodier in a series of papers in the early 1960's [5-36, 5-37]. Later, work by Sih [5-38], Sekine [5-39 through 5-42], and a host of other researchers investigated different crack geometries and thermal loading conditions. The most general analysis appears to be that by Koizumi, et al., [5-43] which considered an infinite plate with a crack or ribbonlike inclusion subjected to a uniform heat flow. Linear heat flow is assumed across the flaw. Most of the papers reviewed presented an analytical solution, derived from assumed thermal and thermoelastic potential functions which were in turn applied to the boundary conditions of the problem in order to obtain a complete, closed form solution. Virtually all of the solutions presented in the above mentioned papers are in the form of power series of singular orthogonal functions, many of which require extensive numerical integration to produce stress solutions to actual problems.

The general results of the analysis demonstrate that Mode I stress intensity factors exist whenever there is a temperature variation over the surface of the crack. Whenever the crack disrupts the flow of heat, Mode II deformations result.

5.2.2 Stress Intensity Factor Calculation

Thermal stresses generally result from differential expansion due to temperature gradients. The maximum thermal stress is not necessarily controlled by the temperature gradient, and the maximum stress intensity factor for a surface crack does not necessarily occur at the time of the maximum surface stress. This has been discussed by Emery [5-44].

Many researchers interviewed in the academic community recommended a standard finite element approach for thermal transient stress analysis, employing the same mesh for the temperature and stress solution. Conversely, most industrial investigators who need to consider numerous thermal crack problems (including the present authors) stressed the use of superposition methods described below, in which no single numerical model is burdened with both the thermal stress field and the crack simultaneously. There was no recommended technique for estimating the time of maximum stress intensity beyond urging that K solutions be obtained at enough times, t, to allow an accurate K(t) plot from which a maximum K could be deduced.

As in normal elasticity, stress intensity factors may be derived from either the closed form solution to the thermoelastic problem or by numerical approximations to it. Generally, the thermal and the elastic problem can be decoupled, and the thermal stresses treated as mechanical stresses. Section

5.2.1 considered the situation where the crack disturbed the temperature gradient thereby generating a stress intensity factor.

Four basic methods of determining stress intensity factors for thermal stress problems were encountered:

1. Finite elements with singular crack tip elements [5-45, 5-46].
2. Finite elements strain energy release methods [5-44, 5-47].
3. Superposition [5-44, 5-48 through 5-58].
4. J-Integral [5-59 through 5-63].

The first two methods are familiar methods in determining stress intensity factors.

Heaton [5-24] has demonstrated that any thermal stress crack problem can be converted into an equivalent problem in which the originally stress-free geometry is subjected to boundary tractions, boundary displacements, and body forces. This equivalent problem can then be solved by the method of elastic superposition. This third method is used extensively by many analysts of advanced aerospace engine hardware, for example, by FaAA, Pratt and Whitney Aircraft, several divisions of the General Electric Company, Teledyne, Rocketdyne and the A. Reynolds Company for thermal stress cracking. Care must be taken with the selection of the proper weight function for a particular problem. If displacement boundary conditions are specified, the weight function must be specific to those particular boundary conditions. This is particularly relevant in the case of thermal stresses, which are frequently dependent on displacement boundary conditions.

Blackburn [5-59] has shown that in the presence of thermal stress, the J-integral no longer becomes path independent. Blackburn, Wilson, Aoki, and others [5-59 through 5-63] have proposed variations on the J-integral to restore path independence. The method documented by Wilson [5-60] appears to produce highly accurate stress intensity factor values.

Given that a weight function exists for a particular geometry and, if relevant, set of boundary conditions, weight function techniques provide a distinct advantage over direct finite element approaches. Since the stress calculation for a weight function analysis is for an uncracked body, the FE mesh need not be as refined as for a finite element crack model, nor as consuming of computer time. Several automated stress intensity computer programs exist -- as discussed in Section 2.3 of this report. One drawback of this aproach is that it may not be able to treat the insulating nature of a crack. If such effects are important, detailed finite element calculations would be required for all but the simplest problems.

5.2.3 Thermal Fatigue

The growth of cracks due to the cyclic stresses imposed by cyclic temperatures is known as thermal fatigue, and is an important problem in many industries. In spite of its importance, surprisingly little literature on this topic was found. Several articles were reviewed, and three methods of life prediction were found. The first method employs linear elastic fracture mechanics and crack growth rate data (da/dn) to evaluate fatigue crack growth and fatigue lifetime. Gemma [5-64], McLean, et al., [5-50], Miller [5-65], and Harris, et al., [5-55 through 5-57] use this approach.

McLean, Miller and Harris use weight functions to calculate stress intensity factors. Gemma employs published formulae for K_I adjusted for particular geometries using experimentally derived and published non-dimensional adjustment factors. Miller calculates a power spectral density of the stress intensity factor using a corresponding surface temperature power spectral density. The integral of the product of stress intensity power spectral density with the crack growth law is calculated to obtain crack length, a, as a function of time. Gemma and McLean use known or estimated stress/strain cycles to obtain a spectrum of K_I cycles.

Leis, et al., [5-66] use a basic S-N approach using finite element generated stresses to attack a crack initiation problem. Cost [5-67] employs a probabilistic model that compares actual stress with an allowable stress, assuming a Gaussian distribution of stress over a particular time period. The allowable stress similarly varies according to temperature and accounts for aging and viscoelastic effects. Both Gemma and Leis present experimental results which agree with their analytical work.

5.3 PROBABILISTIC FRACTURE MECHANICS

The purpose of probabilistic fracture mechanics (PFM) is to estimate or bound the reliability [1-(probability of failure)] of a component subject to cracking, and to quantitatively ascertain the influence of engineering and management decisions on component reliability. Earlier sections of this report have reviewed the various facets of fracture mechanics that are required to analyze crack behavior in structural components. If the analytical procedures were capable of perfectly predicting the crack behavior,

and if all the inputs to the analysis were known exactly, then the future behavior of the crack could be predicted in a deterministic manner, and the moment at which the component would fail could be precisely predicted. The use of probabilistic fracture mechanics would not be called for in such a case. However, all of the necessary inputs to a fracture mechanics analysis are only rarely known with a high degress of certainty, and a deterministic "best estimate" and/or "worst case" analysis is often resorted to. All too often, such calculations are inconclusive, in that the best estimate results are acceptably optimistic and the worst case is unacceptably pessimistic. This is the situation which most clearly calls for probabilistic fracture mechanics.

5.3.1 General Discussion

Probabilistic fracture mechanics is strongly based on deterministic fracture mechanics procedures, but considers many of the input variables to be random -- rather than having deterministic values. The input variable which is usually the least well known is the initial crack size. Rather than assuming a fixed given initial size (which can be based on inspection detection capabilities) this parameter can be taken to be present over a range of sizes, with probabilities estimated for each size. In the simplest case, a deterministic fracture mechanics analysis can then be performed to provide the crack size distribution as a function of time (or stress cycles) in service. The failure probability at any time is then equal to the probability of having a crack larger than the critical size.

Generally speaking, more than one of the fracture mechanics variables is not known with great certainty, and in many cases numerous input variables must be considered to be random. The following list provides examples of input parameters to fracture mechanics analysis that could be considered as random variables:

- initial crack size
  - depth
  - length
  - location
- crack detection probability
  - detection probability as a function of size
  - uncertainty in actual crack size for a given level of indication
- material properties
  - subcritical crack growth characteristics (such as da/dn - ΔK relation for fatigue
  - fracture toughness
  - tensile properties
- service conditions
  - stress levels
  - cycling rate
  - temperature

Not all of these parameters need be considered as random in every application of PFM; only those with uncertainty or scatter that produces the greatest effects on life calculations need be so considered.

5.3.2 Historical Review

The earliest work in probabilistic fracture mechanics appears to have been related to aircraft applications [5-68 through 5-70], although general

early discussions are available [5-71, 5-72]. In more recent years, the most common application has been to pressurized components - primarily pressure vessels and piping in commercial nuclear power reactors. References 5-55 and 5-73 through 5-79 provide examples in this area. Most such applications concentrate on weld areas, because cracks tend to be concentrated in such regions. Recent Japanese work [5-80, 5-81] has been related to civil engineering structures such as buildings and includes a rare instance of actual data on initial crack size distributions. Reference 5-82 provides more recent examples of applications to aircraft and aerospace structures.

5.3.3 Generation of Numerical Results

Once a probabilistic fracture mechanics model of component reliability has been constructed, it is necessary to generate numerical results. This can be accomplished in a variety of ways. In all but the simpliest cases, numerical techniques must be employed. This is usually not an obstacle, because even the underlying deterministic model would often require numerical calculation for crack growth.

Several techniques for generation of numerical results are available. These include stress-strength overlap, variance-covariance, convolution and Monte Carlo. The stress-strength overlap is perhaps the easiest to visualize. The probability of failure is equal to the probability that the applied stress exceeds the residual strength of the component, and can be calculated once the statistical distribution of both stress and strength are known. However, estimation of these distributions themselves may be a difficult task. For example, in the case of fatigue crack growth, the strength distribution would

depend on the statistical distribution of the following input parameters: initial crack size, cyclic stress level and frequency, and material properties in da/dn - ΔK relation. In all but the simplest of cases (such as assuming everything to be normally distributed with small variances) one of the other techniques would still have to be utilized.

The method of analysis of variance and covariance by perturbation techniques is based on the assumption that some variables will deviate by relatively small amounts from their respective means. This technique is also often referred to as the method of generation of systems moments [5-83], and provides estimates of the moments (mean, variance, skewness, etc.) of the dependent variable from the moments of the independent variables and the partial derivatives of the functional relationship between the independent and dependent variables. This technique is only an approximation. It increases in accuracy as the variances of the independent variables decrease. Only the moments of the distribution of the dependent variable are provided; no information on the details of the distribution are obtainable.

Davis [5-84] presents an application of this variance/covariance method to the development of an automated design system for stiffened two-panel aircraft box systems subject to fatigue crack growth and fracture. This method was also employed by Ellingwood [5-85] in assessing the low cycle fatigue behavior of structural welds undergoing both crack initiation and propagation.

The convolution method, which is also sometimes referred to as direct synthesis, involves the establishment of the probability density function of the dependent output random variable from the functional relationhip between the dependent and independent variables and the probability density functions

of the independent variables. In principle, this method is capable of providing closed form results. However, the dimension of the integrals (i.e., the "number" of integral signs) is equal to the number of random independent variables, and setting up the integrals is often tricky and intricate. In the end, numerical integration is usually required, and care must be taken to obtain accurate results. Additionally, the inclusion of dependencies between the input variables is difficult to include. Itagaki, et al. [5-81], utilized the convolution method in assessing the effects of weld repair on weld reliability.

Monte Carlo simulation [5-83, 5-86] is a general numerical technique for determination of the distribution of the dependent variables. It is of wide applicability in the generation of numerical results from probabilistic fracture mechanics models [5-55, 5-87]. The inclusion of dependencies between input variables is relatively straightforward in Monte Carlo techniques.

The procedure consists of selecting a value for each input variable at random from its known statistical distribution. These values are then used to calculate one corresponding value of the output (dependent) variable. This is repeated many times. This provides many values of the output variable, which are then used to construct a histogram. This gives an approximation of the desired probability density function. As more values are generated and the histogram "bins" are made smaller, the results approach the true probability density function. Clearly, much computer time can be consumed in this procedure, but the use of Monte Carlo techniques does not necessarily mean larger computer expenditures. The generality and ease of implementation make Monte

Carlo techniques widely applicable to problems such as encountered in probabilistic fracture mechanics.

5.3.4 Combined Analysis

Probabilistic fracture mechanics as described in earlier portions of Section 5.3 is often not capable of providing results with a high degree of confidence. This is primarily due to uncertainties in the distribution of input variables, such as the initial crack size distribution. A means of partially overcoming such deficiencies is provided by a procedure known as combined analysis or calibrated numerical modeling [5-88 through 5-90]. The "combined analysis" (CA) approach provides improved, quantitative methods of interpreting in-service sructural life data in combination with valid, but incomplete, engineering models to more accurately predict reliability. The CA method provides a systematic means for calibrating an incomplete engineering model with in-service data in order to minimize the effects of analytical modeling errors or missing laboratory or structural simulation data. The methods have been illustrated in two applications [5-89]. The first deals with a wear-out failure mode dominated by the propagation of easily inspectable cracks in a rim slot blade attachment of a turbine where stress analysis is difficult. Knowledge of in-service crack sizes is used to make up for the lack of accurate estimates of loads and stresses in the critical location. The second considers a failure mode in which most of the long-term degradation is caused by creep- or fatigue-induced sharpening of non-metallic subsurface inclusions in turbine rotors. Engineering models of this latter failure mode are fraught with difficulties. The inclusions are assumed to be difficult to inspect, structural degradation (crack sharpening) is assumed to be impossible

to detect, and large life scatter, missing data, and analytical errors are assumed present, including cases in which the failure mode is misdiagnosed. However, in the specific case analyzed the rotor population has a significant, largely successful (one failure, 499 rotors without failure), 25-year history upon which to calibrate the incomplete engineering model and to minimize its sensitivity to errors. The analysis in the first instance relies heavily on in-service inspection data while the analyses in the second relies mainly on proper interpretation of in-service structural failure and success data. The combined analysis approach provides a means of combining engineering modeling and judgement with actual field service information in order to provide a calibrated model of reliability that can then be put to a number of uses, such as predicting the impact on component reliability of altering service conditions.

The work of Shinozuka, et al., [5-91] utilizes a probabilistic fracture mechanics model with Bayesian updating of input distributions to provide agreement between model predictions and field observations. This is a somewhat different approach to the same problem addressed by combined analysis.

5.4 PROOF TEST CRITERIA FOR TOUGH DUCTILE MATERIALS EXHIBITING STABLE FLAW GROWTH

Proof test criteria establish optimum testing techniques for imposing preservice and periodic "safe-condition" in-service loadings as a quality assurance procedure. Typically these safe-condition loads, by virtue of their large magnitude or severe conditions (such as low temperature), are more apt to cause brittle failure or noticeable damage to the structure than any in-service load within the design envelope. A properly designed proof test will

reveal flaws in defective structures, often by damaging or destroying the structure under safe conditions, without causing significant damage to sound structures. The proof test loading should cause critical size flaws (cracks) to grow to failure, either stably or unstably, without significantly enlarging non-critical flaws or otherwise damaging the structure. Consequently, many structural components are difficult to proof test because the required loads would damage other components in the load path.

5.4.1 Review of Proof Test Philosophy

While there is a well-established basis for the effectiveness of proof testing for brittle materials, the logic is not so straightforward for tough ductile materials which exhibit stable flaw growth. For brittle materials, passing a well-designed proof test should generally guarantee that no crack exists in the structure above a size deemed safe for introduction or return to service. This logic is confounded for materials which may exhibit stable flaw growth under proof loading because any given structure might have a benign crack turned into a dangerous crack by the proof test. Proof testing is most effective for materials which exhibit a significant reduction of fracture toughness under viable test conditions, as in low temperature testing of the F-111 wing box at McClellan Air Force Base as reported by Buntin [5-92].

Some investigators, Formby [5-93] for example, have concluded that there is little to be gained or there are no rational methods for proof testing tough ductile materials exhibiting stable flaw growth. Several characteristics of tough ductile material diminish the value of proof testing or add confounding elements to proper design of a proof test progam. These charac-

teristics include: (1) the larger fracture toughness which diminishes the value of the proof test as a screen for catching flaws; (2) the normally lower yield strengths associated with ductile materials which make it harder to develop a high proof load for screening without causing undesirable permanent plastic deformation of the structure; (3) the higher probability and magnitude of stable crack growth under single or multiple proof test loadings.

This third characteristic is especially troublesome because, as will be demonstrated in Sections 5.4.2 and 5.4.3, it often creates a situation in which some, hopefully small, percentage of the structural population will be degraded by the proof tests rather than improved. Thus, stable flaw growth may make it impossible to adhere to the old adage "Doctor, do no harm" for each and every member of the structural "patient" population. This fact, in itself, has caused some people concerned with structural integrity to rule out proof testing of tough ductile materials which exhibit stable flaw growth, especially when protection against future liability and litigation has been an issue. However, if the probability of high-severity in-service failures can be reduced by the proof testing for the aggregate population (by benefiting the vast majority of the population), the concept of proof testing materials exhibiting stable flaw growth certainly deserves some consideration. Thus, most of the emphasis in this section is on obtaining the maximum benefit from the proof test and in evaluating pragmatically whether or not to engage in such a test.

Note that the characteristic behavior of tough ductile materials also leads to several <u>beneficial</u> results from a properly designed proof test. Unfavorable (tensile) residual stresses that existed prior to proof testing

are reduced or eliminated. Favorable (compressive) residual stresses are often imparted by proof test loading. These not only increase the fatigue life of uncracked material but also cause retardation of crack growth from flaws through residual compressive stresses and blunting at the crack front. The crack front residual stresses also have the advantage of maintaining a crack opening gap that greatly enhances crack detectability during post-proof NDE procedures. Conventional NDE procedures can be augmented by inspecting critical areas for evidence of back-face dimpling. Tough ductile materials are known to provide visible evidence of dimpling after stable crack growth when the crack approaches the material back surface.

It is mandatory that proof test criteria include an assessment of proof test damage in the calculation of critical initial flaw sizes. For example, Formby [5-93] has shown that excessive proof testing of a pressure vessel in a military vehicle decreased the safe service life by a factor of two. Proof testing has been found by Irwin [5-94] to decrease the lifetime (time-to-leakage) of natural gas transmission pipelines.

Many manufacturers have adopted successful proof test techniques for crack-susceptible structures made from tough ductile materials with stable flaw growth. Included among these are manufacturers of gas turbine disks which undergo proof spins at speeds more than 20% above maximum operating speed, or in the case of pressure vessels, at pressures much larger than maximum operating pressures.

Four topics appear to be most important in developing these successful proof test techniques. These are:

- Number of loading cycles used to conduct a single proof test.
- Probabilistic modeling of proof test.
- Innovative proof testing techniques.
- Interrelationships between proof testing and non-destructive testing.

An example of the pragmatic approach to proof testing, which embodies the four topics above, is the multi-cycle proof test loading used by the Rocketdyne Division of Rockwell Internation, as detailed by Vroman and colleagues [5-95 through 5-99]. After suffering a significant number of premature failures in rocket engine pressure vessels, Rocketdyne adopted a procedure of applying five pressurization cycles to comprise a single proof test. Since adopting this procedure, they have not had an in-service failure of a pressure vessel that had passed the multi-cycle proof loading. Because of the large number of Rocketdyne rocket engines that have performed successfully, the value of this approach to proof testing cannot be ignored. In 1972, a probabilistic fracture mechanics-based study of multi-cycle proof testing was performed by Vroman and Creager [5-96]. This study included a characterization of stable crack growth behavior, inspection, and several possible statistical distributions of crack sizes. The study concluded that multi-cycle proof loading dramatically decreased the probability of in-service failure in comparison to single-cycle proof loading. However, several investigators [5-93, 5-94, 5-100, 5-101, and 5-102] have not accepted multiple cycle proof testing as a generally valid approach, and care must be exercised for individual applications.

Since proof testing can be thought of as a form of inspection, manufacturers, operators, and consultants evaluating the significance of possible cracking often consider the question of whether or not proof tests should be used as a substitute or supplement for nondestructive inspection. Where tough ductile materials are involved, these investigators invariably recommend monitoring the structure by acoustic emission [5-103] or other inspection techniques [5-104, 5-105] during proof test cycles.

5.4.2 Single and Multiple Cycle Proof Testing of Ductile Materials Exhibiting Stable Flaw Growth

One of the major decisions that must be made in designing a proof test for the purpose of fracture control is whether to use single or multiple "overload" excursions during the test. For the stable flaw growth-susceptible materials under consideration here, Figures 5-1 through 5-4, obtained from Vroman [5-96], illustrate the differences between single- and multiple-cycle loading. Figure 5-1 summarizes the stable flaw growth occurring in a single cycle of loading. Note the presence of a "threshold level" of the parameter a/Q of approximately 0.5 mm, below which no stable flaw growth takes place. (Use of the normalizing parameter "Q" for expressing crack size and accounting somewhat for the effects of semi-elliptical surface crack aspect ratio and proximity to the yield stress level, is purported [5-106] to be an improvement compared to simply considering the crack size parameter, "a". This is itself a subject of controversy, an investigation of which is outside the scope of this project).

Figure 5-2 shows the large increase of stable flaw growth exhibited during five cycles of loading. Note the important assumption/finding by

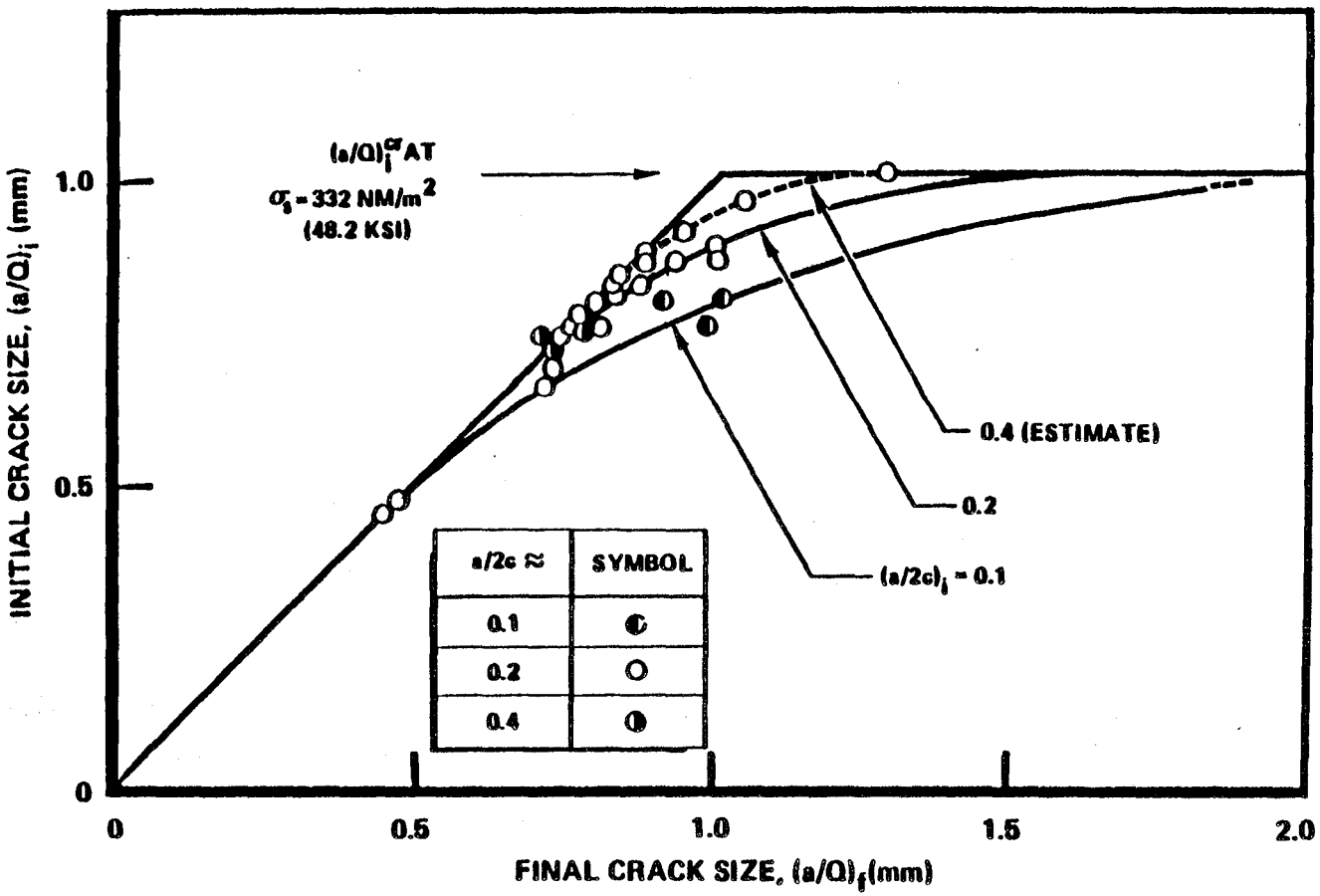

Figure 5-1. Crack Growth During Proof Test - Single-Cycle Loading [5-96].

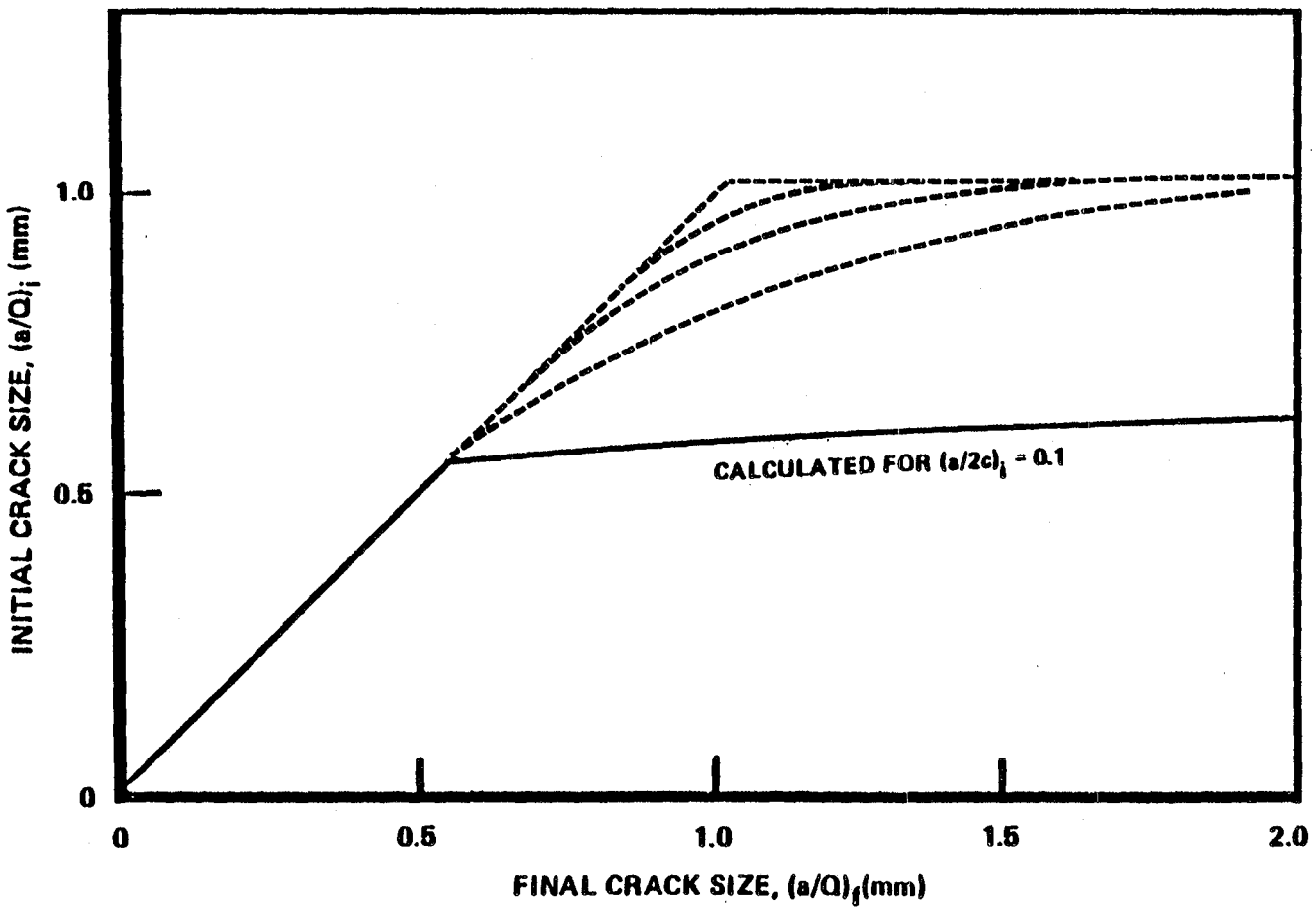

Figure 5-2. Crack Growth During Proof Test - Five-Cycle Loading [5-96].

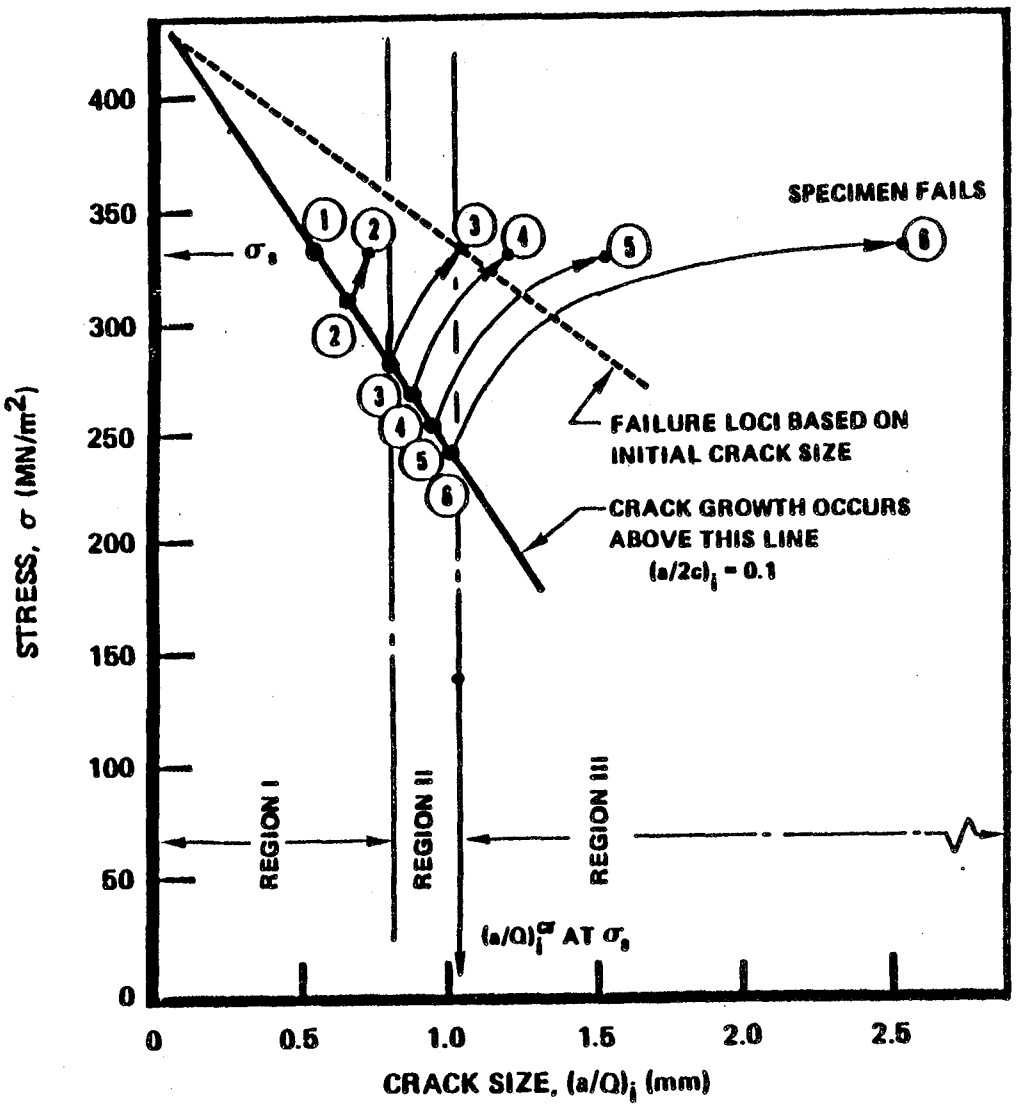

REGION I

IF INITIAL CRACK SIZE IS WITHIN THIS RANGE, SERVICE LIFE CAN BE GUARANTEED

REGION II

IF INITIAL CRACK SIZE IS WITHIN THIS NARROW RANGE, SERVICE LIFE CANNOT BE GUARANTEED.

REGION III

IF INITIAL CRACK SIZE IS GREATER THAN $(a/Q)_i^{cr}$, VESSEL FAILS OR LEAKS DURING PROOF TEST

Figure 5-3. Fracture Mechanics Proof Test Logic - Single-Cycle Loading [5-96].

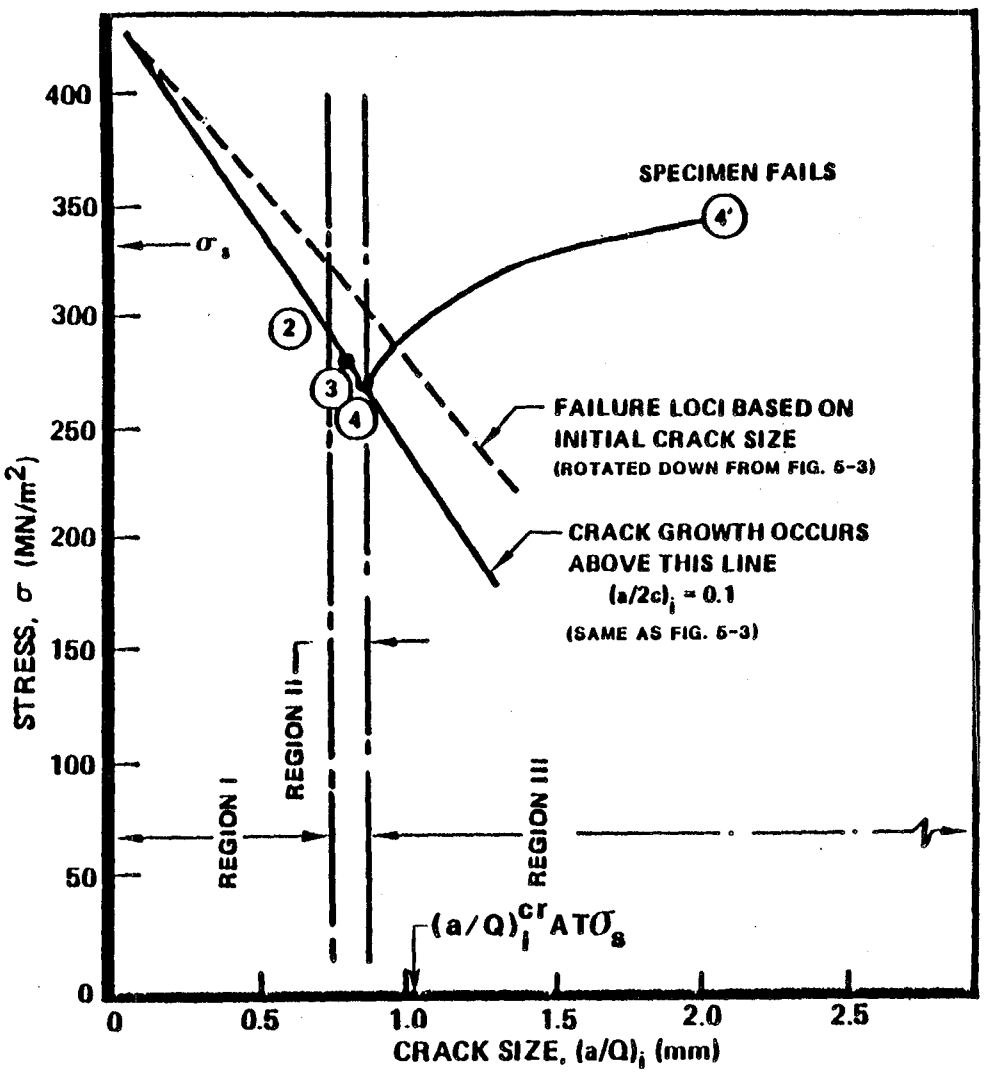

REGION I

IF INITIAL CRACK SIZE IS WITHIN THIS RANGE, SERVICE LIFE CAN BE GUARANTEED

REGION II

IF INITIAL CRACK SIZE IS WITHIN THIS NARROW RANGE, SERVICE LIFE CANNOT BE GUARANTEED

REGION III

IF INITIAL CRACK SIZE IS GREATER THAN $(a/Q)_i^{cr}$, VESSEL FAILS OR LEAKS DURING PROOF TEST

Figure 5-4. Fracture Mechanics Proof Test Logic - Five-Cycle Loading (Modified from [5-96]).

Vroman [5-97], for considered material/loading combinations, that the threshold level below which stable flaw growth does not occur is maintained in spite of the greater number of proof test cycles. If this critical assumption is significantly incorrect, that is if the threshold is to drop from a/Q = 0.5 mm for the first cycle to, say, a/Q = 0.3 mm for the fifth cycle, any advantages of multi-cycle proof testing would disappear and cycles beyond the first cycle would be quite detrimental.

Figure 5-3 shows the results of a single-cycle proof test schematically. It indicates the presence of three regions corresponding to I) initial crack sizes small enough that service life can be guaranteed whether or not a proof test takes place, II) the hopefully narrow range within which the proof test actually causes subsequent field failure through stable flaw growth (i.e., without the proof test, in-service failure would be avoided.) III) initial crack sizes large enough such that failure occurs during proof testing and, consequently, the proof test eliminates what otherwise would have been an in-service failure.

Figure 5-4 summarizes the results of a five-cycle proof test. Both Figure 5-3 and Figure 5-4 contain the simplifying assumption that the proof test level for a single cycle has been set at a value which would cause failure of a crack of size "a/Q^{cr}", the same size as the minimum that can cause an in-service failure. Other graphical constructs could be made for more complex situations.

In Figure 5-4, the greater amount of stable flaw growth associated with multi-cycle loading results in a rotation of the line labeled "failure loci based on the inital crack size". This narrows the proof-test "danger" region

(II) by "promoting" more flaws into a proof-test failure while still having little or no effect upon flaws of size less than a/Q = 0.75 mm. Because some flaws are promoted into the danger region by cycles beyond the first, note that the left side of Region II shifts downward on the inital crack size scale but the right side of Region II shifts downward even further, narrowing the danger zone where service life cannot be guaranteed. Of course, from probabilistic considerations we know that a simple narrowing of Region II, on such plots as Figure 5-3 and Figure 5-4, does not guarantee a reduced risk associated with multi-cycle proof testing. The initial flaw size distribution must also be considered, especially since, in most situations the pre-proof test probability densities associated with small flaws are larger than those associated with slightly larger flaws.

Figure 5-5 exemplifies the all-important impact of the initial flaw size distribution upon the optimum number of proof test loading cycles. The illustrative example is fully specified in Figure 5-5 and is unrelated to that summarized ir Figures 5-1 and 5-4. For the new example, the imposition of the first proof test actually increases the in-service failure probability by 50%, from 0.00020 to 0.00030. This is because more defects are "promoted", with stable flaw growth, from a benign to a dangerous size than are grown from a dangerous size to a proof test failure. The trend reverses for the second proof test cycle, so as to reduce the in-service failure rate to the same value, 0.00020, as for no proof testing whatsoever. The third, fourth, and subsequent proof test cycles reduce the in-service failure probability substantially and monotonically, at the cost of additional proof test failures, as well as their operational costs. Eventually a point of diminishing returns will be reached beyond which additional cycling is not warranted. The results

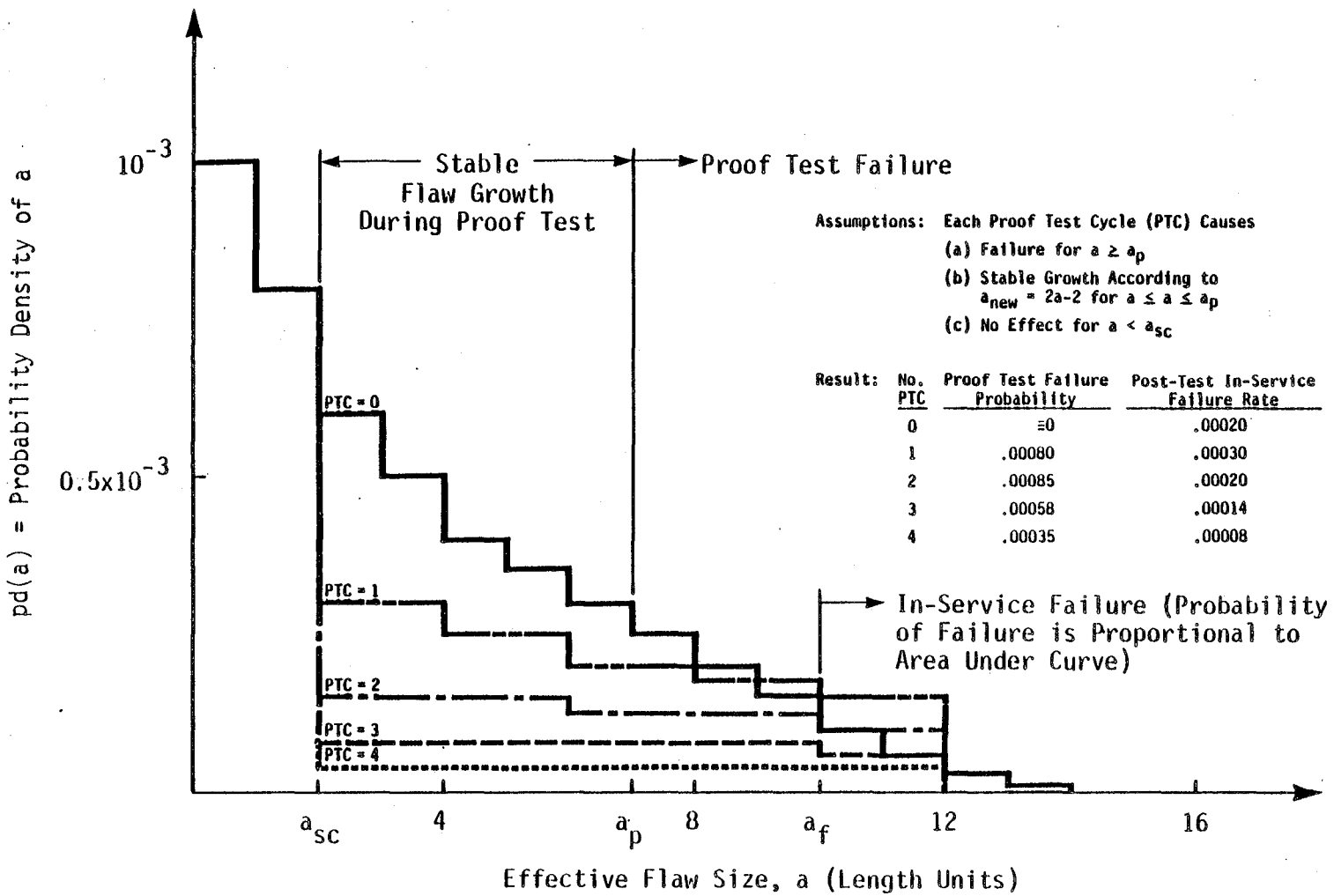

Figure 5-5. Numerical Example Illustrating the Complex Effects of Multiple Cycle Proof Testing Under Stable Crack Growth. Note that for the Assumptions Used, the Highest In-Service Fracture Rate Occurs if a Single Proof Test Cycle is Employed.

of the example in Figure 5-5 could be easily changed by modifying the initial flaw size distribution, stable flaw growth properties, or complexity of the physical and economic models and criteria. Any number of proof test cycles, including zero, could be "made" optimum by changing the example. Thus, it is clear that each problem must be evaluated on its own merits. There is no single number of proof test cycles that are optimum.

To summarize this graphical description, and as reported in Reference 5-96, multi-cycle proof testing offers three possible advantages over single-cycle testing. First, multi-cycle loading can reduce the region of crack sizes, and more significantly but not equivalently the number of components, for which service life cannot be guaranteed. Second, the lower proof test level that can be used in multi-cycle loading promotes leak before burst in, for example, pipes and pressure vessels, and causes less damage to the tested structure which therefore may be repairable. Third, the lower proof test level usually associated with multi-cycle loading reduces the chances of overstraining and cracking regions of low ductility that are otherwise defect free. Two additional advantages to multi-cycle proof tests of certain material/structure combinations are (1) an increased number of opportunities to detect crack-induced damage through non-destructive inspection and (2) the capacity to sharpen defects into cracks during unloading from the first proof cycle so that they will fail during a subsequent proof test cycle.

Several confounding elements can reduce or eliminate advantages of multi-cycle proof testing in some situations. At NASA's request, an effort was made to locate references and experts who tended to favor single-cycle proof testing in order to bring out the controversy in this area. Our search revealed

three references and one interview to support the single-cycle concept. The references are due to Irwin [5-94], Schliessmann [5-100] and Formby [5-93] and the interview was with Tiffany [5-101]. The three references reported specific situations in which the value of multiple proof test cycles was reduced. The reasons for these reductions in value are well understood and, in our opinion, do not constitute grounds for rejecting multiple-cycle testing in general. However, the interview with Tiffany covered, albeit qualitatively, more fundamental objections to multi-cycle testing which, we believe, should be considered before specifying multiple cycles.

In the work of Irwin and Corten [5-94] on proof testing of natural gas transmission lines, a change was recommended from a multi-cycle test to a higher-load single-cycle test, based on special considerations of this engineering problem. These special considerations revolved around the fact that leak-before-burst was considered a severe disadvantage during proof testing of this component, because bursts or leaks had about the same repair costs and burst failures were far easier to find than leaks in the all important phase of inspection following proof testing (Section 5.4.6). Also, some significant costs were avoided, associated with the additional cycles of testing. Thus the findings of Irwin and Corten, that high-load single-cycle testing was preferred, would only be relevent for similar cases in which discovery of the damage caused by the proof test was more important than the severity of the damage to the tested component.

The work of Formby involved pressure vessels with an extremely ductile C-Mn pressure vessel steel of low yield strength levels of between 30 and 40 ksi. Our review of Formby's results indicates that all failure modes were

essentially ductile and associated with plastic collapse (i.e., net section exceedance of ultimate strength under membrane stress and/or plastic hinge due to bending). Essentially, with no elements of brittle or crack-aided fracture involved, none of the proof test strategies Formby explored were of significant value and, under these conditions the higher cost of multi-cycle proof testing would, of course, be unjustified.

Similarly, the comments of Schliessmann [5-100] can be dismissed from our subject area since the steels tested (4335V and D6AC) exhibited little or no stable flaw growth. From the discussion illustrated by Figures 5-1 through 5-4, it is clear that only the stable flaw growth characteristic can make multi-cycle proof testing substantially more beneficial than single-cycle testing and, as stated, our topic covers only those materials that exhibit stable flaw growth.

In the interview with Tiffany, he made several key points. He stated that it is good common sense engineering practice to expose the structure to the high proof test loads as infrequently and for as short of duration as possible to avoid excessive plastic deformation and other damage to the structure. Cost of additional cycles is another factor cited by Tiffany, but his current preference for single-cycle testing is motivated primarily by a desire not to damage the structure in subtle, uninspectable ways during proof testing. Upon our questions regarding the fact that multi-cycle proof testing can be performed at loads less than the single-cycle, Tiffany points out that in most of the proof test applications of which he has knowledge, innovative techniques are available to lower the required single-cycle load level and to make the single-cycle proof testing a more effective screen. He emphasized

the use of proof test temperatures lower than any to be experienced in-service. As the interview preceeded, it appeared that Tiffany's position could be summarized by the statement that "additional cycles could prove to be dangerous and costly and other techniques to increase the screening capability of the proof test should be sought first".

During our first major exposure to the single- versus multi-cycle proof test controversy we developed the opinion that there are several competing effects (discussed above) that could swing the balance between the two procedures. A pervading and confounding element is the probabilistic nature of many of the key parameters such as threshold level below which stable flaw growth does not take place. Thus, while many of the arguments against multi-cycle proof testing available in the literature can be dismissed qualitatively, a quantitative, perhaps probabilistic, analysis (as simplified in the example in Figure 5-5) and revealing structural simulation experiments may be required to decide the number and magnitude of load cycles and to truly optimize the proof test. The rapidly building in-service experience with proof testing must be included in this analysis. For example, the most relevant in-service experience is highlighted by the success at Rocketdyne mentioned before which shows an improved and currently trouble-free record of all component failure modes upon which five-cycle proof testing has been applied.

5.4.3 Probabilistic Characterizations of Proof Testing

The probabilistic fracture mechanics (PFM) models described in Section 5.3 reveal that three elements have important roles in proof test logic and

implementation. These three elements are the probability distribution of crack-like defect size, pd(a), probability of rejection of a component given a certain defect size, $P(R\backslash a)$, and probability of failure given that a component with flaw size "a" has been accepted, $P(F\backslash a,\overline{R})$.

Flaw Size Distribution, pd(a)

With respect to pd(a) as shown in Figure 5-5, the engineer must be concerned with more than one flaw size distribution. The general effect of proof testing tough ductile materials which exhibit stable flaw growth is to eliminate those few components with the largest proof-test critical flaw sizes but to promote intermediate size flaws to levels which may either be innocuous or dangerous for in-service use. As shown in the figure, multiple proof test cycles increase both the elimination of large flaws and the promotion of intermediate size flaws.

The variations of effective initial flaw size within a population of components to be proof tested is, by definition, an important element in the probabilistic characterization of proof testing. Without this variation among components, proof test logic would make no sense in that there would be no need to screen out "bad" components from a population of identical components. Consequently, it is not surprising to see that the three most enlightening probabilistic references emphasize the role of flaw size distribution in the proof test logic. These three references are by Vroman and Creager [5-96], Harris [5-103], and Buntin [5-92]. The difficultly in establishing accurate flaw size distributions is well known although, for welded structures, much useful information is becoming available (see Section 5.3 for a review of

information available in this area). However, the use of bounding or calibrated estimates, rather then precise values, of pd(a) can also lead to a well-designed proof test.

As shown in detail by Vroman and Creager [5-96], innovative techniques may be used to calibrate the flaw size distribution used with the rest of the PFM model. Specifically, Vroman and Creager use an adjustable constant in their function describing the initial flaw size distribution and solve for the value of that constant that would most likely produce precisely the history of proof test failures observed in the structure. This type of innovative reliance on relevent historical data is a good example of what is meant by combined or calibrated numerical analysis (CA) discussed in Section 5.3.4. CA, as applied in Reference 5-96, establishes a valid baseline condition not only for the flaw size distribution, but for the overall PFM model. After a successful application of CA, the engineer is burdened only with the important problems of interpolating and extrapolating the calibrated model to situations which differ significantly from the average historical conditions.

Probability of Rejection via Proof Test Failure or Associated NDE, P(R\a)

With respect to acceptance or rejection of components with a given flaw size [P(R\a)], the proof test is in itself a form of inspection. The simplest characterization of the combined effects of the proof test (and all associated destructive and non-destructive inspections) is by one probabilistic function, P(R\a). However, if enough data is available, sometimes a large amount of knowledge may be gained by considering the effects of inspection separately to

insure for example, that an optimum NDE inspection is used with the proof test (see for example Harris [5-103]).

Conditional In-Service Failure Probability [$P(F\backslash a,\bar{R})$]

The use of proof test logic also complicates the description of failure probabilities in that two failure modes must be considered simultaneously. These are, the failure probability during the proof test (part of $P(R\backslash a)$) and the failure probability in-service given that there was no proof test failure, $P(F\backslash a,\bar{R})$. Any attempt to characterize these two failure probabilities simultaneously should account for any statistical dependence between them. Such factors as a higher- or lower-than-usual fracture toughness, for example, could tend to cause both failure probabilities to increase or decrease together.

5.4.4 Literature Review

As stated above, only three references were located which attempted a PFM model of proof testing of tough ductile materials. Following is a summary of the effects considered and not considered in each of the references.

Vroman and Creager [5-96]

Vroman and Creager developed and executed proof tests of several critical Rocketdyne engine structures. They emphasized the proper characterization and estimation of the flaw size distribution from historical data. They also emphasized the notion of a probabilistic evaluation of single-cycle versus multi-cycle proof testing and the stable flaw growth occurring during proof

test as a critical part of the PFM model. Of all references evaluated, Reference 5-96 contained the most substantial combination of data and analysis for evaluating multi-cycle proof testing.

All important deterministic elements of the proof tests were considered. However, some of the probabilistic elements not considered by Vroman and Creager's PFM model are the statistical variations of (1) failure both during proof testing and in-service, (2) stable flaw growth in-service, (3) fatigue or stress corrosion cracking (SCC) during multiple cycle proof testing, (4) periodic applications of proof testing or NDE, and (5) the role of NDE in probabilistically truncating the flaw size distribution.

Most of the statistical elements lacking are incorporated implicitly or explicitly as "best" or "conservative estimates" in Vroman and Creager's deterministic model. For example, the role of NDE is modeled as a perfect truncation of the flaw size distribution which removes all cracks larger than a given size, a_0. Furthermore, many of the other statistical elements lacking are not important such as the fatigue crack growth rate variations exhibited during multiple cycle proof testing. Since as a practical matter the number of proof test cycles will probably not exceed five, this fatigue crack propagation is negligible. However, in the parameteric study considered in the paper which looks at many more than five proof test cycles, the in-service failure rate is seen to decrease monotonically with increases in the number of proof test cycles. It is believed that incorporation of fatigue crack growth in the model would show that this trend must eventually reverse and that fatigue crack growth during proof testing would be a problem.

Harris [5-103]

Harris concentrates on the use of periodic proof testing for long-life structures in close combination with an acoustic emission NDE technique which appears to be quite effective for the structural/material combination considered. The PFM model emphasizes the effect of proof testing and NDE on a time-dependent flaw size distribution. Among the elements lacking from the PFM analysis are statistical characterization of failure probabilities both during proof and service tests, stable flaw growth, and multiple versus single cycle proof testing. The elements lacking from the PFM formulation may or may not be important for the specific applications of Harris. For purpose of our survey, the prime contribution of Reference 5-103 to show the important interrelationship between proof testing and an effective NDE procedure.

Buntin [5-92]

Buntin's paper on proof testing of the F-111 airplane appears to describe the most complete PFM characterization of proof test logic from our survey. All three probabilistic elements are considered quantitatively in the PFM model. However, modeled statistical dependencies among these elements are not complete. For example, the previously discussed effect of changes in the fracture toughness on both in-service and proof test failure probabilities is not modeled. Buntin's paper describes some innovative proof testing techniques which will be discussed in Section 5.4.5 and models, simultaneously, in-service stress corrosion cracking (da/dt) and fatigue crack growth (da/dn). Among the elements lacking from the overall PFM model is lack of consideration of stable flaw growth (which may or may not be needed with the D6AC material

considered) and a seemingly over-simplified characterization of the alternating stress intensity factor in-service. One major problem with Buntin's alternating stress intensity factor characterization is the use of a yield stress based on monotonic rather than cyclic loading to estimate the effect of plastic zone size on in-service da/dn. Any plastic zone correction must be based on cyclic properties and must be consistently applied for calculation of in-service conditions and reduction of the experimental data upon which the in-service calculations are based.

Summary of Role of PFM Models for Proof Tests

The need to perform some degree of optimization during proof testing, and to address trade-offs between proof tests so stringent that they eliminate an undesireably large fraction of the population and proof tests so liberal that they permit too high of an in-service failure probability, increases the need for more effective PFM models of proof test logic. The confounding element of stable flaw growth is that a hopefully small segment of the population will be damaged to some extent by proof testing and probabilistic considerations are often needed to determine whether the damage accumulated by the small fraction of the population is more than compensated by the aggregate benefit of the proof testing and associated NDE procedures to the majority of the population.

5.4.5 Innovative Proof Testing Techniques

The present investigators were somewhat disappointed in the lack of innovative proof testing ideas and techniques in the literature. The paper by Buntin [5-92] appeared to be the best source of such methods in describing

both a cold test of an entire F-111 aircraft and an innovative technique for optimizing the method for proof testing and, through judicious delay before the post-test NDE inspection, checking residual stress induced stress corrosion cracking around fastener holes of critical wing and body structure on the F-111.

It is believed that many more innovative techniques are available to increase the power and reliability of proof testing. One area lacking from the literature we reviewed, for example, is a discussion of the possible role of alternating hot and cold proof test cycling. For example, one or more high temperature proof test cycles could be used to produce favorable residual stress fields, encourage stable flaw growth to occur, and to open up and blunt cracks for greater inspectability and more benign behavior in service. These warm proof tests could be followed by one or more cold proof test cycles to remove the bad actors from the population with little or no danger of stable flaw growth (which would have been exhausted by the hot proof test with the material in a more tough and ductile state). Clearly, the benefits of any feasible complex combination of proof test cycling loads and temperatures would have to be demonstrated in the laboratory for a whole series of specimens or structural simulators with initial flaws ranging from innocuous to very dangerous.

5.4.6 Relationship Between Non-Destructive Inspection and Proof Testing

It is an old, well-established, engineering practice to throughly inspect structures during and after proof test cycling. It is necessary to pinpoint any undesireable permanent deformation induced in the structure, stable flaw

growth, and any other manifestations of subtle failure modes. Aside from ensuring as much as possible that proof testing has not materially damaged the structure, the need for such intensive NDE is indicated both qualitatively and quantitatively by the fact that, by definition, the proof test loads or environment factors should equal or exceed anything within the in-service design envelope. Thus post-test NDE results can provide the designer with much useful knowledge.

Many interesting qualitative aspects of inspection before, during, and after proof testing are described in two older papers on the interrelationship of NDE and proof testing of large chains [5-105] and light poles [5-104]. These two references and others state emphatically that inspection during proof testing is a critical and well established engineering practice for a wide variety of structures. Harris' quantitative work and experimental demonstration of the positive synergism of acoustic emission NDE and proof testing has already been mentioned [5-103]. The severity of the proof test loads opens the door for more work in this area ranging from the use of NDE techniques during the proof test load (when for example, tensile plastic deformation is at its peak and many critical crack-like defects should be the most wide open and inspectable) and the use of techniques such as "ringing" which is now being introduced successfully to the inspection of large offshore oil-drilling platforms. The notion is to strike (non-destructively) critical members, and record the "ringing" sound both before and after proof testing to see if the free vibration characteristics have been changed. If changes have occurred, more detailed inspections are used to determine their causes, which might include, for example, extensive local plastic deformation or stable flaw growth.

5.5 WELD CRACKS

Fracture mechanics analysis of the behavior of weld defects is an important area in a wide variety of structural components, including those found in aerospace applications. Special aspects of the use of fracture mechanics to determine the influence of weld defects on structural integrity will be covered in this section. The additional topic of methods which do not include fracture mechanics (such as the use of S-N curves to predict fatigue strength) will not be addressed.

Welds, by their very nature, often contain defects. Furthermore, they contain regions of varying microstructure and composition, often with materials of reduced toughness. They often include zones of tensile residual stresses which can accelerate crack initiation and propagation, and commonly include geometric stress concentrations as a result of the shape and location of the weld. As a consequence of these factors, welds are responsible for a high proportion of structural failures, and applying fracture mechanics to weld defects is therefore particularly important.

Many of the facets of applying fracture mechanics to the behavior of weld defects are common to other areas already discussed, such as fatigue crack growth, failure criteria, etc. This section will discuss aspects of the technology peculiar to welds, with special emphasis on areas relevant to the SSME program.

The main types of weld defects encountered in the SSME have been identified in discussions with knowledgeable personnel to be the following [5-107 through 5-110]

- weld porosity,
- microfissuring in the nailhead region of the electron beam welds, possibly associated with Laves phases in the Inconel 718,
- lack of fusion between passes because oxide on a previous pass has not been removed, and
- lack of fusion at root or sidewall.

Porosity in general presents little direct threat to structural integrity, unless it is very extensive [5-111]. The major problems with the presence of porosity are that it may mask more serious defects and that it indicates questionable weld quality. The region subject to microfissuring is limited in size. Furthermore, the cracks are not perpendicular to the maximum tensile stresses. Tests on large welded testpieces showed the microfissuring not to have a significant effect on fatigue or tensile strength [5-110]. The major type of defect to be addressed by fracture mechanics is thus lack of fusion, interpass, root or sidewall. Such defects are generaly sharp and crack-like.

The general approach to evaluating the significance of postulated or actual weld defects has been LEFM, particularly as described in Reference 5-112. The approach uses a computer program to calculate fatigue crack propagation and eventual breakthrough or failure using techniques discussed in Sections 3.6 and 3.7. Postulated defects are based on estimates from NDE personnel as to sizes of defects which might not be detected in certain areas, particularly areas where inspection is difficult. LEFM has been used even though maximum stress levels, taking into account stress concentrations, may reach or considerably exceed yield [5-107]. This approach is thought to be conservative in view of the highly ductile materials used [5-113]. For a more

exact analysis, elastic-plastic fracture mechanics (EPFM) would need to be applied.

Weld defects usually grow due to cyclic loading in field applications. The techniques for analysis of fatigue crack growth outlined in Section 3 are generally applicable to the crack-like weld defects of concern, with References 5-112, 5-114 through 5-124 providing examples of such applications. For crack-like defects agreement between experimental and analytical results has generally been good, and this approach is now well established, including use in codes [5-125]. These papers cover a wide range of materials including steels, aluminum alloys and titanium alloys, although work on nickel alloys appears to have been limited. In spite of this success, some problems remain in application to structures. Some of these are well summed up by Hoeppner [5-126]. They include:

- The variation in composition and/or microstructure throughout the weld and HAZ. It is important to generate crack growth rate data applicable to the region through which the defect is propagating, or at least generate data which form an upper bound to growth rates.
- Growth rate data should be generated for appropriate environments, since environment can have a major effect on crack propagation [5-127, 5-128], and discussion in Section 3.5. Closely tied to environmental effects are frequency effects. Cycling rate must be slow enough to allow environmental interactions to produce their full effect on propagation rates. These effects are discussed in more detail in Section 3.
- Weld residual stresses can have very significant effects on defect propagation [5-123, 5-129]. The complexity of residual stress patterns, unless the weld is adequately stress relieved, can make such effects difficult to predict. This is discussed in more detail in Section 5.1.
- The geometry of many welded joints results in stress concentrations, the magnitude of which can be difficult to predict.

Fracture mechanics methods are essentially limited to crack-like defects and do not treat rounded defects such as porosity accurately (although they do treat such defects conservatively).

The criteria for breakthrough and/or final failure of welds are the same as discussed in earlier portions of this review. Even though the procedures employed are the same, it must be borne in mind that the material parameters involved (such as K_{IC}, J_{IC}, T_{mat}, CTOD, etc.) may be different in welds than in the base material. Such differences must be recognized, and data applicable to the type of welds being analyzed should be used when possible.

The problems associated with applying fracture mechanics to the analysis of the behavior of weld defects result in uncertainties in life prediction. For example, Thielsch [5-130] considers fracture mechanics currently a useful tool in deciding whether or not defects require repair or components need replacement, but only a tool. He relies finally on experience and cites cases where electric utility rotors have run successfully for several years after they would have been rejected on the basis of fracture mechanics. Nevertheless, in spite of these limitations, the overwhelming experience cited in the literature in using LEFM to predict weld defect propagation rates is positive. The problems cited above are, for the most part, not theoretical problems with the methodology but instead practical problems with its application. They can, at least in principle, be solved with improved experimentation.

5.6 REFERENCES

5-1. Ruud, C.O., "A Review and Evaluation of Non-Destructive Methods for Residual Stress Measurement," EPRI Report NP-1971, Project 1395-5, Electric Power Research Institute, Palo Alto, California, September 1981.

5-2. Kino, G.S., Hunter, J.B., Johnson, G.C., Selfridge, A.R., Barnett, D.M., Hermann, G., and Steele, C.R., "Acoustoelastic Imaging of Stress Fields," Journal of Applied Physics, Vol. 50, No. 4., pages 2607-2613, April 1979.

5-3. "Proceedings of a Workshop on Non-Destructive Evaluation of Residual Stress," Air Force Materials Laboratory, NTIAC-76-2, August 13-14, 1975.

5-4. Thompson, D.O., and Chimenti, D.E., editors, Review of Progress in Quantitative Non-Destructive Evaluation, Vol. 1, Plenum Press, 1981.

5-5. Mordfin, L., "Standards for Residual Stress Measurement," Residual Stress Effects in Fatigue, ASTM Special Technical Publication 776, pages 6-12, 1982.

5-6. Tsai, Swe-Den, Schmerling, M., and Marcus, H.L., "Residual Stress Measurement in Metal Matrix Composites," Residual Stress and Stress Relaxation, Proceedings of the Twenty-Eighth Sagamore Army Materials Research Conference, July 13-17, 1981, Plenum Press, New York, pages 425-438, 1982.

5-7. Darlane, A.J.A., "The Determination of Residual Stresses: A Review of Contemporary Measurement Techniques," Proceedings of an International Conference entitled Residual Stresses in Welded Construction and Their Effects, The Welding Institute, November 15-17, 1977.

5-8. Vande Walle, L.J., editor, Residual Stress for Designers and Metallurgists, Proceedings of a conference held 9-10 April 1980, Chicago, Illinois, American Society for Metals, 1981.

5-9. Lessels, J.M., and Brodrick, R.F., "A Critical Study of the Stress Distribution Produced by Shot-Peening," Society of Automotive Engineers.

5-10. Metals Handbook, Heat Treating, Cleaning and Finishing, Vol. 2, 8th Edition, American Society for Metals.

5-11. Shot Peening Applications, 5th Edition, Metals Improvement Company, Teaneck, New Jersey.

5-12. Masubuchi, K., Analysis of Welded Structures, Residual Stresses, Distortion and Their Consequences, Pergamon Press, 1980.

5-13. Rybicki, E.F., and Stonesifer, R.B., "Computation of Residual Stresses Due to Multipass Welds in Piping Systems," ASME 78-PVP-104, June 1978.

5-14. Tall, L., "The Calculation of Residual Stress-In Perspective," Proceedings of an International Conference entitled Residual Stresses in Welded Structures and Their Effects, The Welding Institute, November 15-17, 1977.

5-15. Masubuchi, K., et al., "Analysis of Thermal Stress and Metal Movement During Welding," NASA Contract Report CR-61351, December 1970.

5-16. Liu, Y.J., and Hsu, T.B., "On Residual Stress/Strains in Pressure Vessels Induced by Cyclic Thermomechanical Loads," ASME 82-PVP-27.

5-17. Residual Stress Effects in Fatigue, ASTM Special Technical Publication 776, 1982.

5-18. Residual Stress and Stress Relaxation, Proceedings of the Twenty-Eighth Sagamore Army Materials Research Conference, July 13-17, 1981, Plenum Press, 1982.

5-19. Lawrence, F.V., Burk, J.D., and Yung, J-Y, "Influence of Residual Stress on the Predicted Fatigue Life of Weldments," Residual Stress Effects in Fatigue, ASTM Special Technical Publication 776, pages 33-43, 1982.

5-20. Besuner, P.M., et al., "BIGIF Fracture Mechanics Code for Structures," Research Project 700-5, Electric Power Research Institute, April 1981.

5-21. "Structural Welding Code-Steels," American Welding Society, 1979.

5-22. Maddox, S.J., "Influence of Tensile Residual Stresses on the Fatigue Behavior of Welded Joints in Steel," Residual Stress Effects in Fatigue, ASTM Special Technical Publication 776, pages 63-96, 1982.

5-23. Satoh, K., Transactions of the Japan Welding Society, Vol. 3, No. 1, April 1972.

5-24. Heaton, M.D., "On the Calculation of Stress Intensity Factors Due to Thermal and Residual Stress Fields," Central Electricity Generating Board, England, Research Report No. NW/SSD/RR/158/76, December 1976.

5-25. Parker, A.P., "Stress Intensity Factors, Crack Profiles, and Fatigue Crack Growth Rates in Residual Stress Fields," Residual Stress Effects in Fatigue, ASTM Special Technical Publication 776, pages 13-31, 1982.

5-26. Glinka, G., "Effect of Residual Stresses on Fatigue Crack Growth in Steel Weldments Under Constant and Variable Amplitude Loads,"

Fracture Mechanics, ASTM Special Technical Publication 677, pages 198-214, 1979.

5-27. Nelson, D.V., "Effects of Residual Stress on Fatigue Crack Propagation," Residual Stress Effects in Fatigue, ASTM Special Technical Publication 776, pages 172-194, 1982.

5-28. Harris, D.O., "Stress Corrosion Crack Growth in the Presence of Residual Stress," Residual Stress and Stress Relaxation, Twenty-Eighth Sagamore Army Materials Research Conference, Plenum Press, pages 273-295, 1982.

5-29. Harris, D.O., and Dedhia, D.D., "The Influence of Residual Stresses on the Growth of Semi-Elliptical Stress Corrosion Cracks in Pipes," presented at the ASME Pressure Vessel and Piping Conference session on Crack Growth in Weld Induced Stress Fields, Portland, Oregon, June 1983.

5-30. Boley, B., and Weiner, J., Theory of Thermal Stresses, John Wiley, New York, 1960.

5-31. Manson, S.S., Thermal Stress and Low Cycle Fatigue, Krieger Publishing Company, 1981.

5-32. Hetnarski, R.B., editor, Journal of Thermal Stresses, Hemisphere Publishing Company.

5-33. Hasselman, D.P.H., "Crack Propagation Under Constant Deformation and Thermal Stress Fracture," International Journal of Fracture, Vol. 7, No. 2, pages 157-161, June 1971.

5-34. Chell, G.G., and Ewing, D.J.F., "The Role of Thermal and Residual Stresses in Linear Elastic and Post Yield Fracture Mechanics," International Journal of Fracture, Vol. 13, No. 4, pages 467-479, August 1977.

5-35. Blauel, J.G., Kalthoff, J.F., and Stahn, D., "Model Experiments for Thermal Shock Fracture Behavior," Journal of Engineering Materials and Technology, Transactions of the ASME, Vol. 96, Series H, No. 4, pages 299-304, October 1974.

5-36. Florence, A.L., and Goodier, J.N., "Thermal Stresses Due to Disturbance of Uniform Heat Flow by an Insulated Ovaloid Hole," Journal of Applied Mechanics, Transactions of the ASME, Vol. 82, Series E, pages 635-639, December 1960.

5-37. Florence, A.L., and Goodier, J.N., "The Linear Thermoelastic Problem of Uniform Heat Flow Disturbed by a Penny-Shaped Insulated Crack," International Journal of Engineering Science, Vol. 1, pages 533-540, 1963.

5-38. Sih, G.C., "On the Singular Character of Thermal Stresses Near a Crack Tip," Journal of Applied Mechanics, Transactions of the ASME, pages 587-589, September 1962.

5-39. Sekine, H., "Influence of an Insulated Circular Hole on Thermal Stress Singularities at Tips of a Crack," International Journal of Fracture, Vol. 13, No. 2, pages 133-149, April 1977.

5-40. Sekine, H., and Mura, T., "Thermal Stresses Around an Elastic Ribbonlike Inclusion with Good Thermal Conductivity," Journal of Thermal Stresses, Vol. 2, pages 275-489, 1979.

5-41. Sekine, H., "Thermal Stresses Near Tips of an Insulated Line Crack in a Semi-Infinite Medium Under Uniform Heat Flow," Engineering Fracture Mechanics, Vol. 9, pages 499-507, 1977.

5-42. Sekine, H., "Thermal Stresses Singularities at Tips of a Crack in a Semi-Infinite Medium Under a Uniform Heat Flow," Engineering Fracture Mechanics, Vol. 7, pages 713-729, 1975.

5-43. Koizumi, Takashi, Takahuda, Kazuo, Shibuya, Tashikazu, and Nishizawa, Takao, "An Infinite Plate with a Flaw and Subjected to Uniform Heat Flow," Journal of Thermal Stresses, Vol. 2, pages 341-351, 1979.

5-44. Emery, A.F., "Thermal Stress Fracture in Elastic-Brittle Materials," Thermal Stresses in Severe Environments, International Conference on Thermal Stresses in Materials and Structures in Severe Thermal Environments, Plenum Press, pages 95-121, 1980.

5-45. Stern, M., "The Numerical Calculation of Thermally Induced Stress Intensity Factors," Journal of Elasticity, Vol. 9, pages 91-95, 1979.

5-46. Stern, M., "On Calculating Thermally Induced Stress Singularities," Thermal Stresses in Severe Environments, Plenum Press, pages 123-134, 1980.

5-47. Reynen, J., "Surface Cracks in Cylinders During Thermal Shock," ASME Paper 77-PVP-5, New York, 1977.

5-48. Heaton, M.D., "On The Calculation of Stress Intensity Factors Due to Thermal and Residual Stress Fields," Central Electricity Generating Board, North Western Region, Scientific Services Department, Research Report NW/SSD/RR, pages 158-176, December 1976.

5-49. Bueckner, H.F., "The Propagation of Cracks and the Energy of Elastic Deformation," Transactions of ASME, Vol. 80E, pages 1225-1230, 1958.

5-50. McLean, J.L., Cohen, L.M., and Besuner, P.M., "Effects of Location, Thermal Stress and Residual Stress on Corner Cracks in Nozzles with

Cladding," International Journal of Pressure Vessels and Piping, pages 308-161, 1979.

5-51. Labbens, R.C., Heliot, J., and Pellissier-Tanon, A., "Weight Functions for Three-Dimensional Symmetrical Crack Problems," Cracks and Fracture, ASTM Special Technical Publication 601, pages 448-470, 1976.

5-52. Emery, A.F., Walker, G.E., and Williams, J.A., "A Green's Function for the Stress Intensity Factor of Edge Cracks and Its Application to Thermal Stresses," Journal of Basic Engineering, Transactions of the ASME, Vol. 91, pages 618-624, 1969.

5-53. Kobayashi, A.S., and Enetanya, A.N., "Stress Intensity Factor of a Corner Flaw," Mechanics of Crack Growth, ASTM Special Technical Publication 590, pages 477-495, 1976.

5-54. Peters, W.H., and Blauel, J.G., "A Study of Part-Through Cracks in a Reactor Beltline Subjected to Thermal Shock," Thermal Stresses in Severe Environments, Plenum Press, pages 273-286, 1980.

5-55. Harris, D.O., Lim, E.Y., and Dedhia, D.D., "Probability of Pipe Fracture in the Primary Coolant Loop of a PWR Plant, Vol. 5: Probabilistic Fracture Mechanics Analysis," U.S. Nuclear Regulatory Commission Report NUREG/CR 2189, Vol. 5, Washington, D.C., 1981.

5-56. Dedhia, D.D., Harris, D.O., and Lim, E.Y., "The Influence of Non-Uniform Thermal Stresses on Fatigue Crack Growth of Part-Through Cracks in Reactor Piping," published in the Proceedings of the Fourteenth National Symposium on Fracture Mechanics, American Society of Testing and Materials, Philadelphia, Pennsylvania, 1982.

5-57. Dedhia, D.D., Harris, D.O., and Denny, V.E., "TIFFANY: A Computer Code for Evaluation of Thermal Stress Intensity Factors for Surface Cracks in Clad Piping," SAI-331-82-PA, report to Lawrence Livermore National Laboratory by Science Applications, Inc., Palo Alto, California, November 1982.

5-58. Cruse, T.A., and Besuner, P.M., "Residual Life Prediction for Surface Cracks in Complex Structural Details," Journal of Aircraft, Vol. 12, No. 4, pages 369-375, April 1976.

5-59. Blackburn, W.S., et al., "An Integral Associated with the State of a Crack Tip in a Non-Elastic Material," International Journal of Fracture, Vol. 13, No. 2, pages 183-199, 1977.

5-60. Wilson, W.K., and Yu, I.W., "The Use of the J-Integral in Thermal Stress Crack Problems," International Journal of Fracture, Vol. 15, No. 4, pages 377-387, August 1979.

5-61. Ainsworth, R.A., et al., "Fracture Behavior in the Presence of Thermal Strains," Proceedings of the Institution of Mechanical

Engineers, Conference on Tolerance of Flaws in Pressurized Components, page 197, May 1978.

5-62. Gurtin, M., "On a Path-Independent Integral for Thermoelasticity," International Journal of Fracture, Vol. 15, pages R169-R170, 1979.

5-63. Auki, S., Kishimato, K., and Sakato, M., "Crack-Tip Stress and Strain Singularity in Thermally Loaded Elastic-Plastic Material," Journal of Applied Mechanics, Vol. 48, pages 428-429, June 1981.

5-64. Gemma, A.K., and Philips, J.S., "The Application of Fracture Mechanics to Life Prediction of Cooling Hole Configurations in Thermal-Mechanical.Fatigue," Engineering Fracture Mechanics, Vol. 9, pages 25-26, 1977.

5-65. Miller, A.G., "Crack Propagation Due to Random Thermal Fluctuations: Effect of Temporal Incoherence," International Journal of Pressure Vessels and Piping, Vol. 8, pages 15-24, 1980.

5-66. Leis, B., Hopper, A., Ghadiali, N., Jaske, C., and Hulbert, G., "An Approach to Life Prediction of Domestic Gas Furnace Clam Shell Type Heat Exchangers," Thermal Stresses in Severe Environments, Plenum Press, pages 207-228, 1980.

5-67. Cost, T., "Reliability Analysis of Thermally Stressed Viscoelastic Structures by Monte Carlo Simulations," Thermal Stresses in Severe Environments, pages 431-446, 1980.

5-68. Shinozuka, M., and Yang, J.N., "Optimum Structural Design Based on Reliability and Proof Load Test," Annals of Assurance Science Proceedings of the Reliability and Maintainability Conference, Vol. 8, July 1969.

5-69. Heer, E., and Yang, J.N., "Structural Optimization Based on Fracture Mechanics and Reliability Criteria," AIAA Journal, Vol. 9, pages 621-628, April 1971.

5-70. Yang, J.N., and Trapp, W.J., "Reliability Analysis of Aircraft Structures Under Random Loading and Periodic Inspection," AIAA Journal, Vol. 12, pages 1623-1630, December 1974.

5-71. Graham, T.W., and Tetelman, A.S., "The Use of Crack Size Distribution and Crack Detection for Determining the Probability of Fatigue Failure," AIAA Paper 74-393, presented at AIAA/ASME/SAE Fifteenth Structures, Structural Dynamics and Materials Conference, Las Vegas, Nevada, April 1974.

5-72. Cramond, J.R., "A Probabilistic Analysis of Structural Reliability Against Fatigue and Fracture," Ph.D. dissertation, University of Illinois at Urbana-Champaign, 1974.

5-73. Becher, P.E., and Pedersen, A., "Application of Statistical Linear Elastic Fracture Mechanics to Pressure Vessel Reliability Analysis," Nuclear Engineering and Design, Vol. 27, No. 3, pages 413-425, 1974.

5-74. Harris, D.O., "The Influence of Crack Growth Kinetics and Inspection on the Integrity of Sensitized BWR Piping Welds," Report EPRI NP-1163, Electric Power Research Institute, Palo Alto, California, 1979.

5-75. "An Assessment of the Integrity of PWR Pressure Vessels," report of a Study Group chaired by W. Marshall, Her Majesty's Stationery Office, London, England, 1976.

5-76. Harris, D.O., and Lim, E.Y., "Applications of a Fracture Mechanics Model of Structural Reliability to the Effects of Seismic Events on Reactor Piping," Progress in Nuclear Energy, Vol. 10, No. 1, pages 125-159, 1982.

5-77. Kitigawa, H., and Hisada, T., "Reliability Analysis of Structures Under Periodic Inspection," Third International Conference on Pressure Vessel Technology, Part I: Analysis and Design, American Society of Mechanical Engineers, New York, 1977.

5-78. Arnett, L.M., "Optimization of In-Service Inspection of Pressure Vessels", E.I. duPont de Nemours and Company, Report DP-1428, Savannah River Laboratory, Aiken, South Carolina, August 1976.

5-79. Dufresne, J., et al., "The CEA-Sponsored Research Program on PWR Reactor Vessel Failure Probability Calculation," Probabilistic Analysis of Nuclear Reactor Safety, Vol. 2, Paper III.1, Proceedings of topical meeting sponsored by the American Nuclear Society, Los Angeles, California, May 1978.

5-80. Satoh, K., et al., "Study on Reasonable Inspection Method for Welds Considering Detectability of NDT," Fracture Tolerance Evaluation, Proceedings of a U.S.-Japan cooperative seminar held in Honolulu, Hawaii, edited by Kanazawa, T., Kobayashi, A., and Iida, K., pages 249-256, December 1981.

5-81. Itagaki, H., et al., "Reliability Analysis of Welded Joints with Flaws," Fracture Tolerance Evaluation, Proceedings of a U.S.-Japan cooperative seminar held in Honolulu, Hawaii, edited by Kanazawa, T., Kobayashi, A., and Iida, K., pages 267-274, December 1981.

5-82. Structural Integrity Technology, edited by Gallagher, J.P., and Crooker, T.W., American Society of Mechanical Engineers, New York, 1979.

5-83. Hahn, G.J., and Shapiro, S.S., Statistical Models in Engineering, John Wiley and Sons, New York, 1967.

5-84. Davis, C.S., "Automated Design of Stiffened Panels Against Crack Growth and Fracture Amongst Other Design Constraints," Flaw Growth and Fracture, ASTM Special Technical Publication 631, pages 416-445, 1977.

5-85. Ellingwood, B.R., "Probabilistic Assessment of Low Cycle Fatigue Behavior of Structural Welds," Journal of Pressure Vessel Technology, pages 26-32, February 1976.

5-86. Hammersley, J.M., and Handscomb, D.C., Monte Carlo Methods, Methuen and Company, Ltd., 1964.

5-87. Lim, E.Y., "Probability of Failure in the Primary Coolant Loop of a PWR Plant, Vol. 9: PRAISE Computer Code User's Manual," U.S. Nuclear Regulatory Commission Report NUREG/CR 2189, Vol. 9, Washington, D.C., 1981.

5-88. Rau, C.A., Jr., "Quantitative Decisions Relative to Structural Integrity," Structural Integrity Technology, American Society of Mechanical Engineers, New York, pages 1-15, 1979.

5-89. Besuner, P.M., and Sorenson, K.G., "Retirement for Cause: A Workable Approach for Structural Life Extension and Response to In-Service Problems," Electric Power Research Institute Report EPRI NP-855, Palo Alto, California, 1978.

5-90. Rau, C.A., Jr., and Besuner, P.M., "Statistical Aspects of Design: Risk Assessment and Structural Integrity," Philosophical Transactions of the Royal Society of London, Series A, Vol. 299, pages 111-130, 1980.

5-91. Shinozuka, M., Itagaki, H., and Asada, H., "Reliability Assessment of Structures with Latent Cracks," Fracture Tolerance Evaluation, Proceedings of a U.S.-Japan Cooperative Seminar held in Honolulu, Hawaii, edited by Kanazawa, T., Kobayashi, A., and Iida, K., pages 237-247, December 1981.

5-92. Buntin, W.D., "Concept and Conduct of Proof Test of F-111 Production Aircraft," Aeronautical Journal, Vol. 76, No. 742, pages 587-598, October 1972.

5-93. Formby, C.L., " The Desireability of Proof Testing Reactor Pressure Vessels Periodically," Periodic Inspection of Pressure Vessels Conference, Institute of Mechanical Engineering, Paper C53/72, pages 185-193, London, England, 1972.

5-94. Irwin, G.R., and Corten, H.T., "Evaluating the Feasibility of Basing Pipe Line Operating Pressure on In-Place Hydrostatic Test Pressure," Report to Northern Natural Gas Company and El Paso Natural Gas Company, November 1968.

5-95. Mendoza, J., and Vroman, G.A., "Multiple Cycle Proof Test Logic," Rocketdyne Division, Rockwell International Report SSME 73-410, PUB 572-K-9, Revised 12/73, December 1973.

5-96. Vroman, G.A., and Creager, M., "Multiple Cycle Proof Test Logic," Copy of Rockwell International viewgraphs presented at the 7th National Symposium on Fracture Mechanics, University of Maryland, August 1973.

5-97. Vroman, G.A., personal communications with NASA-MSFC and the Boeing Company "Fracture Mechanics Aspects of Proof Testing," Documentation of telecon of 26 September 1975.

5-98. Vroman, G.A., "SSME Proof Test Logic Based on Fracture Mechanics," Rockwell International Report SSME 72-818, PUB 572-K-13, June 1973.

5-99. Vroman, G.A., "Proof Test Equivalency," personal communication/ monograph, undated.

5-100. Schliessmann, J.A., "Pressure Vessel Proof Test Variables & Flaw Growth," Journal of Materials, Vol. 7, No. 4, pages 465-469, December 1972.

5-101. Tiffany, C., personal communication, telecommunication with P.M. Besuner, February 1983.

5-102. Johnston, R.L., private communication.

5-103. Harris, D.O., "A Means of Assessing the Effect of Periodic Proof Testing and NDE on the Reliability of Cyclically Loaded Structures," Journal of Pressure Vessel Technology, Vol. 100, No. 2, pages 150-157, May 1978.

5-104. Arena, J.R., "How Safe Are Your Poles," ASCE Journal Structural Division, Vol. 99, No. ST7, pages 1333-1347, July 1973.

5-105. "Chain Testing," Works Engineering & Factory Services, Vol. 64, No. 760, pages 50-52, October 1962.

5-106. Vroman, G.A., "Using Compact Specimen Data to Predict PTC Specimen Crack Growth," personal communication/monograph, undated.

5-107. Vroman, G.A., private communication.

5-108. Chandler, W., private communication.

5-109. McIlwain, M., private communication.

5-110. McKown, R., private communication.

5-111. James, L.A., and Mills, W.J., "Fatigue-Crack Propagation Behavior of Defective Welds," International Journal of Pressure Vessel and Piping, Vol. 9, pages 367-383, 1981.

5-112. Peterson, D.E., and Vroman, G.A., "Computer-Aided Fracture Mechanics Life Prediction Analysis," Part-Through Crack Fatigue Life Prediction, ASTM Special Technical Publication 687, pages 129-142, 1979.

5-113. Herring, H., private communication.

5-114. Lawrence, F.V., "Estimation of Fatigue-Crack Propagation Life in Butt Welds," Welding Research Supplement, May 1973.

5-115. Gurney, T.R., Fatigue of Welded Structures, Cambridge University Press, 1968.

5-116. Bouwkamp, J.G., "Cyclic Loading of Full-Size Tubular Joints," 8th Annual Offshore Technology Conference, Houston, Texas, May 3-6, 1976.

5-117. National Academy of Sciences, "Effect of Weldments on the Fatigue Strength of Steel Beams," National Cooperative Highway Research Program Report 102.

5-118. National Research Council, "Fatigue Strength of Steel Beams With Welded Stiffeners and Attachments," National Cooperative Highway Research Program Report 147.

5-119. Maddox, S.J., "Calculating the Fatigue Strength of a Welded Joint Using Fracture Mechanics," Metal Construction and British Welding Journal, pages 33-37, 1970.

5-120. Tenge, P., and Karlsen, A., "Influence of Weld Defects on Low Cycle, High Strain Fatigue Properties of Welds in Offshore Pipelines," Det Norske Veritas, Vol. 5, pages 2-15, 1977.

5-121. Maddox, S.J., and Webber, D., "Fatigue Crack Propagation in Aluminum-Zinc-Magnesium Alloy Fillet-Welded Joints," Fatigue Testing of Weldments, ASTM Special Technical Publication 648, pages 159-184, 1978.

5-122. Sandifer, J.P., and Bowie, G.E., "Fatigue Crack Propagation in A537M Steel," Fatigue Testing of Weldments, ATSM Special Technical Publication 648, pages 185-196, 1978.

5-123. Kapadia, B.M., "Influence of Residual Stresses on Fatigue Crack Propagation in Electroslag Welds," Fatigue Testing of Weldments, ASTM Special Technical Publication 648, pages 244-260, 1978.

5-124. Boulton, C.F., "Acceptance Levels of Weld Defects for Fatigue Service," Welding Journal, 1977.

5-125. ASME Boiler and Pressure Vessel Code, Section XI, 1980.

5-126. Hoeppner, D.W., "Summary," Fatigue Testing of Weldments, ASTM Special Technical Publication 648, Hoeppner, D.W., editor, 1978.

5-127. Morgan, H.G., and Thorpe, T., "An Introduction to Crack Growth Testing in The UKOSRP and its Relevance to the Design of Offshore Structures," Fatigue of Offshore Structural Steel, Institute of Civil Engineers, London, 1981.

5-128. Pettit, D.E., Ryder, J.T., Krupp, W.E., and Hoeppner, D.W., "Investigation of the Effects of Stress and Chemical Environments on the Prediction of Fracture in Aircraft Structural Materials," AFML-TR-74-182, Air Force Materials Laboratory, December 1974.

5-129. Seeley, R.R., Katz, L., and Smith, J.R.M., "Fatigue Crack Growth in Low Alloy Steel Submerged Arc Weld Metals," Fatigue Testing of Weldments, ASTM Special Technical Publication 648, pages 261-284, 1978.

5-130. Thielsch, H., private communication.

Section 6

SUMMARY AND CONCLUSIONS

An assessment of the state-of-the-art of fracture mechanics life technology for applicability to oxygen/hydrogen propulsion components has been provided in this report. This assessment combined a broad search of the literature, contacts with specialists in the field, and the experience provided by the staff at Failure Analysis Associates. Failure of oxygen/hydrogen propulsion components most often occurs due to the growth of cracks or defects caused by cyclic loading. The review therefore concentrates heavily on techniques for analyzing fatigue crack growth by fracture mechanics techniques. The majority of the component lifetime is occupied by cracks growing at relatively slow rates, and the final critical crack size most often does not have a strong influence on the calculated (or observed) lifetimes. Consequently, the final failure criterion is not influential and such criteria therefore receive secondary consideration in the review.

Fracture mechanics-based analyses of fatigue crack growth are based on comparisons of the cyclic crack driving force with the material's response to this force. In the case of linear elastic fracture mechanics, the driving force is measured primarily by the value of the cyclic stress intensity factor, ΔK ($= K_{max} - K_{min}$), and the material response is measured by the corresponding crack growth rate, da/dn. Hence, a stress intensity factor solution is required. This solution relates the applied loads (mechanical, thermal or residual stresses) and crack size and configuration to the value of the stress intensity factor.

Various aspects of the inputs to a fracture mechanics analysis will be summarized in the remainder of this section in roughly the same order as they are covered in this report.

Stress Intensity Factors: Section 2 reviews the current state-of-the-art for elastic stress analysis of cracked bodies. For the case of bodies which can be idealized as two-dimensional, it was found that a very wide variety of stress intensity solutions are currently available and that fairly accessible and economical techniques are available for the generation of new solutions in situations where this is required. Additionally, the use of influence functions, superposition and judicious approximations can readily provide results for new stress systems and cracked configurations. Hence, it appears that the evaluation of stress intensity factors for two-dimensional bodies does not pose an obstacle to the use of fracture mechanics for lifetime prediction. However, additional software developments to make influence function techniques as well as finite element programs optimized for cracked bodies more convenient to use for fracture mechanics practitioners is desireable.

The current stress intensity factor solutions for three-dimensional elastic bodies are not nearly as complete as for two-dimensional bodies, although a wide variety of configurations have been treated. Furthermore, economical numerical procedures for evaluation of K for new geometries are lacking, and the most economical techniques are not readily accessible to the technical community. The less satisfactory status of three-dimensional (as compared to two-dimensional) problems is, of course, due largely to the inherent additional complexities of three-dimensional problems. The majority of cracks that lead to problems in oxygen/hydrogen propulsion components spend

most of their time as partial thickness cracks -- which are inherently three-dimensional. Therefore, such cracks are of special interest in this case. Advances are currently being made in the economical generation of stress intensity factors for cracks in three-dimensional bodies, including cracked plates and shells. Special consideration should be given to the appreciable additional information on crack surface opening displacements that is generated in numerical calculations of stress intensity factors, because this information can be used in the development of influence functions. Such functions can be used to very economically evaluate stress intensity factors for arbitrary stresses. This is especially useful in situations involving complex spatial stress gradients, such as arise in thermal and residual stress fields.

Subcritical Growth of Cracks: The response of the cracked material to the applied driving forces is another piece of information required in the estimation of component lifetime. Oxygen/hydrogen propulsion components are typically subjected to cyclic loads, and the resulting fatigue crack growth is the process leading to final failure. The material's response is measured by the value of the crack growth per cycle, da/dn. Section 3 provides a review of this topic, which comprises a large fraction of this report. Even for the simple case of constant amplitude cycling, many factors influence the crack growth rate for a given material and value of the cyclic stress intensity factor (ΔK). These include the load ratio ($R = K_{min}/K_{max}$), environment, cyclic loading frequency and temperature. There are complex interactions between these factors which are only poorly understood at the present time. Extensive experiments must be conducted for the particular conditions of interest if it is desired to have reliable information for lifetime analyses.

The need for experimentation for the specific conditions of interest is one of the current drawbacks of the use of fracture mechanics, and can add greatly to the cost of performing a reliable lifetime analysis. A more complete understanding of the effect of influencing factors and their interaction would reduce the need for experimentation and circumvent this drawback.

Many propulsion components are subjected to high frequency loadings and any initial cracks must be small in order to survive for the desired lifetime. Some of these cracks are too small to be modeled with typical fracture mechanics methods. Hence, a means of treating the growth of short cracks is necessary, as is briefly reviewed in Section 3.3. Of equal importance is a knowledge of the threshold conditions for the growth of fatigue cracks. Such threshold conditions, and the influence of various factors, are reviewed in Section 3.3. The effects of R-ratio appears to be well understood, at least in an empirical sense, but the influence of environment is only partially documented and conflicting observations have been made. A more thorough understanding of the influence of environment and microstructure on fatigue crack growth thresholds would be highly desireable. Additionally, the influence of load history (such as prior overloads) on thresholds is in need of better understanding.

Matters become increasingly more complex and less well understood as attention is turned towards the more realistic case of variable amplitude cyclic loading. In such cases, the crack growth per cycle is influenced by the past loading history, and the behavior becomes quite complex -- even in the absence of environmental and threshold effects. In the case when the histogram of cyclic load amplitudes is unimodal, crack growth rates can often

be related to RMS values of the cyclic stress intensity factor. Various models have been suggested for periodic overloads and other more general loading cases. These models typically consider the crack growth to be altered by threshold effects and either the presence of residual stresses ahead of the crack, or crack closure and crack surface alteration produced by the overload. These models are reviewed in Section 3.4 and all have been shown to provide good correlations to selected test data. However, they all have been shown to be lacking in some regard, such as not agreeing with test data in some different loading situations. When adverse environments and/or threshold effects become important, the situation is even more uncertain. Hence, the development of a general model for crack growth under variable amplitude loading has yet to be developed. This is especially true for situations involving adverse environments. The influence of time dependencies at elevated temperatures is another related area of uncertainty that is of concern in the life prediction of oxygen/hydrogen propulsion components.

Analytical tools for the analysis of the subcritical growth of part-through cracks are currently not well developed, especially in the case of complex spatial stress gradients. Additionally, criteria for the transition of part-through cracks to become through-wall cracks are currently of a highly empirical nature. Additional analytically based work in this area would be worthwhile, but would be complicated by plasticity effects as the crack depth approached the wall thickness. Such concerns are not of great importance in the prediction of the lifetime of components subjected to high-cycle fatigue, because a relatively small portion of the lifetime is spent in the transition range. However, such transition considerations would be important in the case

of low-cycle fatigue of components initially containing part-through cracks. Plasticity effects would most likely be important in such a situation.

Although considerable additional understanding of fatigue crack growth remains to be attained, much of the current state-of-the-art is distributed among several automated computer programs. These programs provide an adequate level of predictive capability for many applications. The programs appear to be fairly easy to use, are applicable to a wide variety of configurations and materials, and are available to a variety of users. However, none of the programs is comprehensive, and consolidation of all available predictive procedures into one general-purpose program has yet to be accomplished. Other improvements in these programs await the development of more comprehensive descriptions of fatigue crack growth.

Nonlinear Fracture Mechanics: The need for nonlinear fracture mechanics arises when plastic or viscoplastic deformation becomes appreciable and also has an influence on calculated lifetimes. In oxygen/hydrogen propulsion components, plasticity occurs predominately at the crack location, such as at a surface crack emanating from a notch-like stress raiser that causes localized yielding. Plasticity effects can be very important for accurate life prediction, and the few tools available to address these problems are described in Section 4. These methods include adaptation of both Neuber's notch plasticity results to prediction of nonlinear stress fields and attempts to define and use such parameters as the J-integral. The use of cyclic J values, ΔJ, to correlate with crack growth rates is described. However, a comprehensive review of nonlinear fracture mechanics is not attempted.

Three approaches to final failure criteria for nonlinear situations were considered: the failure assessment diagram; the design curve approach; and the J-integral approach. The first two are relatively easy to employ but generally are lacking in precision and generality. The J-integral and related tearing modulus approach are the most strongly mechanics-based, and should be readily applicable to oxygen/hydrogen propulsion components. However, very little information on the J-resistance characteristics of relevant materials is available. Such data would have to be generated in order to employ this approach, but relevant test methods are fairly well advanced based on progress from other fields -- such as nuclear reactor pressure vessels and piping. However, as stated above, such data is of secondary importance in prediction of lifetime for most components, because most of the component life is spent at fairly slow fatigue crack growth rates. In cases of low-cycle fatigue, nonlinear considerations of final failure can be important. Additionally, in cases where large cyclic stresses are imposed, nonlinear consideration of fatigue crack growth can be of use. Section 4.2 reviews the current status of this area.

Additional Topics: Numerous topics of peripheral interest are also reviewed. One of growing interest is probabilistic fracture mechanics (PFM). Scatter in material properties, the stochastic nature of imposed loads, and uncertainties in initial crack sizes often lead to large uncertainties in lifetime calculations that are based on deterministic fracture mechanics predictions. Lower bound or conservative approaches are often inconclusive. Fracture mechanics calculations that incorporate probabilistic considerations provide a means of quantifying these uncertainties and assessing their influence on the reliability of the component. The current state-of-the-art

in this rapidly expanding field is reviewed in Section 5.3. Probabilistic considerations will undoubtedly be of growing importance in future fracture mechanics analyses of oxygen/hydrogen propulsion components.

Another topic of current interest and concern is the use of proof testing to assess the adequacy of component integrity. Various approaches to selecting appropriate proof test loadings and cycles for the tough ductile materials employed in components of interest are reviewed in Section 5.4. The trade-offs between damaging good components during the proof test or allowing unsafe components to go into service are discussed. Basically, it was found that a divergence of opinion exists between various practitioners as to the merit of multiple cycle proof tests. The divergence of opinion is based largely on dissimilar past experience in this area, much of which can be understood and explained with relatively simple analyses. Examples are given in which the use of multiple proof cycles benefits, harms, or has no effect upon structural reliability. The probabilistic nature of the effectiveness and optimization of proof testing is pointed out, and the close interplay between the benefits of proof testing, non-destructive inspection, and PFM is emphasized. The current state-of-the-art in selection and optimization of proof test procedures is fairly rudimentary, and this appears to be a topic for fruitful future efforts -- especially as additional information on the nature of the randomness of various fracture mechanics inputs becomes available. The review is concluded with a discussion of weld cracks, which is of importance because many life-limiting defects in oxygen/hydrogen propulsion components originate in welds and because many cracked-weld problems combine several complexities of fracture mechanics life technology and material behavior.

In summary, the review of fracture mechanics life technology provided in this document revealed that many powerful tools are now available. The elastic stress analysis of cracks is straightforward, at least in principle, but additional useful tools for the day-to-day practitioner would be worthwhile. This is especially true for cracks in three-dimensional bodies. The largest gap of knowledge in areas of importance in lifetime prediction is in characterization of fatigue crack growth for the case of variable amplitude loading in the presence of an adverse environment. Additionally, fatigue crack growth thresholds under such conditions are also only beginning to be understood.

Recommendations for future research efforts to narrow the gaps in important areas are provided in the appendix.

APPENDIX

RECOMMENDATIONS FOR FUTURE RESEARCH ON FRACTURE MECHANICS LIFE TECHNOLOGY

Contract NAS8-34746

September 1983

Prepared by

Failure Analysis Associates
2225 E. Bayshore Road
Palo Alto, California 94303

J.M. Thomas
P.M. Besuner
D.O. Harris

Prepared for

National Aeronautics and Space Administration
George C. Marshall Space Flight Center
Huntsville, Alabama 35812

Table of Contents

RECOMMENDATIONS FOR FUTURE RESEARCH ON FRACTURE MECHANICS LIFE TECHNOLOGY

An extensive review of the current state-of-the-art in analytical life-time prediction of advanced hydrogen/oxygen rocket engine components by use of fracture mechanics was provided in a companion volume to this report. The purpose of this document is to provide recommendations for future research efforts to improve the predictive capabilities of fracture mechanics for this particular application. The review provided in the companion volume revealed that many powerful tools and voluminous materials data now exists, and that the current technology is capable of providing adequate results under many circumstances. However, conflicting theories and inconsistent data have been reported, and there is an obvious need for both a better understanding of underlying phenomena and additional material data. This report will provide recommendations for (i) improved use of existing technology, (ii) research areas to fill the gaps in current understanding, and (iii) research for expanding the technology.

The fracture mechanics analysis of crack growth in engine components often involves consideration of low- and high-cycle variable amplitude fatigue under extreme conditions of temperature and/or aggressive environment. Aside from errors outside the fracture mechanics analysis (such as load estimation errors), inaccuracies in prediction of component lifetime will therefore be dominated by inaccuracies in environmental and fatigue crack growth relations, stress intensity factor solutions, and methods used to model given loads and stresses. Consideration of failure criteria and transition criteria (point at which a part-through crack becomes a through-wall crack) are of secondary

importance. Therefore, the following recommendations will be heavily weighed towards filling the gaps in knowledge of the growth characteristics of cyclically loaded cracks.

Fracture mechanics considerations form only a portion of a comprehensive analysis of component lifetime. Other considerations, such as the initiation of cracks in flaw-free areas are often of primary importance. Additionally, non-destructive evaluations (NDE) of components prior to being placed in service and in-service examinations form other key ingredients in assuring the satisfactory lifetime of a structure. The following recommendations will therefore not be restricted to the fracture mechanics topics touched upon in the companion volume, but will also include closely allied areas that are necessary for comprehensive fracture control.

Future research can cover a very wide range of efforts, from making existing procedures more useable for the day-to-day practitioner to expanding the frontiers of continuum mechanics. In recognition of this diversity, the areas of recommended future research will be broken down into the following three categories:

I. Improvements in Utilization of Existing Technology
II. Filling the Gaps in Existing Technology
III. Expansions of Existing Technology.

Obviously, there will be overlaps and interplay between these three areas.

Research topics in each of these three categories will be enumerated and discussed in the following. Areas of special relevance to lifetime prediction of engine components will be emphasized. Hence, no claim is made regarding the general and comprehensive nature of the following discussion.

I IMPROVEMENTS IN UTILIZATION OF EXISTING TECHNOLOGY

The review provided in the companion volume demonstrated the high degree of sophistication of the current technology of fracture mechanics. However, the high degree of sophistication is often not fully utilized by the fracture mechanics practitioner. The current technology could find more extensive use if easily used and widely accessible software was available. As discussed in Sections 2.3 and 3.7 of the companion volume, numerous computer codes for automated fracture mechanics analyses are available. However, none of these codes fully utilize today's technology. Additionally, for the most part, these codes are not easy to use and are not available to a wide range of users. Therefore, the first step in expanding the usefulness of fracture mechanics for life prediction technology is to provide more easily used and accessed software. To this end, the following efforts are recommended.

I.1 Software Development

Recommendation I.1.1

Development of a widely accessible user-friendly software package for the determination of stress intensity factors for a wide range of crack configurations and loadings is recommended. This could be viewed as a computerized K-handbook, such as provided by Tada, et al., Sih or Rooke and Cartwright. The current state-of-the-art in personal computers would allow this software to be used on such computers which would facilitate the interactive use of these programs. Software that would require no knowledge of computer programming on the part of the user could be developed, and is recommended. Convenient interfaces between the personal computer, mini-computers, and mainframes should be an integral part of such a development. The computer program BIGIF provides an example of a code that covers a very wide range of loading and geometry combin-

ations that could be expanded with available or newly-developed software to include new, or missing capabilities and user-oriented format. The use of influence (or weight) functions to provide a more general approach to a variety of loading conditions is recommended. The use of such influence functions requires information on stresses on the crack plane prior to introduction of the crack. Such information is often provided by strength of materials, theory of elasticity, finite element, or other stress analysis methods. Provisions for easily interfacing the uncracked-structure stress analysis (especially finite element results) with the fracture mechanics code for determination of stress intensity factors by use of influence functions is also recommended.

Recommendation I.1.2

The development of software for treating contained plasticity due to notches and other local stress-raisers using procedures such as that based on the Neuber approach discussed in Section 4.2 of the companion volume is recommended. Such software should be incorporated into the K-determination code discussed immediately above.

Recommendation I.1.3

The development of a widely accessible user-friendly software package for the automated analysis of flaw growth is recommended. Currently publicly available codes could be merged to form a code that would contain most capabilities required for day-to-day fracture mechanics applications. Capabilities for analyzing variable amplitude loading, adverse environments, R-ratio effects and threshold effects should be included. Such efforts could be approximately treated using current technology, but the treatment could be updated based on information gained through research recommended in later sections of this discussion. The software package for automated analysis of flaw growth should be merged with the "computerized K-handbook" software discussed above in order to provide a comprehensive tool for flaw growth calculations.

Recommendation I.1.4

The development of software for predicting critical flaw sizes for various crack configurations in typical engine components and materials is recommended. The resulting software should be merged with the "K-handbook" and flaw growth software discussed in Recommendations I.1.1 and I.1.3 in order to allow lifetime predictions to be made. Since the lifetime of most components is spent growing relatively small cracks, accurate knowledge of critical crack sizes is not required for accurate lifetime predictions. Hence, a high degree of sophistication in this software is not necessary. To the extent possible, the failure assessment diagram, J-integral, and tearing modulus approaches should be employed using materials information developed under efforts recommended in later sections of this discussion.

Recommendation I.1.5

Current state-of-the-art codes and procedures for generation of stress intensity factors for two-dimensional configurations not already analyzed should be made more user-friendly and widely accessible. A user-oriented widely available code for generation of stress intensity factors is recommended for development for an approach to two-dimensional problems. Such a code would be of use to a wide variety of fracture mechanics practitioners. Boundary collocation, finite element or boundary integral equation codes (preferably with singular elements) should be considered.

Recommendation I.1.6

Current state-of-the-art codes and procedures for generation of stress intensity factors for cracked three-dimensional bodies should be made more accessible and user-oriented. Finite element techniques coupled with singular elements and/or the alternating procedure employing recent analytical results for embedded elliptical cracks (Section 2.2 of the companion volume) should be embodied in an easily used software package. Line spring models for cracks in three-dimensional bodies serve as an alternative candidate.

Capabilities for three-dimensional analysis currently reside with the developer of the particular procedure employed and are not useable by a wide variety of practitioners. The development of three-dimensional codes useable by a relatively unsophisticated practitioner would be difficult, but is recommended.

Recommendation I.1.7

J-integral, tearing modulus and C* (energy release rate due to creep) solutions are required in some low cycle fatigue and/or high temperature applications. The development of a user-oriented code for the generation of such solutions is recommended. Nonlinear finite elements appear to be the best candidate for general applicability to two-dimensional problems. This is another example of current capabilities residing only with the code developers, and a readily accessible code would do much to expand the utilization of this technology. The difficulties (and costs) of developing such nonlinear codes must be weighed against the relative unimportance of nonlinear effects in the lifetime prediction of many engine components. An alternative approach would be to generate new nonlinear solutions for geometries of relevance to engine components (see Recommendation I.2.3).

I.2 Generation of New Stress Intensity Factor Solutions and Examples of Software Utilization

The development of widely available and user-friendly software for determination of stress intensity factors in two- and three-dimensional bodies that was recommended above would reduce the need for the efforts to be recommended in this section. However, the following items, which are specifically tailored to engine components, would assist in the transfer of technology to the day-to-day engine fracture mechanics practitioner.

Recommendation I.2.1

Identify typical critical engine components of geometries for which existing stress intensity factor solutions are inadequate and generate such solutions for future use. Careful consideration of the idealizations employed in the modeling must be given. Weight function or influence function techniques should be employed in order to provide results of use under complex stress conditions. The results generated should be incorporated into the software discussed in Recommendation I.1.1. These geometries include all welded joints and other "hot spots" subject to the simultaneous occurrence of high stress and potential material weakness. Crack geometries include the range of observed and worst-case flaw shapes and sizes in weld joints. The state-of-the-art may be such as to allow some numerical, accurate, fully three-dimensional stress intensity factor solutions to be developed as a practical matter. However, a more cost effective approach based on existing technology would be the use of variable (cross-sectional) thickness two-dimensional solutions and approximations for many typical engine component geometries.

Recommendation I.2.2

The new stress intensity factor results generated in Recommendation I.2.1, along with the software developed in Section I.1, should be exercized for both hypothetical and practical problems which encompass most geometries, stress, material and environmental combinations to be expected in the field. The 15 to 100 analyses created can serve as modeling examples and guidelines for the rocket engine engineering community.

Recommendation I.2.3

In the event that the cost of development of a general purpose code for calculation of J-integral solutions (Recommendation I.1.7) was not warranted by the need for such results in engine component lifetime predictions, a recommended alternative approach is to generate

J-integral solutions for configurations of interest that cannot be treated by currently available results. Generation of solutions relevant to stress gradient conditions should be considered.

I.3 Generation of Additional Test Results

The current state-of-the-art of fracture mechanics life prediction technology, as reviewed in the companion volume, provides powerful tools for the prediction of crack growth -- once the appropriate test data is available. This section will provide recommendations for generation of additional test data within the framework of current technology. Additional recommendations for testing and analysis to expand the current technology will be provided in Section II.1.

Recommendation I.3.1

Identify key material/environment combinations of relevance to hydrogen/oxygen engine components for which adquate fatigue crack growth data is unavailable. Perform tests to characterize the subcritical crack growth of the material to serve as inputs to fracture mechanics analyses of component lifetime. Such results could be input to the software developed under Recommendation I.1.3. Due consideration of R-ratio, threshold and frequency effects should be given, and it is recommended that data be generated over a wide range of crack growth rates (such as 10^{-8} to 10^{-3} inches/cycle).

Recommendation I.3.2

Additional fatigue crack growth data under variable amplitude loading should be generated in combination with Recommendation I.3.1 if such loading is easily characterized for the specific application being considered.

Recommendation I.3.3

Key testing to discriminate between various proposed models of crack growth under variable amplitude loading is recommended. As discussed in the companion volume (Section 3.4) several models have been proposed and voluminous data generated to demonstrate the usefulness of the various models. However, additional testing is recommended that involves carefully selected load histories that would discriminate between the various models. The results of such testing would be useful in incorporating the appropriate model into the software discussed in Recommendation I.1.3, as well as in development of new models -- as will be discussed in Section II of this document.

Recommendation I.3.4

Limited additional testing aimed at a clearer understanding of transition behavior of part-through cracks is recommended. Since such behavior occupies only a small fraction of the lifetime of most hydrogen/oxygen components, this item is of secondary importance.

Recommendation I.3.5

The generation of J-resistance curves for ductile materials at temperatures at which critical crack lengths have an important influence on predicted lifetimes is recommended. The technology of such testing is fairly advanced, and these tests would therefore not be overly expensive.

Recommendation I.3.6

J-resistance curve testing for use in analysis of part-through cracks is suggested.

Recommendation I.3.7

Crack growth under mixed mode cyclic loading can be important in the complex situations encountered in engine components and a research effort to better understand such growth in typical engine materials is suggested.

Recommendation I.3.8

Procedures for analyzing the growth of part-through cracks under complex stress conditions should be subjected to experimental confirmation in typical engine materials and environment. The assumption of "self-similar" flaw growth can lead to serious error in many situations, and this assumption can and should be avoided.

II FILLING THE GAPS IN EXISTING TECHNOLOGY

The previous section provided recommendations for research to facilitate the more effective use of existing technology for the prediction of component lifetime. This section will provide recommendations for research to expand and fill in gaps in current technology. Hence, recommendations in this section are more research oriented, but of more direct and immediate applicability than items to be discussed in Section III.

II.1 Development of Improved Models of Subcritical Crack Growth

Recommendation II.1.1

A general model for estimation of fatigue crack growth under aggressive environments would be very useful -- even for the relatively simple case of constant cyclic load amplitude. Research for the development of such a model is strongly recommended. This is one of the most difficult undertakings recommended here, but is also the one with potentially the largest payoff. This model would allow predictions to be made of the influence of a particular environment on fatigue crack growth, including the effects of temperature, loading frequency and R-ratio. This would circumvent the need to perform numerous tests each time a new loading condition or environment was encountered. Such a model has proved very elusive in the past, because of the complexity of the phenomena involved as well as the interdisciplinary nature of the problem. Lacking a general model, several viable techniques for "interpolating" or "extrapolating" from test conditions to the desired conditions are available and should be pursued. The results of these efforts should be incorporated into the software discussed in Recommendation I.1.3.

Recommendation II.1.2

Improved methods of predicting crack growth under variable amplitude cyclic loading would be beneficial in improving the accuracy of lifetime predictions. Initiation of research efforts in this area is recommended. Such efforts should be coordinated with the general model development discussed in Recommendation II.1.1, and the testing included in Recommendation I.3.3. Such a model would ideally provide a means of treating crack retardation that does not require extensive additional testing.

Recommendation II.1.3

A research program to provide a better understanding of the influence of environment and previous load history on fatigue crack growth thresholds is recommended. The results of these efforts should be combined with Recommendations II.1.1 and II.1.2 to provide a general model of fatigue crack growth that is incorporated into a widely available computer program code such as discussed in Recommendation I.1.3.

Recommendation II.1.4

Creep crack growth in some engine components is important, and further research in this area is recommended. Considerable research on characterizing high temperature sustained load crack growth in selected relevant materials has already been performed and serves as a foundation upon which to build. Further research to explore the influence of hold times at elevated temperatures on crack retardation is recommended. Such efforts should be based on solid mechanics concepts, such as the C* parameter approach.

Recommendation II.1.5

Further research to explore the interactions of creep and fatigue are recommended in order to gain a better understanding of this complex area.

Recommendation II.1.6

Additional testing to provide crack growth rate-C* correlations for relevant materials and temperatures is recommended.

Recommendation II.1.7

Solid mechanics-based studies of the relevant parameters for correlation of creep crack growth under typical hydrogen/oxygen engine conditions is recommended. The conditions under which net section stress (σ_n), K, J and/or C* provide the suitable parameters for engine conditions needs to be clarified. If C* is applicable to fully creeping materials and engine conditions are "contained creep" (in which σ_n, K or J is controlling), then C* should be eliminated from consideration and test conditions designed to simulate typical engine conditions -- rather than doing what is easiest in the laboratory.

Recommendation II.1.8

A research effort is recommended to develop applicable tools for analyzing creep crack growth. The J or C* "solutions" for relevant defects should be developed so that the laboratory correlations with crack growth characteristics can be used to predict the behavior of actual cracked components operated at high temperatures.

II.2 Integration of Crack Initiation Analysis with Fracture Mechanics

Many hydrogen/oxygen engine components are currently designed based on a fatigue analysis that assumes an initially flaw-free material. The analysis then proceeds with an "S-N" type of approach for predicting component lifetime. NASA currently has a research project underway on "Verify Fatigue Life" to develop procedures for calculating lifetimes under random cyclic loading, and to verify the prediction by comparison with observed service conditions and corresponding failures. A research program is recommended to develop

methodologies that combine the "S-N" approach with fracture mechanics in order to provide a consistent tool for life estimation of initially unflawed components that includes both the initiation and propagation of cracks. Improved tools for the treatment of short cracks (i.e., cracks too small to be modeled adequately with current continuum fracture mechanics methods) would be important in the treatment of the early behavior of initiated cracks. Procedures for treating the randomness of the initiation phase would be useful in probabilistic fracture mechanics (PFM) analyses.

II.3 Residual and Assembly Stresses

Residual stresses, such as due to welding, and assembly stresses can be introduced into engine components during fabrication. These stresses can have an important influence on subcritical and catastrophic crack growth. A research effort to better characterize such stresses is recommended. Through-thickness variations of welding residual stresses have an important influence on the effect of such stresses on the behavior of cracks, and should be included in any research efforts in this area.

II.4 Probabilistic Fracture Mechanics (PFM)

A research program to expand the usefulness of PFM for engine components is recommended. Such efforts would be closely coupled to the improvements in (deterministic) fracture mechanics resulting from research efforts recommended above, because any PFM analysis is no better than the deterministic models upon which it is based.

Recommendation II.4.1

The development of data bases for improved definition of the statistical distribution of the materials-related random variables is recommended. This would include studies of the distribution of toughness of typical engine materials as well as the distribution of cyclic crack growth properties for a given ΔK and cycles to initiation for a given stress history.

Recommendation II.4.2

Research into the statistical distribution of initial defect sizes and numbers is recommended. The applicability and utility of "effective-initial-crack-size" distributions presented in the literature should be explored. Additional investigations into initial crack sizes is recommended, including more data on initial crack depth and length -- as well as the relationship between these two random variables. The often-made assumption that the crack depth and the aspect ratio are independent should be scrutinized.

Recommendation II.4.3

It is recommended that any PFM efforts be coordinated with on-going NASA programs related to NDE of engine components. Coordination of projects would improve the likelihood that the NDE procedures would concentrate on the most relevant types and features of defects from a fracture mechanics standpoint while also providing information on flaw detection probabilities that is necessary for the PFM evaluation.

II.5 Optimization of Proof Testing Procedures

A coordinated effort is recommended for the development of procedures to apply PFM to the optimization of proof test procedures. The costs of failure during proof loading and the cost of a service failure would be important inputs to such procedures. The magnitude of proof loading and the number of

proof cycles could be optimized based on the cost of various types of failure and their probability of occurrance. The J-resistance curve information on engine materials subject to stable flaw growth discussed in Recommendation I.3.5, and the improved data bases for random variables mentioned in Section II.4 would provide important inputs to proof test optimization.

III EXPANSIONS OF EXISTING TECHNOLOGY

Previous sections provided research recommendations that are concerned with the existing framework of fracture mechanics technology. This section will discuss areas that deal with expanding the current technology, and will therefore touch upon more fundamental topics. The areas to be covered were identified during the survey summarized in the companion volume. Therefore, this section is certainly not intended to be a general set of recommendations for long range comprehensive research efforts.

III.1 Generalization of J-Integral

The J-integral is strictly applicable only to nonlinear elastic materials. This lack of generality makes its use suspect in applications involving either non-monotonic loading or crack growth. Research efforts to provide a more general parameter for the characterization of crack stress fields and/or energy release rates is recommended. The T-integral of Atluri, which was briefly mentioned in the Introduction to Section 4 of the companion volume, appears to provide a fruitful path for future research efforts.

III.2 Cyclic Plasticity - Fatigue Crack Growth Interfaces

A research effort aimed at unifying the fracture mechanics approach to fatigue crack growth and the cyclic plastic deformation characteristics of the material would be worthwhile, in that it would unify these two largely independent areas to provide a better and more fundamental understanding of fatigue crack growth. Progress in this area could have an important impact on

the development of models of fatigue crack growth suggested for development in Section II.1 of this document.

III.3 Transient Creep Crack Growth

Current theories of creep crack growth assume that creep is occurring under steady-state conditions (i.e., secondary creep, for which $\dot{\varepsilon} \propto \sigma^n$). This allows J-integral approaches to be employed. This ignores the transient portion of the creep behavior (primary creep), which could be important for the time-temperature combinations relevant to creep cracking of typical hydrogen/oxygen engine components. As additional information is gained on the creep crack behavior under relevant conditions, the suitability of ignoring transient creep should become apparent. The desireability of a research effort into this area could be assessed at that time.

TECHNICAL REPORT STANDARD TITLE PAGE

1. REPORT NO.	2. GOVERNMENT ACCESSION NO.	3. RECIPIENT'S CATALOG NO.
NASA CR-3957		

4. TITLE AND SUBTITLE	5. REPORT DATE
A Review of Fracture Mechanics Life Technology	February 1986
	6. PERFORMING ORGANIZATION CODE

7. AUTHOR(S)	8. PERFORMING ORGANIZATION REPORT #
Philip M. Besuner, David O. Harris, and Jerrell M. Thomas	

9. PERFORMING ORGANIZATION NAME AND ADDRESS	10. WORK UNIT NO.
Failure Analysis Associates 2225 East Bayshore Road P.O. Box 51470 Palo Alto, California 94303	M-509
	11. CONTRACT OR GRANT NO. NAS8-34746
	13. TYPE OF REPORT & PERIOD COVERED
12. SPONSORING AGENCY NAME AND ADDRESS	
National Aeronautics and Space Administration Washington, DC 20546	Contractor Report (Final)
	14. SPONSORING AGENCY CODE

15. SUPPLEMENTARY NOTES

Science and Engineering
Structures and Propulsion Laboratory
Marshall Technical Monitor: Larry Salter

16. ABSTRACT

A review of current lifetime prediction technology for structural components subjected to cyclic loads was performed. The central objectives of the project were (1) to report the current state of the art and (2) recommend future development of fracture mechanics-based analytical tools for modeling subcritical fatigue crack growth in structures. Of special interest was the ability to apply these tools to practical engineering problems and the developmental steps necessary to bring vital technologies to this stage. The authors conducted a survey of published literature and numerous discussions with experts in the field of fracture mechanics life technology. One of the key points made is that fracture mechanics analyses of crack growth often involve consideration of fatigue and fracture under extreme conditions. Therefore, inaccuracies in predicting component lifetime will be dominated by inaccuracies in environment and fatigue crack growth relations, stress intensity factor solutions, and methods used to model given loads and stresses. Suggestions made for reducing these inaccuracies include development of improved models of subcritical crack growth, research efforts aimed at better characterizing residual and assembly stresses that can be introduced during fabrication, and more widespread and uniform use of the best existing methods.

17. KEY WORDS	18. DISTRIBUTION STATEMENT
Fracture Fracture Mechanics Crack Crack Growth Flaw Flaw Growth	Unclassified - Unlimited Subject Category: 39

19. SECURITY CLASSIF. (of this report)	20. SECURITY CLASSIF. (of this page)	21. NO. OF PAGES	22. PRICE
Unclassified	Unclassified	429	A19

MSFC - Form 3292 (May 1969)

For sale by National Technical Information Service, Springfield, Virginia 22161

End of Document